Spring 2019

ACCURACIES, ERRORS, AND UNCERTAINTIES OF GLOBAL CROPLAND PRODUCTS

Kamini Yadav
University of New Hampshire, Durham

ACCURACIES, ERRORS, AND UNCERTAINTIES OF GLOBAL CROPLAND PRODUCTS

BY

KAMINI YADAV
B.S., University of Delhi, 2008
M.S., TERI University, 2010

DISSERTATION

Submitted to the University of New Hampshire
in Partial Fulfillment of
the Requirements for the Degree of

Doctor of Philosophy
in
Natural Resources and Environmental Studies

May 2019

This dissertation was examined and approved in partial fulfillment of the requirements for the degree of Doctor of Philosophy in Natural Resources and Environmental Studies by:

Dissertation Director, Dr. Russell G. Congalton,
Professor of Remote Sensing and Geographic Information Systems, Natural Resources and the Environment

Dr. Mark J. Ducey, Professor of Forest Biometrics and Management, Natural Resources and the Environment

Dr. Richard Smith, Associate Professor, Natural Resources and the Environment

Dr. Meghan Graham MacLean, PhD, Research Associate, Harvard Forest, Harvard University

Dr. Barrett N. Rock, Professor Emeritus, Natural Resources and the Environment

On January 10, 2019

Approval signatures are on file with the University of New Hampshire Graduate School.

ACKNOWLEDGEMENTS

I would like to thank my advisor, Dr. Russell G. Congalton, for providing a continuous support and guidance during my exploration and research in the field of science of where and through the process of defining my thoughts and hard work. Also, I want to thank my committee: Dr. Mark Ducey, Dr. Richard Smith, Dr. Meghan G. Maclean, and Dr. Barry Rock, for offering me their expertise knowledge and motivation throughout this process.

I would like to thank the entire team of the Global Food Security Data Analysis project led by Dr. Prasad Thenkabail. Working with this group of scientists on this project has been a great learning experience and I appreciate all the work we did together. The team includes Pardhasaradhi Teluguntla, Jun Xiong, Adam Oliphant, Corryn Hola, Justin Poehnelt, Ying Zhong, Aparna Phalke, Richard Massey, Temmulen Sankey, James Charles Tilton, Murali Krishan Gumma, Mutlu Ozdogan, Varsha Vijay, Chandra Giri, and Itiya Aneece. I would like to thank Dr. Prasad Thenkabail for giving me the opportunity to be a part of this project and learn from the people expertise in the field of remote sensing and agriculture. I would like to thank Dr. James Charles Tilton for requesting and ordering the high spatial resolution imagery from the Digital Globe. Thank you to all the BASAL Lab students (Heather Grybas, Ben Fraser, Lindsay Melendey, Jianyu Gu, Christine Healy, Linnea Dwyer, and Peijun Sun without whom I could not have done such a wonderful work by helping in writing, brain storming with ideas, and putting all their efforts to achieve the task.

I want to thank my friends and family for making my life cheerful as I completed my dissertation. The constant love and support from my family has made my time as PhD student that much more fun and rewarding. A special thanks to my mom and grandma for loving, caring, and

supporting me to accomplish the completion of this dissertation and of course my husband Munendra and daughter Navika for keeping me motivated and hopeful to get my dissertation done.

This research was supported in part by the Global Food Security Analysis Project, NASA MEaSUREs grant number: NNH13AV82I and the USGS Sales Order number is 29039. Additionally, this project was supported in part by Grant/Cooperative Agreement Number G14AP00002 from the United States Geological Survey via a sub award from AmericaView. Its contents are solely the responsibility of the authors and do not necessarily represent the official views of the USGS. Thank you to the NRESS tuition waiver (2018) for making my research possible.

TABLE OF CONTENTS

ACKNOWLEDGEMENTS……... iv

TABLE OF CONTENTS……....vi

LIST OF TABLES……...viii

LIST OF FIGURES……..... xi

ABSTRACT……. xv

CHAPTER PAGE

I. INTRODUCTION……... 1
II. BACKGROUND AND LITERATURE REVIEW…….. 8
Global Cropland Extent Products……. 8
Accuracy Assessment of Global Cropland Extent Maps…….11
Uncertainty Analysis of Global Cropland Extent Maps……...……..…. 14
Sampling Strategies for Collecting Reference Data……...….17
Object-Based Image Analysis (OBIA) of High-spatial Resolution Imagery (HRI) ….……. 20
III. ISSUES WITH LARGE AREA THEMATIC ACCURACY ASSESSMENT FOR MAPPING CROPLAND EXTENT: A TALE OF THREE CONTINENTS……. 25
Abstract……... 25
Introduction……. 26
Study Area…….. 30
Methods……....33
Stratification……. 34
Collecting Reference Data……36
Sampling……...37
Computing Descriptive Statistics……. 39
Results……. 41
Discussion……60
Lessons Learned……...65
Conclusions……. 67
IV. ACCURACY ASSESSMENT OF GLOBAL FOOD SECURITY-SUPPORT ANALYSIS DATA (GFSAD) CROPLAND EXTENT MAPS PRODUCED AT THREE DIFFERENT SPATIAL RESOLUTIONS……69
Abstract……69
Introduction……. 70
Study Area……...77

Datasets……78
Methods……85
Assessment……86
Comparison…….. 89
Results…… 93
Discussion…… 111
Conclusions……....116
V. EVALUATING SAMPLING DESIGNS FOR ASSESSING THE ACCURACY OF CROPLAND EXTENT MAPS IN DIFFERENT CROPLAND PROPORTION REGIONS…… 119
Abstract…… 119
Introduction……120
Study Area……123
Datasets…… 124
Methods…..…… 125
Selecting Probability-based Sampling……126
Choosing an Optimum Sample Size……...127
Comparison of sampling designs for different crop proportion regions…….……...… 128
Results……129
Discussion…… 141
Conclusions……....146
VI. AUGMENTING AND EXTENDING LIMITED CROP TYPE REFERENCE DATA USING AN INTERPRETATION AND PHENOLOGY-BASED APPROACH……...148
Abstract…… 148
Introduction……149
Study Area……154
Datasets…… 156
Methods…… 161
Augmentation…….....162
Extension……163
Accuracy Assessment of Augmentation and Extension……166
Results……167
Discussion…… 181
Conclusions……190
VII. OVERALL CONCLUSIONS……192

LITERATURE CITED

LIST OF TABLES

Table 1. Zone-wise accuracy estimates listed for all the AEZ's of the United States……...46

Table 2. An overall accuracy matrix for the cropland extent map of US…… 47

Table 3. Zone-wise accuracy estimates listed for all the AEZ's in Africa……... 52

Table 4. An overall accuracy matrix for the cropland extent map of Africa…….53

Table 5. The error matrix generated using unbalanced ground collected reference samples……59

Table 6. The error matrix generated using balanced ground collected reference samples augmented with HRI interpreted samples……...……... 59

Table 7. The error matrix generated using balanced reference samples generated in crop buffer zone 1…….59

Table 8. The error matrix generated using balanced reference samples generated in crop buffer zone 2…….59

Table 9. Distribution of random study sites in different agriculture field sizes of different continents……...78

Table 10. Description of the three different GFSAD cropland extent maps…….……80

Table 11. Different sources of reference data used to assess the three different GFSAD cropland extent maps……....83

Table 12. The list of regions used in the assessment of the three different GFSAD cropland extent maps…….…….....88

Table 13. An example of a similarity matrix……..... 90

Table 14. Regions, their area, and number of samples that were used to assess the GFSAD1km Cropland extent map……...…..... 95

Table 15. The accuracy measures of GFSAD1km map in eight regions……..... 95

Table 16. The error matrix showing the overall accuracy of the GFSAD1km cropland extent map……..... 96

Table 17. The accuracy measures of the GFSAD250m cropland extent map……97

Table 18. The error matrix showing the overall accuracy of the GFSAD250m cropland extent map…….98

Table 19. Regions and number of reference samples used to assess the GFSAD30m cropland extent map……...100

Table 20. The accuracy measures of GFSAD30m GFSAD cropland extent map……...100

Table 21. The error matrix showing the overall accuracy of the GFSAD30m cropland extent map……...101

Table 22. Overall similarity between cropland extent maps with different resolutions…….… 105

Table 23. Omission Error (OE) and Commission Error (CE) of crop in the coarser-resolution maps as compared to fine resolution for nine different study sites……... 107

Table 24. Landscape parameters in different resolution maps for all study sites…… 108

Table 25. The specific recommendations for when to apply the three spatial resolutions of GFSAD cropland extent map with respect to different agriculture field sizes……... 116

Table 26. The calculations of cropland and non-cropland sample sizes…….……. 128

Table 27. Cropland and non-cropland area proportion and probability class of the various cropland regions……. 129

Table 28. The allocation of cropland and non-cropland reference samples using SRS and SMPS designs……. 131

Table 29. Error matrices showing the accuracy measures achieved with SRS and SMPS designs in the very low cropland proportion regions. ……...…....133

Table 30. Error matrices showing the accuracy measures achieved with SRS and SMPS sampling designs in the low crop proportion regions……. 135

Table 31. Error matrices showing the accuracy measures achieved with SRS and SMPS designs in the medium cropland proportion regions……. 137

Table 32. Error matrices showing the accuracy measures achieved with SRS and SMPS designs in high cropland proportion regions……...……. ….138

Table 33. Error matrices showing the accuracy measures achieved with SRS and SMPS designs in the very high cropland proportion regions…….……. 140

Table 34. The comparison of sampling designs in different crop probability classes…..……145

Table 35. The description of the six regions selected in three AEZs for different field sizes….154

Table 36. The cropping calendar of the crop types for three agriculture field sizes……... 155

Table 37. List of vegetation indices that were explored and used in the classification of crop types…….……..….. 157

Table 38. The training data collected from the 2015 CDL of the TR regions to classify the crop type maps of the TR and TE regions…….. 173

Table 39. The reference data used to assess the crop/no-crop and crop type maps of the three TR and three TE regions……176

Table 40. The evaluation of the augmented crop type reference data collected from GSV……177

Table 41. The error matrices of crop and no-crop maps of TR and TE regions for the large, medium, and small field sizes……...……. 178

Table 42. The overall accuracy of the crop type maps of the three TR regions developed from one, two, and three dates of satellite imagery……. 178

Table 43. The error matrix of crop type map generated from multi-dates of World View-2 imagery for the TE region in the large agriculture field size…….……. 179

Table 44. The error matrix of crop type map generated from multi-dates of World View-2 imagery for the TE region in the medium agriculture field size……. 179

Table 45. The error matrix of crop type map generated from multi-dates of World-View 2 imagery for the TE region in the small agriculture field size……. 180

LIST OF FIGURES

Figure 1. Map showing the location of three selected continents and their respective homogeneous regions such as Agro-ecological zones (AEZs) and crop buffer…….32

Figure 2. Flowchart of the process used to conduct the continent-based accuracy assessment of the GFSAD mapping products…….....34

Figure 3. The distribution of Agro-ecological zones in the United States. …….....42

Figure 4. The graphical representation of sample size simulation in AEZ's of the US…….44

Figure 5. The distribution of randomly generated reference samples within each of the AEZ's of the US. …….. 44

Figure 6. The difference image derived using reference data and cropland map of the US showing 2% Omission and 0% commission error (Massey et al., 2017a)……..... 46

Figure 7. Agro-Ecological Zones (AEZ's) of Africa……..... 49

Figure 8. The graph showing the sample simulation in AEZ's of Africa……. 50

Figure 9. The distribution of Cropland and Reference Samples in Africa……..... 51

Figure 10. Crop buffer zones delineated using Euclidean Distance buffering approach…….. 54

Figure 11. The distribution of ground collected samples used in the accuracy assessment of cropland map of Australia……. 56

Figure 12. The distribution of ground collected and augmented no-crop samples in Australia…56

Figure 13. The distribution of reference samples in buffer zones of Australia……..... 57

Figure 14. The location of the nine randomly selected study sites for the world……... 78

Figure 15. The GFSAD 1 km, 250 m, and 30 m cropland extent maps generated by multiple producers……82

Figure 16. The overall flowchart showing the methods step followed to assess and compare different resolution GFSAD cropland extent maps……...86

Figure 17. The implementation scheme of similarity matrix to compare the area of cropland on different resolution maps……...92

Figure 18. The distribution of eight regions along with the entire reference data of 1800 samples (Source: Geo-Wiki) used in the assessment of GFSAD1km cropland extent map...……... 94

Figure 19. The distribution of reference samples distributed in the four regions (Source: Independent datasets generated by assessment team and field data collected for Australia (Teluguntla et al., 2017a) used to assess GFSAD250m cropland extent map…….. 97

Figure 20. The distribution of regions and reference samples (Source: Independent reference datasets generated by assessment team from CDL and high-resolution imagery and field data collected for Australia (Teluguntla et al., 2017a) used to assess the GFSAD30m cropland extent map……..... 99

Figure 21. Difference images representing the disagreement in the GFSAD250m (A) and GFSAD30m (B) cropland extent map of the US as compared to the reference map……. 102

Figure 22. Visual comparison of the three different GFSAD cropland extent maps with high-resolution images acquired for small, medium, and large field sizes at random study sites around the entire world. The gray area represents the crops…….. 104

Figure 23. The similarity in the cropland areas mapped at the three different spatial resolutions in different agriculture landscapes……... 105

Figure 24. The differences in the percentage of cropland areas in different field size landscapes……109

Figure 25. PPU Landscape heterogeneity of different-resolution maps in landscapes with different field sizes…….……109

Figure 26. The comparison of landscape heterogeneity and area proportions in small, medium, and large field sizes…… 110

Figure 27. The location of various cropland regions around the world and the GFSAD30m cropland extent map…….124

Figure 28. The flow chart showing the steps involved to perform the assessment of cropland extent maps of the various cropland regions……..... 126

Figure 29. The distribution of 250 reference samples using SRS and SMPS designs in the Canada Zone 3……..... 130

Figure 30. Graphical representation of the overall accuracy achieved with SMPS design using the sample sizes from 50 to 300…….132

Figure 31. Graphical representation of the accuracy measures achieved with SRS and SMPS designs in the very low crop proportion regions……. 133

Figure 32. Graphical representation of the accuracy measures achieved with SRS and SMPS designs in the low crop proportion regions……. 134

Figure 33. Graphical representation of the accuracy measures achieved with SRS and SMPS designs in the medium cropland proportion regions……136

Figure 34. Graphical representation of the accuracy measures achieved with SRS and SMPS designs in the high cropland proportion regions……. 138

Figure 35. Graphical representation of the accuracy measures achieved with SRS and SMPS designs in the very high cropland proportion regions……. 139

Figure 36A and 36B. The location of three pairs of Training (TR) and TEst (TE) regions selected each in three AEZs and three agriculture field sizes……154

Figure 37. The World View-2 images used to investigate the use of multi-dates of imagery for extending the crop type reference data from the Training (TR) (left panel) to Test (TE) regions (right panel) in large (L), medium (M), and small (S) field sizes……..... 156

Figure 38. Cropland Database Layer (CDL) of TR (first row) and TE (second row) regions used as reference data to evaluate the results of augmentation and extension approaches…….....158

Figure 39. The hierarchical classification scheme followed to classify the agriculture crops of the six regions……159

Figure 40. The overall methodology flow chart showing the augmentation and extension of the limited crop type reference data for the six regions…….161

Figure 41. Augmented crop type reference data of three TR regions collected from GSV for large (L), medium (M), and small (S) field sizes…….....167

Figure 42. The crop/no-crop maps of the three TR and three TE regions in large (L), medium (M), and small (S) field sizes…….....168

Figure 43. The Decision Trees (DTs) built from the 2015 CDL reference data of the three TR regions for large (L), medium (M), and small (S) field sizes……. 170

Figure 44. The relationship between Vegetation Indices (MSR, DVI, NDVI, and GNDVI) in different growing seasons in the large agriculture field size TR region……. ……171

Figure 45. The relationship between Vegetation Indices (MSR, DVI, and SARVI) in different growing seasons in the medium agriculture field size TR region.……... 172

Figure 46. The relationship between Vegetation Indices (GNDVI, EVI, and MCARI) in different growing seasons in the small agriculture field size TR region……... 172

Figure 47. Crop type maps of three TR regions produced from one, two, and three dates of satellite imagery in the large, medium, and small field sizes…… 174

Figure 48. The crop type maps of the three TE regions produced from the classification of multi-dates of satellite imagery in large, medium, and small field sizes……...175

Figure 49. The World View-2 images of the medium field size TR region showing the unique spectral characteristics of the fallow land……....183

Figure 50. The comparison of CDL reference data of the small field size TR region with the satellite imagery……...184

ABSTRACT

ACCURACIES, ERRORS, AND UNCERTAINTIES OF GLOBAL CROPLAND PRODUCTS

By

Kamini Yadav

University of New Hampshire, May 2019

Global cropland products are continuously being produced at different spatial resolutions using remotely sensed satellite imagery. Recently, with our increased accessibility to higher computing processing, three different cropland extent maps have been developed as a part of Global Food Security-Support Analysis Data (GFSAD) project at three spatial resolutions (i.e., GFSAD1km, GFSAD250m, and GFSAD30m). All cropland maps should be assessed for their accuracy, errors, and uncertainty for various agriculture monitoring applications. However, in previous assessment efforts appropriate assessment strategies have not always been applied and many have reported only a single accuracy measure for the entire world. This research was divided into four components to provide more attention and focus on the accuracy assessment of large area cropland products.

First, a valid assessment of cropland extent maps was performed addressing different strategies, issues, and constraints depending upon various conditions related to the cropland distribution, proportion, and pattern present in each continent. This research focused on dealing

with some specific issues encountered when assessing the cropland extent of North America (confined to the United States), Africa and Australia. Continent-specific sampling strategies and accuracy assessments were performed within homogenous regions (i.e., strata) of different continents to ensure that an appropriate reference data set was collected to generate rigorous and valid accuracy results indicative of the actual cropland proportion.

Second, all the three different GFSAD cropland extent maps were assessed using appropriate sampling and collection of a cropland reference data based on the cropland distribution and proportion for different regions in the entire world. In addition to the accuracy assessment, the cropland extent maps developed at the three spatial resolutions were compared to investigate the differences among them and provide guidance for users to select the appropriate resolution given different agriculture field sizes. The comparison of three different GFSAD cropland extent maps was performed based on the similarity of the cropland area proportion (CAP) and landscape clumping at different spatial resolutions to provide specific recommendations for when to apply these maps in different agriculture field sizes.

Third, an issue was discovered with the accuracy assessment of 30m global cropland extent map (i.e., GFSAD30m) in that insufficient samples were collected resulting in an ineffective assessment when the cropland map class was rare as occurred in some regions around the world. This research evaluated the sampling designs for different cropland regions to achieve sufficient samples and effective accuracy of rare cropland map class by comparing the distribution, allocation of samples and accuracy measures. The evaluation of sampling designs demonstrated that the cropland regions of <15% CAP must be sampled with an appropriate stratified sampling combined with a predetermined minimum sample size for each map class.

Finally, the accuracy assessment of all thematic maps (e.g., crop type maps) needs sufficient reference data to conduct a valid assessment. The availability of reference data is a severely limiting factor over large geographic region because of the time, effort, cost, and accessibility in different parts of the world. The objectives of this research were to augment and extend the limited availability of crop type reference data using non-ground-based sources of crop type information for creating and assessing large area crop type maps. There is the potential to either interpret the photographs available from Google Street View (GSV) or classify High Resolution Imagery (HRI) using a phenology-based classification approach to generate additional reference data within similar agriculture ecological zones (AEZs) based on the crop characteristics, their types, and growing season. These two methods of augmenting and extending crop type reference data were developed for the United States (US) where high-quality crop type reference data already exist so that the methods could be effectively and efficiently tested.

This research described a tale of three continents providing recommendations to adapt accuracy assessment strategies and methodologies for assessing global cropland extent maps. Based on these results, the assessment and comparison of different resolution GFSAD cropland extent maps were performed to provide specific recommendations for when to apply each of the maps for agriculture monitoring based on the agriculture field sizes. When assessing the cropland extent maps, different sampling strategies perform differently in the various cropland proportion regions and therefore, must be selected according to the cropland extent maps to be assessed. Finally, this research concluded that the limited crop type reference data can be effectively extended using a phenology-based classification approach and is more efficient than the interpretation of photographs collected from GSV.

CHAPTER I

INTRODUCTION

Food security is one of the major challenges that human beings are facing (Pena-Barragan et al., 2011; Yang et al., 2011; Zhong et al., 2014). The global population, which is expected to reach a 9.8 billion mark by 2050, will demand 70% more food than they are consuming today (Alexandratos and Bruinsma, 2012). Cropland areas have expanded considerably to provide more production for closing this yield gap (Lobell et al., 2009; Foley et al., 2011; Tollefson, 2011). This expansion causes the increase in greenhouse gas (GHG) emissions and environment degradation and conflicts with the global need for sustainable agriculture (Adams and Eswaran, 2000; Beach et al., 2008). The essential inputs to improve agriculture practices and predict GHG emissions includes the mapping of cropland extent, distribution, and their specific characteristics (i.e., crop types) (Ramankutty et al., 2008; Pena-Barragan et al., 2011; Gong et al., 2013; Atzberger et al., 2015; See et al., 2015). Therefore, cropland mapping has a significant role to ensure food security, environment stability, and provide help to farmers on crop yield predictions and decision makers for policy and planning actions on large geographic areas (Yang et al., 2011; Foerster et al., 2012). Remote sensing technology provides reliable and cost-effective methodologies for cropland mapping over space and time, repeatedly, and consistently at various spatial and temporal domains (Ustuner et al., 2014; Zhou et al., 2014). Remotely sensed satellite imagery provides multiple spectral, spatial, and temporal resolution characteristics that can be effectively utilized to map the cropland extent and crop type characteristics of the earth's surface (Ulabay et al., 1982; Congalton et al., 1998; Oetter et al., 2000).

Various global cropland extent products such as the Global Map of Irrigation Areas (GMIA), the Global Map of Rain-fed Areas (GMRCA), the Global Monthly Irrigated and Rain-fed Crop Areas (MIRCA2000), the Global Rain-fed, Irrigated, and Paddy Croplands (GRIPC), and the Moderate Resolution Imaging Spectroradiometer-Cropland (MODIS) have been developed at multiple spatial resolutions from 10km to 250m (Biradar et al., 2009; Thenkabail et al., 2009; Pittman et al., 2010; Portmann et al., 2010; Salmon et al., 2015). Recently, with our increased accessibility to advanced computing platforms for processing large datasets, an improved spatial and thematic dataset compared to previous cropland mapping efforts called the GFSAD Project (Global Food Security Support-Analysis Data) was completed. These three new GFSAD cropland extent maps were created separately at three different spatial resolutions (1km, 250m, and 30m) using Landsat and MODIS imagery along with other existing cropland data (Teluguntla et al., 2016; Massey et al., 2017a and b; Xiong et al., 2017a, b, and c; Teluguntla et al., 2017a and b; Gumma et al., 2017; Phalke et al., 2017; Oliphant et al., 2017; Zhong et al., 2017; Teluguntla et al., 2018; Massey et al., 2018).

However, the cropland mapping at different spatial resolutions cause large uncertainty and differences in the estimates of cropland area and their spatial extent (Chen et al., 2017; Pérez-Hoyos et al., 2017). The cropland maps either have ineffective accuracies generated from insufficient reference data or their resolution is too coarse for use in other than global applications (Fritz et al., 2013). The quality and reliability of the cropland extent maps are required to be established as the base map for generating higher level cropland products such as crop type and crop intensity maps (Thenkabail et al., 2010). Therefore, the newly developed three GFSAD cropland extent maps must be assessed with a large area accuracy assessment strategy involving

an appropriate sampling of collecting sufficient cropland reference data over large areas to provide meaningful and effective map accuracy.

Previous attempts at rigorous accuracy assessment of large area cropland extent maps has been very limited. Considerable ambiguity exists in the implementation and interpretation of large area thematic map accuracy assessment (Congalton, 2016). Individual measures and guidelines for assessing thematic map accuracy established by many researchers are not often followed due to various limitations in the assessment process (e.g., thematic resolution, geo-location accuracy and availability of reference data) (Congalton, 1991; Stehman, 1997; Stehman and Czaplewski, 1998; Congalton and Green, 1999; Olofsson et al., 2013). As such, large area assessment and crop type mapping efforts have mostly relied on insufficient, sparsely distributed reference data (Bicheron et al., 2008; Fritz et al., 2009a; Foody, 2010; Gong et al., 2013; Yu et al., 2013). The assessments performed with limited and insufficient reference dataset reported overall accuracies ranging from 66% to 78% with considerably lower accuracies from 10% to 50% for the cropland class (Sedano et al., 2005; Frey and Smith, 2007). Therefore, more work must be done to create additional global cropland reference datasets to effectively assess large area cropland extent maps.

In the past, different sampling approaches have been used for collecting reference data to achieve appropriate accuracy results for different landscapes. Many researchers have expressed opinions on using different sampling strategies (e.g., simple random and systematic selection protocols, and structures imposed on the population such as strata clusters) for assessing the thematic maps (Hord and Brooner, 1976; Ginevan, 1979; Rhode, 1978; Congalton, 1991; Stehman and Czaplewski, 1998; Stehman, 1999; Stehman, 2009; Congalton and Green, 2009). While assessing the global cropland extent maps, different sampling approaches might result in

insufficient samples and ineffective assessments of the rare cropland map class due to the equal probability of selecting a sample area in areas that have a low proportion and distribution of cropland (Foody, 2002; Gallego, 2004; Foody and Boyd, 2013; Waldner et al., 2015). The effective use of statistically valid and probability-based sampling designs still needs to be established for various cropland regions around the world (Bayas et al., 2017). Therefore, an alternate probability-based sampling design imposed within strata defined by the map classes combined with minimum sample size is one method to provide sufficient samples and useful accuracy measures for the rare cropland map class (Stehman, 1999; Olofsson et al., 2014).

Bayas et al., (2017) has suggested that a larger sample size be implemented for assessing the cropland maps that have between 25-75% cropland and that a smaller sample size would be enough to efficiently assess the cropland maps in areas with very high or very low cropland proportion. However, in most cropland assessments, mostly small samples sizes that are sparsely distributed have been used resulting in an ineffective assessment of the cropland extent maps of various cropland regions (e.g., Fritz et al., 2009a; Gong et al., 2013). A larger sample size can achieve more appropriate and useful accuracy of the cropland extent maps (Tsendbazar et al., 2015). However, even a larger total sample size can result in insufficient samples and ineffective accuracies of the rare cropland map class if the samples are not distributed effectively. Rather than selecting sample size and strategy by the map complexity, the cropland distribution and proportion of each cropland region must be carefully considered to choose an optimum sample size to efficiently assess the cropland extent maps. Therefore, an optimum sample size must be chosen using a sample simulation analysis based on a Monte Carlo method for an effective and useful

assessment of the cropland extent maps of the various cropland regions (Hay, 1979; Congalton, 1988; Yadav and Congalton, 2018a and b).

Once the global cropland maps are assessed with appropriate strategy, sufficient sample size, and meaningful accuracy results, they can be effectively used to generate high order cropland products (e.g., crop type maps). Crop type mapping at high spatial resolution requires sufficient high-quality crop type reference data which is limited over large geographic regions from ground-based surveys because of the time, effort, cost, and accessibility in different parts of the world. However, sufficient cropland and crop type reference data are difficult to be collected from ground-based surveys because of their limited time, effort, cost, and accessibility to different parts of the world. The collection of sufficient crop type reference data can be challenging for different field size regions. Therefore, limited crop type reference data needs to be augmented or extended at multiple place using non-ground-based sources for collecting additional crop type reference data to create and assess large area crop type maps.

Possible non-ground-based sources to augment and extend the limited crop type reference data to every region are: (1) the interpretation of photographs that are readily available from sources such as Google Street View (GSV) and (2) the classification of High-spatial Resolution Imagery (HRI). The interpretation of photographs available from GSV has the potential to augment the limited availability of crop type reference data. The classification of HRI has been used to extend the crop type information to multiple years to develop year by year crop type maps without considering region to region re-training of the satellite imagery (Zhong et al., 2014). The Object-Based Image Analysis (OBIA) of the multi-dates of HRI has replaced the conventional pixel-based classification approach to achieve the improved accuracy of the crop type maps (Castillejo-

González et al., 2009; Yang et al., 2011; Conrad et al., 2014). It may be possible to use such OBIA approach along with different phenology-based classification algorithms to extend the limited crop type reference data within a single year to similar regions. These methods of augmentation and extension could save the labor, cost, and time of field surveys required to collect the crop type reference data over large regions (Tatsumi et al., 2015).

In summary, the focus of my dissertation was to assess the large area GFSAD cropland extent maps developed at three different spatial resolutions to estimate the uncertainty, errors, and accuracy of cropland areas and their spatial extent at global and regional scales. Throughout the process, many related issues involving the cropland proportion and reference data availability in different continents, appropriate sampling approaches for collecting valid cropland reference data, and crop type reference data extension to multiple regions were addressed. The specific objectives were to:

1. **Determine an appropriate assessment strategy for large area cropland maps based on the cropland distribution and pattern in different regions.**
2. **Assess and compare the three different GFSAD cropland extent maps to establish their suitability and provide specific recommendations for agriculture monitoring in different agriculture field sizes.**
3. **To evaluate sampling strategy for assessing the cropland extent maps of different crop proportion regions.**
4. **To generate additional crop type reference data with augmentation and extension approaches from non-ground-based sources using the visual interpretation of photographs and classification of multi dates of satellite imagery.**

The results of this dissertation are valuable to provide effective and meaningful accuracy results for large area cropland extent maps (i.e., GFSAD1km, GFSAD250m, and GFSAD30m). The assessment strategy employed for specific spatial resolutions allow the users to make a choice of an appropriate cropland extent map from the three different GFSAD cropland maps for their specific use. More specifically, the assessment strategy provides suitable recommendations for when to apply the three different resolution maps for different field sizes. Since, the low cropland proportion regions had insufficient samples and ineffective accuracy of rare cropland map class, an alternate sampling design was evaluated to assess the cropland extent maps of different cropland regions. Finally, the limited crop type reference data was augmented and extended to every region using non-ground-based sources to create sufficient reference data for large area crop type mapping.

CHAPTER II

BACKGROUND AND LITERATURE REVIEW

Multiple independent efforts have incorporated detailed agriculture statistical surveys with the spatial information derived from satellite imagery to produce global cropland extent maps at different spatial resolutions (e.g. Leff et al., 2004; Monfreda et al., 2008; Portmann et al., 2010). The accuracy assessment and comparison of existing cropland maps have identified uncertainties, errors, and discrepancies in the estimated cropland area and ineffective accuracy of the cropland class. To understand the previous work on the uncertainty analysis and accuracy assessment of global cropland products developed using satellite imagery that serves as the basis and motivation for this dissertation, five major components should be reviewed. They are: (1) Global cropland extent maps; (2) Accuracy assessment of global cropland extent maps; (3) Uncertainty analysis by comparing global cropland extent maps; (4) Sampling for collecting cropland reference data; (5) Object-based image analysis of multi dates of High Spatial Resolution Imagery (HRI) for mapping cropland products.

Global Cropland Extent Maps

A wide range of approaches have been investigated and evaluated to collect cropland information (e.g. ground-based field surveys, satellite based cropland classification maps, blending of field-based and satellite data, crowd sourced data and blending of crowd sourced data and satellite data). Ramankutty, (2008) and Monfreda et al., (2008) have compiled census and survey-based agriculture information reported by the Food and Agriculture Organization (FAO). Independent

evaluation by the World Bank (e.g., The World Bank, 2010) has recognized that there are both quality and quantity related problems in agriculture information provided by different countries. Alternatively, remote sensing technology provides effective tools and the necessary imagery to generate frequent and consistent cropland information at different spatial resolutions over large areas (See et al., 2014).

The use of remote sensing in agriculture began four decades ago through a series a large area field experiments: The Corn Blight Watch Experiment (MacDonald et al., 1971), the Large Area Crop Inventory Experiment (LACIE) (MacDonald et al., 1975), and the Agriculture and Resources Inventory Surveys Through Aerospace Remote Sensing experiment (AgRISTARS, 1981). Remotely sensed satellite imagery has multiple spectral, spatial, radiometric, and temporal resolution characteristics that can be effectively utilized for mapping cropland areas and crop type identification (Congalton et al., 1998; Yang et al., 2011). Therefore, remotely sensed satellite imagery is increasingly used for cropland and crop type mapping at different spatial resolutions because of its high temporal and spectral characteristics even at moderate and coarse spatial resolutions (e.g. Chang et al., 2007; Wardlow and Egbert 2008; and Vintrou et al., 2012).

Operational global cropland products that are available at spatial resolutions from 10 km to 250 m at best, such as MODIS based products, have limited ability to capture land use patterns in complex landscapes (Ozdogan and Woodcock, 2006). Examples of these products include: the Global Map of Irrigation Areas (GMIA), the Global Map of Rain-fed Areas (GMRCA), the Global Monthly Irrigated and Rain-fed Crop Areas (MIRCA2000), the Global Rain-fed, Irrigated, and Paddy Croplands (GRIPC), and the Moderate Resolution Imaging Spectroradiometer-Cropland (MODIS) (Thenkabail et al., 2009; Pittman et al., 2010). These products are poor at detecting

croplands in low agricultural intensification areas because of the inter-mixing of the spectral and temporal responses of croplands with grasslands and the mixing of different crop types within a single pixel at these coarse resolutions (Pittman et al., 2010). The estimates from these cropland maps are highly divergent due to the lack of details and incompatible legend definitions (i.e., different classification schemes).

It was not until the release of the Landsat archive in 2008 (Wuldner et al., 2012), that higher spatial resolution global products at 30m resolution were possible. With our increased accessibility to advanced computing platforms for processing large datasets, a refined spatial and thematic dataset compared to previous cropland mapping efforts called the GFSAD Project (Global Food Security Support-Analysis Data) has been produced. The GFSAD project created cropland extent maps at three different spatial resolutions (1km, 250m, and 30m) using Landsat, MODIS, and other existing cropland data (Teluguntla et al., 2016; Massey et al., 2017a and b; Teluguntla et al., 2017a and b; Xiong et al., 2017a, b, and c; Phalke et al., 2017; Oliphant et al., 2017; Zhong et al., 2017; Gumma et al., 2017; Massey et al., 2018; Teluguntla et al., 2018). Mapping from a variety of spatial resolutions raises many inconsistencies, differences, and uncertainties among the estimated cropland areas, visualizations of the map, and spatial distributions of cropland patches in different cropping patterns (Giri and Long, 2014; Bai et al., 2015). Mapping of cropland areas at different spatial resolutions causes large differences in the estimates of cropland area and spatial extent (Chen et al., 2017; Bayas et al., 2017; Pérez-Hoyos et al., 2017). Therefore, the cropland extent maps developed at these varying spatial resolutions must be compared and assessed both at the global and regional scales to establish their accuracy and uncertainty for using them as base maps for generating higher level cropland products such as crop type maps (Thenkabail et al., 2010).

Accuracy Assessment of Global Cropland Extent Maps

Accuracy assessment is an essential step in creating a thematic map from remotely sensed imagery. However, previous attempts at rigorous accuracy assessment of large area cropland extent maps developed at various spatial resolutions has been very limited. It has been observed that considerable ambiguity exists in the implementation and interpretation of large area thematic map accuracy assessment (Congalton, 2016). In the literature, individual measures and guidelines of accuracy assessment are well established by many researchers (Congalton, 1991; Stehman, 1997; Stehman and Czaplewski, 1998; Congalton and Green, 1999). However, these guidelines are not often followed due to different constraints of uncertainty components in the assessment process (Olofsson et al., 2013). The most important uncertainty components in the large area accuracy assessment process includes inconsistent availability of valid reference data, inappropriate sampling designs for collecting reference data, and invalid reporting of accuracy results for different crop proportions regions or continents. Therefore, the issues and constraints observed in the cropland maps of different continents must be addressed with an appropriate assessment strategy involving a valid and high-quality independent reference dataset, logistically feasible and statistically valid sampling strategies, and meaningful and informative accuracy measures (Franklin and Wulder, 2002).

Historically, large area assessment efforts have relied mostly on relatively sparsely distributed reference data (Fritz et al., 2009a; Foody, 2010; Gong et al., 2013b; Yu et al., 2013b). Insufficient availability of reference data limits the value of the land cover maps for informed decision making and usefulness for different studies. For example, 39 international experts have interpreted 379 confidence sites during a two-week workshop for the IGBP-DIS dataset (Scepan et al., 1999); 253

Landsat images were pre-processed, and international experts interpreted 1265 sample sites for the GLC2000 dataset (Mayaux et al., 2006); and 16 international experts have completed an on-screen collection of reference data for 4258 sample sites for the GlobCover validation dataset (Defourny et al., 2011b). All the reference samples collected from different sources were used to validate various land cover classes including forest, water, and cropland and vary in their classification schemes. Consequently, very limited number of samples were collected to assess the cropland class in different region. When large area cropland maps are assessed with extremely limited reference data, inconsistent accuracy measures were observed for different cropland regions (Foody, 2002; Foody and Boyd, 2013; Waldner et al., 2015).

However, a few large global reference datasets (e.g., FAO-GFRA (Food and Agriculture Organization Global Forest Resources Assessment), GOFC-GOLD (Global Observation for Forest Cover and Land Dynamics), and Geo-wiki) have been developed to perform the assessment of global land cover maps (Fritz et al., 2009b; Olofsson et al., 2012). These datasets were collected over large areas with the expectation that they would continue to be augmented and used for a variety of global map assessments (Olofsson et al., 2012; Stehman et al., 2012). Despite the efforts put into generating these reference datasets and the scarcity of other reference data, their use has been mainly limited to the original intended use and only a few studies reported re-using these datasets for other uses (Göhmann et al., 2009). Currently, there is no assessment providing information on how these datasets can be used beyond their original scope and what the implications would be for specific user applications having different requirements for a land cover map and its assessment. Consequently, the efficient use of these few global datasets remains

questionable for assessing the current and future cropland maps developed at different spatial resolutions. More work must be done to create additional global cropland reference datasets.

Any future cropland reference dataset can be collected either from the ground-based field visits or non-ground-based sources using augmentation and extension approaches. Ground collected information is considered as the best quality reference data compared to other sources. However, ground reference data is expensive, labor and time consuming, and unable to be collected in some parts of the globe due to inaccessible terrain conditions. In this situation, volunteer-based Geo-Wiki, Virtual interpretation of earth web-interface tool (View-IT), degree confluence points, existing cropland maps, and Google Street View may provide an effective and inexpensive way of collecting potentially useful cropland reference data (Fritz et al., 2009b; Clark and Aide, 2011). In addition, the interpretation and classification of HRI with an adequate temporal resolution might serve as high quality reference data to classify and assess the cropland extent and crop type maps (Congalton and Green, 2009). However, the suitability of the reference data collected from different sources varies in their quality and accessibility. Therefore, non-ground-based sources (e.g., classification of HRI, Google street view) must be evaluated for their potential use of collecting sufficient cropland reference data for creating and assessing global cropland products.

Finally, the assessment of the thematic maps is required to be reported in the form of an error matrix which is the most common way of expressing meaningful and informative accuracy measures (Congalton and Green, 2009; Comber et al., 2012). A global summary of the accuracy measures including kappa, total accuracy, user's accuracy and producer's accuracy can be calculated from this error matrix (Story and Congalton, 1986; Congalton, 1991). While the standard individual accuracy measures are reported in the error matrix, there are few related

limitations associated with the error summary represented in the error matrix: invalid and inappropriate accuracy measures for low cropland proportion regions where regional errors may be much larger or smaller than the overall omission and commission errors and no description on the regional differences in the overall accuracy measures (Foody, 2002). Therefore, region specific accuracy measures are required to be generated for different cropland proportion regions to provide more detailed user's and producer's accuracy.

Uncertainty Analysis of Global Cropland Extent Maps

Many studies have compared existing cropland maps of different spatial resolutions with each other and/or with statistical survey information to analyze their uncertainty for choosing an appropriate one for specific user requirements (Latifovic et al., 2004; Giri et al., 2005; Fritz and See, 2005; Neumann et al., 2007; Herold et al., 2008; Fritz et al., 2010; Ran et al., 2010; Kaptué Tchuenté et al., 2011; Pérez-Hoyos et al., 2012; Vancutsem et al., 2013; and Kuenzer et al., 2014). These comparative studies have identified discrepancies and inconsistencies in the crop area estimates and disagreement in their spatial extent when compared with each other and the reference data. The differences in these maps could be a function of many different factors including differences in classification methodology, the imagery used, the date of the imagery, and the classification scheme used. It is, therefore, not possible to conclusively determine if the disagreement and uncertainty in cropland maps is real or just a result of one or more of these many other factors. Despite identifying spatial discrepancies and inconsistencies, particularly in the cropland class over large geographic regions, these comparison studies have not focused on the adequacy of different spatial resolutions for mapping agriculture fields of varying sizes (See et al.,

2013). The uncertainties in the cropland map class for different spatial resolution maps could be due to: (1) errors in the precise spatial location of the cropped areas, (2) the coarse resolution of the map products with significant uncertainties in areas, locations, and detail, and (3) invalid assessments of these cropland extent maps. However, with recent high spatial resolution cropland mapping efforts, the uncertainties in cropland areas have been reduced and therefore should be analyzed from comparison with these other coarser resolution maps.

The uncertainty of different resolution cropland maps is usually performed by comparing the cropland definitions and areas using an overlap comparison method. The overlap (i.e., pixel-by-pixel) comparison method accounts for the differences in class definitions between the cropland maps by using a legend translation or cross-walk between the map classes to establish a one-to-one relationship for an error analysis of the cropland areas (Fritz and See, 2008). Two different approaches have been considered in the past for legend translation: (1) a Boolean approach and (2) a fuzzy set theory approach in which the Land Cover Classification System (LCCS) acts as a general bridging system (Fritz and See, 2005). The Boolean or crisp approach has been used to match the legend categories in different maps using an overlap method based on pixel by pixel basis. The fuzzy approach served to highlight the consistency of the land cover maps under consideration, especially for datasets that showed higher divergences. However, a Boolean approach minimizes part of the uncertainty introduced by ambiguity of legends and results in an overall increase of agreement of around 10% in absolute terms while comparing different pixel-based cropland maps developed at different spatial resolution with each other. Therefore, different resolution cropland maps must be cross-walked and resampled to bring them to a comparable resolution and map classes for implying a Boolean-based comparison.

Once the cropland maps are resampled to a comparable resolution and the map classes reconciled, three measures of comparison based on the class labels can be implemented as: (1) agreement and disagreement, (2) area similarities between map classes as similarity in area proportions, and (3) clumping of the cropland patches as similarity of landscape metrics. The pixels with the same map class in both maps retain their class values as agreement, whereas pixels with different map class were labeled as areas of disagreement. These agreement and disagreement maps show the areas of commission and omission error in one cropland map as compared to the other. In addition, the similarities in the characteristics of agriculture landscapes (e.g., crop area proportions and landscape metrics) observed at different resolutions can also be used to predict the suitability of cropland extent maps in different agriculture field sizes for different continents (Frohn, 1997). This area-based comparative analysis can be effectively implemented by using a similarity matrix. This approach is based on a contingency table or error matrix and categorizes the landscape metrics such as landscape proportion for different agriculture field sizes (Sun et al., 2018). The percent of cropland areas omitted and committed to the coarse-resolution cropland extent maps due to the change in the pixel size can be estimated as omission and commission errors in the cropland map of different regions. The spatial distribution of classification errors is related to some of the explanatory variables associated with landscape characteristics. Stehman et al., (2003) used a logistic regression model to assess the impact of patch size and local heterogeneity on per pixel classification accuracy. The clumping of the cropland patches (i.e., Per Patch Unit) characteristic of the cropland landscape experiences changes at different spatial resolutions and field sizes due to fragmentation of the large cropland patches at a smaller pixel size. The clumping of the cropland areas decreases with increasing spatial resolution, as the landscape becomes more

generalized and aggregated from high-resolution to low-resolution cropland extent maps (Frohn, 1997). Therefore, the variations observed in the area proportion and clumping of the cropland landscape are very crucial for determining the similarity among the three crop extent maps in different agriculture field sizes. Based on the similarities and differences of cropland areas and extent within small regions distributed within different field sizes, specific recommendations can be established for when to apply the three different cropland extent maps in different agriculture landscapes of different continents.

Sampling Strategies for Collecting Reference Data

Limited and sparsely distributed cropland extent and crop type reference data have been used to generate cropland extent and crop type maps for large geographic regions. Any large area cropland reference data are required to be collected from ground-based or non-ground-based sources of cropland information. The cropland information collected from field surveys are limited due to time, cost, and accessibility in different parts of the world. Additional non-ground-based sources must be effectively used to collect cropland reference data and augment or extend the crop type reference data to every region for large area mapping. To collect valid reference data for the accuracy assessment of cropland maps, a sampling protocol must be designed to select a sample of reference locations at which the reference classification can be compared with the map classification (Congalton, 1991; Stehman,1999, Congalton and Green, 2009). The sampling protocol depends on the sampling unit, sample size, and sampling strategy that must be defined to collect reference samples for classification and assessment. The sampling unit is the fundamental unit on which the accuracy assessment is based; it is the link between a spatial location on the map

and the corresponding spatial location on the earth (Stehman and Czaplewski,1998). A sampling unit can be a pixel, a group of pixels, or a polygon. The choice of sampling units must be based on the classification approach. When the reference units are collected for assessing a pixel based coarse or moderate spatial resolution map, a 3x3 grouping of pixels must be used for collecting the reference classification in order to compensate for positional accuracy. Various sized polygons can be used as reference units to assess the cropland map developed with polygons depending on the project objectives and the spatial resolution of the imagery.

The approach to assess the cropland maps of different continents must include an appropriate sampling design and sample size. Many researchers have expressed opinions on using different sampling designs (e.g., simple random sampling, stratified, and systematic unaligned sampling) to be used for assessing thematic map accuracy (Congalton, 1991; Stehman, 1999; Congalton and Green, 2009). While different sampling approaches have been studied for achieving appropriate accuracy results in different landscapes, their effective use still needs to be established for various cropland regions around the world (Bayas et al., 2017). The probability-based, simple random sampling (SRS) design, while statistically valid and easy to implement for large area assessments, could result in insufficient sample sizes for the rare cropland map class because each sample area has equal probability of selection. Therefore, an alternate probability-based sampling design imposed within strata defined by the map classes combined with a predetermined minimum sample size is one method to provide sufficient samples and useful accuracy measures of these rare cropland maps (Stehman, 1999; Olofsson et al., 2014).

Bayas et al., (2017) has suggested that a larger sample size be implemented for assessing cropland regions that have between 25-75% cropland and that a smaller sample size would be

enough to efficiently assess the cropland maps in areas with very high or very low cropland proportion. However, in most cropland assessments, mostly small samples sizes that are sparsely distributed have been used for the entire map resulting in an ineffective assessment of the cropland extent maps of various cropland regions (e.g., Fritz et al., 2009a; Gong et al., 2013). A larger sample size is necessary to achieve more appropriate and valid assessments of the cropland extent maps (Tsendbazar et al., 2015). However, even a larger total sample size can result in insufficient samples and ineffective accuracies of the rare cropland map class if the samples are not distributed effectively. Rather than selecting sample size and strategy by the map complexity, the cropland distribution and proportion of each cropland region must be carefully considered to choose an optimum sample size to efficiently assess the cropland extent maps. The optimum sample size is the one where the accuracy reaches plateau and do not increase with addition of more samples. Therefore, an optimum sample size must be chosen using a sample simulation analysis based on a Monte Carlo method for an effective and useful assessment of the cropland extent maps of various cropland regions (Hay, 1979; Congalton, 1988; Yadav and Congalton, 2018a).

Object-Based Image Analysis (OBIA) of High-spatial Resolution Imagery (HRI)

With an increasing demand of spatially detailed crop type maps, many researchers have recognized the potential of high-resolution imagery (HRI) such as Ikonos, Quick Bird, World-View, and Rapid Eye in mapping cropland products (e.g., crop types) (Castillezo-Gonzalez et al., 2009; Conrad et al., 2014). Crop type identification has become more detailed and accurate at a smaller pixel size which acts to remove the spectral mixing that is common for moderate and coarse resolution pixels (De Wit and Clevers, 2004; Palchowdhuri et al., 2018). Single date multi-spectral

imagery is often used for crop type mapping, but many researchers have recognized the benefits of using multi-date imagery within a given year to map agriculture crops (Ehrlich et al., 1994; Panigrahy and Sharma, 1997; Simonneaux et al., 2008). Huang et al., (2014) emphasized the importance of exploring temporal information, as some crops (e.g., corn) are often grown in rotation with other crops (e.g., winter wheat and paddy rice). Zhong et al., (2014) and Li et al., (2014) observed that interannual differences in image quality and crop growing stages often lead to error when only spectral features are used, remarking that error rates can be significantly reduced by also using phenological parameters. The inclusion of phenological information of crops may guarantee the separaibility of different crop type classes grown in different growing seasons of the same year. Consequently, the cropland mapping methods applied to multi-date HRI have proven to perform better than single-date mapping methods (Long et al., 2013; Gómez et al., 2016) and offers more opportunities to generate crop type maps of different cropland regions (Castillejo-González et al., 2009; Conrad et al., 2014). The high spatial, spectral, and temporal resolution satellite images taken over the growing season provide additional details to capture crop characteristics even in complex cropping patterns. Therefore, the classification of HRI could possibly be used as non-ground-based sources for collecting an efficient, high-quality, consistent, and sufficient crop type reference data required to generate and assess large area crop type maps.

The classification of satellite images began with the visual interpretation and has progressed to the current digital, computer-based processing. In computer-based classification, there are generally two ways to classify an image: the traditional pixel-based approach and the Object based Image Analysis (OBIA) approach. Pixel-based methods have been dominating the analysis of remote sensing images since its beginning. There are various studies dedicated to cropland

mapping at pixel level using supervised or unsupervised algorithms focused on the classification of multi-date high resolution images (e.g., Arvor et al., 2011; Petitjean et al., 2012b; Yan and Roy, 2015). Petitjean et al., (2012b) argue that the increasing spatial resolution of satellite imagery, creates the possibility of applying object-based image analysis (OBIA) to extract crop types from multi-date images. Object-based approaches tend to be advantageous with high resolution images because these significantly increase the within-class spectral variability and, therefore, decrease the statistical separability between classes with traditional pixel-based classification approaches (Blaschke et al., 2014).

Laliberte et al., (2004) mentioned that much information is contained in the relationship between adjacent pixels, including texture and shape information, which allows for identification of individual objects as opposed to single pixels, coming closer to the way humans interpret information. OBIA is a new approach which coincides well with the human perception and the way we extract information from visual impression (Blaschke et al., 2007; Blaschke and Strobl, 2001; Congalton and Green, 2009). The pixel-based approach classifies each pixel individually without considering other spatial information. The OBIA approach groups contiguous pixels with similar spectral response into segments or polygons (Baatz et al., 2001; Desclee et al., 2006). This process mimics human perception of an image's content which is mainly based on objects and is considered to provide potentially more accuracy than the traditional pixel-based approaches (Warner et al., 1998; Blaschke and Strobl, 2001; Desclee et al., 2006; Congalton and Green, 2009; Vieira et al., 2012; Toscani et al., 2013). In addition to spectral and textual features, image objects allow us to make use of shape features which are not considered in pixel-based approach of classification (Hay et al., 2008; Blaschke, 2010). Consequently, object-based classification

approach is more effectively used than pixel-based for delineating agriculture fields and mapping different crop types using HRI (Castillejo-González et al., 2009; Song et al., 2017; Lebourgeois et al., 2017; Belgiu and Csilik, 2018).

OBIA is an iterative method that starts with the segmentation of satellite imagery into homogeneous and contiguous image segments (also called image objects) (Blaschke, 2010). The resulting image objects are then assigned to the target classes using supervised or unsupervised classification algorithms. The OBIA approach groups contiguous pixels with similar spectral response into segments or polygons (Baatz et al., 2001; Desclee et al., 2006). Regarding suitable segmentation algorithms, a variety of alternatives exist (Dey et al., 2010). All algorithms have advantages and disadvantages, and there is no perfect segmentation algorithm for defining object boundaries (Munoz et al., 2003; Forster et al., 2010; Yan et al., 2014). Many scientific studies rely on the Multiresolution Segmentation algorithm (Baatz and Schäpe, 2000; Blaschke, 2010; Liu and Xia, 2010; Stumpf and Kerle, 2011; Dronova et al., 2011; Myint et al., 2011; Peña-Barragán et al., 2011; Vieira et al., 2012; Taşdemir et al., 2012; Long et al., 2013; Pena et al., 2014). This algorithm starts with one-pixel image segments, and merges neighboring segments together until a heterogeneity threshold is reached (Benz et al., 2004). Using OBIA, the main problem relates to the fine-tuning of segmentation parameters (Peña-Barragán et al., 2011; Vieira et al., 2012; Duro et al., 2012). Only well-chosen segmentation parameters ensure good segmentation results. Manually defining the suitable segmentation parameters can be a time-consuming approach, necessarily leads to optimum results for the classification of different crop types in different agriculture field size regions.

Object-based image classification approach integrates textural features, which describe spatial and structural attributes of crops at image object level. However, conventional supervised classifiers (e.g., maximum likelihood method) are inefficient for determining the separability of a large volume of features (such as spectral, temporal, texture and vegetation indices) at an object-level under complex cropping conditions. Recently developed nonparametric machine learning algorithms (e.g., Decision Tree (DT) (Friedl and Brodley, 1997; Shao and Lunetta, 2012), Random Forest (RF) (e.g. Akar and Gungor, 2018; Song et al., 2017; Tatsumi et al., 2015), and Rule-Based Classification (RBC) (e.g. Schlager et al., 2013)) provide effective tools to identify different crop type classes, as they are not constrained by the assumption that the input parameters are normally distributed (Breiman, 2001; Mathur and Foody, 2008; Tatsumi et al., 2015). The non-parametric phenology-based classifier (e.g., decision tree and random forest) can handle an information class (e.g., crop) with multiple sub-classes (e.g., crop types) to accommodate the intra-class variability at multiple places. The classification algorithms based on multi-dates spectral characteristics (i.e., phenology-based) combined with the OBIA are very effective for mapping cropland products using high spatial resolution imagery (Arvor et al., 2011; Long et al., 2013; Muller et al., 2015; Gómez et al., 2016; Palchowdhuri et al., 2018).

Random Forest classifier has been given increasing attention with regards to crop mapping (Ok et al., 2012; Sonobe et al., 2012; Fletcher et al., 2016). The random forest algorithm has the potential to incorporate multiple spectral and texture variables to discriminate different crop types and improve the classification performance (Lawrence et al., 2006; Oliveira et al., 2012). The RF classifier has been proven to be stable and relatively efficient to yield overall accuracy levels that are either comparable to or better than other classifiers such as decision trees, neural networks and

SVM (Duro et al., 2012). Additionally, RF can not only deal with a large volume of spectral, temporal and texture features (even those that are highly correlated), but it can also measure feature importance and enable automatic generation of a structured knowledge, which may be a promising method for crop classification when using high spatial resolution images. Therefore, the performance of a combination of RF approaches with object-based image analysis for crop mapping has garnered much attention (Duro et al., 2012, Vieira et al., 2012, Lebourgeois et al., 2017).

The rule-based classification algorithm is another example that uses a spectral or texture condition to assign the crop and no-crop class. This algorithm allows the analyst to combine different features of objects to assign a class membership degree (between 0 and 1) to each object based on a fuzzy membership function or strict thresholds (Walker et al., 2008; Benz et al., 2004). It has a hierarchical capability to classify the entire scene into general classes (e.g., vegetation and non-vegetation areas). These general classes are called parent classes. Then, each parent class is divided to sub classes (child class) containing more detailed land cover types (e.g., crop types). This hierarchical capability allows the developer to incorporate objects in different levels of segmentation for individual levels of class hierarchy. Therefore, phenology-based classification algorithms (e.g., RBC, DT, RF) can be effectively used to generate crop reference data based on the spectral characteristics of different crop types derived from multi dates of HRI.

CHAPTER III

ISSUES WITH LARGE AREA THEMATIC ACCURACY ASSESSMENT FOR MAPPING CROPLAND EXTENT: A TALE OF THREE CONTINENTS

Abstract

Accurate, consistent and timely cropland information over large areas is critical to solve food security issues. To predict and respond to food insecurity, global cropland products are readily available from coarse and medium spatial resolution earth observation data. However, while the use of satellite imagery has great potential to identify cropland areas and their specific types, the full potential of this imagery has yet to be realized due to variability of croplands in different regions. Despite recent calls for statistically robust and transparent accuracy assessment, more attention regarding the accuracy assessment of large area cropland maps is still needed. To conduct a valid assessment of cropland maps, different strategies, issues and constraints need to be addressed depending upon various conditions present in each continent. This study specifically focused on dealing with some specific issues encountered when assessing the cropland extent of North America (confined to the United States), Africa and Australia. The process of accuracy assessment was performed using a simple random sampling design employed within defined strata (i.e., Agro-Ecological Zones (AEZ's) for the US and Africa and a buffer zone approach around the cropland areas of Australia. Continent-specific sample analysis was performed to ensure that an appropriate reference data set was used to generate a valid error matrix indicative of the actual cropland proportion. Each accuracy assessment was performed within the homogenous regions (i.e., strata) of different continents using different sources of reference data to produce rigorous

and valid accuracy results. The results indicate that continent-specific modified assessments performed for the three selected continents demonstrate that the accuracy assessment can be easily accomplished for a large area such as the US that has extensive availability of reference data while more modifications were needed in the sampling design for other continents that had little to no reference data and other constraints. Each continent provided its own unique challenges and opportunities. Therefore, this paper describes a tale of these three continents providing recommendations to adapt accuracy assessment strategies and methodologies for validating global cropland extent maps.

Introduction

Accurate and consistent cropland information is crucial to answer the issues of global food security to make future policy, investment and logistical decisions (Fritz and See, 2008; Husak et al., 2008; Pflugmacher et al., 2011; Olofsson et al. 2012; Thenkabail and Wu, 2012; Giri et al., 2013). Global cropland mapping provides baseline cropland information to accurately assess the drivers and implications of cropland dynamics both at regional and global scale (Fritz et al., 2013; Grekousis, et al., 2015; Foody, 2015). To predict and respond to food insecurity, global cropland products are readily available from coarse and medium spatial resolution earth observation data. Therefore, remote sensing has been recognized as an extremely effective, economical and feasible approach to create cropland thematic maps over a range of spatial and temporal scales (Barrett and Curtis, 1992; Wu et al., 2008; Gallego et al., 2014).

Cropland maps such as Global Map of Irrigation Areas (GMIA), Global Map of Rain-fed Areas (GMRCA) (Thenkabail et al., 2009), Global Monthly Irrigated and Rain-fed Crop Areas

(MIRCA2000) (Portmann et al., 2010), Global Rain-fed, Irrigated and Paddy Croplands (GRIPC) (Salmon et al., 2015) and MODIS-Cropland (Pittman et al., 2010) derived from coarse-resolution satellite data are currently some of the main sources of cropland information on a global scale. However, these types of products either have insufficient accuracy or their resolution is too coarse for use in other than global applications (Fritz et al., 2013). More recently, with advances in remotely sensed imagery and classification algorithms implemented on cloud computing platforms such as Google Earth Engine, cropland products are available at higher spatial resolutions. For example, global cropland products were generated at 250 m spatial resolution by the NASA MEaSURES (Making Earth System Data Records for Use in Research Environments) GFSAD (Global Food Security Data Analysis) project (Massey et al., 2017a; Xiong et al., 2017a; Teluguntla et al., 2017a).

Previously, accuracy assessments performed on most global cropland extent maps were conducted to produce a single global accuracy measure (i.e., overall accuracy) without regard to continental or regional differences (Foody, 2002; Tsendbazar et al., 2015). These measures could then be used to make a statement about the overall accuracy of the global map, but not about specific continents or regions (Congalton and Green, 2009). The accuracy of a specific continent or region could only be determined if an assessment was done for that area. Insufficient availability of reference data in most regions of the world along with significant variations in agricultural landscape patterns offers unique challenges to conduct a more detailed accuracy assessment of any global mapping product. The reference data required to perform the assessment over large area cropland maps are not uniformly available for all the continents. For instance, some of the continents have extensive reference data available for assessment (such as US and Canada) while

other continents (such as Africa) have very little to none. Additionally, mapping in some continents exhibits larger errors than others simply depending on the complexity of the agriculture landscapes (DeGloria et al., 2000; Ung et al., 2000). For example, it has been reported that an accurate map is difficult to achieve in developing countries with small holder agricultural landscape by the International Food Policy Research Institute (IFPRI) (Fritz et al., 2015). Therefore, most of the global assessments have not attempted to provide a more regionalized measure of accuracy encompassing continents/regions or different agriculture landscapes (Strahler et al., 2006).

Clearly, a single accuracy estimate will not provide a holistic view of the ability to map variation within the agriculture landscapes of different continents. However, these continental variations could be reported by assessing the map accuracy in response to different issues observed in the cropland maps of different continents (Congalton, 1991; Congalton and Green, 1999; Foody, 2002; Foody, 2005). Therefore, a continent-based assessment strategy will provide more intensive evaluation of the cropland maps in agriculture landscapes for different continents. This kind of intense and efficient assessment strategy for different continents will also help to understand the efficacy, quality and variations of large area cropland maps (Wardlow and Egbert, 2008). Therefore, the question is how to implement such a continent-based assessment strategy effectively for each continent while also considering the different kinds of issues and constraints related to both reference data availability and complexity of agriculture landscapes.

While individual measures of accuracy are well established in literature (e.g., Congalton, 1991; Stehman, 1997; Congalton and Green, 1999), considerable ambiguity remains about the implementation and interpretation of accuracy assessment for large areas. The most widely accepted approach to perform an accuracy assessment is through the use of an error matrix

(Congalton, 1991). The error matrix is a cross tabulation of the class labels predicted by the image classification against that observed from the reference dataset. The key issue in generating a valid error matrix is the collection of sufficient and appropriate reference data. The collection of such data must be conducted using an appropriate sampling scheme with sufficient samples in consideration of the complexities of the area being mapped (Congalton and Green, 2009).

In order to conduct a detailed continent-based assessment of cropland extent maps generated in the GFSAD project, it was important to consider how the mapping was performed in each continent. The cropland extent maps for each continent were created by dividing the area into homogeneous regions (i.e., stratification) rather than just producing a single map of the entire continent. As a result, the accuracy assessment was also performed within these homogeneous areas using traditional assessment methods with modified sampling designs for collecting reference data depending on the agriculture landscapes in each continent (Congalton and Green, 1999; Foody, 2002). Such modified sampling designs for collecting reference data ensured an optimum sampling approach considering different agriculture landscapes in each continent. Therefore, continent-based accuracy assessment of the cropland maps generated in GFSAD project was conducted by continent in response to different issues and constraints observed in the cropland extent maps.

The goal of this research is to provide specific approaches and recommendations for modifying existing accuracy assessment strategies and methodologies to validate global cropland extent maps considering the issues and constraints unique to each continent. Meaningful and statistically valid assessment results demonstrate that these methods and approaches contribute a better understanding of global cropland distribution by continent. This work is specifically focused on

dealing with unique issues encountered when assessing cropland extent for North America (confined to the USA), Africa and Australia. These three continents were selected as a representative of different cropping patterns with variable size agriculture fields and availability of reference data. Lessons learned from this work can be further extended to other continents to provide appropriate methods of accuracy assessment where different scenarios of reference data availability and agriculture landscapes exist. The approach of stratifying the continents based on Agro-Ecological Zones (AEZ's) for the US and Africa provided rigorous and valid accuracy results (Foody, 2005). The buffer-based stratification approach used in Australia also provides an alternative methodology for when crops are clustered only in certain areas of the continent and are not appropriately represented by AEZ's.

Study Area

The study area for this paper includes three continents (i.e., North America (confined to United States), Africa and Australia) where a wide variety of climate, topography, moisture and crop growing periods prevail due to the large size, range of geographic features and non-contiguous arrangement of homogeneous agriculture landscapes (Ramankutty et al., 2008) (Figure 1). For North America, the United States (US) was chosen as a representative of the continent. This assumption is appropriate here as the issues and constraints found in the US also hold for Canada and Mexico. For the other two continents, the entire continent has been assessed. Food and Agriculture Organization (FAO) Agro-Ecological Zones (AEZ's) that are defined by the length of the growing period days derived from temperature, precipitation and soil water holding capacity were used to stratify both the US and Africa (Fischer et al., 2012). Both the mapping and the

accuracy assessment were performed within these homogeneous areas (AEZ's). However, this AEZ-based stratification method resulted in more fragmented zones when applied to Australia because of a single, large area in the center of the continent having low probability of cropland. Therefore, a different and more effective stratification method (i.e., buffering approach) was used instead to define an appropriate sampling area around the cropland patches for the Australian continent.

The US is composed mostly of large, agriculturally homogeneous regions and large area farming is prevalent due to abundant land availability (Ramankutty et al., 2008). The cropland areas are roughly concentrated in the central regions of the US; pastures are in the more arid west; and forest land in the East, where the topography and precipitation patterns are conducive to growing trees (USDA, Economic Research, 2012). Dominant crops such as corn and soybeans are grown in large, homogeneous, agriculture fields. In contrast, there are some heterogeneous regions in the US that grow rare crops and have a high diversity of crop types. All of these crop areas along with their specific types have been regularly mapped by USDA-NASS (i.e., United States Department of Agriculture-National Agricultural Statistics Service) every year since 2009 for all 48 conterminous states with a 30 m pixel resolution (Boryan et al., 2011). Before 2009, cropland was mapped at 56 m spatial resolution. All these data are readily available in a database called the Cropland Database Layer (CDL) and can be used as reference data for other mapping efforts including the GFSAD project. Therefore, in the US, assessing cropland maps is much easier than any other part of the world.

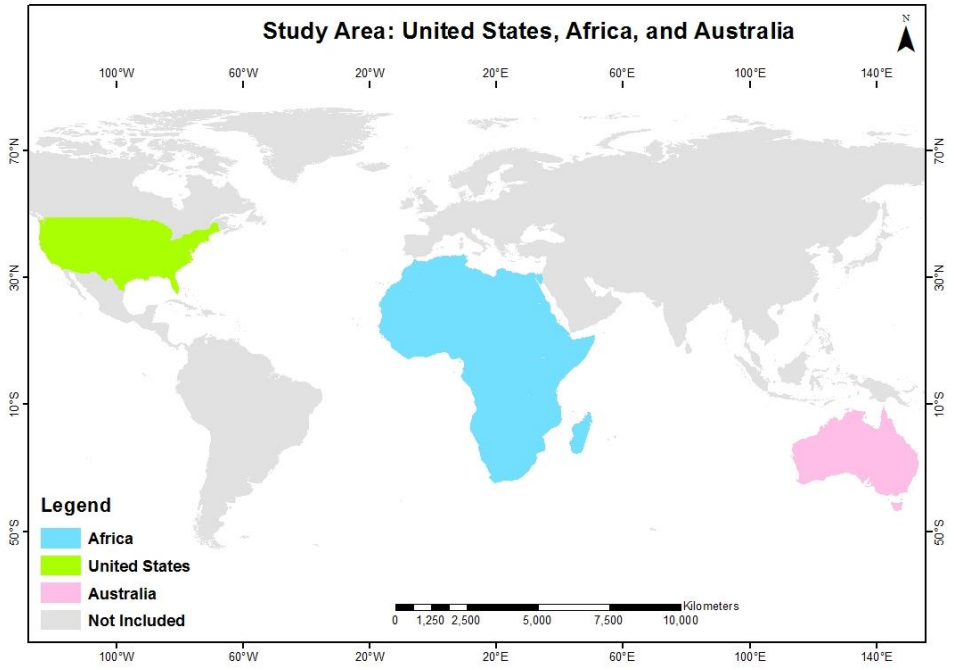

Figure 1. Map showing the location of three selected continents and their respective homogeneous regions such as Agro-ecological zones (AEZs) and crop buffer.

Africa has more scattered cropland distribution than any other cropping region of the world. The variation between AEZ's in Africa is large, ranging from the dry and barren desert, through the rich soil of the Rift, Nile and Niger River Valleys, to the southern extremes. However, unlike any other parts of the world, there are no large crop belts in Africa. Rather, there are agricultural regions within which different combinations of crops are cultivated (Ramankutty et al., 2008).

Australia closely resembles other temperate regions of the world. Wheat is the dominant crop in Australia; it is interrupted only briefly by a combination of wheat and barley in the southern part of the continent. In the western portion of the Australian Wheat Belt, pulses are the most prominent secondary crop, while barley is the secondary crop in the eastern portions. Pulses are the third most dominant crop (about 11%) (Leff et al., 2004). However, the total cropland

distribution is restricted to a ring-like region around the edges of the continent. Therefore, to minimize cropland omission and commission errors and to avoid sampling where there was no possibility of finding a crop, the area surrounding the crop patches was chosen for sampling through the use of a buffering approach instead of using AEZ's.

Methods

The typical approach to perform a statistically rigorous thematic accuracy assessment of any map generated from remotely sensed imagery includes collecting reference data and then computing descriptive statistics (Congalton, 1991). This chapter focuses on the accuracy assessment of large area cropland extent maps generated for the entire world. The methods to perform such an accuracy assessment must include the consideration of specific issues, concerns and characteristics for each continent including: (1) the appropriate stratification; (2) the effective and valid collection of reference data; (3) the appropriate sampling; and (4) the application of a descriptive analysis protocol (Figure 2).

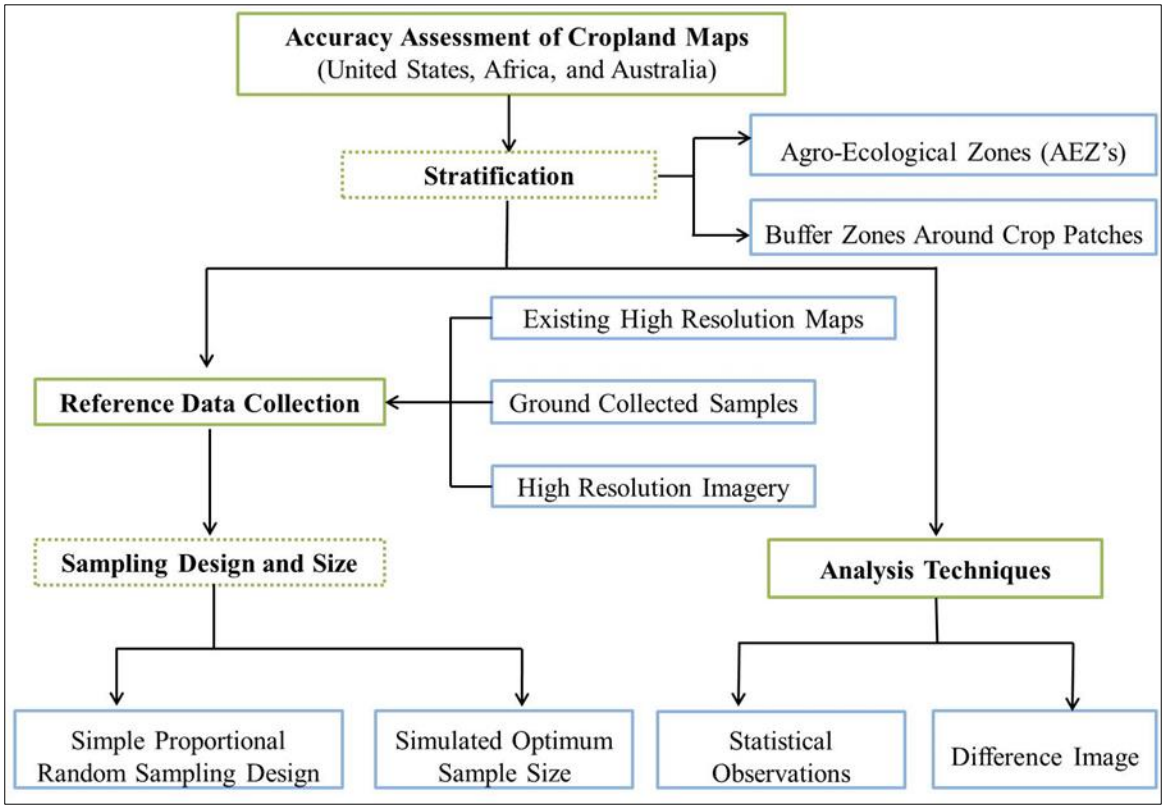

Figure 2. Flowchart of the process used to conduct the continent-based accuracy assessment of the GFSAD mapping products.

Stratification

Continents with diverse cropping patterns are expected to have variations in classification accuracy due to a number of reasons including: these diverse cropping patterns, differences in the classifiers employed to create the maps and the different spatial resolutions of the satellite images used (Shao and Lunetta, 2012; Champagne et al., 2014). It is more likely that low accuracy and confidence levels are achieved in mapping rare classes due to their limited population size (Champagne et al., 2014). When comparing the cropland maps of different continents, it has been shown that high

agreement and consistency in accuracy is associated with areas of no or almost fully covered agricultural classes (Vancutsem et al., 2013). However, the regions with scattered and sparse cropping patterns contained more uncertainty and inconsistency. The issue of variations in different agriculture landscapes must be considered and addressed by modifications to the accuracy assessment strategy. The assessment of cropland maps and reporting the accuracy estimates for homogeneous regions of similar cropping patterns using some type of stratification approach will result in more meaningful, representative and applicable mapping products (Champagne et al., 2014).

There are two advantages of implementing a stratification method while mapping cropland areas and assessing their accuracy. First, implementing a stratification method of dividing a large mapping area into homogeneous regions reduces the extent of the area to be mapped and assessed. The stratification then results in more efficient performance of the classification algorithm in response to the variations of each region and allows for more effective validation (Vancutsem et al., 2012). Secondly, the stratification method also helps to optimize the efforts required to collect a valid and efficient reference dataset required for mapping and assessing the accuracy of the cropland areas (Waldner et al., 2015). The choice of an appropriate stratification method could be either based on the mapped classes or homogeneous zones of different cropping and climatic conditions such as Agro-Ecological Zones (AEZ's) in any particular area of interest (i.e., a continent).

AEZ-based stratification methods were used to divide the study area into more homogeneous regions in previous research such as simulating crop yield potentials (Van Wart et al., 2013), global change assessment (Vittorio et al., 2016) and climate change (Seo, 2014) projects. Therefore,

AEZ-based stratification method will also help to divide different continents into homogeneous regions to implement the assessment strategy required to assess the cropland extent maps (Stehman and Czaplewski, 1998). However, it is difficult to divide sparse cropland regions into homogeneous zones based on AEZ's. In such sparse cropland regions, AEZ-based stratification methods result in more fragmented zones rather than homogeneous ones. Therefore, a more representative stratification method is required to define an appropriate sampling area around the sparse cropland patches (for example, Australia). Upon close examination of the cropland distribution in the three selected continents (i.e., US, Africa and Australia), two stratification methods (i.e., AEZ's and Euclidean distance buffering) were used to divide the continents into zones before assessing the cropland maps. In US and Africa, the cropland extent was stratified using the AEZ approach based on the number of growing period days. In Australia, the cropland distribution is mostly concentrated in a narrow belt towards the edges of the continent leaving a large portion toward the center with a very low likelihood of crops. Therefore, a buffering approach rather that an AEZ approach was used for stratification in Australia.

Collecting Reference Data

The reference data can be sourced either from ground-collected data, or from any existing appropriate reference maps (e.g., USDA CDL), or from interpretation of high-resolution imagery (HRI). However, in many cases, a difference in the classification scheme between the existing reference data and the map to be assessed and/or the size of the sample unit (often too small) can limit the use of any existing reference data (Thenkabail, 2005; Congalton et al., 2014). Therefore, ground collected data are considered as the optimal, yet most expensive, reference data. The timing

of the reference data collection for assessing agricultural maps is also a very important factor. Significant errors can occur when not keeping the reference data collection to as near as possible to the image collection date (Congalton and Green, 2009). It is critical that the reference data be independent of any other data used for training and initial testing of the thematic mapping. Once the independency, timing and source of the reference data are achieved, it is important to choose the appropriate sampling design and sample size.

Upon completion of a thorough search for any readily available reference data for the three continents, an independent source of reference data was generated using an appropriate sampling design in the homogeneous regions for each continent. For example, existing reference maps (e.g., CDL for the US with an accuracy range of 85–95% (Boryan et al., 2011) can be used as reference data to perform the assessment of cropland extent map while ground sampling or interpretation of high-resolution imagery (HRI) might be performed for continents such as Africa with little to no existing reference data. In addition, a field campaign (i.e., ground sampling) usually focuses on collecting the reference data for the map class of interest (in our case, crops). Therefore, to generate a proportionally balanced reference dataset, additional reference samples may need to be interpreted from HRI. In this study, a combination of the three different sources of reference data (i.e., existing reference maps, independent generated random samples and ground collected samples) were ultimately used to assess the cropland extent maps of the three selected continents.

Sampling

Many researchers have published suggestions regarding the proper sampling scheme to use for collecting reference data depending on different regions of interest (e.g., Hord and Brooner, 1976;

Ginevan, 1979). These suggestions vary from simple random sampling to stratified, systematic and other sampling approaches for assessing the accuracy of remotely sensed maps. There are both pros and cons associated with each of these types of sampling schemes. Another study (Stehman, 2009) has proposed the relative strengths and weakness of these different sampling designs based on seven desirable criteria. These criteria are: (1) probability-based; (2) practical implications; (3) cost effectiveness, (4) spatially balanced; (5) precise estimates of class-specific accuracy; (6) ability to estimate standard errors; and (7) flexibility to change the sample size.

Systematic and spatially stratified designs were generally rated as strong on the spatially balanced criterion, whereas the designs stratified by thematic map classes were strong for determining class-specific accuracy. Systematic sampling was usually rated as weak due to non-availability of an unbiased variance estimator. A key issue in sampling is that of randomness such that each sample (in this case, crop and no-crop) has an equal and independent chance of being selected (Congalton and Green, 2009). Given that in this project there were only two map classes, simple random (probability-based) sampling with flexibility to modify the sample size for each continent is the best scheme. Therefore, a simple random sampling design was selected to distribute samples in different agriculture landscapes of the three selected continents to assess the accuracy of the cropland maps.

Once the sampling scheme was selected, then the next question is to decide the size of the sample unit. In literature, a cluster of pixels has been suggested to be used as the sample unit when assessing the accuracy of cropland maps derived from medium resolution imagery. Selecting a homogeneous cluster of 3 × 3 pixels accounts for issues in positional accuracy for maps derived from 30 m or so satellite imagery to ensure that thematic accuracy is being analyzed and not

positional error (Congalton and Green, 2009). However, it is extremely difficult to find a 3 × 3 homogeneous cluster of pixels for coarse resolution satellite imagery (250 m pixels). Therefore, a single pixel sample unit was used to collect reference samples to assess the accuracy of the 250 m cropland maps in the three selected continents.

The most challenging component of assessing the accuracy of a thematic map is collecting enough samples to perform a valid assessment. Different equations and guidelines have been established by many researchers for choosing an appropriate sample size (Hord and Brooner, 1976; Genderen and Lock, 1977; Hay, 1979; Ginevan, 1979; Rosenfield et al., 1982; Congalton, 1988). In the literature, a method based on Monte Carlo simulation (Congalton, 1988) suggested that most thematic maps can be assessed using a sample size of 50 for each mapped class. However, given that the areas to be assessed here (AEZ or buffer zones) are quite large, a sample simulation using the Monte Carlo method was performed to determine the appropriate sample size. Based on the results of the sample simulation, an appropriate sample size was selected for each of the selected continent.

Computing Descriptive Statistics

The last step in an accuracy assessment is the descriptive analysis protocol to report accuracy measures in the form of an error matrix and, in some cases, spatial agreement and disagreement analysis using a difference image. Once an error matrix has been properly generated, it can be used as a starting point to calculate individual class accuracies (i.e., producer's and user's accuracies) in addition to an overall accuracy (Story and Congalton, 1986). The producer's and user's accuracy are often called commission and omission errors, respectively. A commission error is defined as

including an area into a thematic class when it does not belong to that class while an omission error is excluding that area from the thematic map when it belongs to the map. Omission errors can be calculated by dividing the total number of correctly classified sample units in a category by the total number of sample units in that category from the reference data (Story and Congalton, 1986; Congalton, 1991). Commission errors, on the other hand, are calculated by dividing the number of correctly classified sample units for a category by the total number of sample units that were classified in that category (Story and Congalton, 1986; Congalton, 1991; Congalton and Green, 1999).

In addition to these statistical measures, a difference image can also be created by comparing the map with an existing cropland map created by other researchers for each continent and spatially depicting the agreement and disagreement in the map classes. This image can only be generated when there is another thematic map available such as in the US, where reference data sets are available that cover the entire study area. In most areas of the world, these reference maps do not exist, and only limited reference data samples are available.

When the reference map is assumed to be 100% correct, the difference image is used to depict the omission and commission errors that occurred between the two cropland maps. Unless the comparison is being conducted using a reference map, the different image demonstrates similarity between the two maps rather than an omission and commission error. Once the difference image is created, the results can also be shown in a similarity matrix, which is generated in the same way as an error matrix.

Results

The results of the accuracy assessment process that was performed including specific issues and constraints observed in the cropland maps are presented in the following three major components for each of the three selected continents: (1) Stratification: dividing each continent into homogeneous regions; (2) Collecting reference data and sampling design: developing continent specific procedures for effective and valid collection of reference data using an appropriate sampling design; and (3) Accuracy measures: generating error matrices and difference image of spatial agreement using the collected reference data for different continents. The results are presented by continent beginning with the US, then Africa and finally Australia.

United States (US)

The cropland extent map of the US was created by Northern Arizona University (NAU) in NASA MEaSURES's GFSAD project for the year 2008 at 250 m spatial resolution (Massey et al., 2017). An extensive and easily available high-quality reference data set (i.e., USDA CDL) is available at a spatial resolution of 56 m to perform the assessment of this cropland extent map. The availability of such an extensive reference data set (i.e., CDL) and the well-distributed cropland areas in the US make it extremely easy to perform an accuracy assessment. The following sections present the major components of AEZ-based assessment strategy with a modified sampling design that was used to assess the cropland map of the US.

Stratification

The agriculture landscape of the US was stratified or divided into homogeneous regions using an AEZ-based stratification method. The entire US was divided into 13 zones based on the length of growing period days (from 0 to 365 days) using Global Agro-Ecological Zones (GAEZ) layer provided by FAO (Fischer et al., 2012) (Figure 3). AEZ 1 has no likelihood of cropland areas and therefore sampling was not employed in this zone while performing the assessment.

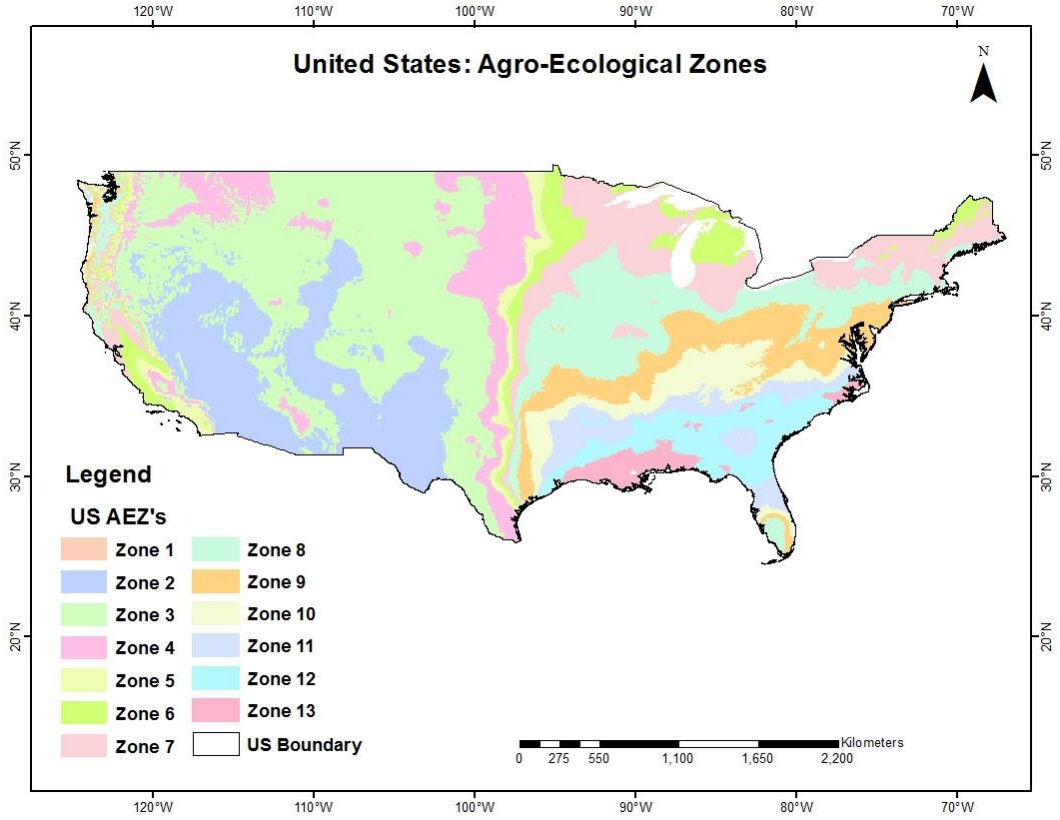

Figure 3. The distribution of Agro-ecological zones in the United States.

Reference Data Collection and Sampling

The reference data for US were samples selected from the CDL (Source: USDA, NASS) for the year 2008. The availability of such an extensive and easily accessible cropland reference dataset made the process of accuracy assessment in the US extremely easy. The samples selected for accuracy where independent of any samples used by the mapping team at NAU to create the cropland map. To perform the assessment of the 250 m cropland map, the CDL (available at https://nassgeodata.gmu.edu/CropScape) was resampled from 56 m to 250 m and the CDL classification scheme was simplified into crop and no-crop classes.

Simple random sampling was implemented in all the AEZ's of the US to perform the accuracy assessment of the cropland extent map. The samples were distributed randomly in each AEZ with a minimum distance of 10 km apart minimizing the spatial autocorrelation that could possibly occur in near-distant samples. An appropriate sample size was selected by sample simulation analysis performed in all the AEZ's. An optimum sample size of 350 was selected when the proportion of crop samples reached a stable level (asymptote) and did not increase further with a further increase in sample size (Figure 4). Figure 4 shows the variability in the proportion of cropland samples as 4-8% increase and decrease from the sample size of 50 to 350 after which it is expected to remain stable in all the zones. Figure 5 shows the distribution of the 350 samples in each of the AEZ in the US.

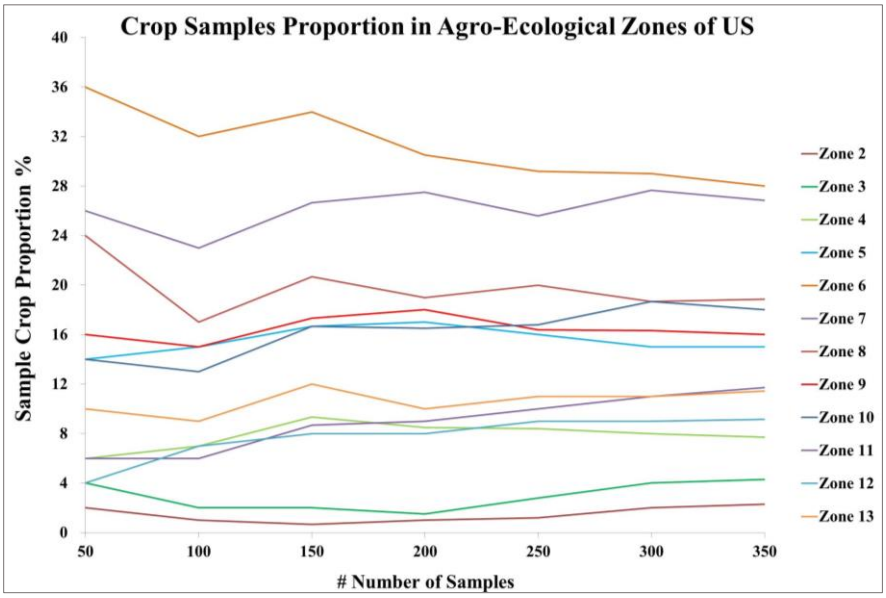

Figure 4. The graphical representation of sample size simulation in AEZ's of the US.

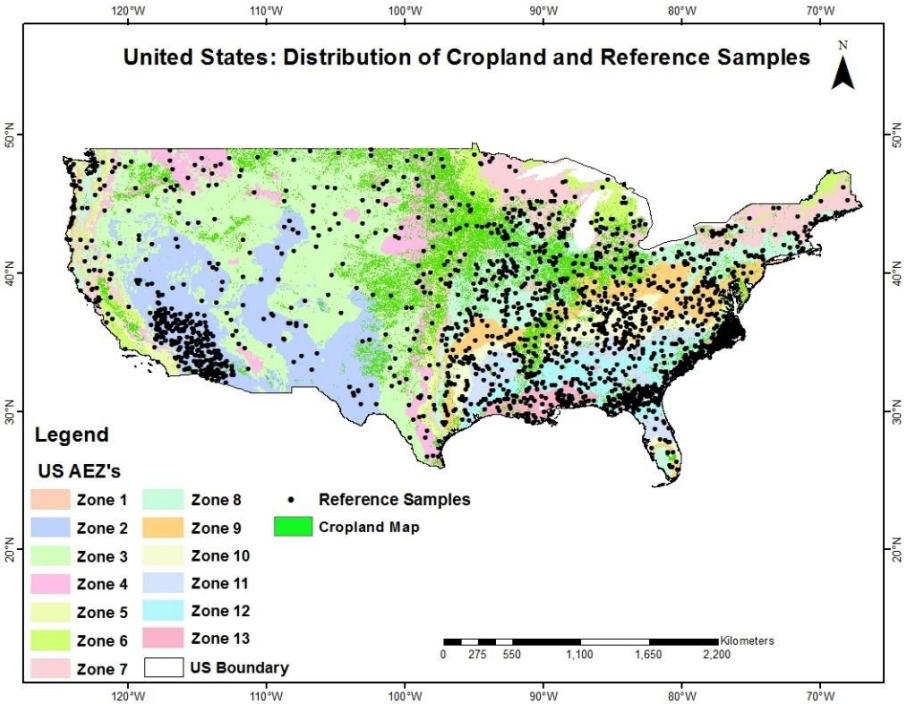

Figure 5. The distribution of randomly generated reference samples within each of the AEZ's of the US.

Computing Accuracy Statistics

Both error matrices and a difference image were generated to report the accuracy measures and spatial distribution of agreement and disagreement respectively in the US. The error matrices were generated for each of the AEZ's separately to present the statistical and quantitative assessment of the cropland map. The accuracy measures including an overall, producer's and user's accuracy of the individual class (i.e., crop and no-crop) have been listed for all the AEZ's in Table 1.

An overall accuracy was also calculated for the entire US in addition to accuracy estimates for each AEZ using the entire validation dataset. The error matrix in Table 2 shows an overall accuracy of 98.0%. There is no misclassification of No-Crop samples into the Crop class on the map. It indicates that there is no commission error in the cropland class on the map. There is only omission error in the cropland extent map (i.e., only some crop areas have been mapped as no-crop) (Table 2).

A difference image (i.e., the spatial map of agreement and disagreement in the crop and no-crop classes) was created to show the spatial distribution of omission and commission errors in the cropland map. The results from the difference image can be presented as a similarity matrix, which is generated the same way as an error matrix. The difference image of the US cropland extent map with CDL showed only 2% omission errors in the map (Figure 6). The difference image in Figure 6 showed a small area of 2% disagreement in the crop class that has been omitted or mapped as no-crop in the map. The agreement in the two maps was depicted by the class labeled as "No-Difference" in Figure 6.

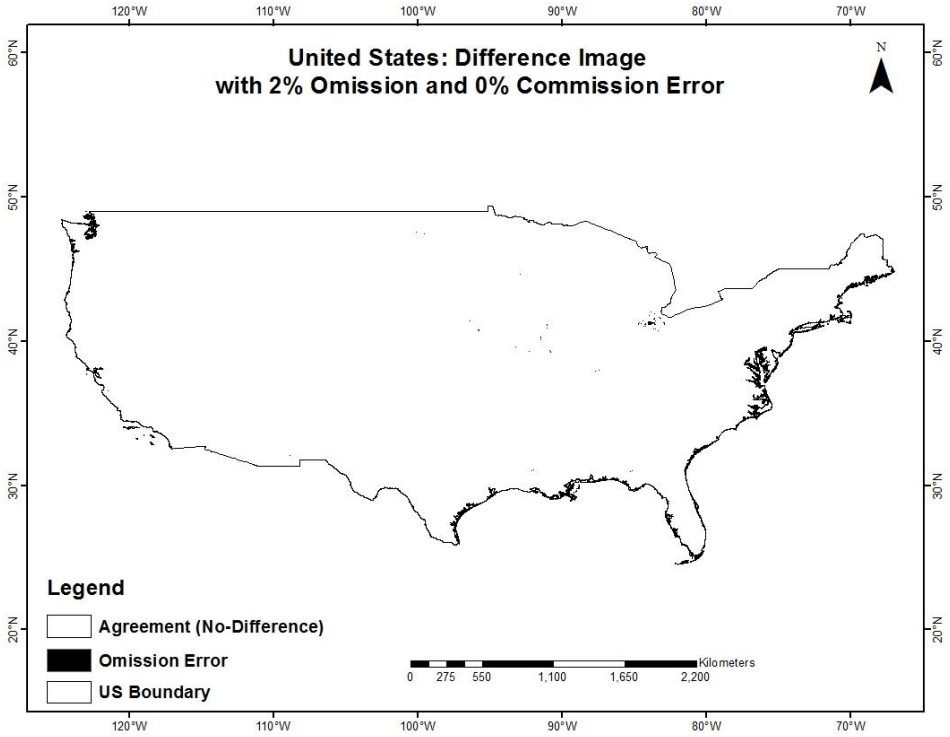

Figure 6. The difference image derived using reference data and cropland map of the US showing 2% Omission and 0% commission error (Massey et al., 2017a).

Table 1. Zone-wise accuracy estimates listed for all the AEZ's of the United States.

Zone	C/C	C/NC	NC/C	NC/NC	RCS	RNCS	MCS	MNCS	PAC	PANC	UAC	UANC	OA
Zone 2	5	1	0	344	6	344	5	345	83.3%	100.0%	100.0%	99.7%	99.7%
Zone 3	14	1	0	335	15	335	14	336	93.3%	100.0%	100.0%	99.7%	99.7%
Zone 4	25	3	0	322	28	322	25	325	89.3%	100.0%	100.0%	99.1%	99.1%
Zone 5	46	11	0	293	57	293	46	304	80.7%	100.0%	100.0%	96.4%	96.9%
Zone 6	89	12	0	249	101	249	89	261	88.1%	100.0%	100.0%	95.4%	96.6%
Zone 7	82	12	0	256	94	256	82	268	87.2%	100.0%	100.0%	95.5%	96.6%
Zone 8	60	6	0	284	66	284	60	290	90.9%	100.0%	100.0%	97.9%	98.3%
Zone 9	53	11	0	286	64	286	53	297	82.8%	100.0%	100.0%	96.3%	96.9%
Zone 10	49	14	0	287	63	287	49	301	77.8%	100.0%	100.0%	95.4%	96.0%
Zone 11	34	7	0	309	41	309	34	316	82.9%	100.0%	100.0%	97.8%	98.0%
Zone 12	30	2	0	318	32	318	30	320	93.8%	100.0%	100.0%	99.4%	99.4%
Zone 13	33	7	0	310	40	310	33	317	82.5%	100.0%	100.0%	97.8%	98.0%

C: Crop; NC: No-Crop; Symbol /: Classified as; RCS: Number of Reference Crop Samples; RNCS: Number of Reference No-Crop Samples; MCS: Number of Map Crop Samples; MNCS: Number of Map No-Crop Samples; PAC: Producer's Accuracy of Crop; UAC: User's Accuracy of Crop; PANC: Producer's Accuracy of No-Crop; UANC: User's Accuracy of No-Crop OA: Overall Accuracy.

Table 2. An overall accuracy matrix for the cropland extent map of US.

All Zones Combined		**Reference Data**			
		Crop	No-Crop	Total	User's Accuracy
Map Data	Crop	520	0	520	100.0%
	No-Crop	87	3593	3680	97.6%
Total		607	3593	4200	
Producer's Accuracy		85.7%	100.0%		**98.0%**

Africa

The cropland extent map of Africa was generated by the USGS team of the NASA MEaSURES's GFSAD project for the year 2014 at 250 m spatial resolution (Xiong et al., 2017a). Upon close examination of the cropland distribution and reference data availability in Africa, some issues and constraints of concern were considered before choosing the stratification method and sampling analysis to assess the cropland maps. These were: (1) the lack of an extensive and easily accessible reference data and (2) the scattered distribution of cropland areas throughout the entire continent. Due to non-availability of easily accessible reference data and non-uniform cropland distribution of Africa continent, the basic traditional strategy of accuracy assessment was modified.

Stratification

Like the US, the AEZ-based stratification method (Fischer et al., 2012) was used to divide Africa into 8 homogeneous cropping pattern regions or AEZ's (Figure 7). According to the distribution of cropland area, different growing period days provided by FAO were combined together to create fewer and more reasonable zones. As a result, these combined eight AEZ's were well structured based on the distribution of cropland areas in Africa continent. The AEZ's with less number of growing period days had sparse distribution of cropland as compared to the ones with high number of growing period days. Therefore, the AEZ-based stratification method helped to understand and describe the cropland distribution to perform the assessment of the croplands of Africa. For example, AEZ 1 and 2 have a scattered and sparse cropland distribution and therefore, could be assessed with a lower sample size as compared to other AEZ's with more cropland areas. The stratification method facilitates the process of collecting the reference data and performing the sampling analysis in each AEZ's based on the distribution of cropland areas and results in a more detailed, meaningful and valid accuracy results.

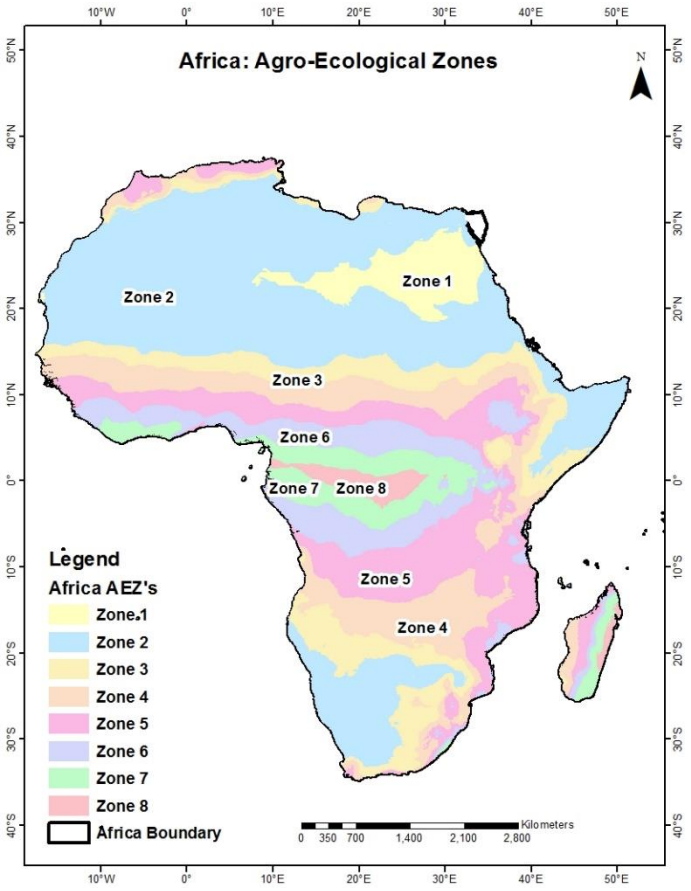

Figure 7. Agro-Ecological Zones (AEZ's) of Africa.

Collecting Reference Data and Sampling Design

Upon completion of a thorough search for reference data availability for the African continent, it was determined that there is a lack of any extensive reference data required to perform the assessment of the cropland map. In addition, ground collected reference data were also limited due to the high costs and effort required to obtain them (Strahler et al., 2006). Therefore, the reference data to perform the accuracy assessment of the cropland map of Africa was obtained from visual interpretation of HRI.

To collect the reference data from HRI, it was necessary to decide on an appropriate sampling design and an optimum sample size for the continent. Samples were distributed randomly using a simple random sampling design to account for the variability in the cropping pattern in all the 8 AEZ's of Africa. The sample size for each AEZ was selected based on a sample simulation analysis performed ranging from a sample size of 50 to 250. A small sample size of 50 was enough for the sparse cropland regions (i.e., AEZ 1 and 2) as compared to other zones where the proportion of crop samples was not stable until a sample size of 250 was obtained (Figure 8). The choice of a less intensive sample size for scarce cropland regions allowed for more sampling effort to be dedicated to areas with more croplands.

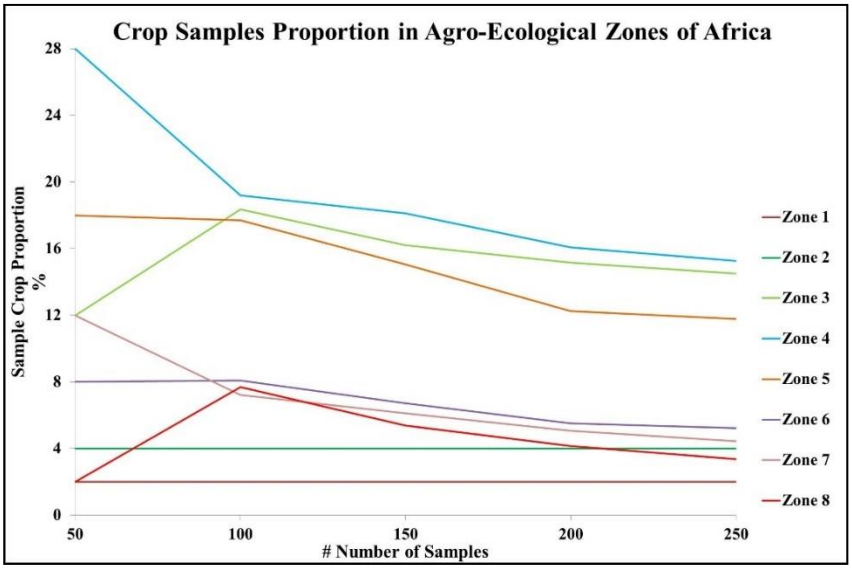

Figure 8. The graph showing the sample simulation in AEZ's of Africa.

Randomly generated reference samples were interpreted using high-resolution imagery by two independent interpreters. The crop and no-crop samples were labeled by interpreting a 250 m ×

250 m homogeneous sample unit on HRI. A sample size of 1600 was used for the overall zone-wise assessment of cropland map of Africa. Only when both interpreters independently agreed on the same map classes were the samples used for assessment. Figure 9 shows the distribution of the 1600 reference samples (2 zones at 50 samples and 6 zones at 250 samples) along with the cropland distribution in all the AEZ's of Africa.

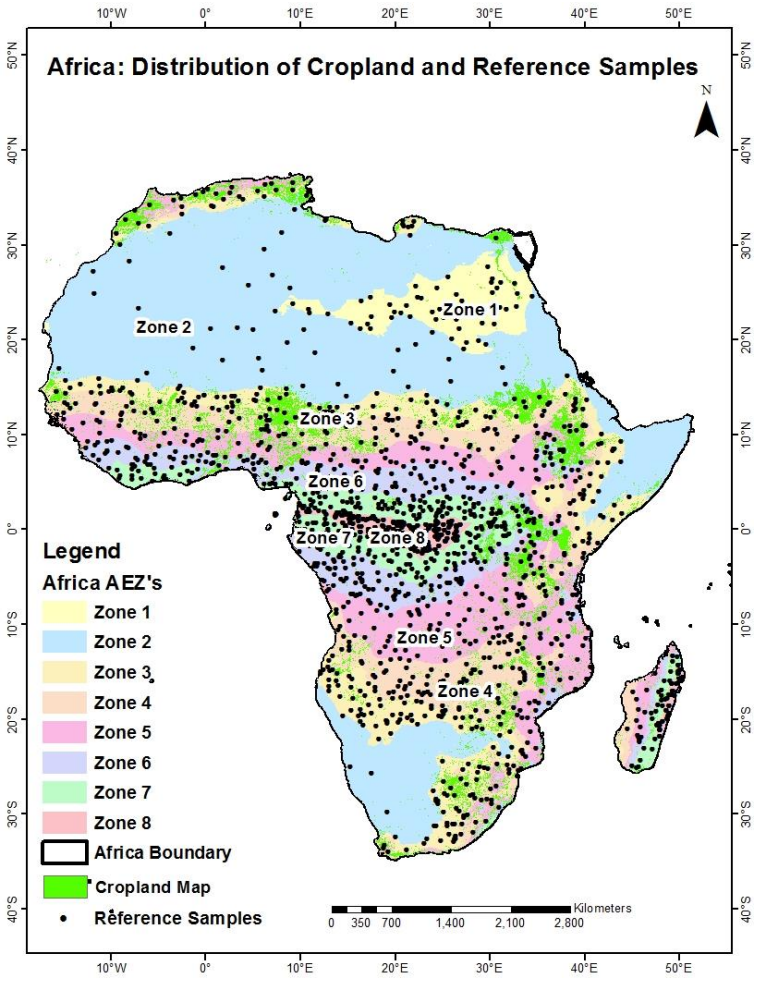

Figure 9. The distribution of Cropland and Reference Samples in Africa.

Computing Accuracy Statistics

Only the error matrices were generated to report the accuracy measures of the cropland extent map of Africa due to non-availability of a reference thematic map required to conduct the spatial comparison of the two maps. An overall accuracy along with user's and producer's accuracy was computed for each AEZ from the error matrices. The comparison of accuracy estimates in all the zones provides knowledge of how much effort, time and costs are required to collect appropriate reference data to perform the accuracy assessment.

Table 3 shows the comparison of the accuracies in all 8 AEZ's. An overall accuracy of 100.0% was achieved using a sample size of 50 in AEZ 1 and 2. AEZ 3–8 used a sample size of 250. The overall accuracies for these six zones (i.e., from AEZ 3–8) ranged from 90.4% to 96.4%. The samples from all the AEZ's were combined to generate an overall accuracy for the entire Africa continent (Table 4).

Table 3. Zone-wise accuracy estimates listed for all the AEZ's in Africa.

Zone	C/C	C/NC	NC/C	NC/NC	RCS	RNCS	MCS	MNCS	PAC	PANC	UAC	UANC	OA
Zone 1	1	0	0	49	1	49	1	49	100.0%	100.0%	100.0%	100.0%	100.0%
Zone 2	2	0	0	48	2	48	2	48	100.0%	100.0%	100.0%	100.0%	100.0%
Zone 3	24	13	11	202	37	213	35	215	64.9%	94.8%	68.60%	94.0%	90.4%
Zone 4	29	12	8	201	41	209	37	213	70.7%	96.2%	78.4%	94.4%	92.0%
Zone 5	14	8	14	214	22	228	28	222	63.6%	93.9%	50.0%	96.4%	91.2%
Zone 6	5	10	7	228	15	235	12	238	33.3%	97.0%	41.7%	95.8%	93.2%
Zone 7	3	4	5	238	7	243	8	242	42.9%	97.9%	37.5%	98.4%	96.4%
Zone 8	4	12	0	234	16	234	4	246	25.0%	100.0%	100.0%	95.1%	95.2%

C: Crop; NC: No-Crop; Symbol /: Classified as; RCS: Number of Reference Crop Samples; RNCS: Number of Reference No-Crop Samples; MCS: Number of Map Crop Samples; MNCS: Number of Map No-Crop Samples; PAC: Producer's Accuracy of Crop; UAC: User's Accuracy

of Crop; PANC: Producer's Accuracy of No-Crop; UANC: User's Accuracy of No-Crop OA: Overall Accuracy.

Table 4. An overall accuracy matrix for the cropland extent map of Africa.

All Zones Combined		**Reference Data**			
		Crop	No-Crop	Total	User's Accuracy
Map Data	Crop	82	45	127	64.6%
	No-Crop	59	1414	1473	96.0%
Total		141	1459	1600	
Producer's Accuracy		58.2%	96.9%		**93.5%**

Australia

The cropland extent map of Australia was created by the USGS team of the NASA MEaSURES's GFSAD project for the year 2014 at 250 m spatial resolution (Teluguntla et al., 2017a). The assessment strategy to assess the cropland map of Australia was modified in response to the cropland diversity, which is different from the pattern observed in the other selected continents. The cropland area in Australia is mostly concentrated in a narrow belt towards the edges of the continent leaving a large, single portion towards the center with very low probability of cropland areas. Sampling in the area with a very low probability of cropland would not be indicative of the ability to accurately map cropland. Therefore, the continent was divided into a homogeneous region where the crops occurred using a buffering approach rather than the AEZ-based stratification method. Consequently, this method provided a more appropriate sampling design creating a sampling frame around the cropland patches and excluding the areas with no chance of cropland.

Stratification

The stratification method for Australia was performed using a buffering strategy instead of AEZ's. The buffer zones (Figure 10) were generated using the Euclidean distance method. This method calculates the distance between crop and no-crop pixels from a raster layer of the cropland map and results in a buffer around the crop areas. Using this method, two crop buffers were generated around the cropland patches with a Euclidean Distance (ED) of 1 (~100 km) and 2 (~200 km). These buffer zones represent the reduced regions where a reasonable occurrence of cropland areas can be expected. No sampling was performed in areas outside the buffer zones.

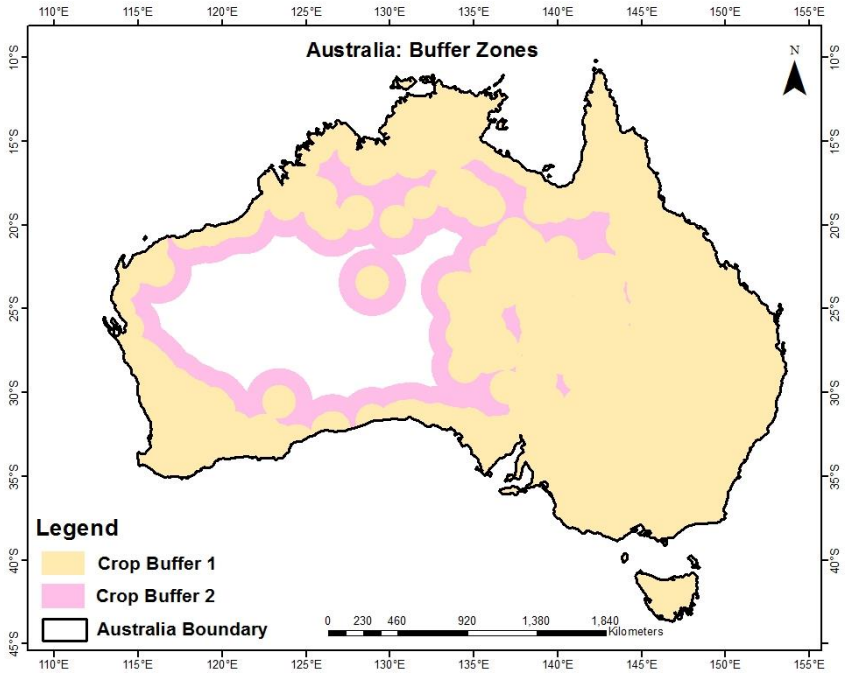

Figure 10. Crop buffer zones delineated using Euclidean Distance buffering approach.

Collecting Reference Data and Sampling Design

To perform the assessment of the cropland extent map of Australia, reference data were collected both from ground-based samples and from HRI for the year 2014. A field campaign was initially conducted in which 3343 samples were collected (3234 crop samples and 109 no-crop samples) for the southern region of Australia where croplands are prevalent (Teluguntla et al., 2017a). One-third (1118 samples with 1082 crop and 36 no-crop samples) of these ground collected reference data were set aside and used to assess the cropland map of Australia independently from the samples that were used as training data for making the cropland map (Figure 11). Most of the ground samples were collected in the cropland areas of southern Australia with few no-crop samples being collected. Therefore, it was necessary to supplement the ground-collected samples with more no-crop samples in order to achieve a balanced, valid and effective reference dataset. More no-crop samples were collected from visual interpretation of HRI in a sampling frame around the cropland patches making sure to exclude areas with no chance of cropland (Figure 12). The 36 no-crop ground collected samples were augmented with an additional 787 no-crop samples interpreted using HRI. Given that the proportion of cropland across Australia was approximately 12%, it is necessary to sample the reference data such that it represents this proportion. Therefore, since there were 823 (787 + 36) no-crop samples, we randomly selected 106 crop samples (about 12%) from the 1082 ground collected crop samples to achieve a balanced reference data set for generating the error matrix.

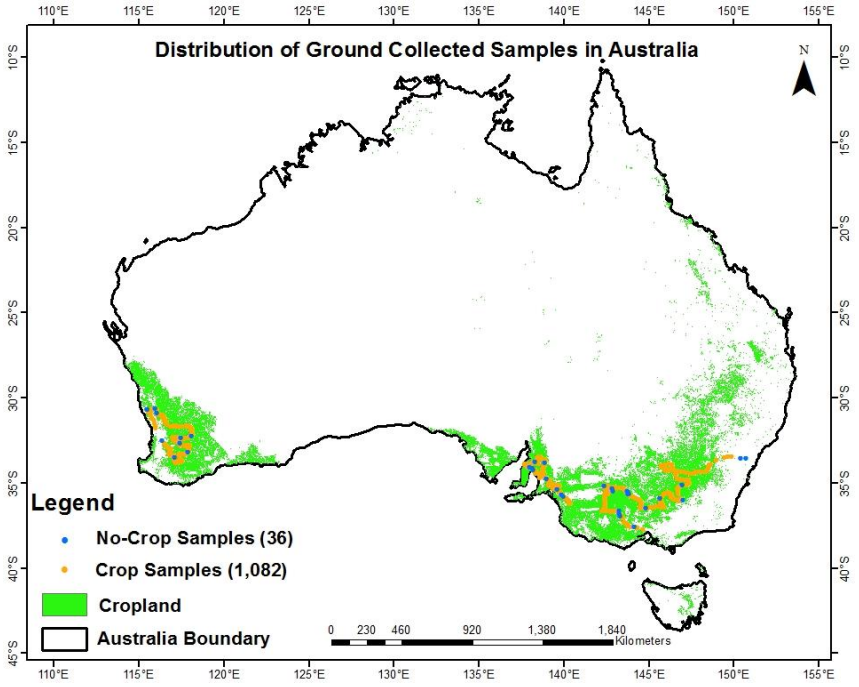

Figure 11. The distribution of ground collected samples (Teluguntla et al., 2017a) used in the accuracy assessment of cropland map of Australia.

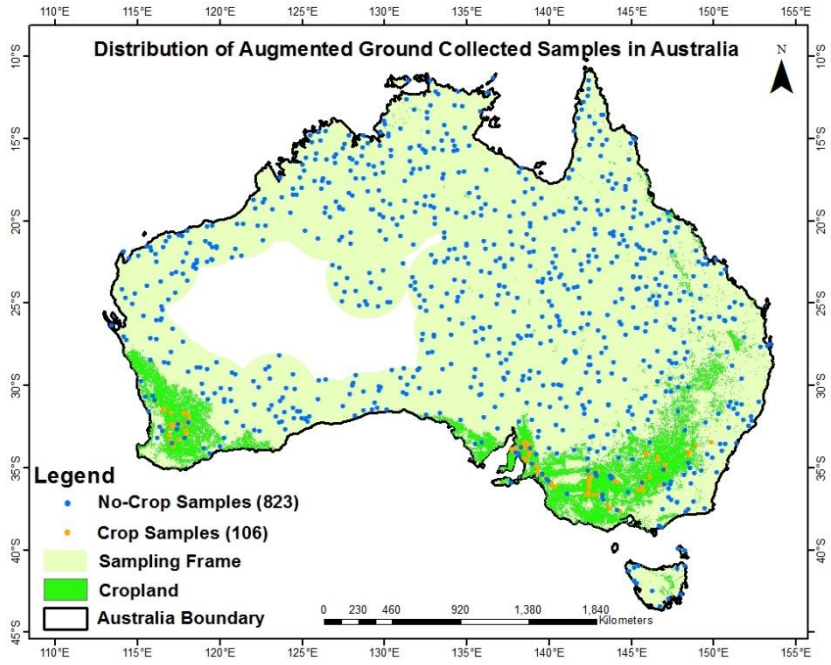

Figure 12. The distribution of ground collected and augmented no-crop samples in Australia.

As a result of this initial analysis, it was clear that only portions of Australia (mostly around the coastal area) grow crops. The center of Australia has very little chance of cropland because of extremely dry conditions. Therefore, in order to effectively validate the cropland areas a buffering approach was employed instead of AEZs that would have included the entire continent. This approach resulted in the collection of 700 and 800 reference samples independently for the two buffer zones, respectively using visual interpretation of HRI (Figure 13). The final analysis then resulting in having four sets of reference data with different sample sizes (i.e., 1118, 929, 700 and 800) with the first two based on the ground reference data collection (initial and balanced assessments) and the last two based on the buffering approach (buffer 1 and buffer 2) that were used to assess the cropland map of Australia.

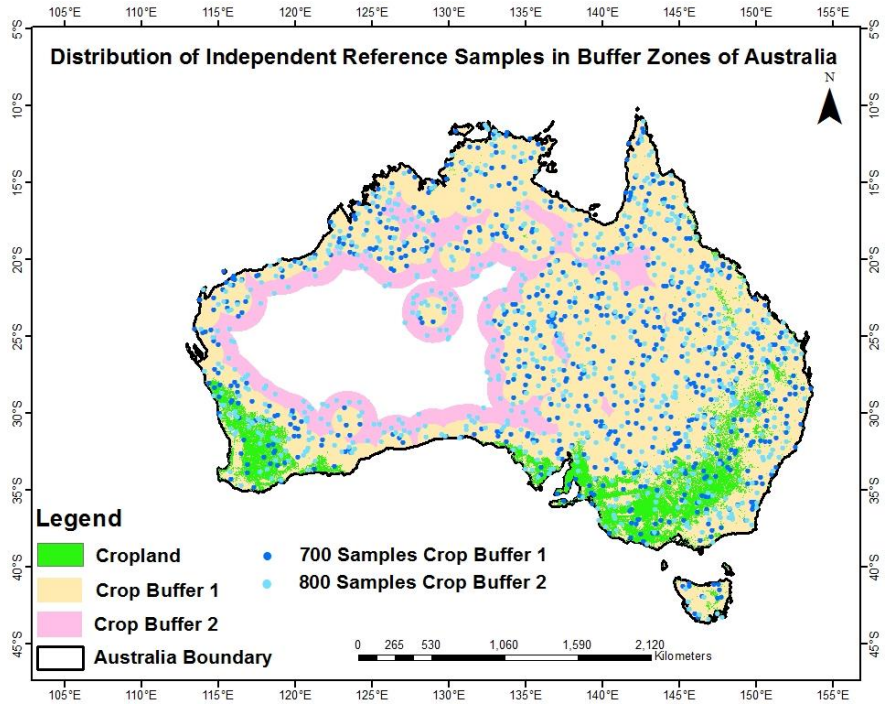

Figure 13. The distribution of reference samples in buffer zones of Australia.

A simple random sampling design was used to distribute all the reference samples to perform the accuracy assessment of the cropland map of Australia. Figures 11–13 show the distribution of these reference samples used in the accuracy assessment process. Figure 11 shows the original and complete ground-based field campaign reference data. Figure 12 shows the augmentation of the ground-based data with HRI interpreted no-cropland samples to achieve a balanced data set. Finally, Figure 13 shows the results of the buffering approach (buffers 1 and 2) to extend the crop sampling across the entire continent minus the area in the center where there was no chance of cropland existing.

Computing Accuracy Statistics

The accuracy assessment of cropland extent map of Australia was performed using a combination of ground collected and HRI interpreted samples generated with the stratification (buffer zones) of Australia. Error matrices were generated from the ground collected samples from the initial field campaign resulting in an unbalanced sampling approach (Table 5), a combination of ground and HRI samples to create a balanced (proportional) sampling approach (Table 6) and then within the buffer zones 1 and 2 (Tables 7 and 8) for Australia. The error matrix in Tables 5 and 6 depicts the accuracy estimates when the cropland map of Australia was assessed separately with ground collected samples only and with the ground samples augmented with HRI respectively to augment the non-cropland samples to produce a proportional sample. The error matrix in Tables 7 and 8 are generated for the buffer zones 1 and 2 respectively using reference samples interpreted from HRI.

Table 5. The error matrix generated using unbalanced ground collected reference samples.

		Reference Data			
		Crop	No-Crop	Total	User's Accuracy
Map Data	Crop	1040	13	1053	98.77%
	No-Crop	42	23	65	35.38%
Total		1082	36	1118	
Producer's Accuracy		96.12%	63.89%		**95.08%**

Table 6. The error matrix generated using balanced ground collected reference samples augmented with HRI interpreted samples.

		Reference Data			
		Crop	No-Crop	Total	User's Accuracy
Map Data	Crop	102	13	115	88.70%
	No-Crop	4	810	814	99.51%
Total		106	823	929	
Producer's Accuracy		96.23%	98.42%		**98.17%**

Table 7. The error matrix generated using balanced reference samples generated in crop buffer zone 1.

		Reference Data			
		Crop	No-Crop	Total	User's Accuracy
Map Data	Crop	55	15	70	78.57%
	No-Crop	48	582	630	92.38%
Total		103	597	700	
Producer's Accuracy		53.40%	97.49%		**91.00%**

Table 8. The error matrix generated using balanced reference samples generated in crop buffer zone 2.

		Reference Data			
		Crop	No-Crop	Total	User's Accuracy
Map Data	Crop	58	31	89	65.17%
	No-Crop	24	687	711	96.62%
Total		82	718	800	
Producer's Accuracy		70.73%	95.68%		**93.13%**

Discussion

The accuracy assessment of large area cropland extent maps was performed in response to specific issues, constraints of concern, limitations and a few advantages observed in different continents throughout this project. The assessment strategy was adapted for the selected continent in order to determine measures in homogeneous regions and provide more information for the large area cropland maps. It is important to note how the assessment strategies were modified from one continent to another globally in response to the cropping patterns in different agriculture landscapes. The heterogeneity in the agriculture landscapes of different continents was minimized by dividing each continent into homogeneous Agro-Ecological Zones (i.e., AEZ's), which were then used to perform the accuracy assessment. Indeed, there is no single sampling design for collecting global reference data that can serve as a universally appropriate everywhere (Strahler et al., 2006). Therefore, modified sampling designs were employed in the AEZ-based assessment strategies for the different continents. Where the use of an AEZ-based stratification failed to produce more homogeneous regions (e.g., Australia), a buffering approach was selected instead. The following is a discussion of the results for each of the selected continents.

United States

The US has dynamic cropping patterns where dominant crop types are well distributed in large homogeneous agriculture field sizes and rare crop types are scattered across heterogeneous agricultural landscapes. Therefore, these variations in agriculture landscape need to be considered while performing an assessment of the cropland maps. The issues and constraints of cropland diversity were incorporated by dividing the US into homogeneous regions using a stratification

method based on AEZ's. The accuracy results for homogeneous regions of a continent can be more meaningful for the users to implement various region-based cropland models for planning and decision-making.

There is a great advantage in the US of having an extensive and easily accessible reference data set (i.e., USDA CDL). Due to the availability of such a high-quality reference data (i.e., accuracy ranges from 85–95%) (Boryan et al., 2011), it was easy to perform an accuracy assessment of cropland maps in the US as compared to other continents. AEZ-based assessment strategy was employed with only a few modifications in the sampling design to choose an appropriate sample scheme and size. The task of achieving an appropriate sample size was determined by a sample simulation analysis that provided insight into how many samples were required to perform a continent specific accuracy assessment. Therefore, AEZ-based assessment strategy using high-quality reference data with some modifications in the sampling design was employed to report the accuracy measures in all the AEZ's.

The accuracy assessment of cropland extent map in the US provided both accuracy measures in the form of error matrices and spatial distribution of agreement and disagreement in the form of a difference image. The compiled accuracy estimates generated for all the AEZ's showed high overall accuracies for the crop and no-crop classes with no commission errors in the cropland areas (Table 1). These results were also confirmed with a difference image that showed spatial agreement and disagreement between the reference data and the map (Figure 6). The cropland class on the map has no-commission error and only 2% omission error. Overall, there were no complications in performing the accuracy assessment of the cropland maps of the US. The results show that performing an accuracy assessment of the cropland extent map for a continent with an

extensive reference data set can easily be done, but that care still must be taken to determine homogeneous cropping regions which result in more meaningful, representative and valid mapping products.

Africa

In Africa, different issues and constraints were observed when compared to the other selected continents due to: (1) the heterogeneous and scattered cropland distribution across the AEZ's; and (2) the lack of effective and valid reference data. In Africa, AEZ's were quite diverse from each other with a few zones having very sparse cropland distribution as compared to others where the cropland areas were more uniformly distributed. These issues and concerns were considered and planned for well before assessing the cropland maps using the AEZ-based accuracy assessment strategy with a modified sampling design. The AEZ-based strategy was different from the one employed in the US as it was specific to each AEZ according to each zone's cropping pattern variability. In response to these cropping patterns and the lack of availability of valid reference data, the traditional method of accuracy assessment was conducted using a modified sampling design.

To perform the accuracy assessment of the cropland extent map of Africa, the reference data had to be collected from interpretation of HRI for the year 2014 because no other data existed. Before collecting this reference data, it was necessary to determine where and how many samples were required. Another sampling simulation was performed to determine appropriate sample sizes for the various AEZs. Because of the large variability in the cropland distribution of the AEZ's in Africa, zones with low crop diversity (i.e., AEZ 1 and 2) were sampled with a minimum number

of samples (50) as compared to the other zones (250). Such modified sampling in Africa demonstrates the power of being able to selectively devote effort and time in collecting reference data based on the variability in the cropland distribution.

The results in Table 3 show that there is a high overall accuracy in all the zones. It is very important to note the producer's and user's accuracy of the crop class in each AEZ. In Zone 5, 6 and 7, the producer's and user's accuracy of the crop class are low due to low crop intensity and spatial structure of cropland areas. However, Zone 1 and 2 also has low crop proportion but the spatial structure of crop patches is different in these zones as compared to zone 5, 6 and 7. Therefore, different users' and producers' accuracies were observed in each zone due to spatial fragmentation of cropland areas in specific zones. These accuracies provide a more detailed view for each mapped class beyond just the overall accuracy and are indicative of the AEZ-based assessment strategy. Specific to Africa, it is very important to observe the cropping pattern in each AEZ and how much effort is required to generate the reference data necessary to perform the AEZ-based assessment strategy. These results show that the AEZ's with low crop proportions do not require large sampling efforts as these zones have smaller geographic extent and less cropland area to assess. It is, therefore, reasonable to assume that if the sample size was increased for these zones; neither the number of crop samples nor the map accuracy would increase. Throughout this process of assessing the cropland map of Africa, the AEZ-based assessment strategy helped to provide a more detailed view of the accuracies of homogeneous regions within the continent.

Australia

The accuracy assessment process to validate the cropland extent map of Australia was modified differently than the process used in the US and Africa. In Australia, the cropland distribution is concentrated only along a narrow belt towards the edges of the continent. There is a very low chance of cropland areas towards the center region of Australia because of the very dry conditions there. This concentrated cropping pattern was considered in the assessment strategy by choosing a reduced region around these cropland patches. AEZ's in Australia do not exhibit much diversity due to low crop variability in the continent and therefore, were not appropriate to stratify the continent. Rather than an AEZ-based assessment strategy, a buffering approach was used to divide the continent into homogeneous regions to perform a valid assessment of the cropland map of Australia.

In addition to a different method of stratification, two different sources of reference data were used in Australia. The first were ground collected samples and the second were collected from interpretation of HRI. As a result of the ground-collected reference data, a new set of issues needed to be considered. This ground data was collected during a field campaign that emphasized identifying cropland areas. As a result, very little non-cropland samples were recorded. Therefore, creating an error matrix from the reference data resulted in an error matrix in which there were many cropland samples and few non-cropland samples (Table 5). However, given that only approximately 12% of Australia is cropland, this error matrix was highly imbalanced and not representative of the map accuracy. The non-cropland samples were augmented appropriately using interpretation of HRI to obtain sufficient samples to generate a balanced error matrix indicative of the actual cropland/non-cropland proportion (Table 6).

While the balanced error matrix generated from the ground reference data augmented with interpretation of HRI demonstrates good overall cropland mapping, it is not representative of the entire continent since the ground data were collected all in the southern region. To solve this problem, a stratification approach using buffer analysis was adopted. This method provides a buffer around the cropland areas of Australia at two distances and eliminates sample collection from the center of the continent where there was very low chance of finding crops.

The error matrices generated for the buffer zones (Tables 7 and 8) have high accuracies but are lower than the error matrix in Table 6. However, these error matrices from the buffering approach should be viewed as more representative and meaningful than the matrix that used reference data from only part of the continent. As demonstrated in Australia, the entire continent might not be considered as an appropriate sampling area for assessing the accuracy of the cropland maps. In such places, therefore, the sampling area needs to be modified to accommodate sparse and concentrated cropping pattern to provide meaningful and representative accuracy results.

Lessons Learned

Accuracy assessment is an expensive, yet essential, component of the mapping projects. Maps without their associated accuracy estimates will not be valuable to the users (Thenkabail, 2005; Strahler et al., 2006). While there is a well-established traditional method to perform the accuracy assessment of thematic maps (Congalton, 1991), there remains considerable need for future research and development to perform the accuracy assessment of large area thematic maps. There are few important lessons that were learned from a modified assessment strategy conducted for three different continents while assessing large area cropland extent maps:

1. Before assessing the cropland extent maps of different continents, some sort of stratification must be employed to divide the area into homogeneous regions. The stratification approach must be considered and recommended to address the issues of variation in different agricultural landscapes within each continent.

2. It is important to ensure that the accuracy assessment of large area cropland extent maps is performed in accordance with how the map was created. Failure to consider the methodologies used including any stratification that was performed will result in unresolved issues.

3. In order to conduct a modified accuracy assessment for the homogeneous regions within the continent, different issues, constraints and characteristics observed in the cropland maps for different continents must be considered carefully. These issues can be either related to complex agricultural landscapes or the availability of reference data for different continents.

4. Performing an accuracy assessment for a continent with an extensive reference data can be easily done, but still the sampling scheme and size must be modified carefully to determine enough samples for the homogeneous cropping regions to result in meaningful, representative and valid mapping products.

5. A modified sampling scheme and size must be chosen using a sample analysis approach for each homogeneous region in response to their cropping pattern variability. Such modified sampling can demonstrate the power of being able to selectively devote effort and time in collecting reference data based on the cropping pattern variability.

6. Any ground collected samples especially if only certain map classes (i.e., crops) area collected must be augmented to create a balanced and effective reference data set. However, this balanced

error still might be representative of the entire continent if the ground data were collected in only one region.

7. When the entire continent cannot be considered as an appropriate sampling area for assessing the accuracy of cropland maps, the sampling area should be modified to accommodate the sparse and concentrated cropping pattern using stratification method.

Conclusions

This paper presents modified accuracy assessment strategies used to assess the accuracy of large area cropland extent maps in response to different issues such as variations of cropping pattern and reference data availability in different continents. Considering and addressing these issues, the modified assessment strategies helped to understand the efficacy and quality of cropland extent maps for different agricultural landscapes to implement economic planning and policymaking. The information derived from large area cropland maps with agricultural landscapes of different continents can be enriched, improved and analyzed with modified assessment strategies. Such modified assessment strategies promise to achieve more meaningful, representative and applicable mapping products for each continent. Therefore, the need for a continent-specific assessment strategy developed by modifying the sampling design for collecting reference data and computing accuracy measures was demonstrated to be valuable. However, different sampling methods can be employed and compared in the future to analyze the accuracy results for different cropping scenarios.

A modified assessment strategy was employed to assess the accuracy of the cropland extent maps of three selected continents developed as a part of GFSAD project. The variability of

cropping pattern in the agricultural landscapes and reference data availability were considered and addressed to provide meaningful and valid accuracy results for mapping products within these selected continents. The stratification approach based on AEZ's or buffer zones used to divide the continent into homogeneous cropping regions: (1) minimized the heterogeneity of different cropping patterns and (2) helped to rationalize the validation efforts for different continents. Finally, the sampling scheme and size were modified for the homogeneous regions using a sample analysis approach based on the variations of cropping pattern within the continent.

In summary, continent-specific modified assessments performed for three selected continents demonstrate that the accuracy assessment can be easily done for a continent such as the US with extensive availability of a reference dataset while more modifications were needed in the sampling scheme for the continents with little to no reference datasets. The result of the modified sampling performed in the AEZ's of Africa show that the effort and time in collecting reference data can be selectively devoted based on the variability in the cropland distribution. Finally, a modified sampling was employed in the buffer zones of Australia using two different sources of reference data. An unbalanced number of ground samples collected during a field campaign that emphasized identifying cropland areas were augmented and balanced to be indicative of the crop/no crop area proportion of the map to generate a balanced and valid error matrix for Australia. The analysis performed with this modified strategy shows that the entire continent might not be considered as an appropriate sampling area for assessing the cropland maps due to little chance of cropland in center of Australia because of extremely dry conditions.

CHAPTER IV

Accuracy Assessment of Global Food Security-support Analysis Data (GFSAD) Cropland Extent Maps Produced at Three Different Spatial Resolutions

Abstract

Monitoring global agriculture systems relies on accurate and timely cropland information acquired worldwide. Recently, the NASA Making Earth System Data Records for Use in Research Environments (MEaSUREs) Program has produced Global Food Security-support Analysis Data (GFSAD) cropland extent maps at three different spatial resolutions, i.e., GFSAD1km, GFSAD250m, and GFSAD30m. An accuracy assessment and comparison of these three GFSAD cropland extent maps produced and published by different researchers was performed to establish their quality and reliability for monitoring croplands both at global and regional scales. Large area (i.e., global) assessment of GFSAD cropland extent maps was performed by dividing the entire world into regions using a stratification approach and collecting a reference dataset using a simple random sampling design. All three global cropland extent maps were assessed using a total reference dataset of 28,733 samples. The assessment results showed an overall accuracy of 72.3%, 80-98%, and 91.7% for GFSAD1km, 250m (only for four continents), and 30m maps, respectively. Additionally, a regional comparison of the three GFSAD cropland extent maps was analyzed for nine randomly selected study sites of different agriculture field sizes (i.e., small, medium, and large). The similarity among the three GFSAD cropland extent maps in these nine study sites was represented using a similarity matrix approach and two landscape metrics (i.e., Proportion of Landscape (PLAND) and Per Patch Unit (PPU)) which categorized the crop

proportion and the crop pattern. A comparison of the results showed the similarities and differences in the cropland areas and their spatial extent when mapped at the three spatial resolutions and considering the different agriculture field sizes. Finally, specific recommendations were suggested for when to apply each of the three different GFSAD cropland extent maps for agriculture monitoring based on these agriculture field sizes.

Introduction

Agriculture monitoring plays a significant role for ensuring food security, social stability, and for providing information to farmers on crop yield predictions and decision makers for policy and planning purposes (Liang and Gong, 2013). These global monitoring systems require large area cropland information as a key input source to estimate crop yield and identify cropping patterns (Atzberger et al., 2015; See et al., 2015). The acquisition of consistent cropland information over large areas relies heavily on the use of earth observation data to describe their precise location on the earth's surface. Since the early 1990's, satellite imagery has been used to produce cropland maps because of its consistent, timely, and systematic observations. Some examples of previous cropland datasets are: the Global Map of Irrigation Areas (GMIA) (Thenkabail et al., 2009), the Global Map of Rain-fed Areas (GMRCA) (Biradar et al., 2009), the Global Monthly Irrigated and Rain-fed Crop Areas (MIRCA2000) (Portmann et al., 2010), the Global Rain-fed, Irrigated, and Paddy Croplands (GRIPC) (Salmon et al., 2015), and the Moderate Resolution Imaging Spectroradiometer-Cropland (MODIS) (Pittman et al., 2010).

Recently, with our increased accessibility to advanced computing platforms for processing large datasets, an improved spatial and thematic dataset compared to previous cropland mapping efforts called the GFSAD Project (Global Food Security Support-Analysis Data) was completed. Three new GFSAD cropland extent maps were created separately at three different spatial resolutions (1km, 250m, and 30m) using Landsat and MODIS imagery along with other existing cropland data (Teluguntla et al., 2016; Massey et al., 2017a; Massey et al., 2017b; Teluguntla et al., 2017a; Teluguntla et al., 2017b; Xiong et al., 2017a; Xiong et al., 2017b; Xiong et al., 2017c; Phalke et al., 2017; Oliphant et al., 2017; Gumma et al., 2017; Zhong et al., 2017; Teluguntla et al., 2018; Massey et al., 2018). It is well known that mapping of cropland areas at different spatial resolutions can result in large differences in the estimates of cropland area and spatial extent (Chen et al., 2017; Pérez-Hoyos et al., 2017). Therefore, these three GFSAD cropland extent maps must be assessed and compared both at the global and regional scale to establish their quality and reliability as the base map for generating higher level cropland products such as crop type and crop intensity maps (Thenkabail et al., 2010). These maps provide for both large area (i.e., global) comparisons between the different spatial resolutions including the identification of similarities and differences and for determining their suitability for more regional analysis, especially when considering different agriculture field sizes (Chen et al., 2017). Therefore, the main objectives of this paper are to (1) perform a large area accuracy assessment of the three GFSAD cropland extent maps and (2) conduct a regional comparison of nine representative study sites selected randomly to explore the impact of different agriculture field sizes.

Previous attempts at rigorous accuracy assessment of large area cropland extent maps has been very limited. Considerable ambiguity exists in the implementation and interpretation of large area

thematic map accuracy assessment (Congalton, 2016). In the literature, individual measures and guidelines for assessing thematic map accuracy have been well established by many researchers (Congalton, 1991; Stehman, 1997; Stehman and Czaplewski, 1998; Congalton and Green, 1999). However, these guidelines are not often followed due to various limitations in the assessment process (e.g., thematic resolution, geo-location accuracy and availability of reference data) (Olofsson et al., 2013). The biggest limitation in the large area accuracy assessment process is the availability of valid reference data. As such, large area assessment efforts have mostly relied on insufficient, sparsely distributed reference data (Bicheron et al., 2008; Fritz et al., 2009a; Foody, 2010; Gong et al., 2013; Yu et al., 2013b). The assessments performed with limited and insufficient reference dataset reported overall accuracies ranging from 66% to 78% with considerably lower accuracies from 10% to 50% for the cropland class (Sedano et al., 2005; Frey and Smith, 2007).

Cropland reference data are extremely limited in most parts of the world resulting in insufficient sample sizes and thus, an inability for assessing the accuracy of large area thematic maps (Foody, 2002; Gallego, 2004; Foody and Boyd, 2013; Waldner et al., 2015). Recently, a few global reference datasets (e.g., FAO-GFRA (Food and Agriculture Organization Global Forest Resources Assessments) (Kooistra et al., 2010; Potapov et al., 2011) and the Geo-wiki sample set (Fritz et al., 2009b; Fritz et al., 2011a)) have been developed to perform the assessment of global land cover maps. Despite the increasing number of initiatives to collect reference datasets freely in the public domain such as Geo-wiki (Fritz et al., 2009b; Fritz et al., 2011a) and GOFC-GOLD (Global Observation of Forest and Land Cover Dynamics) (Olofsson et al., 2012), cropland reference datasets are still lacking. More work must be done to create additional global cropland reference datasets. Any new cropland reference dataset must be generated using an appropriate

sampling design based on the inclusion probability of occurrence of crop and no-crop areas to assess these cropland extent maps (Strahler et al., 2006). If the inclusion probabilities of crop and no-crop areas are ignored, a significant bias is likely to occur resulting in a non-proportional and insufficient number of samples. Unless the reference data represents the entire cropland distribution, accuracy results will not be statistically valid and meaningful.

Basic probability-based sampling designs can be constructed from simple random and systematic selection protocols, and structures imposed on the population such as strata or clusters (Stehman and Czaplewski, 1998; Stehman, 2009). The sampling design needs to be easy to implement and capable of accounting for the proportions of high and low map categories such as crop and no-crop distribution in different continents to perform the assessment on a global scale (Card, 1982). In simple random sampling, each sample of crop and no-crop class has an equal and independent chance of being selected (Congalton and Green, 2009). However, such sampling designs might result in insufficient number of samples in the low crop proportion regions of different continents. The sufficient number of samples must be allocated using an appropriate sampling design. Where possible (e.g., Landsat or Sentinel imagery), a homogeneous cluster of 3 × 3 pixels should be used as the sampling unit to account for the positional error at each location (Congalton and Green, 2009). For coarser resolution imagery (e.g., MODIS), it is difficult to find large homogeneous regions and therefore, a single coarse resolution pixel is used as the sample unit in these situations. The goal is to select the best sampling unit to ensure that only thematic error is considered in the accuracy measures and not error due to mis-registration or positional accuracy.

Another issue or limitation when conducting large area assessments is that most have reported just a single accuracy value for the entire world. This approach does not provide any details or information about the accuracy results for different continents or regions. Given the differences in crop growing strategies and patterns between continents, a more appropriate assessment strategy must be used. Such an assessment strategy has been recently used to assess the cropland extent maps of three different continents (i.e., the United States, Africa, and Australia) (Yadav and Congalton, 2018a). This paper described an appropriate assessment strategy for these continents based on their cropland distribution and reference data availability. This strategy employed a stratification approach to divide the entire world into homogeneous regions and a sample simulation analysis was conducted to determine the appropriate sample size. Implementing a stratification approach prior to the actual assessment provided an effective means of evaluating the cropland extent maps by considering the diverse cropping patterns of different continents (Waldner et al., 2015).

The most widely accepted approach for reporting thematic map accuracy results is using an error matrix (Congalton, 1991; Congalton and Green, 2009). The error matrix is a cross tabulation of the map classes determined by the image classification against that observed from a reference dataset. The error matrix presents the comparison of reference samples with the map and allows computation of overall, producer's, and user's accuracy (Story and Congalton, 1986). This assessment technique can be used to report these accuracy measures for different regions. In addition, there are some regions such as the United States and Canada, where a reference cropland data layer (e.g., CDL in the US) exists for comparing the entire map on a pixel by pixel basis. Such comparison results can then also be presented in the form of a similarity analysis which represents

the spatial distribution of agreement and disagreement that occurred in the map as compared to the reference map.

Finally, in addition to evaluating each of the three different GFSAD cropland extent maps separately, it is useful to perform a comparison between the maps to evaluate the effectiveness of each spatial resolution for specific user requirements (Kaptué Tchuenté et al., 2011; Kuenzer et al., 2014). Mapping at a variety of spatial resolutions raises many inconsistencies, differences, and uncertainties among the estimated cropland areas that can be visualized on the map and are the result of the spatial distribution of cropland patches in different cropping patterns (Giri and Long, 2014; Bai et al., 2015). Therefore, existing and newly developed cropland extent maps must be compared with each other to investigate, determine, and recommend the appropriate spatial resolution for agriculture monitoring given different agriculture field sizes and patterns. Many comparative studies have been performed for existing datasets such as GLC2000, MODIS, International Geosphere-Biosphere Program (IGBP), and National Land Cover Dataset (NLCD) (Giri et al., 2005; Fritz et al., 2011b). Despite identifying spatial discrepancies and inconsistencies, particularly in the cropland class at a global scale, these comparison studies have not focused on the adequacy of different spatial resolutions given different agriculture field sizes (See et al., 2013, Liang and Gong, 2013). The uncertainties in the cropland class of these existing maps could be due to: (1) absence of precise spatial location of the cropped areas, (2) coarse resolution of the map products with significant uncertainties in areas, locations, and detail, and (3) invalid assessments of these cropland extent maps.

The recent production of the three different GFSAD cropland maps promises to provide more detailed and accurate cropland information with a high amount of certainty in the geographic

location of the cropland areas. Therefore, these three different resolution cropland maps must be assessed with an appropriate large area accuracy assessment strategy describing their use, reliability, and quality for different continents. However, cropland mapping in different agriculture fields sizes can be inconsistent at different spatial resolutions because of the spectral similarity of different fields and differences in similar agriculture fields (Bayas et al., 2017). The similarities and differences in the characteristics of agriculture landscapes (i.e., crop area proportions and landscape metrics) must also be explored to provide specific recommendations for when to apply the three different cropland extent maps with respect to different field sizes (Frohn, 1997). This kind of regional comparison can be effectively implemented by using a similarity matrix based on a contingency table approach like an error matrix and by categorizing the landscape metrics such as landscape proportion for different agriculture field sizes.

Therefore, the two primary objectives of this study are to perform an accuracy assessment of the three different GFSAD cropland extent maps of the world and then evaluate the impact of different agriculture field sizes on global and regional agriculture monitoring. To accomplish the first objective, a large area accuracy assessment was conducted separately for each spatial resolution GFSAD cropland extent map. Three different assessments were performed using a valid, large reference data set collected from different sources and sampling simulations to choose the appropriate sample size for each region (Congalton and Green, 2009; Yadav and Congalton, 2018a). Second, regional comparisons of the three GFSAD cropland extent maps were performed by calculating similarity in crop area proportions and landscape heterogeneity in nine random 10 km by 10 km study sites or regions selected in each of three agriculture field sizes (i.e., small, medium, and large). The specific goal of this paper is to provide an appropriate assessment and

comparison of three different GFSAD cropland extent maps to resolve many of the short-comings and uncertainties of other cropland mapping efforts. Finally, the results of this analysis are used to recommend when it is appropriate to apply each map given the different agriculture field sizes for each continent of the world.

Study Area

Two different study areas were used in this investigation. These are: (1) the entire world divided into eight, four, and 15 zones to perform the assessment of GFSAD1km, 250m, and 30m cropland datasets, respectively and (2) nine random 10km by 10km analysis areas used to perform the comparison of GFSAD maps by field size.

To perform the comparison, the agriculture field sizes of the entire world were grouped into three classes using a global field size map from International Institute for Applied Systems Analysis and International Food Policy Research Institute (IIASA-IFPRI). This map classified global field sizes ranging from 10 to 40 hectares (ha) at 1km spatial resolution based on data collected via a Geo-Wiki crowdsourcing campaign (Fritz et al., 2015). The three classes of agriculture field size used in the study were: 10-20 ha (small), 20-30 ha (medium), and 30-40 ha (large). Nine study sites were randomly selected with three in each agriculture field size across the entire world (Figure 14). Table 9 shows the distribution of selected study sites in different continents and agriculture field sizes.

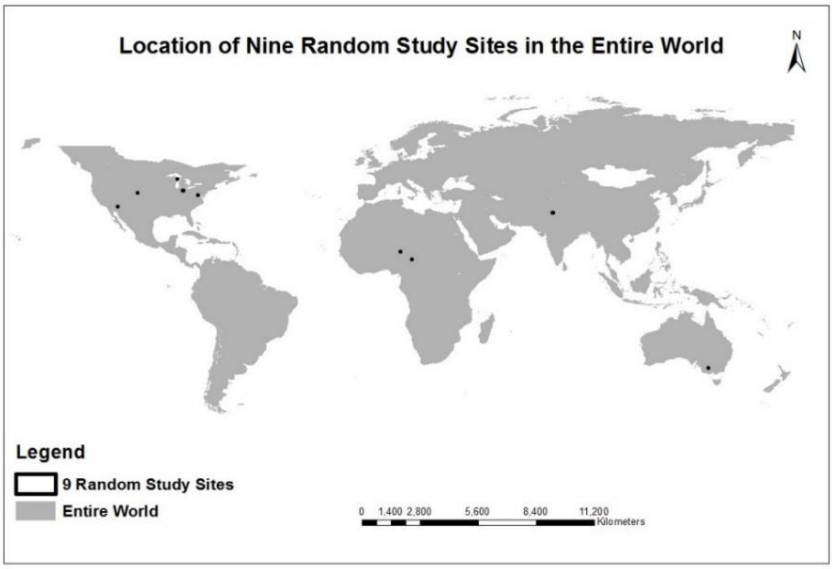

Figure 14. The location of the nine randomly selected study sites for the world.

Table 9. Distribution of random study sites in different agriculture field sizes of different continents.

Field Size	US	Africa	South-Asia	Australia
Small (10-20ha)	-	2	1	-
Medium (20-30ha)	3	-	-	-
Large (30-40ha)	2	-	-	1

Datasets

Four datasets were necessary to conduct the accuracy assessment of the GFSAD cropland extent maps. The first three datasets were the maps themselves at the three spatial resolutions (Figure 2) and the fourth was the reference data set used for comparison. The basic requirements and techniques to perform the thematic map assessment have been reviewed by many researchers

in the past (Congalton, 1991; Stehman and Czaplewski, 1998; Congalton and Green, 2009). One of the key elements of the assessment is to ensure that the same appropriate classification scheme was used for collecting both the training data and the reference data. A well-defined classification scheme helps to reduce the risk of misunderstanding and inconsistencies while comparing and assessing the mapping products (Congalton and Green, 2009; Congalton et al., 2014). Therefore, a common GFSAD classification scheme was used to generate the three GFSAD cropland extent maps at different spatial resolutions and to collect the reference dataset used to validate these cropland extent maps. This classification scheme defines the cropland class as "lands cultivated with plants, harvested for food, feed, and fiber, including both seasonal crops (e.g., wheat, rice, corn, soybeans, and cotton) and continuous plantations (e.g., coffee, tea, rubber, cocoa, and oil palms)". While fallow croplands are defined as "lands uncultivated during a season or a year but are farmlands and are equipped for cultivation, including plantations (e.g., orchards, vineyards, coffee, tea, rubber"). The cropland extent maps include all the planted crops and fallow lands. Non-croplands include all other land cover classes other than croplands and cropland fallow.

Accuracy assessment was conducted on the three cropland extent maps (GFSAD1km, GFSAD250m, and GFSAD30m). These maps were produced for the entire world with the exception of the GFSAD250m cropland map which is only available for four of the continents. These cropland extent maps are listed in Table 10 describing their mapping year, spatial resolution, input data, assessment regions, and classification scheme.

The GFSAD1km cropland extent map was derived as a disaggregated five class global cropland extent map at nominal 1 km resolution using four existing multi-study crop mask layers (Thenkabail et al., 2009; Pittman et al., 2010; Yu et al., 2013). Two of the five classes are

dominated by irrigated and rain-fed agriculture. The other three classes have minor/very minor fractions of croplands. The irrigation minor class represents the areas irrigated by small reservoirs, irrigation tanks, open wells, and other minor irrigation. The GFSAD1km cropland map is available online with these five irrigated and rainfed classes, was downloaded, and a cross-walk was developed to simplify the five classes into a crop/no-crop class map for assessment and comparison with other GFSAD cropland extent maps (Figure 15).

Table 10. Description of the three different GFSAD cropland extent maps.

Datasets	Year	Spatial Resolution	Input Data	Assessment Regions	Classification Scheme	Source	References
GFSAD 1km	2010	1km	Existing cropland maps	Entire world (8 Regions)	Irrigated and Rain-fed cropland classes	https://lpdaac.usgs.gov/dataset_discovery/measures/measures_products_table/gfsad1kcm_v001	Teluguntla et al., 2016
GFSAD 250m	2008, 2014	250m	MODIS	4 Continents (US, Africa, Australia, and South-Asia)	Cropland and Non-Cropland		Teluguntla et al., 2017a; Xiong et al., 2017a; Massey et al., 2017a
GFSAD 30m	2014	30m	Landsat	Entire world (15 regions)	Cropland and Non-Cropland	Africa: https://lpdaac.usgs.gov/node/1276 North-America: https://lpdaac.usgs.gov/node/1277 South-America: https://lpdaac.usgs.gov/node/1278 Europe, Central Asia, Russia, Middle-East: https://lpdaac.usgs.gov/node/1279 South-Asia: https://lpdaac.usgs.gov/node/1280 South-East Asia: https://lpdaac.usgs.gov/node/1281 Australia, China, New Zealand, Mongolia: https://lpdaac.usgs.gov/node/1282	Teluguntla et al., 2017b; Massey et al., 2017b; Xiong et al., 2017b and c; Gumma et al.,2017; Phalke et al., 2017; Oliphant et al., 2017; Zhong et al., 2017; Teluguntla et al., 2018; Massey et al., 2018

The GFSAD250m was developed at a spatial resolution of 250m using MODIS satellite data for only selected regions of the world (the United States (US), Australia, Africa, and South-Asia as shown in Figure 15). These cropland extent maps of each selected region were developed by different mapping teams as a part of the GFSAD project (Massey et al., 2017a; Teluguntla et al., 2017a; Xiong et al., 2017a).

The GFSAD30m cropland extent map was developed at a spatial resolution of 30m for 6 continents using multi-temporal Landsat satellite imagery (Xiong et al., 2017b; Xiong et al., 2017c; Gumma et al., 2017; Phalke et al., 2017; Oliphant et al., 2017; Zhong et al., 2017; Teluguntla et al., 2018; Massey et al., 2018). This cropland extent map was generated for the nominal year 2014 using an automated classification algorithm (i.e., random forest classifier) on the cloud-computing Google Earth Engine (GEE) platform. Figure 15 shows the cropland areas mapped in the GFSAD30m cropland map for the entire world.

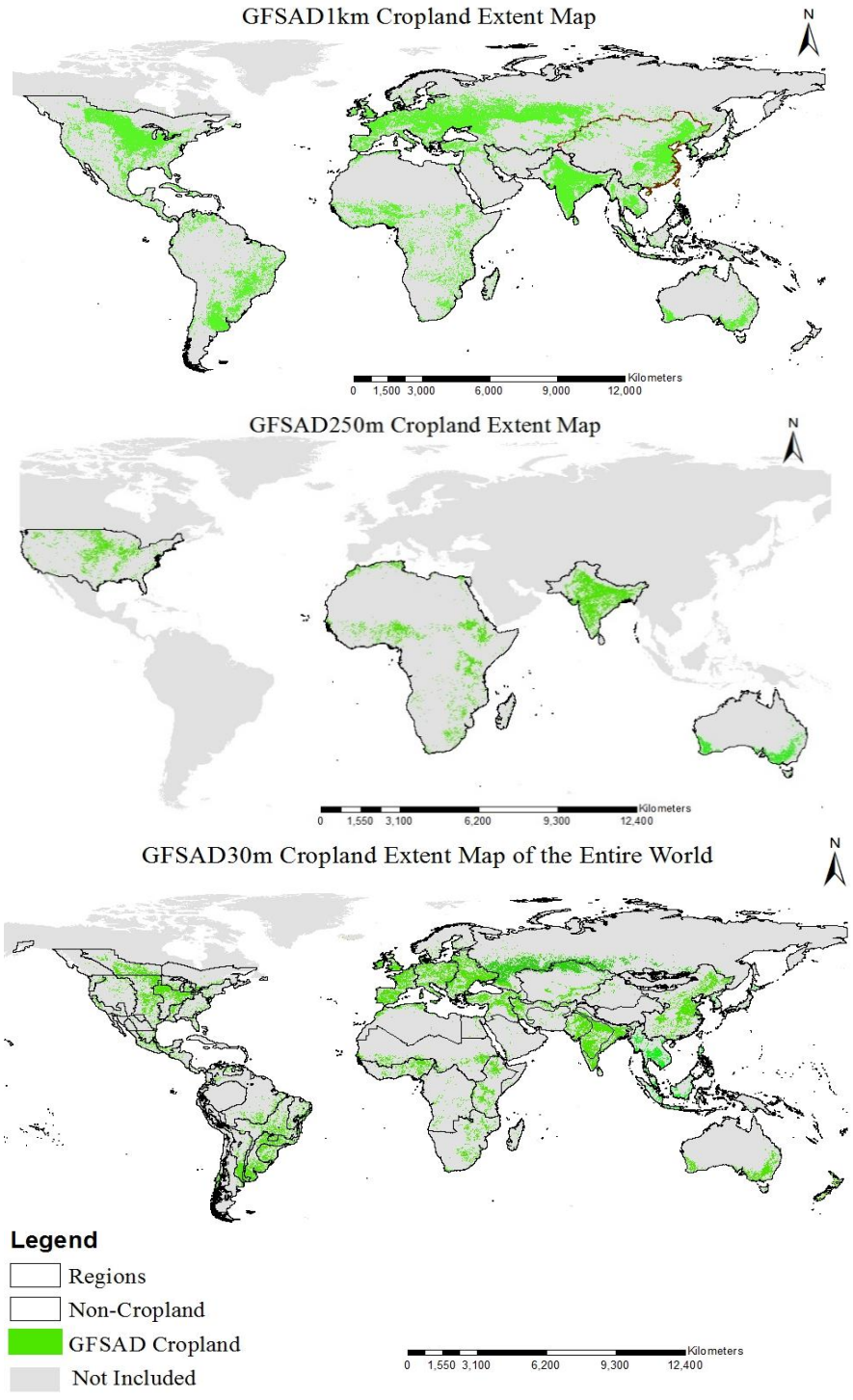

Figure 15. The GFSAD 1 km, 250 m, and 30 m cropland extent maps generated by multiple producers (as listed in Table 10).

In addition to the three different GFSAD cropland extent maps, the fourth and final dataset used in this study is the global reference dataset collected at the same three spatial resolutions from various sources to perform the accuracy assessment. These different sources of reference data include existing reference samples and maps (e.g., crowd sourced Geo-wiki data and USDA Cropland Data Layer), ground collected data, high-resolution image (HRI) interpreted reference samples collected by a GFSAD team member stored on the cropland.org database, and an independently generated reference data by the accuracy assessment team (Table 11).

Table 11. Different sources of reference data used to assess the three different GFSAD cropland extent maps.

Datasets	FAO Geo-wiki	Existing Cropland Maps	Ground Reference Data	Cropland.org Database	Independent Reference Data
GFSAD1km	✓				
GFSAD250m		✓	✓		✓
GFSAD30m		✓	✓	✓	✓

One of the existing reference data sources is IIASA's Geo-wiki reference data which is a global, but sparsely distributed crowd sourced dataset usually collected by experts using high resolution images (Fritz et al., 2009b; Gong et al., 2013). Geo-wiki reference data consists of varying size polygons located across the entire world and a legend showing the percentage of cropland in each sample (Vancutsem et al., 2013). The reference samples were evaluated by IIASA experts using high resolution images through the Geo-wiki crowdsourcing land cover validation tool (Fritz et al., 2009b). This dataset has been proven to be valuable in accuracy assessment of 1km mapping products (Fritz et al., 2009b; Tsendbazar et al., 2015). Both crop and no-crop

reference samples selected in our work were 1km by 1km homogeneous polygons which were reviewed, re-interpreted, and used to assess the GFSAD1km cropland map for the year 2010.

A second existing reference source is high-quality reference cropland maps such as the USDA Cropland Data Layer (CDL) and the Agriculture and Agri-Food Canada (AAFC) cropland layers. The National Agricultural Statistics Service (NASS) of the United States Department of Agriculture (USDA) developed the CDL product for the entire United States (Boryan et al., 2011). The CDL product is a comprehensive, raster-formatted, geo-referenced, and crop-specific land cover map that utilizes ortho-rectified imagery to identify field crop types accurately and geospatially. Similarly, the AAFC Annual Space-Based Crop Inventory for Canada provides information at 30m spatial resolution for the location, extent and changes in Canadian crops (Fisette et al., 2013). Since 2011, AAFC has consistently delivered an annual crop inventory for all the Canadian provinces. These existing data sources provide annual and continuous cropland information at a high spatial resolution.

To supplement existing maps and sample datasets, new reference data on croplands were also generated from: (1) the field campaigns conducted by the GFSAD mapping teams and (2) the interpretation of high-resolution imagery (HRI) by the team members of GFSAD project. These field campaigns provided reference data not only on crop extent (cropland vs. no-cropland), but also on crop type, irrigated vs. rain-fed, and crop intensity (single, double crop per year). For example, campaigns were conducted for Australia and South-East Asia in the year 2014 and 2015, respectively.

Most of the new reference data was obtained by interpretation of HRI. Two collection efforts were employed. First, one GFSAD project team member interpreted a great deal of HRI imagery

for use by the entire GFSAD team. These interpreted samples were split 60/40 with 60 percent of the data being used by the mapping teams for training and testing of their classification algorithms. Forty percent was set aside and hidden from the mapping teams and used in the process of accuracy assessment. The accuracy assessment team used this 40 percent of the reference data, but only after reviewing each sample and confirming the interpretation. If both interpreters agreed, then the sample was selected for use. Second, a supplemental independent set of reference samples was generated by visual interpretation of Google Earth imagery solely by the accuracy assessment team. Again here, two interpreters were used to insure high accuracy in the reference data. These samples were collected for many regions to either supplement for the low sample size or to achieve a proportional reference data size necessary to perform a valid accuracy assessment of the three different GFSAD cropland extent maps.

Methods

The objectives of this study were accomplished using two main methods: (1) thematic map accuracy assessment and (2) map comparison. First, to perform large area thematic accuracy assessment of the three GFSAD cropland extent maps, an assessment strategy was employed based on the availability of reference data, cropland distribution, and mapping strategies used for each continent (Yadav and Congalton, 2018a). Second, the comparison of GFSAD cropland extent maps was performed on randomly selected analysis areas of 10km by 10km in the three different agriculture field sizes. The overall methodology (Figure 16) that was followed to assess and compare the three different GFSAD cropland extent maps is described in the following two sub-sections:

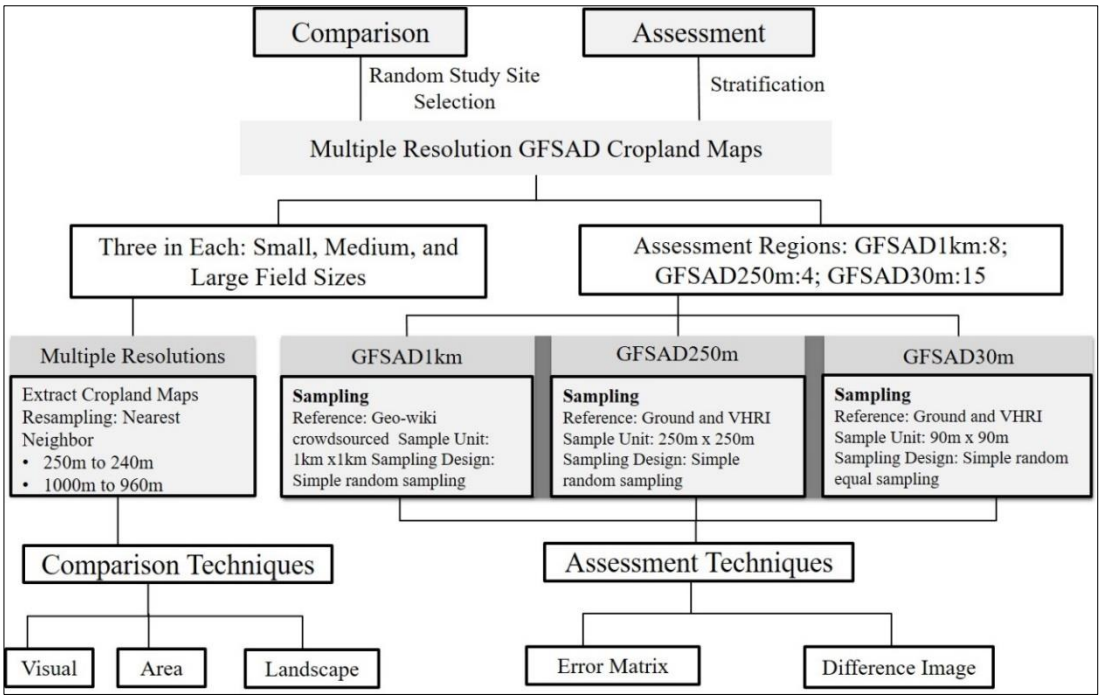

Figure 16. The overall flowchart showing the methods step followed to assess and compare different resolution GFSAD cropland extent maps.

Assessment

The accuracy assessment of the three GFSAD cropland extent maps was executed in the following steps: (1) Stratification, (2) Sampling, and (3) Assessment Technique. An appropriate assessment strategy employed a stratification approach to divide the entire world into homogeneous regions followed by a sampling design derived from the results of a sampling simulation analysis.

First, the process of dividing an area into homogeneous regions based on some relevant factor is referred to as stratification. This relevant factor could be either an administrative or ecological parameter or a combination of both to provide a more meaningful and useful assessment. The stratification of the three different cropland extent maps into homogeneous regions in this study

was based on one of the following three different criteria: (1) Agro-Ecological Zones (AEZs) provided by FAO, (2) a buffer approach, or (3) AEZs combined with country boundaries. Agro-Ecological Zones (AEZs) are created based on the length of the growing period days of crops in homogenous climatic and topographic conditions or regions (Fischer et al., 2012). Because it was difficult to stratify areas using the AEZ approach in some parts of the world due to the very low proportion of cropland, a more effective stratification method (i.e., buffering approach) was used to define an appropriate sampling area around these cropland patches instead (e.g., Australia, Alaska, Iceland, and Mongolia). Finally, in some areas, the AEZ approach was combined with country boundaries to stratify the area into a more reasonable number of regions.

The three cropland extent maps were stratified specifically according to their mapping strategy, reference data availability, and the spatial resolution. For example, the GFSAD1km cropland map was assessed using 8 regions based on the availability of a proportional and optimum size of reference data available from IIASA's Geo-wiki. Similarly, the GFSAD250m cropland map was assessed using 4 regions mapped simply as the four different continents. Finally, the GFSAD30m cropland map was assessed using 15 regions which were combined with country boundaries from the original 72 AEZ-based homogeneous regions (Table 12).

Table 12. The list of regions used in the assessment of the three different GFSAD cropland extent maps.

Datasets	Regions
GFSAD1km	8 (Africa, North-America, South-America, Australia, Europe, South-Asia, South-East Asia, and China/Mongolia)
GFSAD250m	4 (South-Asia, North-America, Africa, and Australia)
GFSAD30m	15 (United States, Canada, Mexico, Central America, Car. Islands, Iceland, South-America, Africa, Europe, Russia, and Mid-East, South-Asia, South East Asia, Australia, New Zealand, China, Mongolia)

Second, an appropriate sampling approach is comprised of a sampling scheme, a sample unit, and a sample size (i.e., appropriate number of samples) for collecting valid reference data. The sampling design needs to be easy to implement and capable of accounting for the proportion of high and low map categories such as crop and no-crop distribution in different continents in order to perform the assessment on a global scale (Card, 1982). A simple random sampling scheme was employed for each region to collect a sample proportional to the cropland and non-cropland map class distribution. A sample unit of 90m x 90m was used to collect reference samples to assess the GFSAD30m cropland map. In contrast, sample units of 250m x 250m and 1km x 1km were used to assess the GFSAD250m and GFSAD1km cropland extent maps, respectively. The most challenging component of sampling is the collection of a sufficient number of samples. The number of samples to assess the GFSAD1km cropland map was determined based on the availability of Geo-wiki samples and the proportional area of the different regions. After a thorough review of Geo-Wiki dataset, it was observed that all the eight regions could be sampled with a minimum sample size of 200. This minimum sample size was balanced with the area

proportions in each region. To assess the GFSAD250m and GFSAD30m cropland extent maps an optimum sample size of 250 was selected based on a Monte Carlo sampling simulation analysis.

Third, the accuracy of the three different GFSAD cropland extent maps was evaluated using two different assessment techniques: (1) an error matrix and (2) a difference image. First, error matrices were generated using the following steps: (1) extract the map and reference labels for the random samples from the cropland extent map and reference map, respectively, (2) output an attribute table using ArcGIS that lists the map and reference labels, and (3) generate the error matrix by comparing these two labels using a program written in R. The error matrix was then used to calculate various measures of accuracy including overall, producer's, and user's accuracies (Story and Congalton, 1986; Congalton, 1991). Second, a difference image was generated by comparing the GFSAD250m and GFSAD30m cropland map for the United States with the resampled and cross-walked CDL reference map. This analysis was possible only for the US because of the availability of this CDL reference map. The two difference images generated at two different spatial resolutions clearly demonstrated the spatial distribution of agreement and disagreement between these two thematic maps.

Comparison

The three different resolution cropland maps were compared for the three different agriculture field sizes based on the following three characteristics observed at the three different spatial resolutions: (1) the look of the map, (2) cropland area similarity, and (3) heterogeneity or clumping in the cropland landscape. First, the look of the spatial extent of the cropland patches at three different spatial resolutions was compared with the expected cropland distribution from high resolution

reference images to show how the map looks at each resolution. This method is simply a qualitative comparison. Second, the similarity of cropland areas mapped at different spatial resolutions was determined based on a contingency table approach in the form of a similarity matrix (Sun and Congalton, 2018). The area of each mapped class of the fine resolution cropland map was presented in the rows while the area of each class on the coarse resolution map was presented in the columns of the similarity matrix (Table 13).

Table 13. An example of a similarity matrix

		Coarse map		
		Class 1	Class 2	Total
Fine map	Class 1	A_{11}	A_{12}	A_{1+}
	Class 2	A_{21}	A_{22}	A_{2+}
	Total	A_{+1}	A_{+2}	

In the Table 13, A_{11} and A_{22} denotes the area that is classified as Class 1 and Class 2, respectively both in the fine and coarse resolution cropland extent maps. The diagonal values represent the consistency or the similarity for each class between the fine and coarse resolution maps. The column totals A_{+1} and A_{+2} sums the area of class 1 and class 2 on the coarse resolution map, respectively. Likewise, A_{1+} and A_{2+} represent the row totals of class1 and class 2, respectively on fine resolution cropland map. The commission error (CE) for class *i* can be evaluated by $A_{+i} - A_{ii} \,/\, A_{+i}$, which represents the percentage of area for class i that is committed from the fine resolution map. The omission error (OE) for class *i* of the coarse map can be evaluated by $A_{i+} - A_{ii} \,/\, A_{i+}$ which represents the percentage of area for class i that is omitted from the coarse map.

The overall similarity (OS) was evaluated by $\sum_{i=0}^{n} A_{ii} / \sum_{i=0}^{n} A_{i+} = \sum_{i=0}^{n} A_{ii} / \sum_{i=0}^{n} A_{+i}$, which represents the percentage of the area for all classes that are correctly represented in the coarse resolution map. The calculation of similarity matrix for crop and no-crop classes was performed in the following seven steps:

1. The area comparison was initialized with a resampling of 250m to 240m map and 1km to 960m map respectively making all three cropland extent maps comparable with each other. This resampling was necessary to incorporate the 30 m spatial resolution map.

2. Compute the total number of the square windows (N_{SW}) of coarse resolution map required to cover the fine resolution map.

3. Place square window over the fine resolution map. The value of square window corresponds to the class label of the coarse resolution map.

4. Identification of class label of coarse and fine resolution map pixels within the square windows.

5. Calculate the area of class 1 and class 2 of the fine resolution map within the coarse pixel.

6. This comparison was performed by moving a 240m and 960m window over different resolution cropland extent maps (Figure 17). Within the moving window, the high-resolution cropland map area was calculated. In Figure 17, each moving coarse resolution square window represents the area of cropland calculated from high resolution cropland pixels.

7. Finally, all the comparisons were reported is a tabular array i.e., a similarity matrix comparing the two pairs of cropland extent maps (Sun and Congalton, 2018).

All the above-mentioned comparison steps were implemented on three pairs of combinations (i.e., 960m-30m, 960m-240m, and 240m-30m) for calculating the cropland area mapped at fine spatial resolution within the coarse resolution pixels at nine study sites in different agriculture field sizes (Figure 17).

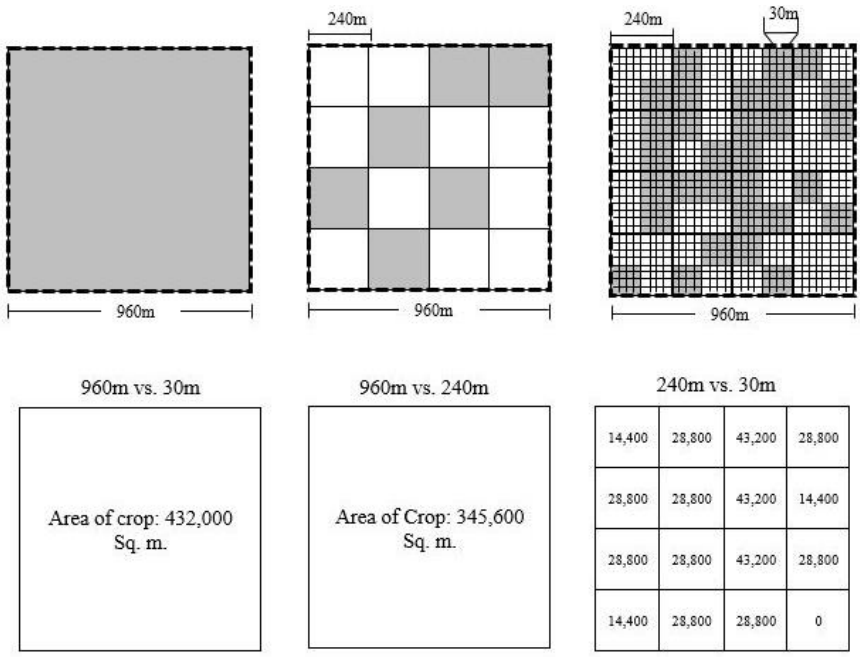

Figure 17. The implementation scheme of similarity matrix to compare the area of cropland on different resolution maps.

Third, two landscape metrics, Per-Patch-Unit (PPU) and the Percentage of LANDscape (PLAND), were calculated and compared for each study site to understand the heterogeneity and clumping in the cropland landscape at three different resolutions with respect to different agriculture field sizes (Frohn, 1997). The most common landscape clumping metric, contagion, was replaced with an alternative, more suitable landscape metric, PPU, because it is less sensitive

to spatial resolution and more sensitive to landscape pattern. The PPU values are expected to be low for less fragmented landscapes and increase with landscape fragmentation. The PPU metric was calculated by using $PPU = m / (nx\lambda)$ for each study site, where m is the total number of patches, n is the total number of pixels, λ is a scaling constant equal to the area of a pixel and expressed in sq. m. units. In addition to PPU, the PLAND metric was calculated in the Fragstats software for each study site for measuring landscape composition (i.e., how much of the landscape is comprised of a patch type (e.g., cropland)). The PPU (clumping or fragmentation levels) and PLAND (the percentage of landscape in cropland) were compared by plotting their values for different agriculture field sizes to understand and analyze the discrepancies and similarities among the three different cropland extent maps. Finally, based on the comparison results, more specific insights, suggestions, and recommendations were provided for when to apply the three different GFSAD cropland extent maps considering different agriculture field sizes.

Results

The accuracy assessment of the three different cropland extent maps follow an appropriate assessment strategy implemented in three main steps: (1) stratification, (2) sampling, and (3) accuracy. The first three sub-sections present the accuracy results for three different cropland extent maps performed in a similar fashion. The fourth subsection presents the comparison of the three cropland extent maps.

GFSAD1km Assessment

The accuracy assessment of GFSAD1km cropland extent map was performed in eight regions using 1,800 crop and no-crop samples as shown in Figure 18. Table 14 presents the area of each region, the area proportion of each region, and the number of reference samples used for each. Table 15 reports the overall, producer's and user's accuracy of GFSAD1km map achieved by region while Table 16 is the summary error matrix for the entire world. The regional overall accuracies range from 73.3% to 85.2%. The overall accuracy of GFSAD1km cropland map is 78.7% with a low (59.3%) user's accuracy of crop.

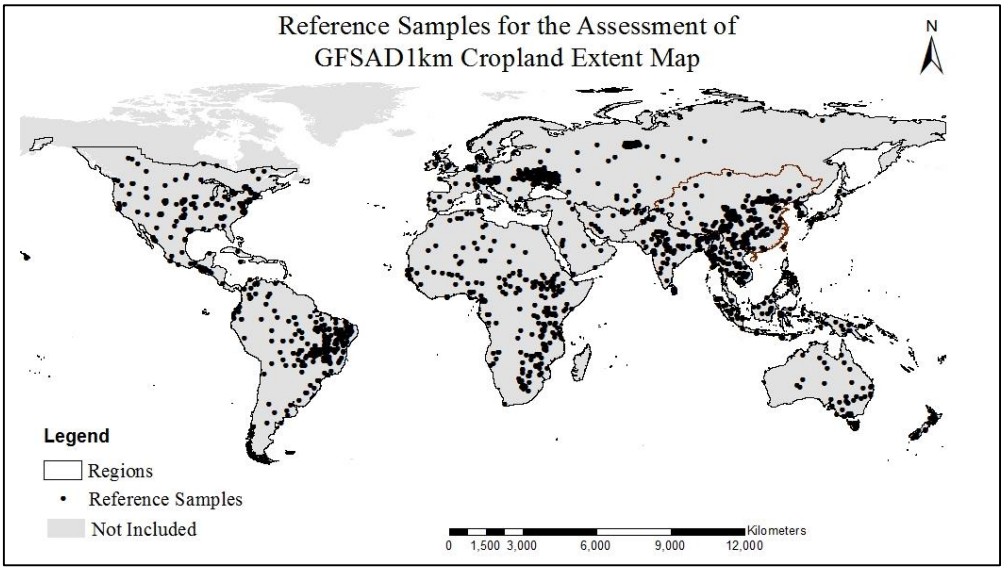

Figure 18. The distribution of eight regions along with the entire reference data of 1800 samples (Source: Geo-Wiki) used in the assessment of GFSAD1km cropland extent map.

Table 14. Regions, their area, and number of samples (Source: GeoWiki) that were used to assess the GFSAD1km Cropland extent map.

Regions (1km)	Area (sq. km.)	Area Proportion	Reference Samples
China and Mongolia	10,950,070	8.72	217
Africa	29,887,900	23.79	248
Europe	31,546,600	25.11	250
North America	15,248,925	12.14	224
South East Asia	5,603,730	4.46	209
South America	17,730,232	14.12	228
South-Asia	6,684,930	5.32	211
Australia and New Zealand	7,957,355	6.33	213
Total	125,609,742	100	1,800

Table 15. The accuracy measures of GFSAD1km map in eight regions.

Regions	OA%	UAC%	UANC%	PAC%	PANC%
China and Mongolia	73.3	41.4	94.6	83.7	70.7
Africa	79.4	50.7	90.5	67.3	82.7
Europe	73.6	59.7	96.8	96.9	59.1
North America	81.7	70.4	93.6	92.1	75.0
South East Asia	85.2	67.7	93.7	93.6	85.7
South America	76.8	66.2	81.5	61.8	84.2
South-Asia	75.4	45.1	98.3	95.4	70.2
Australia and New Zealand	85.1	76.3	88.5	71.4	90.8

OA: Overall Accuracy; UAC: User's Accuracy Crop; UNAC: User's Accuracy No-Crop; PAC: Producer's Accuracy Crop; PANC: Producer's Accuracy No-Crop

Table 16. The error matrix showing the overall accuracy of GFSAD1km cropland map.

		Reference Data			
		Crop	No-Crop	Total	User's Accuracy
Map	Crop	424	291	715	59.3%
Data	No-Crop	92	993	1,085	91.5%
Total		516	1,284	1,800	
Producer's Accuracy		82.2%	77.3%		78.7%

GFSAD250m Assessment

The results of the accuracy assessment of GFSAD250m cropland map performed in four regions using a reference dataset of 7,762 samples includes overall, producer's, and user's accuracy reported in the form of an error matrix (Figure 19, Table 17). The user's accuracy of crop in Africa is slightly less than other regions (64.6%) because of the cropland variability in this continent. The overall error matrix and the overall accuracy of the four regions combined (94.8%) are presented in Table 18.

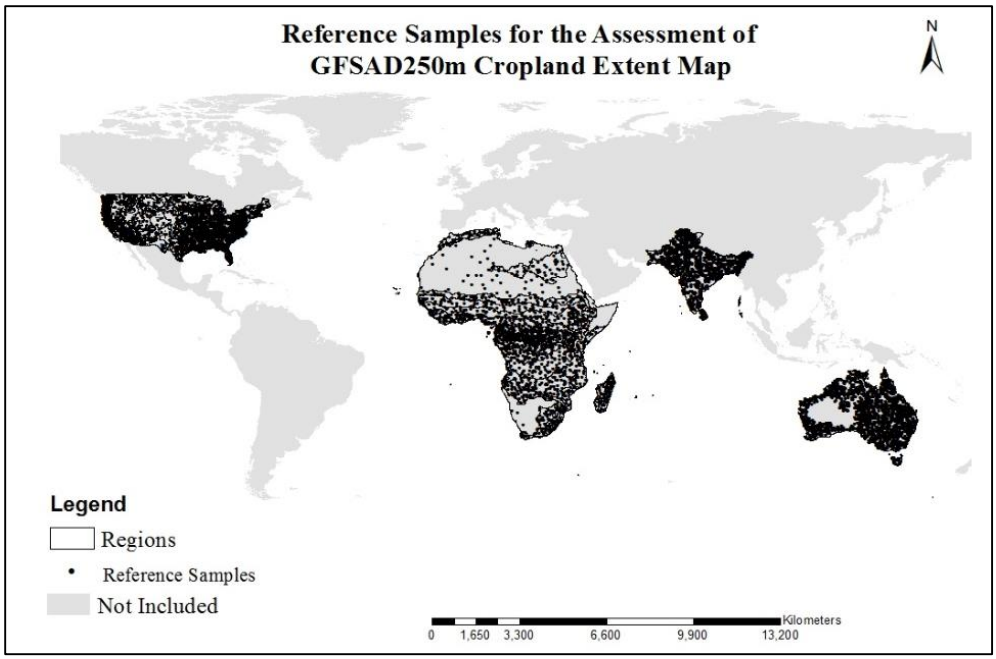

Figure 19. The distribution of reference samples distributed in the four regions (Source: Independent datasets generated by assessment team and field data collected for Australia (Teluguntla et al., 2017a) used to assess GFSAD250m cropland extent map.

Table 17. The accuracy measures of GFSAD250m cropland map.

Regions	OA%	PAC%	UAC%	PANC%	UANC%	Samples
United States	98.0	85.7	100	100	97.6	4,200
Africa	93.5	58.2	64.6	96.9	96.0	1,600
South-Asia	80.7	71.7	85.2	88.8	77.8	1,033
Australia	98.2	96.2	88.7	98.4	99.5	9,29
Total						7,762

OA: Overall Accuracy; PAC: Producer's Accuracy Crop; UAC: User's Accuracy Crop; PANC: Producer's Accuracy No-Crop; UANC: User's Accuracy No-Crop.

Table 18. The error matrix showing the overall accuracy of GFSAD250m cropland map.

		Reference Data			
		Crop	No-Crop	Total	User's Accuracy
Map	Crop	1,054	119	1,173	89.9%
Data	No-Crop	288	6,301	6,589	95.6%
Total		1,342	6,420	7,762	
Producer's Accuracy		78.5%	98.2%		94.8%

GFSAD30m Assessment

The accuracy assessment of GFSAD30m cropland was map performed in 15 regions using a reference dataset of 19,171 samples as shown in Figure 20. Table 19 shows the total number of regions, their area, and the reference samples selected for each of the 15 combined regions. The accuracy results of GFSAD30m cropland map are presented in an error matrix for the entire world and a difference image, just for the US. First, the overall, producer's, and user's accuracy were calculated for all the 15 regions and presented in Table 20 along with total number of samples. Most of the regions have high overall accuracy ranging from 84.5% for South-Asia to 98.3% for Mongolia. The overall error matrix and the overall accuracy of GFSAD30m cropland map for the entire world (91.7%) are presented in Table 21.

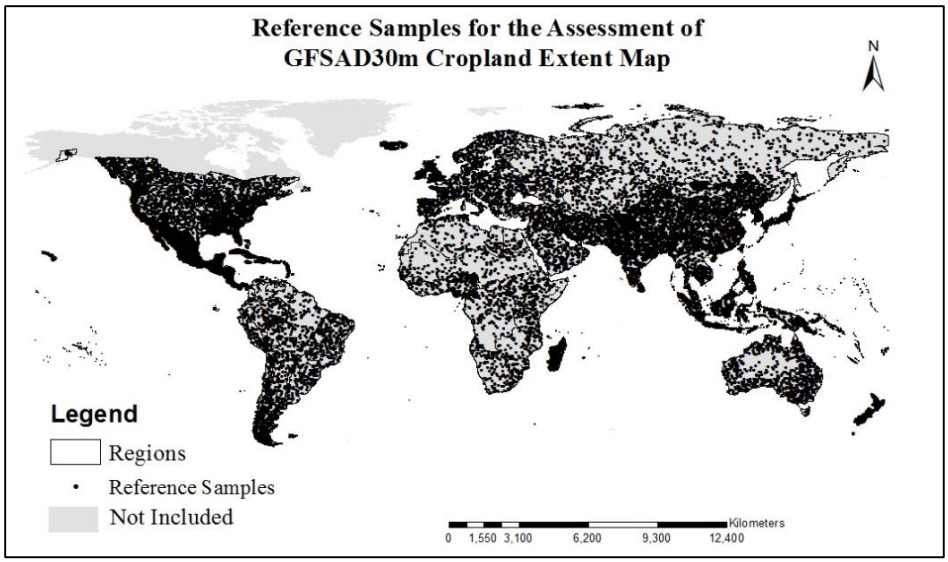

Figure 20. The distribution of regions and reference samples (Source: Independent reference datasets generated by assessment team from CDL and high-resolution imagery and field data collected for Australia (Teluguntla et al., 2017a) used to assess the GFSAD30m cropland extent map.

Table 19. Regions and number of reference samples used to assess GFSAD30m cropland map.

Combined Regions	Area (Mha)	Original Regions	Samples
United States	13.35	9	2250
Canada	10.86	3	750
Mexico	2.36	6	1463
Central-America	0.68	2	496
Cuba, Car. Is., DR Haiti, Alaska, Hawaii	64.67	5	1240
Iceland	0.17	1	250
South-America	20.60	5	1250
South-East Asia	6.21	7	1750
Africa	33.31	7	1750
Mongolia	2.28	3	300
New Zealand	26.3	2	500
China	14.86	3	1972
Europe, Russia, and Mid-East	3,076	12	3000
South-Asia	861.64	6	1500
Australia	768.7	1	700
Total	7,000.60	72	19,171

Table 20. The accuracy measures of GFSAD30m GFSAD cropland map.

Regions	**OA %**	**PAC %**	**UAC %**	**PANC %**	**UANC %**
Africa	93.7	85.9	98.5	94.8	98.1
South America	94.7	82.6	76.7	96.4	97.5
Europe/Mid-East, Russia	90.8	86.5	85.7	92.9	93.3
South-Asia	84.5	74.8	82.0	90.2	85.8
South-East Asia	88.6	81.6	76.7	91.2	93.3
Mongolia	98.3	75.0	92.3	99.7	98.6
China	94.0	80.0	84.2	96.9	95.9
Australia	93.1	71.4	64.1	95.6	96.8
New Zealand	93.4	91.7	82.7	94.0	97.3
North America	92.8	87.2	75.8	94.0	97.1
Iceland	97.6	68.4	100.0	100.0	97.5

OA: Overall Accuracy; PAC: Producer's Accuracy Crop; UAC: User's Accuracy Crop; PANC: Producer's Accuracy No-Crop; UANC: User's Accuracy No-Crop

Table 21. The error matrix showing the overall accuracy of GFSAD30m cropland map.

		Reference Data			
		Crop	No-Crop	Total	User's Accuracy
Map Data	Crop	3,339	924	4,263	78.3%
	No-Crop	666	14,242	14,908	95.5%
Total		4,005	15,166	19,171	
Producer's Accuracy		83.4%	93.9%		91.7%

In addition to the error matrix, the disagreement in the cropland areas mapped in the GFSAD250m and GFSAD30m cropland extent maps are presented in the form of difference images for the US. Creation of the difference images is possible because of the availability of a complete reference map (i.e., CDL). Figures 21A and 21B show the spatial distribution of agreement and disagreement in the cropland areas mapped in the GFSAD250m and GFSAD30m as compared to the reference cropland map. The GFSAD250m cropland map has only 2% omission error and no commission error in the cropland areas as compared to resampled CDL 250m reference map. The GFSAD30m cropland map has 7% omission and 8% commission error in the cropland areas as compared to CDL 30m map. In other words, the GFSAD30m cropland map is 85% similar to the CDL 30m reference map.

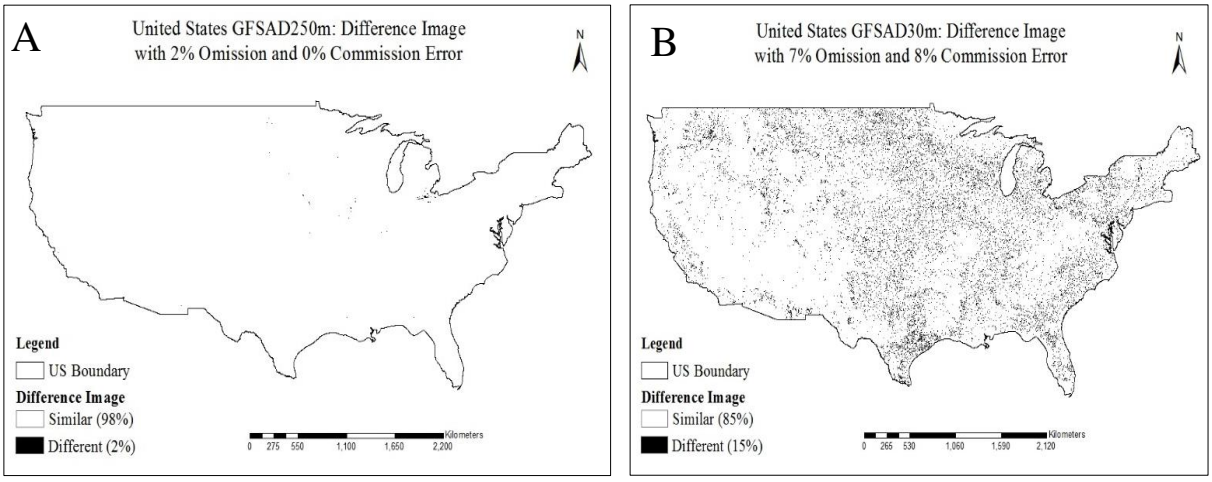

Figure 21A and 21B. Difference images representing the disagreement in the GFSAD250m (A) and GFSAD30m (B) cropland map of the US as compared to the reference map.

<u>Comparison of the three different GFSAD cropland extent maps</u>

Figure 22 presents a visual comparison of the GFSAD1km, GFSAD250m, and GFSAD30m cropland extent maps with the high spatial resolution imagery at nine random study sites for three different field sizes. All the three cropland maps look similar to each other in the large agriculture field sizes of the US and Australia. The GFSAD250m and GFSAD30m cropland maps look more similar to each other than the GFSAD1km cropland map in the medium field sizes of the US and the small agriculture field sizes of South-Asia and Africa. Finally, the visual comparison shows that the cropland areas mapped in GFSAD30m cropland map looks more similar to the spatial extent of the agriculture fields as seen on the high-resolution imagery (HRI) acquired for the same mapping year.

Second, the area comparison performed using the similarity matrix approach shows the overall similarity between the three different cropland maps with respect to different agriculture field sizes

(Table 22, Figure 23). All three cropland maps (i.e., GFSAD30m, GFSAD250m, and GFSAD1km) have high similarity in their cropland areas with respect to the large agriculture field sizes of the US and Australia and small field sizes of South-Asia. However, the GFSAD1km cropland map has low similarity with the other two cropland maps (i.e., GFSAD30m and GFSAD250m) with respect to medium and small field sizes for each continent.

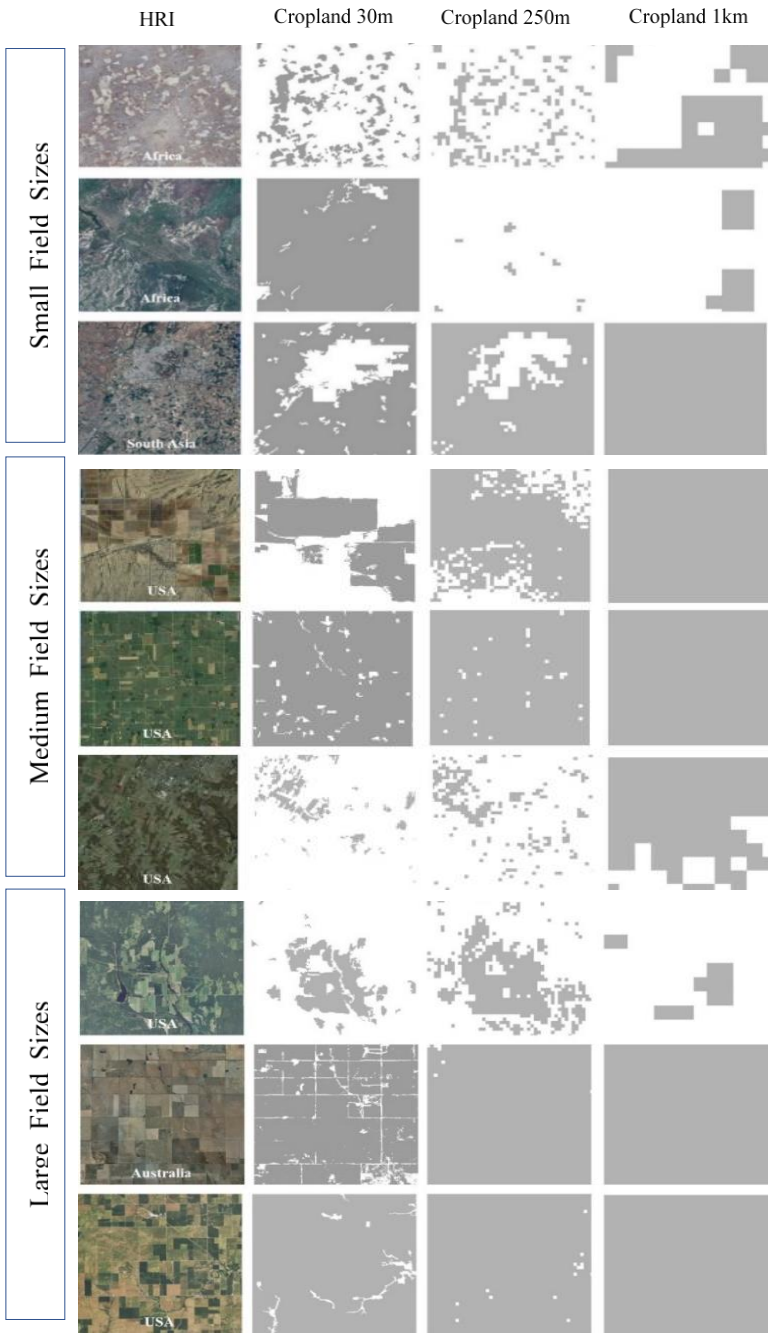

Figure 22. Visual comparison of the three different GFSAD cropland extent maps with high resolution images acquired in the small, medium, and large field sizes at random study sites in the entire world. The gray area represents the crops.

Table 22. Overall Similarity between different resolution cropland extent maps.

Overall Similarity (%) between 30m, 250m, and 1km GFSAD maps in different field sizes			
Field Sizes	30m-250m	30m-1km	250m-1km
Small Africa 1	77.9	51.1	51.5
Small Africa 2	7.2	18.2	85.1
Small South-Asia 3	82.9	72.5	84.3
Medium USA 1	69.0	42.6	72.1
Medium USA 2	93.6	91.4	95.4
Medium USA 3	87.6	35.9	40.8
Large USA 1	95.4	42.2	41.3
Large Australia 2	91.4	91.0	99.3
Large USA 3	80.1	82.4	72.2

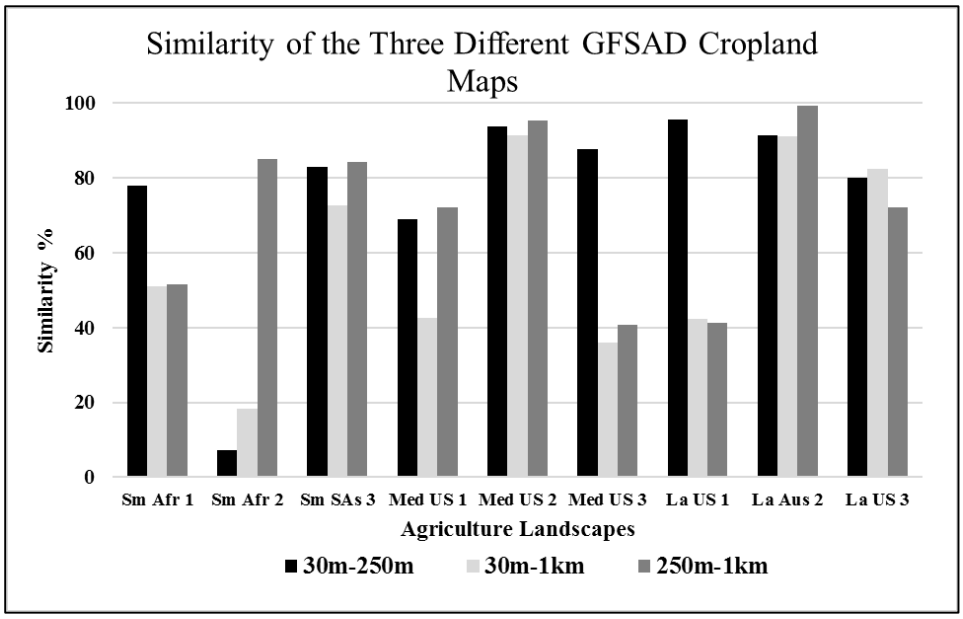

Figure 23. The similarity in the cropland areas mapped at the three different spatial resolutions in different agriculture landscapes.

In addition to the overall similarity, the similarity matrix approach provided omission and commission errors introduced in the cropland areas mapped at coarse spatial resolution when compared with the fine spatial resolution. The estimated errors of each study site are represented as the percent of cropland areas which were either omitted from or committed to the coarse resolution cropland maps (Table 23). For each study site, three different omission (OE) and commission errors (CE) were calculated, one for each of the three combinations of coarse and fine resolution cropland maps. For example, the omission error presented in the third column of the Table 23 (i.e., 58.0%) represents the percentage of cropland areas omitted from the 250m map as compared to the 30m map in the small agriculture fields of Africa. The additional rows in the third column (i.e., 82.3% and 82.7%) represents the omission in the cropland areas from the 1km map when compared to 30m and 250m cropland maps, respectively.

Table 23. Omission Error (OE) and Commission Error (CE) of crop in the coarser resolution maps as compared to fine resolution for nine different study sites.

Resolution	Study Site	OE	CE
250m vs 30m	Small Africa 1	58.0	59.7
1km vs 30m		82.3	57.5
1km vs 240m		82.7	56.8
240m vs 30m	Small Africa 2	0	98.2
1km vs 30m		4.9	85.9
1km vs 240m		100	100
250m vs 30m	Small South-Asia 3	14.9	7.2
1km vs 30m		27.4	0
1km vs 250m		15.7	0
250m vs 30m	Medium USA 1	42.0	1.8
1km vs 30m		57.4	0
1km vs 250m		27.9	0
250m vs 30m	Medium USA 2	5.4	1.3
1km vs 30m		8.5	0
1km vs 250m		4.6	0
250m vs 30m	Medium USA 3	67.4	51.4
1km vs 30m		89.4	7.7
1km vs 250m		84.5	19.8
250m vs 30m	Large USA 1	3.3	1.4
1km vs 30m		4.2	59.4
1km vs 250m		3.0	59.7
250m vs 30m	Large Australia 2	8.5	0.2
1km vs 30m		8.9	0
1km vs 250m		0.8	0
250m vs 30m	Large USA 3	53.3	22.1
1km vs 30m		47.2	82.4
1km vs 250m		32.3	86.4

Third, the comparison of two landscape metrics (i.e., PLAND and PPU) calculated for each study site shows the similarity between the three different GFSAD cropland maps in for the three different agriculture field sizes and spatial resolutions (Table 24). Figure 24 and Figure 25 show the values of PLAND and PPU, respectively as calculated for the three different spatial resolution maps for the three different agriculture field sizes. Figure 26 presents the comparison of the two landscape metrics separately in each agriculture field size to clearly show the similarity among the three different cropland maps.

Table 24. Landscape parameters in different resolution maps for all the nine study sites.

Study Site	Resolution	TA(ha)	NP	PLAND	PPU
Small Africa 1	30m	10,072.1	120	19	1.19
	250m	10,593.7	64	17.3	0.60
	1km	11,000	7	46.4	0.06
Small Africa 2	30m	10,029.6	61	97.2	0.60
	250m	10,318.7	9	1.5	0.08
	1km	11,000	3	12.7	0.02
Small South-Asia 3	30m	13,951.8	83	57.5	0.59
	250m	10,450	12	85.3	0.11
	1km	10,200	1	100	0.01
Medium USA 1	30m	10,030.1	67	8.5	0.66
	250m	10,443.7	61	13	0.58
	1km	11,900	5	77.3	0.04
Medium USA 2	30m	10,059.9	69	96.2	0.68
	250m	10,337.5	20	98.6	0.19
	1km	11,500	1	100	0.01
Medium USA 3	30m	10,133.9	37	43.6	0.36
	250m	10,337.5	20	1.4	0.19
	1km	11,700	2	99.1	0.02
Large USA 1	30m	10,045.17	14	96.49	0.14
	250m	10,076.85	13	98.1	0.13
	1km	9,946.35	7	40	0.07
Large Australia 2	30m	9,581	67	100	0.69
	250m	10,437.5	5	99.76	0.05
	1km	10,500	1	100	0.01
Large USA 3	30m	10,054.8	40	17.2	0.39
	250m	10,356.25	41	28.5	0.39
	1km	112,000	4	5.4	0.00

TA: Total Area; NP: Number of Patches; PLAND: Percentage of Crop in the Landscape; PPU: Per-Patch Unit

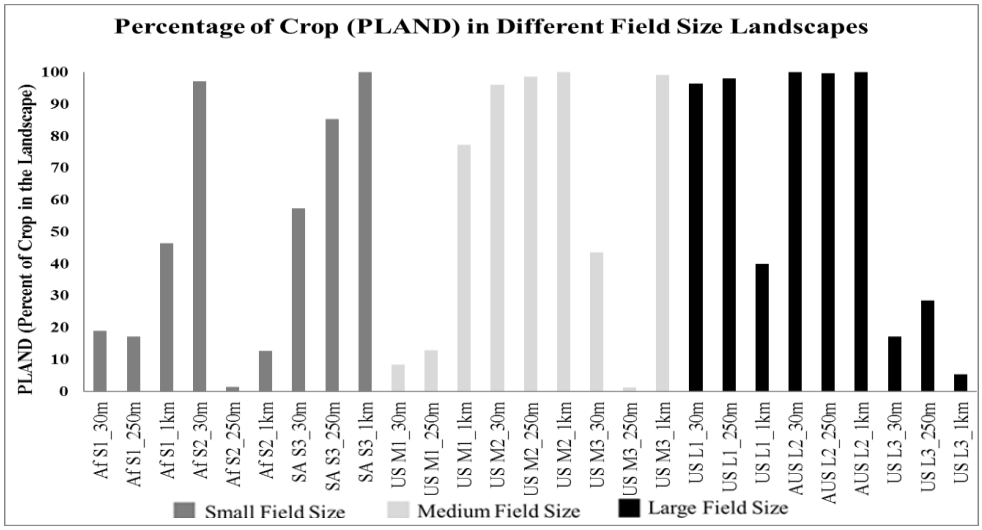

Figure 24. The differences in the percentage of cropland areas in different field size landscapes.

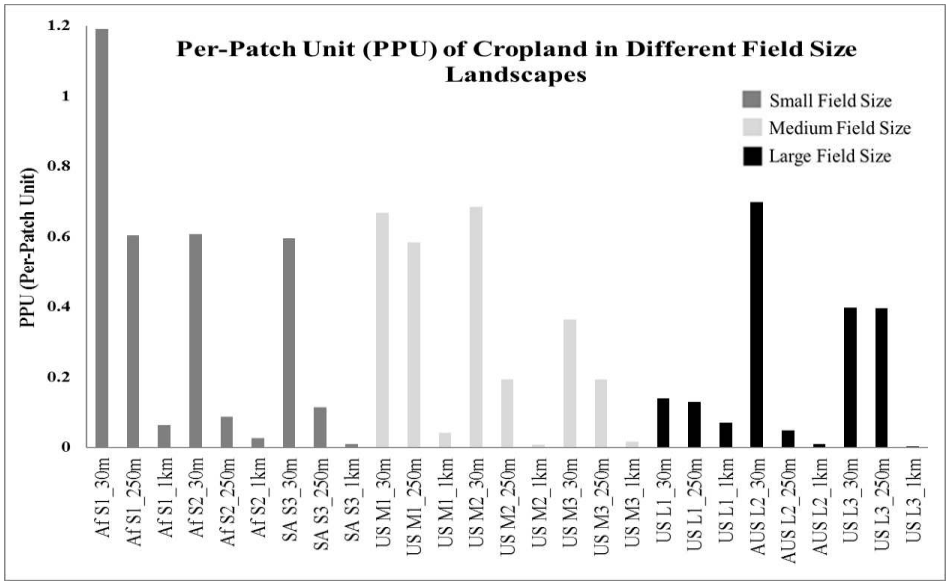

Figure 25. PPU Landscape heterogeneity of different resolution maps in different field size landscapes.

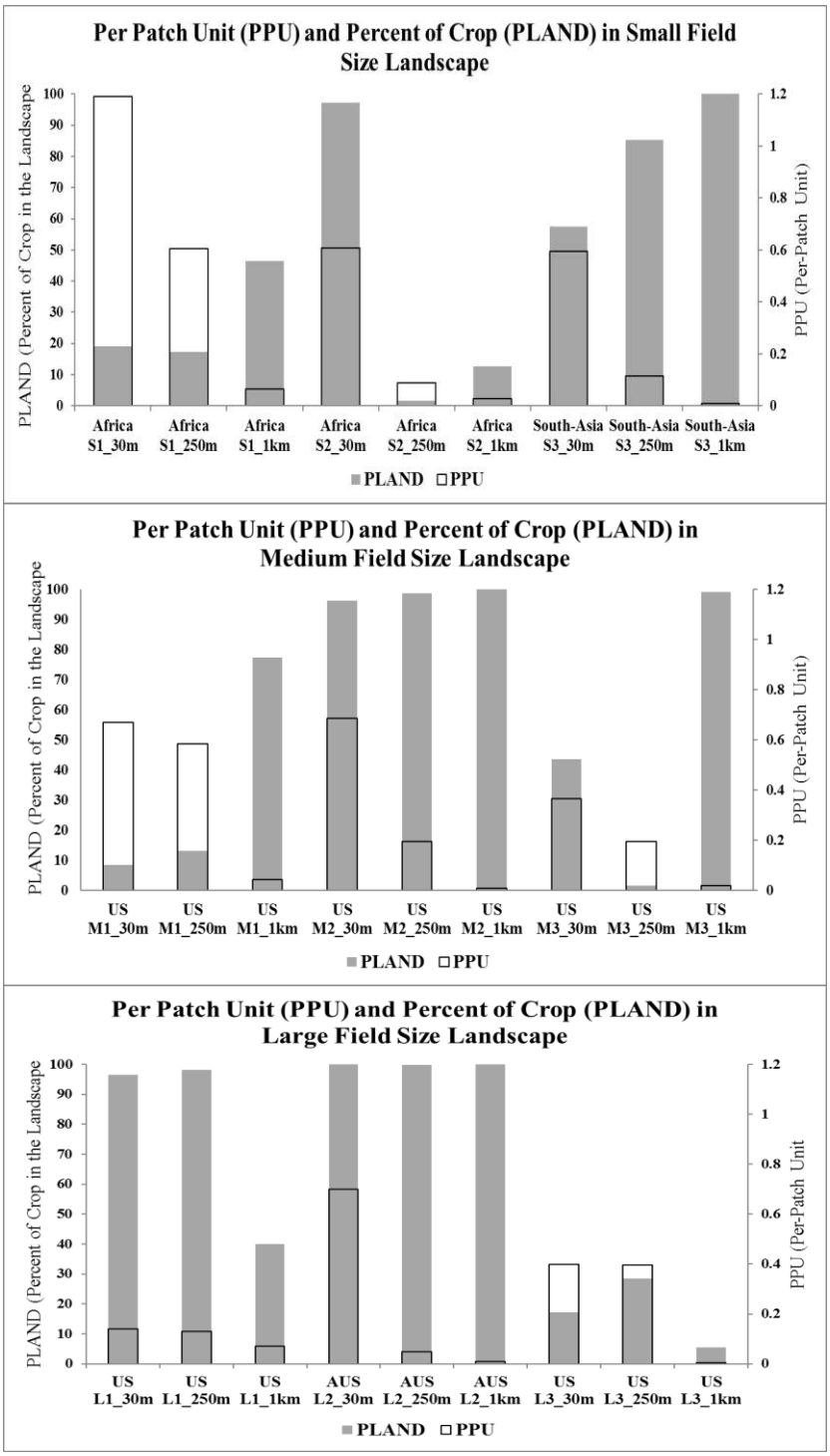

Figure 26. The comparison of landscape heterogeneity and area proportions in small, medium, and large field sizes.

Discussion

With the release of three different resolution GFSAD cropland maps, it becomes crucial to know their individual accuracy and comparative similarity to make a choice on using either coarse or high-resolution map in different agriculture field sizes. This paper presented an appropriate accuracy assessment and detailed comparison of the three cropland maps at random study sites in different agriculture landscapes that are consistent with previous assessment and comparison studies (Vancutsem et al., 2013). Therefore, the results of an appropriate assessment methodology must be discussed to provide insight into the quality, reliability, (un)certainty, and similarity of cropland maps in different regions and spatial resolutions and how the specific recommendations were determined for their use in different agriculture field sizes (Olofsson et al., 2012; Stehman et al., 2012).

Assessment of the three different GFSAD cropland extent maps

The assessment of the three different cropland maps was performed using an accuracy assessment approach involving stratification and appropriate sampling resulting in accuracy measures for different regions of the entire world. The accuracy measures (e.g., overall, user's, and producer's accuracy) estimated for the entire world and different regions establish the quality of the three GFSAD cropland maps and how it varies with the distribution and size of the agriculture fields of each region. It has been well established in the past that the cropland mapping provides accurate results towards a high spatial resolution due to the detailed mapping of the agriculture fields of the heterogeneous cropland landscapes at a smaller pixel size (i.e., 30m) (Pérez-Hoyos et al., 2017). This assumption is also supported by the overall accuracy results of this paper showing high

accuracy of the GFSAD30m cropland extent map (91.7%) than the coarse resolution GFSAD1km map (78.7%) by removing the spectral mixing that is common at coarse resolution pixels of 250m and 1000m (Table 17 and Table 22). However, the overall accuracy of the GFSAD250m crop extent map (94.8%) was estimated from the reference data of the four continents and therefore, cannot be compared with the 30m and 1km map accuracies.

The overall accuracy of the three different cropland maps were also estimated for each region in addition to a single overall accuracy of the entire world. The overall accuracy of the GFSAD1km, GFSAD250m, and GFSAD30m cropland map range from 73.3% to 85.2% in the eight regions, 80.7% to 98.2% in the four regions, and 84.5% to 94.7% in the fifteen regions, respectively (Table 16, 18, and 21). The range of overall accuracy of the three cropland maps in different regions are different due to differences in the distribution, proportion, and size of the agriculture fields in the homogeneous and heterogenous cropping patterns of each region. However, the overall accuracy of the GFSAD30m cropland map of each region are still higher than the coarse resolution GFSAD 250m and GSFAD1km maps. Therefore, the single overall accuracy of the three cropland maps of each region and the entire world indicates that the high resolution GFSAD30m cropland map is more accurate than the coarse resolution maps both at global and regional scale.

In addition to a single overall accuracy of the cropland maps that has been typically reported in the literature, the assessment of each region provides an additional information including crop extent user's and producer's accuracies. It has been observed that the GFSAD1km crop extent user's accuracy is low (50.7%) than the GFSAD250m (64.6%) and GFSAD30m cropland maps (98.5%) in some regions (e.g., Africa) (Table 16, 18, and 21) due to differences in the distribution,

proportion, and size of the agriculture fields of each region. In contrast, the GFSAD250m crop extent map user's and producer's accuracies of the US, South-Asia, and Australia are high compared to Africa. However, Australia also has a sparse distribution of cropland like Africa, but the cropland distribution is more compact and concentrated toward the edges of the continent. Therefore, the differences in the cropland distribution and field size of Australia and Africa achieve different user's accuracy of the GFSAD250m and GFSAD1km crop extent maps.

The accuracy measures estimated in Table 20 shows that the GFSAD30m crop extent user's accuracy ranges from 64.1% (Australia) to 100.0% (Iceland). The GFSAD30m crop extent map user's accuracy of Africa (98.5%) indicates that the small size of agriculture fields of Africa in a heterogeneous cropping pattern can be accurately mapped at high spatial resolution. However, the GFSAD30m user's accuracy of Australia is low because of the sparse cropland distribution and large agriculture field sizes. It is commonly observed from the assessment results of this paper that the low user's accuracies of crop were mostly reported in the low crop proportion regions of the entire world irrespective of the spatial resolution of the crop extent map. Therefore, this paper suggests a detailed analysis of the accuracy measures of low crop probability regions must be performed in future to achieve meaningful assessment results.

In addition to the crop extent user's and producer's accuracy, the assessment results also present the difference image generated based on a pixel-by-pixel comparison of the reference and classified maps. The difference image shows the spatial distribution of the omission and commission errors introduced in the cropland maps of the US at different spatial resolutions. The high spatial resolution crop extent map (i.e., GFSAD30m) has more omission and commission errors in the cropland areas than the coarse resolution maps (Figure 21). The probability of errors

occurring for the high spatial resolution is increased due to identification of the edges of agriculture fields using an object-based classification and removal of spectral mixing caused by the natural vegetation that is common in a coarse resolution pixel.

Comparison of the three different GFSAD cropland maps

The comparison of the three different resolution cropland maps was performed highlighting the similarity in their look, crop area proportion, and clumping at nine random study sites in three different agriculture field sizes of different continents (e.g., Australia, United States (US), South-Asia, and Africa) (Chen et al., 2017; Pérez-Hoyos et al., 2017). The results of the comparison of the three different GFSAD crop extent maps show that the looks, proportion, and clumping of the cropland areas mapped at different spatial resolutions vary with the size of the agriculture fields (Figure 22, 23, 24, and 25). The clumping of the cropland areas (PPU) also decrease with increasing spatial resolution as the landscape becomes more generalized and contagious from high resolution to low resolution cropland maps (Figure 25) (Frohn, 1997). However, these decreasing trends are not uniform in different agriculture field sizes of different continents.

As the size of the agriculture fields becomes smaller, the characteristics of the cropland areas are mapped more accurately towards the higher spatial resolutions by minimizing the spectral mixing of agriculture fields caused by surrounding natural vegetation that is more common at coarse resolution pixel (Figure 22, 23, and 24) (Bayas et al., 2017). In the small field sizes of Africa and South-Asia, the spatial extent, proportion, and patches of the cropland areas of high spatial resolution crop extent map (GFSAD30m) more similar to the reference map than the coarse resolution GFSAD250m and 1km maps. However, in medium field sizes of the US, only GFSAD30m and GFSAD250m crop maps follow the decreasing trend to look similar as the

reference map compared to GFSAD1km map. In large field sizes of the US and Australia, the characteristics of all the three crop extent maps decrease from coarse spatial resolution to high resolution and look similar to the reference map. Therefore, the similarity in the characteristics of cropland areas mapped at different spatial resolutions provide an appropriate consideration and recommendations for using the three different crop extent maps in different agriculture field sizes (Figure 24 and 25). It can also be stated that the agriculture monitoring must be carefully executed even in the same field sizes of different continents (e.g., Africa, South-Asia, Australia, and the US) using an appropriate spatial resolution cropland map.

Determining specific recommendations for when to apply the three GFSAD cropland maps

The similarity in the characteristics of the cropland areas were used to determine the suitability recommendations for when to apply the three different cropland maps for agriculture monitoring in different agriculture field sizes (Figure 26). Table 25 indicates the similarity of the proportion and clumping of cropland areas among the three crop extent maps as low and high based on the PLAND and PPU estimates, respectively achieved in different field sizes. In the large agriculture fields of Australia and the US, the two cropland characteristics are highly similar among all the three different cropland maps. In the medium field sizes of the US, the cropland characteristics are similar in the GFSAD30m and GFSAD250m crop extent maps as compared to the GFSAD1km map. In small agriculture field sizes of Africa and South-Asia, only the GFSAD30m crop extent map presents highly similar and accurate characteristics of the cropland areas. Therefore, Table 24 presents the suitable spatial resolution crop extent maps that could be recommended in different field sizes to perform the agriculture monitoring practices.

Table 25. The specific recommendations for when to apply three spatial resolution GFSAD cropland extent maps with respect to different agriculture field sizes.

Landscape/ Sites	Continents	Similarity in Proportion	Similarity in Clumping	Suitable Spatial Resolution
Small, S1	Africa	Low	Low	30m
Small, S2	Africa	High	High	30m, 250m
Small, S3	South-Asia	High	High	30m, 250m
Medium, M1	US	High	Low	30m, 250m
Medium, M2	US	High	Low	30m, 250m
Medium, M3	US	Low	High	30m
Large, L1	US	Low	Low	30m
Large, L2	Australia	High	Low	30m, 250m, and 1km
Large, L3	US	High	Low	30m, 250m, and 1km

US: United States, CAP: Cropland Area Proportion

Conclusions

Over the last few years, the mapping of global cropland datasets has been rapidly increasing. With the recent release of the three different GFSAD cropland extent maps produced by different researchers, their quality and reliability must be evaluated at global and regional scales. To our knowledge, the accuracy assessment of the GFSAD cropland extent maps are the first investigations on large area accuracy assessment. Although assessments of global thematic maps were implemented with the same purpose, small size reference data were used to report one single global accuracy for the entire world. The large area accuracy assessment of three different GFSAD cropland maps provides an appropriate sampling strategy for collecting a large cropland reference data to achieve meaningful accuracy results for different continents. The assessment report of the

GFSAD30m cropland extent map is available online at https://lpdaac.usgs.gov (Congalton et al., 2017, Yadav and Congalton, 2018b). The assessment results of the three different GFSAD cropland extent maps revealed that the high-resolution cropland extent map (i.e., GFSAD30m) is more accurate than the coarse resolution maps. The significant differences in the accuracy results at different spatial resolutions make the tendency of using high resolution datasets more frequently unless the coarse resolution maps are not required for any user's specific interest. Despite differences in the accuracy measures among three cropland maps, the differences were also observed for a single cropland map in different regions due to the prevalent cropland distribution, proportion, and distribution of reference samples (i.e., sampling). Low producer's and user's accuracies along with an insufficient sample size were noticed for low crop proportion regions of different continents in the entire world due to the equal probability consideration of simple random sampling design. Therefore, this paper provides a future implication of performing more detailed error analysis for different crop proportion regions with respect to the sampling methods of accuracy assessment.

The coarse resolution cropland maps cannot be discarded completely in the presence of more detailed high-resolution cropland products. They should be compared with each other to quantify the similarity among the cropland areas mapped at different spatial resolutions. Large area comparisons might not provide a clear holistic view on the similarity in the proportion and heterogeneity of cropland areas in different field size landscapes of different continents. However, the site-specific comparison of different resolution cropland maps could be more effective in intelligently selecting an appropriate map to help farmers, crop yield predictors, food market researchers, and policy or decision makers for agriculture monitoring. Therefore, this paper

concludes on the following three main recommendations that must be considered to apply the three different cropland maps in three agriculture field sizes:

1. The cropland extent maps developed at 30m spatial resolution must be specifically recommended for their use in small agriculture field sizes of Africa. While, the cropland map developed at 30m and 250m spatial resolutions can be used for agriculture monitoring in small agriculture fields of South-Asia.
2. The cropland extent maps developed at 30m and 250m spatial resolutions are recommended for using them in the medium field sizes of the United States for different agriculture monitoring purposes.
3. The cropland extent maps developed at 30m, 250m, and 1km spatial resolutions (i.e., any of the different spatial resolution cropland maps) can be possibly used in the large agriculture field size of Australia and the United States.

CHAPTER V

Evaluating Sampling Designs for Assessing the Accuracy of Cropland Extent Maps in Different Cropland Proportion Regions

Abstract

The GFSAD30m cropland extent map has been recently produced at a spatial resolution of 30m as a part of NASA MEaSUREs' Program Global Food Security Data Analysis (GFSAD) project. Accuracy assessment of this GFSAD30m cropland extent map was initially performed using an assessment strategy involving a simple random sampling (SRS) design and an optimum sample size of 250 for each of 72 different regions around the world. However, while statistically valid, this sampling design was not effective in regions of low cropland proportion (LCP) of less than 15% cropland area proportion (CAP). The SRS sampling resulted in an insufficient number of samples for the rare cropland class due to low cropland distribution, proportion, and pattern. Therefore, given our objective of effectively assessing the cropland extent map in these LCP regions, the use of an alternate sampling design was necessary. A stratified random sampling design was applied using a predetermined minimum number of samples followed by a proportional distribution (i.e., SMPS) for different cropland proportion regions to achieve sufficient sample size of the rare cropland map class and appropriate accuracy measures. The SRS and SMPS designs were compared at a common optimum sample size of 250 which was determined using a sample simulation analysis in ten different cropland proportion regions. The results demonstrate that the two sampling designs performed differently in the various cropland proportion regions and therefore, must be selected according to the cropland extent maps to be assessed.

Introduction

The cropland regions of different continents distributed around the world exhibit different cropland proportions, cropping pattern, spatial extent, and heterogeneity due to their climatic, topography, and ecological conditions. The cropland maps of various cropland proportion regions are important for cropland monitoring and modeling, cropland change analysis, resolving food security issues, and improving crop productivity in different continents (Yu et al., 2017). To accomplish these objectives, cropland maps of various cropland regions have been generated continuously and effectively using remote sensing data at different spatial resolutions (Bartholome and Belward, 2005; Thenkabail et al., 2009; Yu et al., 2013; Gong et al., 2013). The GFSAD30m cropland extent map is one of the three GFSAD (Global Food Security Data Analysis) cropland extent maps (produced at 30, 250, and 1000 meter resolutions) which has been generated for various cropland proportion regions distributed around the world from satellite imagery and effective classification algorithms (Teluguntla et al., 2016; Xiong et al., 2017a, b, and c; Teluguntla et al., 2017a and b; Massey et al., 2017a and b; Gumma et al., 2017; Phalke et al., 2017; Oliphant et al., 2017; Zhong et al., 2017; Teluguntla et al., 2018; Massey et al., 2018).

The accuracy assessment of the GFSAD30m cropland extent map was initially performed using an assessment strategy involving a simple random sampling (SRS) design and an optimum sample size of 250 for 72 cropland regions around the world (Yadav and Congalton, 2018b). The results of this accuracy assessment reported accuracy measures in the form of error matrices for each region (e.g., overall, user's, and producer's accuracy) (Congalton, 1991). However, while statistically valid, this sampling design was ineffective in regions of low cropland proportion (LCP) of less than 15% cropland area proportion (CAP). The SRS design resulted in an insufficient

number of samples when the cropland class was rare due to low cropland distribution, proportion, and pattern (Stehman, 1999). As a result, the error matrices generated with such an insufficient distribution and allocation of samples for the rare cropland map class reported accuracy measures in the LCP regions that were not useful for our analysis (Pittman et al., 2010; Fritz et al., 2010; Fritz et al., 2011; Pérez-Hoyos et al., 2012; Waldner et al., 2015; Pérez-Hoyos et al., 2017). Therefore, given our objective of effectively assessing the cropland extent maps in these LCP regions, the use of an alternate sampling design was desirable and necessary.

Many researchers have expressed opinions on using different sampling designs (e.g., simple random sampling, stratified, and systematic unaligned sampling) to be used for assessing thematic map accuracy (Hord and Brooner, 1976; Rhode, 1978; Ginevan, 1979; Fitzpatrick-Lins, 1981; Congalton, 1991; Stehman, 1999; Congalton and Green, 2009). While different sampling approaches have been studied for achieving appropriate accuracy results in different landscapes, their effective use still needs to be established for various cropland regions around the world (Bayas et al., 2017). Determination of the cropland area proportion (CAP) of various cropland regions aids in defining an effective sampling area for applying probability-based sampling designs characterized either by simple random or stratified protocols for selecting the samples (Stehman, 1999). The probability-based simple random sampling (SRS) design, while statistically valid, results in an insufficient sample size of the rare cropland map class because each sample area has equal probability of selection and there is not enough area covered by cropland in the LCP regions. Therefore, an alternate probability-based sampling design imposed within strata defined by the map classes combined with a predetermined minimum sample size is one method to provide

sufficient samples and useful accuracy measures of these rare cropland maps (Stehman, 1999; Olofsson et al., 2014).

A minimum of 50 samples for each map category has been recommended as sufficient to generate statistically valid and meaningful accuracy measures (Congalton, 1991). This predetermined minimum sample size of 50 can be allocated to each stratum or map class with additional samples allocated proportionally to the cropland and non-cropland area depending on the total sample size and the cropland regions to be assessed (Olofsson et al., 2014). Bayas et al., (2017) has suggested that a larger sample size be implemented for assessing cropland regions that have between 25-75% cropland and that a smaller sample size would be enough to efficiently assess the cropland maps in areas with very high or very low cropland proportion. However, in most cropland assessments, mostly small samples sizes that are sparsely distributed have been used resulting in an ineffective assessment of the cropland extent maps of various cropland regions (e.g., Fritz et al., 2009; Gong et al., 2013). A larger sample size can achieve more appropriate and useful accuracy of the cropland extent maps (Tsendbazar et al., 2015). However, even a larger total sample size can result in insufficient samples and ineffective accuracies of the rare cropland map class if the samples are not distributed effectively. Rather than selecting sample size and strategy by the map complexity, the cropland distribution and proportion of each cropland region must be carefully considered to choose an optimum sample size to efficiently assess the cropland extent maps. Therefore, an optimum sample size must be chosen using a sample simulation analysis based on a Monte Carlo method for an effective and useful assessment of the cropland extent maps of various cropland regions (Hay, 1979; Congalton, 1988; Yadav and Congalton, 2018a).

This paper evaluates two sampling designs to perform an effective assessment of the GFSAD30m cropland extent maps of the various cropland proportion regions. The first is the simple random sampling (SRS) approach. The second is an alternate sampling design which is primarily a stratified design using a predetermined minimum of 50 samples per strata and a proportional allocation of the remaining total samples (SMPS). The SRS and SMPS designs were evaluated by comparing summary plots and detailed error matrices of the sample size and accuracy measures of the rare cropland map class.

Study Area

The study area comprises ten different cropland proportion regions selected from the 72 regions located around the world in which the GFSAD30m cropland extent map was initially assessed using the SRS design and an optimum sample size of 250 (Yadav and Congalton, 2018b; Fischer et al., 2012). Five of these study sites were purposely selected from the Low Cropland Proportion (LCP) regions and the other five were randomly selected from rest of the 72 regions. Figure 27 depicts the location of the ten selected cropland proportion regions for this study.

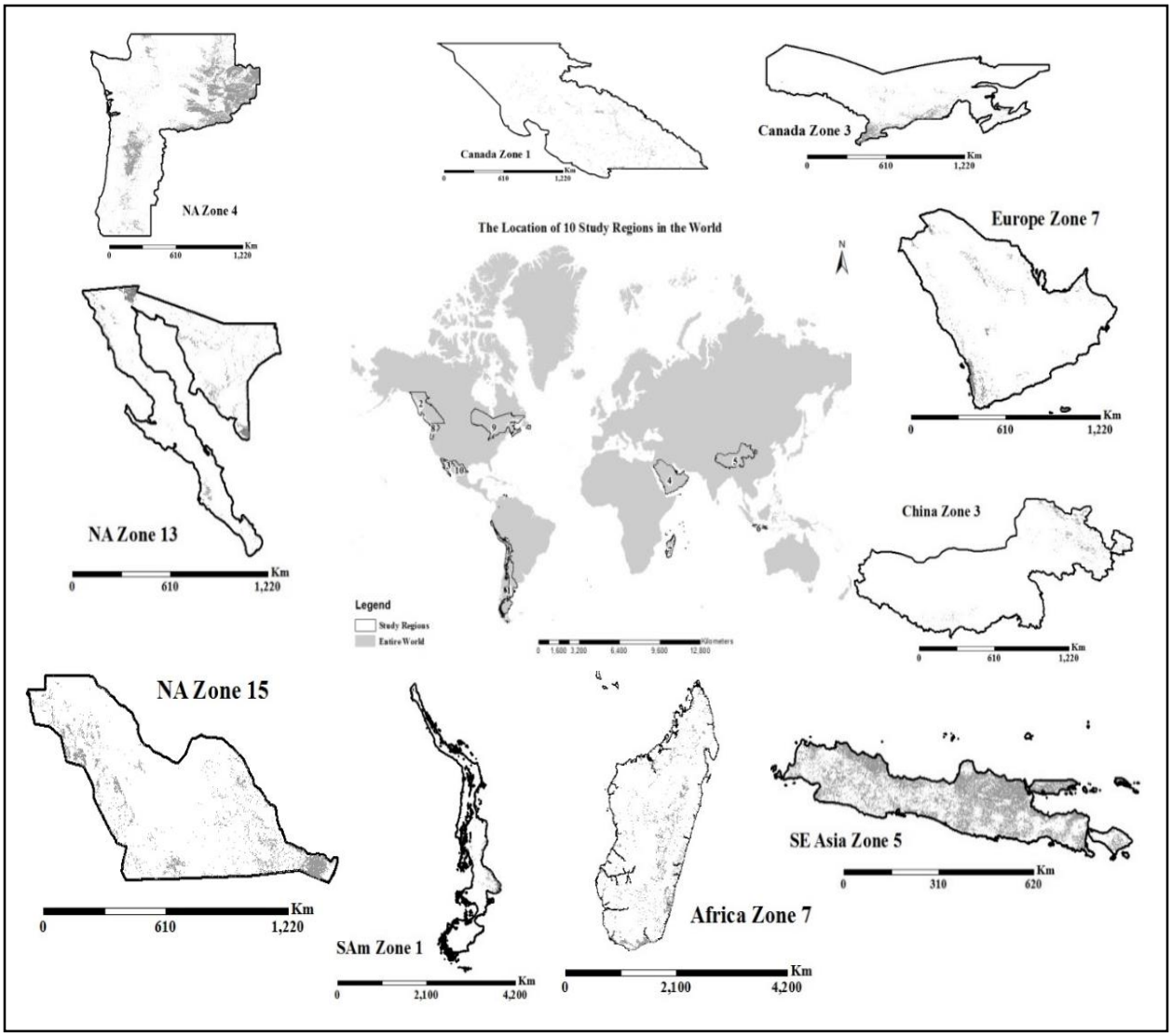

Figure 27. The location of various cropland regions around the world and the GFSAD30m cropland extent map.

Datasets

The ten selected study regions of the GFSAD30m cropland extent map which has been recently produced as a part of NASA MEaSUREs' (Making Earth System Data Records for Use in Research Environments) GFSAD project at 30m spatial resolution for the entire world were

evaluated using two different sampling designs. Separate reference datasets were necessary and were collected using the two different sampling designs from Google Earth imagery and existing cropland maps (e.g., Cropland Data Layer of the United States) to assess the ten regional GFSAD30m cropland extent maps. The first reference dataset was collected as a part of an initial assessment of the GFSAD30m cropland map using the SRS sampling design and an optimum sample size of 250 for the 72 cropland regions around the world (Yadav and Congalton, 2018b). The second reference dataset was collected using an alternate sampling design (i.e., SMPS) and simulated sample sizes from 50 to 300 only for the ten study cropland regions.

Methods

This section describes the methodology for evaluating the initial SRS and the alternate SMPS designs for assessing the GFSAD30m cropland extent maps in four steps: (1) estimating cropland area proportion (CAP), (2) applying the sampling designs, (3) choosing an optimum sample size for the SMPS approach, and (4) generating appropriate accuracy measures for the ten study cropland regions (Figure 28).

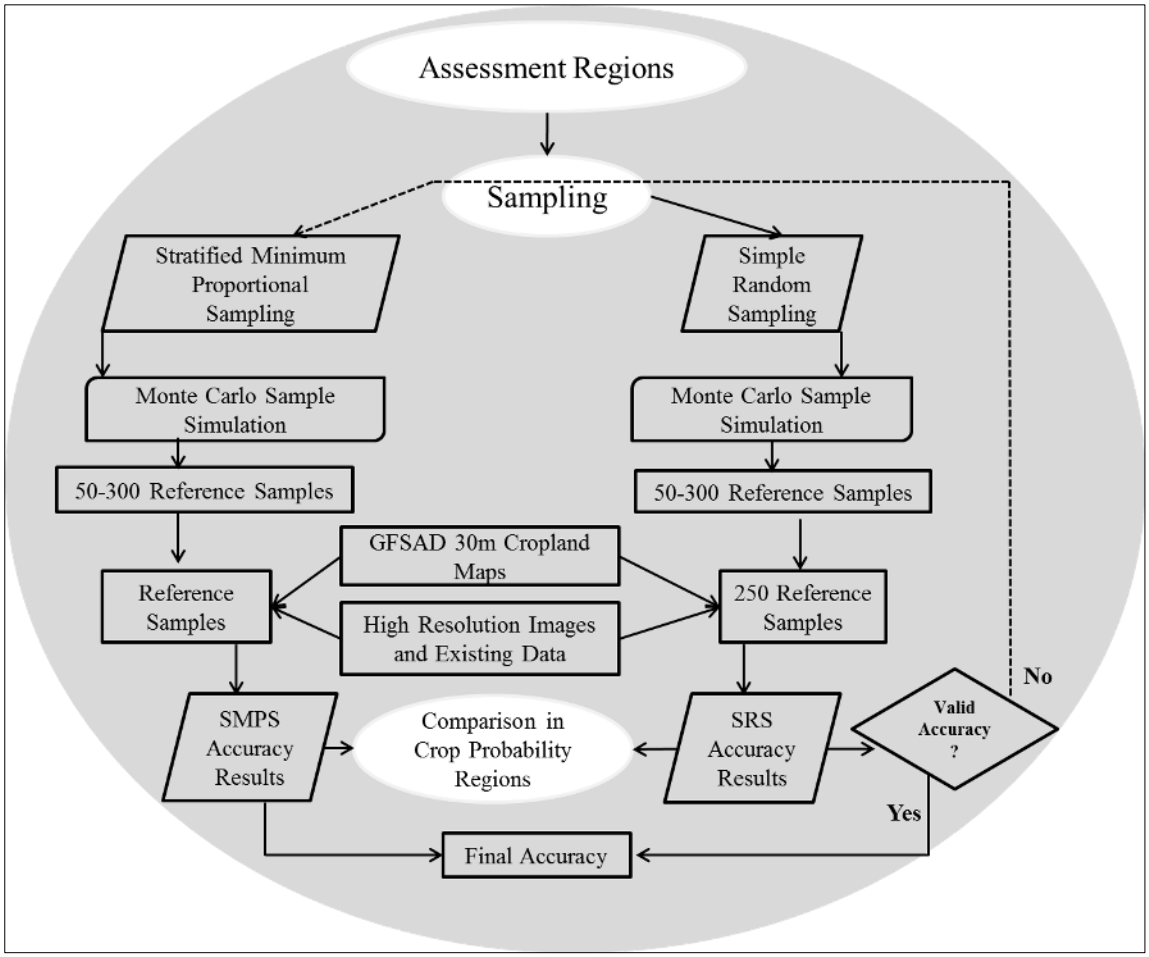

Figure 28. The flow chart showing the steps involved to perform the assessment of cropland extent maps of the various cropland regions.

First, the Cropland Area Proportion (CAP) was estimated for each of the ten study regions using the GFSAD30m cropland extent map classes. The CAP of a region is defined as the percent of cropland area as compared to the total area of the region. The cropland regions with CAP from 0.9% (China Zone 3) to 43.2% (South-East Asia Zone 5) were then grouped into five cropland

probability classes from Class 1 to Class 5 as: (1) very low (0-1%), (2) low (>1-2%), (3) medium (>2-6%), (4) high (>6-15%), and (5) very high (>15%).

Second, the sampling designs were applied in each cropland region based on the following two protocols: (1) Simple Random Sampling (SRS) and (2) Stratified Minimum Proportional Sampling (SMPS) (Stehman and Czaplewski, 1998; Olofsson et al., 2014). The SRS design was applied initially to assess the GFSAD30 cropland extent map for all 72 cropland regions around the world (Yadav and Congalton, 2018b). This sampling design resulted in a random distribution of samples in the cropland and non-cropland map classes based on the equal probability characteristic of random sampling. The cropland map class was rare in low cropland proportion regions and achieved insufficient sample size and ineffective accuracy measures (i.e., producer's and user's accuracies) with this design. Therefore, a second alternative sampling design (i.e., SMPS) was applied to ten randomly selected cropland regions. The SMPS design approach used a predetermined minimum sample size of 50 randomly distributed in each map class (i.e., strata) followed by a proportional distribution of the remaining total samples. This approach was adopted to provide sufficient samples and useful accuracy measures (i.e., user's and producer's accuracy) for the rare cropland map class in the LCP regions.

Third, a sample simulation analysis based on a Monte Carlo method was employed as in Yadav and Congalton, (2018a) with sample sizes ranging from 50 to 300 to determine the optimum sample size. Table 26 shows the allocation of samples tested between 50 and 300 in increments of 50. Once the predetermined minimum sample size of 50 was reached (total samples more than 100) then the additional samples were allocated to each map class proportionally to the cropland and non-cropland area (i.e., CAP and NCAP) (Olofsson et al., 2014).

Table 26. The calculations of crop and no-crop samples for each sample simulation.

Sample Size	Cropland Samples	No-Cropland Samples
50	25	25
100	50	50
150	50+ (CAP % of 50)	50+ (NCAP % of 50)
200	50+ (CAP % of 100)	50+ (NCAP % of 100)
250	50+ (CAP % of 150)	50+ (NCAP % of 150)
300	50+ (CAP % of 200)	50+ (NCAP % of 200)

CAP: Cropland Area Proportion; NCAP: Non-Cropland Area Proportion

Finally, the accuracy measures of the cropland extent map classes were generated in each of the ten cropland regions at the determined optimum sample size for the two sampling designs. The accuracy measures (e.g., overall, producer's, and user's accuracy) were presented in the form of error matrices. The sample size and accuracy measures of the rare cropland map class achieved with different sampling designs at an optimum sample size were compared and evaluated for each cropland region (i.e., probability class from Class 1 to Class 5).

Results

The results of the assessment of the cropland maps of different crop proportion regions describe the comparison of the two different sampling designs with respect to the distribution and allocation of reference samples for each map class and the accuracy measures in the following two sections:

The evaluation of the two sampling designs was performed by comparing the distribution and allocation of reference samples and accuracy measures of the rare cropland map class in each of the ten cropland proportion regions. The results are divided into (1) the grouping of the ten cropland regions into five probability classes, (2) the distribution and allocation of the reference samples, (3) the determination of optimum sample size for the SMPS design, and (4) the accuracy measures of the cropland extent map classes using SRS and SMPS designs.

Five cropland probability classes

The grouping of cropland area proportion of the ten cropland regions resulted in five cropland probability classes in which the two sampling designs were applied, evaluated, and compared to achieve effective accuracy measures of the cropland map class. Table 27 presents the assigned cropland probability class of each region derived from the cropland and non-cropland area proportions (i.e., CAP and NCAP).

Table 27. Cropland and non-cropland area proportion and probability class of the various cropland regions.

	Zones	CAP%	NCAP%	Probability Class
1	South-America Zone 1	1.85	98.15	Class 2 (>1-2%)
2	Canada Zone 1	0.99	99.01	Class 1 (0-1%)
3	North-America Zone 13	4.19	95.81	Class 3 (>2-6%)
4	Europe Zone 7	1.90	98.10	Class 2 (>1-2%)
5	China Zone 3	0.90	99.10	Class 1 (0-1%)
6	South-East Asia Zone 5	43.2	56.8	Class 5 (>15%)
7	Africa Zone 7	5.65	94.35	Class 3 (>2-6%)
8	North-America Zone 4	14.85	85.15	Class 4 (>6-15%)
9	Canada Zone 3	4.8	95.2	Class 3 (>2-6%)
10	North-America Zone 15	9.88	90.12	Class 4 (>6-15%)

Class 1: Very Low; Class 2: Low; Class 3: Medium; Class 4: High; Class 5: Very High

Distribution and Allocation of Reference Samples using SRS and SMPS designs

The SRS and SMPS sampling designs resulted in different distributions and allocation of reference samples of each map class in the ten cropland study regions. An example of the distribution of the 250 reference samples selected using the SRS and SMPS designs are presented for Canada Zone 3 (4.8% CAP) (Figure 29). In addition to the distribution, the allocation of reference samples in the cropland and non-cropland map classes using the two different sampling designs is also presented for the ten cropland regions (Table 28). For example, in Table 28, Canada Zone 3 shows an allocation of 11 and 57 cropland reference samples at a sample size of 250 using SRS and SMPS designs, respectively.

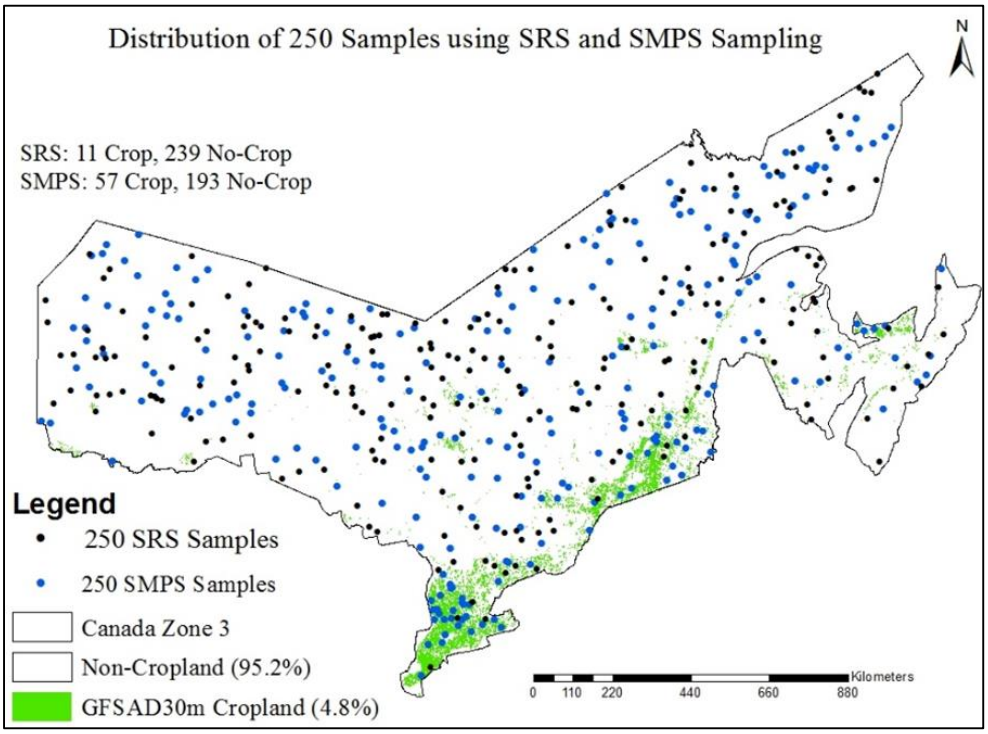

Figure 29. The distribution of 250 reference samples using SRS and SMPS designs in the Canada Zone 3.

Table 28. The allocation of cropland and non-cropland reference samples using SRS and SMPS designs.

	CAP%	SMPS 50		SMPS 100		SMPS 150		SMPS 200		SMPS 250		SMPS 300		SRS 250	
Regions		Crop	NC	Crop	NC	Crop	NC	Crop	NC	Crop	NC	Crop	NC	Crop	NC
SAm Zone 1	1.85	25	25	50	50	51	99	52	148	**53**	197	54	246	**8**	242
Canada Zone 1	0.99	25	25	50	50	50	100	51	149	**51**	199	52	248	**5**	245
NA Zone 13	4.19	25	25	50	50	52	98	54	146	**56**	194	58	242	**11**	238
Europe Zone 7	1.90	25	25	50	50	51	99	52	148	**53**	197	54	246	**8**	242
China Zone 3	0.90	25	25	50	50	50	100	51	149	**51**	199	52	248	**4**	345
SE Asia Zone 5	43.2	25	25	50	50	72	78	93	107	115	135	136	164	116	134
Africa Zone 7	5.65	25	25	50	50	53	97	56	144	**58**	192	61	239	**17**	233
NA Zone 4	14.85	25	25	50	50	57	93	65	135	**72**	178	80	220	**11**	238
Canada Zone 3	4.8	25	25	50	50	52	98	55	145	**57**	193	60	240	**11**	239
NA Zone 15	9.88	25	25	50	50	55	95	60	140	**65**	185	70	230	**24**	223

SAm: South-America; NA: North-America; SE: South-East; SRS: Simple Random Sampling; SMPS: Stratified, Minimum, Proportional Sampling; C: Cropland; NC: Non-Cropland

The optimum sample size for the SMPS design

The determination of the optimal sample size for the SRS sampling was conducted using a sampling simulation analysis (Yadav and Congalton, 2018a). A sample size of 250 was selected. The optimal sample size for the SMPS design was determined by plotting the overall accuracy of the cropland extent maps at sample sizes from 50 to 300 for each of the ten cropland proportion regions (Figure 30). The graphical representation shows a plateau in the overall accuracy of eight of the cropland extent maps at a sample size of 250 using the SMPS design beyond which the accuracy did into increase with the addition of more samples. While two regions, Canada Zone 1 and Africa Zone 7, do not show this plateau a sample size of 250 was selected as optimal.

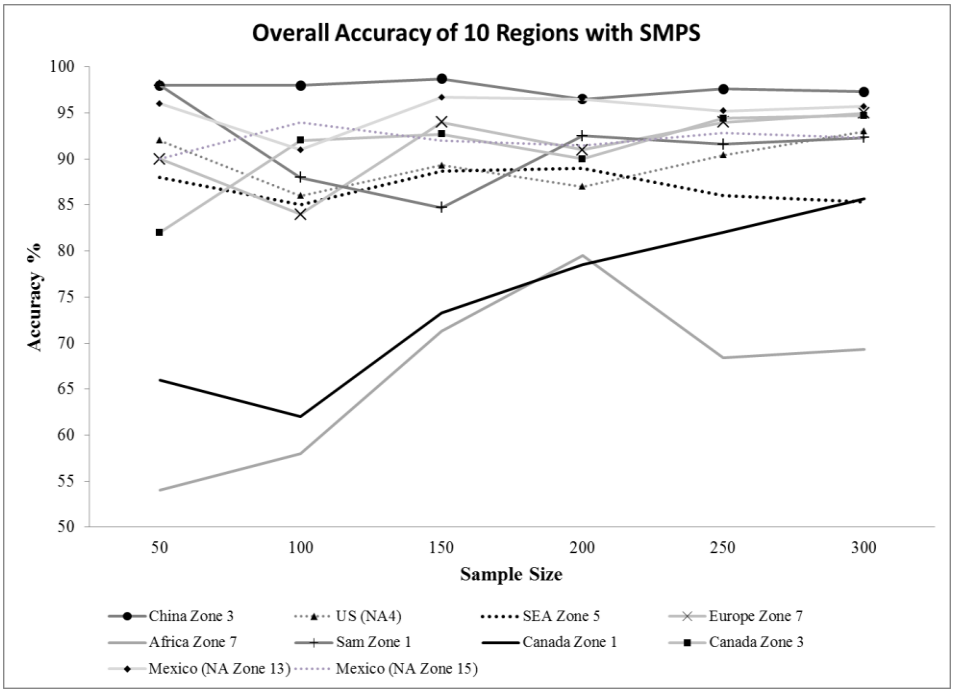

Figure 30. Graphical representation of the overall accuracy achieved with SMPS design using the sample sizes from 50 to 300.

Accuracy measures of the cropland extent map in the ten cropland regions

The SRS and SMPS designs resulted in different accuracy measures of the cropland map class of the GFSAD30m cropland extent map in the ten cropland proportion regions. These accuracies determined at a sample size of 250 are presented graphically and in error matrix form for each of the ten cropland proportion regions by five cropland probability classes.

Very low cropland proportion regions of less than 1% CAP (Class 1)

Canada Zone 1 and China Zone 3 are grouped as very low cropland proportion regions of <1% CAP determined from the GFSAD30m cropland extent map. The accuracy measures (i.e., user's and producer's accuracy) of the cropland map class of these regions achieved at a sample size of

250 using SRS and SMPS designs are presented graphically and in error matrix form for these regions (Figure 31 and Table 29). Large differences in the producer's accuracy of the rare cropland map class were observed between the SRS and the SMPS sampling designs for China Zone 3 (Figure 31). The user's accuracy of the rare cropland map class for the SRS sampling design more closely agrees with the SMPS design for Canada Zone 1. Insufficient samples in the rare cropland map class using the SRS design for these two regions results in accuracy measures that are not indicative of the actual errors the SRS design for these two regions (Table 29).

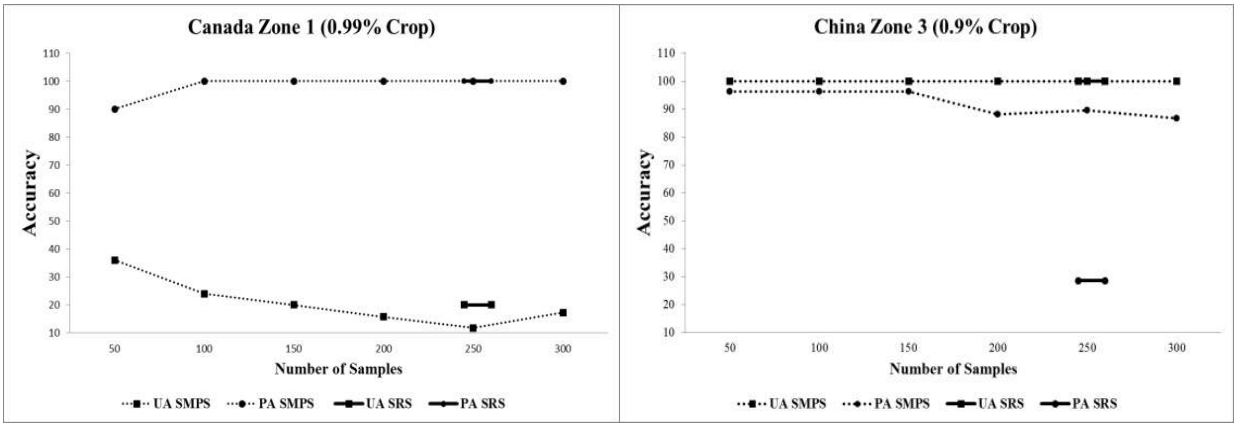

Figure 31. Graphical comparison of the accuracy measures achieved with SRS and SMPS designs in very low cropland proportion regions.

Table 29. Error matrices showing the accuracy measures achieved with SRS and SMPS designs in the very low cropland proportion regions.

SMPS		**Canada Zone 1 Reference Data**			
		Crop	No-Crop	Total	User's Accuracy
Map Data	Crop	6	45	51	11.7%
	No-Crop	0	199	199	100.0%
Total		6	244	250	
Producer's Accuracy		100.0%	81.5%		82.0%

SRS		**Canada Zone 1 Reference Data**			
		Crop	No-Crop	Total	User's Accuracy
Map Data	Crop	1	4	5	20.0%
	No-Crop	0	245	245	100.0%
Total		1	249	250	
Producer's Accuracy		100.0%	98.4%		98.4%

SMPS		China Zone 3 Reference Data			
		Crop	No-Crop	Total	User's Accuracy
Map Data	Crop	51	0	51	100.0%
	No-Crop	6	193	199	96.9%
Total		57	193	250	
Producer's Accuracy		89.5%	100.0%		**97.6%**

SRS		China Zone 3 Reference Data			
		Crop	No-Crop	Total	User's Accuracy
Map Data	Crop	4	0	4	100.0%
	No-Crop	10	335	345	97.1%
Total		14	193	349	
Producer's Accuracy		28.6%	100.0%		97.1%

Low cropland proportion regions of >1-2% CAP (Class 2)

South-America Zone 1 and Europe Zone 7 are grouped as low cropland proportion regions of >1-2% CAP derived from the GFSAD30m cropland extent map. The accuracy measures (i.e., user's and producer's accuracy) of the cropland map class of these regions using the SRS and SMPS designs are presented graphically and in error matrix form for these low cropland proportion regions (Figure 32 and Table 30). Large differences in the user's and producer's accuracy of the rare cropland map class were observed between the SRS and the SMPS sampling designs for South-America Zone 1 (Figure 32). The user's accuracy of the rare cropland map class for the SRS sampling design more closely agrees with the SMPS design for Europe Zone 7. Insufficient samples in the rare cropland map class using the SRS design for these two regions results in accuracy measures that are not indicative of the actual errors (Table 30).

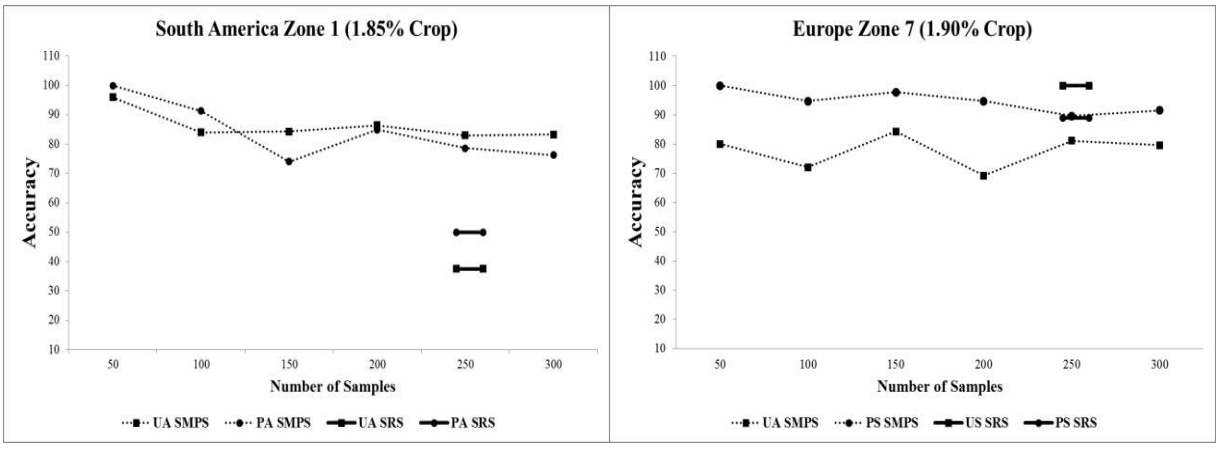

Figure 32. Graphical comparison of the accuracy measures achieved with SRS and SMPS designs in the low cropland proportion regions.

Table 30. Error matrices showing the accuracy measures achieved with SRS and SMPS sampling designs in the low cropland proportion regions.

SMPS	**South-America Zone 1 Reference Data**				
		Crop	No-Crop	Total	User's Accuracy
Map Data	Crop	44	9	53	83.0%
	No-Crop	12	185	197	93.9%
Total		56	194	250	
Producer's Accuracy		78.5%	95.3%		**91.6%**

SRS	**South-America Zone 1 Reference Data**				
		Crop	No-Crop	Total	User's Accuracy
Map Data	Crop	3	5	8	37.5%
	No-Crop	3	239	242	98.8 %
Total		6	250	250	
Producer's Accuracy		50.0%	98.0%		**96.8%**

SMPS	**Europe Zone 7 Reference Data**				
		Crop	No-Crop	Total	User's Accuracy
Map Data	Crop	43	10	53	81.13%
	No-Crop	5	192	197	97.46%
Total		48	202	250	
Producer Accuracy's		89.58%	95.05%		**94.00%**

SRS	**Europe Zone 7 Reference Data**				
		Crop	No-Crop	Total	User's Accuracy
Map Data	Crop	8	0	8	100.0%
	No-Crop	1	241	242	99.6 %
Total		9	241	250	
Producer's Accuracy		88.9%	100.0%		**99.6%**

Medium cropland proportion regions of >2-6% CAP (Class 3)

Canada Zone 3, Africa Zone 7, and North-America Zone 13 are grouped as medium cropland proportion regions of >2-6% CAP determined from the GFSAD30m cropland extent map. The accuracy measures (i.e., user's and producer's accuracy) of the cropland map c lass of these regions using SRS and SMPS designs are presented graphically and in error matrix form for these medium cropland proportion regions (Figure 33 and Table 31). Large differences in the user's accuracy of the rare cropland map class were observed between the SRS and the SMPS sampling designs for Canada Zone 3 and Africa Zone 7 (Figure 33). The user's and producer's accuracy of the rare cropland map class for the SRS sampling design more closely agrees with the SMPS design for North-America Zone 13. Insufficient samples in the rare cropland map class using the SRS design

for these three regions results in accuracy measures that are not indicative of the actual errors (Table 31).

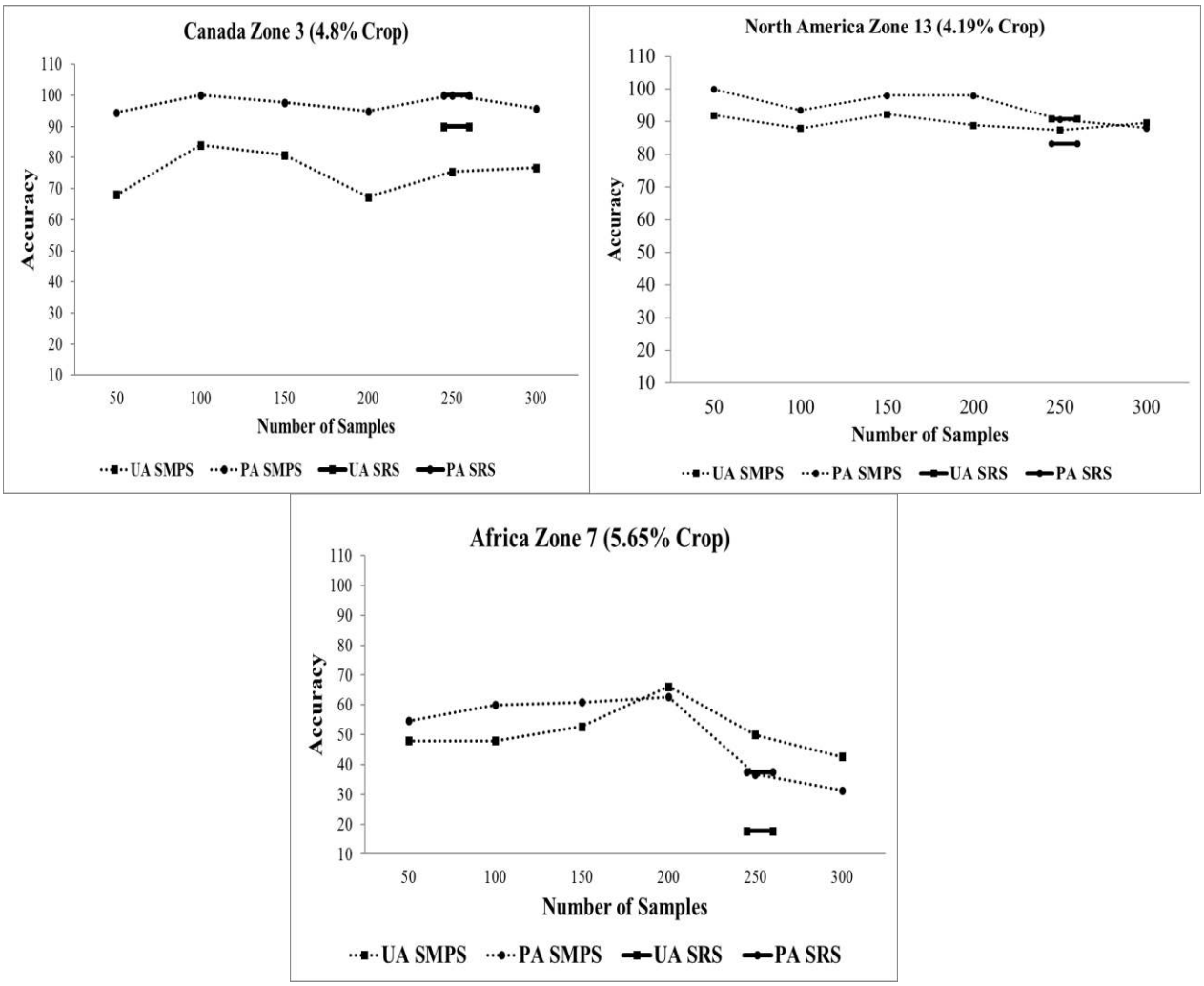

Figure 33. Graphical comparison of the accuracy measures achieved with SRS and SMPS designs in the medium cropland proportion regions.

Table 31. Error matrices showing the accuracy measures achieved with SRS and SMPS designs in the medium cropland proportion regions.

SMPS	Canada Zone 3 Reference Data				
		Crop	No-Crop	Total	User's Accuracy
Map Data	Crop	43	14	57	75.4%
	No-Crop	0	193	193	100.0%
Total		43	207	250	
Producer's Accuracy		100.0%	93.2%		**94.4%**

SRS	Canada Zone 3 Reference Data				
		Crop	No-Crop	Total	User's Accuracy
Map Data	Crop	10	1	11	90.9%
	No-Crop	0	239	239	100.0%
Total		10	240	250	
Producer's Accuracy		100.0%	99.7%		**99.6%**

SMPS	Africa Zone 7 Reference Data				
		Crop	No-Crop	Total	User's Accuracy
Map Data	Crop	29	29	58	50.0%
	No-Crop	50	142	192	73.9%
Total		79	171	250	
Producer's Accuracy		36.7%	83.0%		**68.4%**

SRS	Africa Zone 7 Reference Data				
		Crop	No-Crop	Total	User's Accuracy
Map Data	Crop	3	14	17	17.7%
	No-Crop	5	228	233	97.9%
Total		8	242	250	
Producer's Accuracy		37.5%	94.2%		**92.4%**

SMPS	North-America Zone 13 Reference Data				
		Crop	No-Crop	Total	User's Accuracy
Map Data	Crop	49	7	56	87.5%
	No-Crop	5	189	194	97.4%
Total		54	196	250	
Producer's Accuracy		90.7%	96.4%		**95.2%**

SRS	North-America Zone 13 Reference Data				
		Crop	No-Crop	Total	User's Accuracy
Map Data	Crop	10	2	12	83.3%
	No-Crop	2	236	238	99.2%
Total		12	237	250	
Producer's Accuracy		83.3%	99.6%		**98.8%**

High cropland proportion regions of >6-15% CAP (Class 4)

North-America Zone 15 and North-America Zone 4 are grouped as high cropland proportion regions of >6-15% CAP derived from the GFSAD30m cropland extent map. The accuracy measures (i.e., user's and producer's accuracy) of the cropland map class of these regions using SRS and SMPS designs are presented graphically and in error matrix form for these high cropland proportion regions (Figure 34 and Table 32). Large differences in the user's and producer's accuracy of the rare cropland map class were observed between the SRS and the SMPS sampling designs for North America-Zone 15 (Figure 34). The user's and producer's accuracy of the rare

cropland map class for the SRS sampling design more closely agrees with the SMPS design for North-America Zone 4. Insufficient samples in the rare cropland map class using the SRS design for these two regions results in accuracy measures that are not indicative of the actual errors (Table 32).

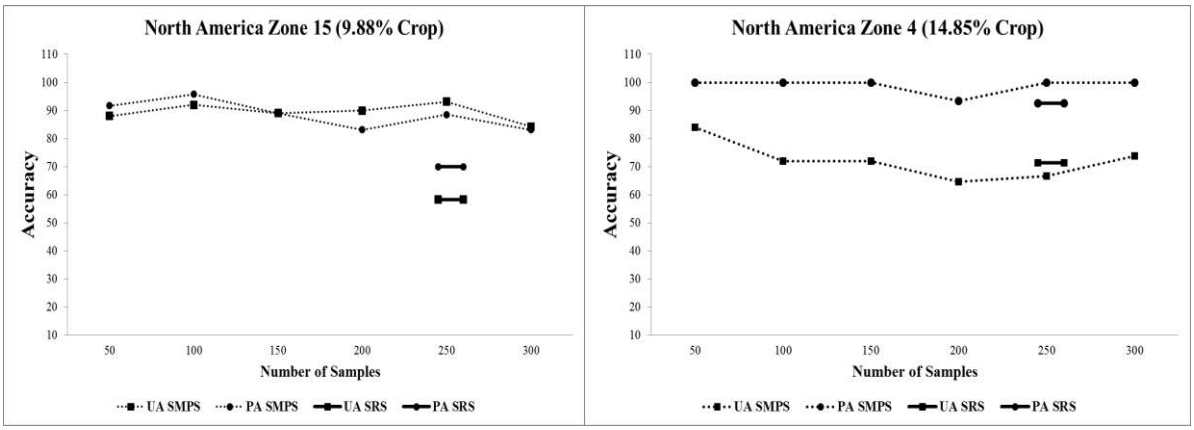

Figure 34. Graphical comparison of the accuracy measures achieved with SRS and SMPS designs in the high cropland proportions regions.

Table 32. Error matrices showing the accuracy measures achieved with SRS and SMPS designs in the high cropland proportion regions.

SMPS	**North-America Zone 15 Reference Data**				
		Crop	No-Crop	Total	User's Accuracy
Map Data	Crop	54	11	65	83.0%
	No-Crop	7	178	185	96.2%
Total		61	189	250	
Producer's Accuracy		88.5%	94.1%		**92.8%**

SRS	**North-America Zone 15 Reference Data**				
		Crop	No-Crop	Total	User's Accuracy
Map Data	Crop	14	10	24	58.3%
	No-Crop	6	217	223	97.3%
Total		48	227	247	
Producer's Accuracy		70.0%	95.6%		**93.5%**

SMPS North-America Zone 4 Reference Data					
		Crop	No-Crop	Total	User's Accuracy
Map Data	Crop	48	24	72	66.6%
	No-Crop	0	178	178	100.0%
Total		48	202	250	
Producer's Accuracy		100.0%	88.1%		**90.4%**

SRS North-America Zone 4 Reference Data					
		Crop	No-Crop	Total	User's Accuracy
Map Data	Crop	25	10	35	71.4%
	No-Crop	2	213	215	99.1%
Total		27	223	250	
Producer's Accuracy		92.6%	95.5%		**95.2%**

Very high cropland proportion regions of >15% CAP (Class 5)

South-East Asia Zone 5 is grouped as very high cropland proportion region of >15% CAP derived from the GFSAD30m cropland map. The accuracy measures (i.e., user's and producer's accuracy) of the cropland map class of this region using SRS and SMPS designs are presented graphically and in error matrix form (Figure 35 and Table 33). The user's and producer's accuracy of the rare cropland map class for the SRS sampling design more closely agrees with the SMPS design for South-East Asia Zone 5 (Figure 35). Sufficient samples in the rare cropland map class using the SRS design results in accuracy measures that are indicative of an effective and meaningful assessment of the cropland map for this region (Table 33).

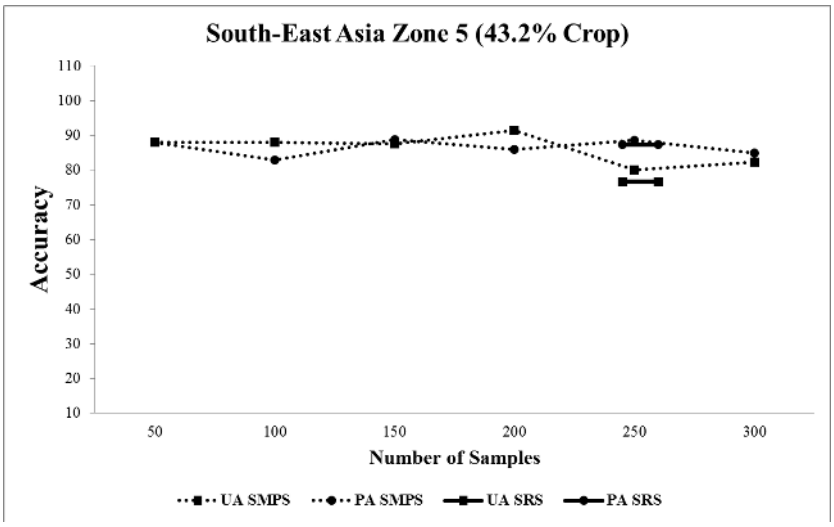

Figure 35. The comparison of the accuracy measures achieved with SRS and SMPS designs in the very high cropland proportion regions.

Table 33. Error matrices showing the accuracy measures achieved with SRS and SMPS designs in the very high cropland proportion regions.

SMPS South-East Asia Zone 5 Reference Data					
		Crop	No-Crop	Total	User's Accuracy
Map Data	Crop	92	23	115	80.0%
	No-Crop	12	123	135	91.1%
Total		104	146	250	
Producer's Accuracy		88.4%	84.2%		**86.0%**

SRS South-East Asia Zone 5 Reference Data					
		Crop	No-Crop	Total	User's Accuracy
Map Data	Crop	89	27	116	76.7%
	No-Crop	13	121	134	90.3%
Total		102	148	250	
Producer's Accuracy		87.3%	81.8%		**84.0%**

Discussion

The accuracy assessment of the GFSAD30m cropland extent map was initially performed using SRS design at a sample size of 250 for various cropland regions around the world (Yadav and Congalton, 2018b). This sampling design resulted in an insufficient sample and ineffective accuracy measures of the rare cropland map class in the low cropland proportion regions due to the cropland proportion, distribution, and pattern of the cropland extent map being assessed. Very limited research has been done so far to evaluate and choose an appropriate sampling design to perform an effective accuracy assessment of the cropland maps of different regions (Bayas et al., 2017). After thorough research, it was found that there are no suggestions available for employing appropriate sampling approaches to assess the cropland maps of different cropland regions in the literature. To achieve sufficient samples and effective accuracy measures of the rare cropland map class, an alternate SMPS design was applied in ten selected cropland regions. The comparison of two different sampling designs presents novel results by providing recommendations on performing an appropriate sampling for different cropland regions. Therefore, the novel results of

performing an appropriate sampling in different cropland proportion regions are discussed in the following sections with respect to number of samples and achieved accuracy measures.

Assigning cropland probability classes

The cropland area proportion (CAP) of the ten selected regions were estimated using the GFSAD30m cropland extent map to provide an effective sampling area for applying and evaluating the sampling designs. The ten cropland regions were grouped into five probability classes from very low to very high cropland probability based on their estimated percent of cropland area proportion from 0.9% to 43.2% (Table 27). The very high cropland probability class was assigned to the regions of >15% CAP while four probability classes (e.g., very low, low, medium, and high cropland probability) were assigned to the regions of <15% CAP. The cropland regions of <15% CAP were purposely grouped into four probability classes from Class 1 to 4 to evaluate the sampling designs in all the possible low cropland proportion regions. The grouping of the ten cropland regions into five cropland probability classes was necessary to determine the range of CAP of the low cropland proportion regions to be effectively assessed using an appropriate sampling design.

Distribution and allocation of samples with SRS and SMPS designs

The distribution and allocation of samples of the rare cropland map class at a sample size of 250 using SRS and SMPS designs were compared spatially and in tabular form for the ten cropland regions. An example comparison of the distribution and allocation of samples of the rare cropland map class at a sample size of 250 using SRS and SMPS designs was presented for Canada Zone 3 (Figure 29 and Table 28). This comparison shows an allocation of only 11 samples in the rare

cropland map class using the SRS design at a sample size 250 due to the equal probability of selecting a sample area in the low cropland class. As a result, computation of producer's and user's accuracy is problematic as even a small number of incorrect classifications can generate very low accuracies. Similar insufficient sample allocations for the rare cropland map class were also observed in other cropland regions of <15% CAP (Table 28). Therefore, an alternate SMPS design was developed and achieved appropriate distribution and allocation of samples of the rare cropland map class in the LCP regions (Table 28) (Stehman, 1999). The SMPS design resulted in an appropriate distribution and allocation of 57 samples of the rare cropland map class at a sample size of 250 for Canada Zone 3 (Figure 29). In contrast, the high cropland proportion regions of >15% CAP achieved appropriate distribution and sufficient number of samples at a sample size of 250 both with SMPS and SRS designs due to more uniform and prevalent cropland distribution in these regions. These results demonstrate that the sampling designs achieve different distribution and allocation of samples of the rare cropland map class in the ten cropland regions and therefore, the appropriate design must be selected according to the proportion of cropland extent in the maps to be assessed.

The optimum number of samples for SRS and SMPS designs

The sample simulation analysis performed by Yadav and Congalton, (2018a) determined an optimum sample size of 250 for the SRS design in various cropland regions. Similarly, the optimal sample size for the SMPS design was also determined by plotting the overall accuracy of the cropland extent maps at sample sizes from 50 to 300 for each of the ten cropland proportion regions (Figure 30). The graphical representation shows a plateau in the overall accuracy of eight of the cropland extent maps at a sample size of 250 using the SMPS design beyond which the accuracy

did into increase with the addition of more samples. However, the overall accuracy of the cropland extent map of Africa Zone 7 decreased while that of Canada Zone 1 increased with the addition of more samples beyond the sample size of 250. Unlike the other low cropland proportion regions, these two regions did not reach a plateau in the overall accuracy at 250 samples due to errors (i.e., omission or commission) in the rare cropland map class of the cropland extent map.

The rare cropland map class of the cropland extent map of Africa Zone 7 had serious omission errors when compared with the Google Earth imagery. The methodology used to accurately classify the cropland regions of the entire African continent do not seem to have worked as well to map the very small fields of Africa Zone 7 (Madagascar) given their unique cropland distribution and pattern. On the other hand, the rare cropland map class of the cropland extent map of Canada Zone 1 had a large number of commission errors. These errors are a result of missing cropland patches in the AAFC (Agriculture and Agri-Food Canada) reference cropland layer that was used for the assessment. Comparing this reference data with Google Earth imagery showed that for this region the reference data missed a large number of cropland patches. It is clear that the overall accuracy of the cropland extent map of Africa Zone 7 and Canada Zone 1 did not reach plateau at a sample size of 250 due to omission and commission errors of the rare cropland map class, respectively. Therefore, a sample size of 250 was selected as optimal for SMPS design based on the simulation analysis of eight of the cropland regions excluding Africa Zone 7 and Canada Zone 1. Finally, the results demonstrate that choosing an alternate design (i.e., distribution and allocation of samples) is more important than increasing the sample size to achieve sufficient samples and effective accuracy of the rare cropland map class in the ten cropland regions.

Accuracy measures with SRS and SMPS designs

The SRS and SMPS designs resulted in different accuracy measures of the cropland map class of the GFSAD30m cropland extent map in the ten cropland proportion regions. The SRS design resulted in insufficient and ineffective accuracy measures of the rare cropland map class in the Low Cropland Proportion (LCP) regions around the world (Yadav and Congalton, 2018b). However, the alternate SMPS design achieved effective and useful accuracy measures of the rare cropland map class in the LCP regions of <15% CAP (e.g., China Zone 3, South-America Zone 1, Africa Zone 7, and North-America Zone 15) (Figure 31, 32, 33, and 34). The reasons for achieving different accuracy results with the two sampling designs can be explained by examining the cropland proportion, distribution, and pattern of the cropland extent maps of the different cropland regions to be assessed. It should be noted that not all the LCP regions produced the same result. In a few of the LCP regions of <15% CAP, the accuracy measures of the rare cropland map class were the same for the SRS and SMPS designs due to: (1) omission errors in the cropland class of the reference cropland extent map (e.g., Canada Zone 1) (Figure 31) and (2) the more evenly scattered and uniformly distributed cropland pattern (e.g., Europe Zone 7) (Figure 32).

The evaluation of the SRS and SMPS designs in the regions of >15% CAP (e.g., South-East Asia Zone 6) did not show any change in the accuracy measures of the rare cropland map class (Figure 35). The high cropland proportion regions (>15% CAP) can be sampled using either of the sample designs at a sample size of 250. It is important to note that regions of more than 85% cropland proportion (i.e., <15% non-cropland area proportion (NCAP)) should be considered the same as the LCP regions. In this case, non-cropland becomes the rare map class and the sampling issues are the same. Therefore, the evaluation of SRS and SMPS designs demonstrates that the

regions of <15% CAP or NCAP need to be assessed using the SMPS design while the regions between 15-85% cropland proportion can be assessed using either of the sampling designs.

Conclusions

In this paper, we have evaluated two sampling designs to effectively assess the cropland extent maps of the ten selected cropland regions. The evaluation of the SRS and SMPS designs with respect to the sample allocation and accuracy of the rare cropland map class at a sample size of 250 demonstrates their suitability for implementation given different cropland probability classes and cropping patterns (Table 34).

Table 34. The comparison of sampling designs in different cropland probability classes.

Cropland Probability Class	Cropping Pattern	Sampling Design	Sample Allocation	Accuracy
0-1%	No Pattern	**SMPS**	**Sufficient**	**90-100%**
		SRS	Insufficient	20-30%
1-2%	Clustered and limited to small areas	**SMPS**	**Sufficient**	**80-90%**
		SRS	Insufficient	40-50%
	Scattered, uniformly-distributed	SMPS	**Sufficient**	Remain same
2-6%	Limited to small areas	SMPS	**Sufficient**	70-90%
		SRS	Insufficient	80-90%
	Uniformly distributed	SMPS	**Sufficient**	Remain same
6-15%	No Pattern	**SMPS**	**Sufficient**	**85-90%**
		SRS	Insufficient	70-80%
>15%	No Pattern	SRS/SMPS	No Difference	70-90%

Based on the evaluation and comparison of the sampling designs (Table 9), the following conclusions can be used to perform an effective assessment of the cropland extent maps of various cropland regions:

1. To perform an effective assessment of the cropland extent map in various cropland regions, the three P's must be determined for each cropland region to be assessed: (1) Proportion of cropland, (2) Possibility of rare map class, and (3) Predetermined minimum sample size of the rare map class.
2. While choosing a sampling strategy to effectively assess the rare cropland map class of various cropland regions, the distribution of samples is more important than increasing or decreasing the number of samples (once a sufficient number of samples is determined).
3. The distribution of samples combined with the predetermined minimum number of samples must be chosen appropriately to achieve sufficient sampling and effective accuracy assessment of the rare cropland map class in the low cropland proportion (LCP) regions.
4. The regions of <15% CAP that have clustered and limited to small areas cropping pattern can be effectively assessed using the SMPS design as compared to the scattered and uniform cropping pattern. However, the regions of >15% CAP (those maps that do not contain a rare cropland map class) can be effectively assessed using either of the sampling designs at a sample size of 250.

CHAPTER VI

Augmenting and Extending Limited Crop Type Reference Data using an Interpretation and Phenology-based Approach

Abstract

The combination of high spatial resolution and multi-date satellite imagery offers new opportunities for mapping and monitoring crop types of different agricultural field sizes. However, mapping of crop types at high spatial resolution requires high-quality crop type reference data typically collected from the ground-based surveys to create the maps and/or to assess the map accuracy. The availability of sufficient crop type reference data is limited over large geographic regions because of the time, effort, cost, and accessibility in different parts of the world. To generate large area crop type maps, this limited reference data must be augmented and spatially extended to every region using appropriate and available non-ground-based sources of reference data. There is the potential to either interpret the photographs available from Google Street View (GSV) or classify High Resolution Imagery (HRI) using a phenology-based classification approach to generate additional reference data within similar agriculture ecological zones (AEZs) based on the crop characteristics, their types, and their growing season. Therefore, the objective of this study was to augment and extend the limited crop type reference data using this approach. First, the limited reference data within selected training regions was augmented using the interpretation of field photographs collected from GSV for three different field sizes. Then, multi-date, high spatial resolution satellite images were used to spatially extend the limited crop type reference data from one region (called the training region (TR)) to another region (called the test

region (TE)) within the same AEZ using a phenology-based Decision Tree (DT) classifier for three different field sizes. These two methods of augmenting and extending crop type reference data were developed for the United States (US) where high-quality crop type reference data already exist so that the methods could be effectively and efficiently tested. The results demonstrate that the GSV shows promise to augment the limited reference data for the more common/dominant agriculture crops, while the phenology-based classification approach can efficiently extend the limited crop type reference data to every region in same AEZ for different field sizes.

Introduction

Food security is one of the major challenges that human beings are facing (Zhong et al., 2014). By 2050, the global population of 9.8 billion will demand 70% more food than is consumed today (Alexandratos and Bruinsma, 2012; Schwab et al., 2014). To shape the future of food security and agriculture, new cropland areas are increasing under current agriculture practices causing greenhouse gas (GHG) emissions and environmental degradation (Adams and Eswaran, 2000; Beach et al., 2008). The essential inputs to improve the current agriculture practices and modeling GHG variability in different agriculture systems include the identification of different crop types (Ramankutty et al., 2008; Peña-Barragán et al., 2011; Gong et al., 2013). Therefore, acquiring crop type information over large geographic regions is extremely relevant for decision making and policy actions (Yang et al., 2011; Foerster et al., 2012).

Remote sensing technology provides reliable and cost-effective satellite imagery and tools for crop type mapping over space and time, repeatedly, and consistently at different spatial and

temporal domains (Barrett and Curtis, 1992; Asner et al., 2002; Jakubauskas et al., 2003; Castillejo-González et al., 2009; Vinciková et al., 2010; Rodriguez-Galiano et al., 2012; Thenkabail and Wu, 2012; Ustuner et al., 2014; Zhou et al., 2014). Remotely sensed satellite imagery has multiple spectral, spatial, and temporal resolution characteristics that can be effectively utilized for crop type identification (Ulabay et al., 1982; Congalton et al., 1998; Oetter et al., 2000). Satellite imagery such as that available from Landsat (Ryerson et al., 1985; Williams et al., 1987; Oetter et al., 2000), SPOT (Büttner and Csillag, 1989; Murakami et al., 2001), Indian Remote Sensing satellite data (Dutta et al., 1994; Panigrahy and Sharma, 1997), ASTER (Peña-Barragán et al., 2011), and MODIS (Gumma et al., 2014; Teluguntla et al., 2017a) have been used to identify different crop types in the past.

With the development of high spatial resolution sensors such as Rapid Eye (2008), GeoEye-1 (2008), World View-2 (2009), and Sentinel-2 (2015), crop type identification has become more detailed and accurate as a result of removing the spectral mixing that is common at moderate and coarse resolution pixels (De Wit and Clevers, 2004; Palchowdhuri et al., 2018). Multi-date High-spatial Resolution Imagery (HRI) is being continuously used to generate crop type maps of different regions around the world (e.g., Castillejo-González et al., 2009; Conrad et al., 2014; Gumma et al., 2016). However, the potential use of a single, or two, or multi-dates of imagery are still yet to be evaluated to generate effective crop type maps especially for different agriculture field sizes.

The mapping of crop types at high spatial resolution requires high-quality crop type reference data typically collected from ground-based surveys to create the maps and/or to assess the map accuracy. A well-distributed, consistent, and sufficient amount of crop type reference data over

large areas substantially reduces the mapping cost and improves the accuracy of the crop type maps. However, the availability of sufficient crop type reference data from ground-based methods is typically severely limited over large geographic regions because of the time, effort, cost, and accessibility in most parts of the world (South et al., 2004; Peña-Barragán et al., 2008). Therefore, whatever limited reference data that does exist must be augmented and spatially extended using non-ground-based sources of reference data in order to generate and/or assess large area crop type maps.

Possible non-ground-based sources to augment and extend the limited crop type reference data to every region are: (1) the interpretation of photographs that are readily available from sources such as Google Street View (GSV) and (2) the classification of HRI. The interpretation of photographs available from GSV has the potential to augment the limited availability of crop type reference data. The classification of HRI has been used to extend the crop type information to multiple years to develop year by year crop type maps without considering region to region re-training of the satellite imagery (Zhong et al., 2014). It may be possible to use such a classification approach to extend the limited crop type reference data within a single year to similar regions. These methods of augmentation and extension could save the labor, cost, and time of field surveys required to collect the crop type reference data over large regions (Tatsumi et al., 2015).

Regional intra-class variation exists in a single agriculture crop type due to farmer's decisions to plant crops at different dates in different regions (Wardlow et al., 2007). These variations remain consistent within similar agriculture ecological zones (AEZs) and field size landscapes (e.g., large, medium, and small) due to similar agriculture and ecological conditions (Serra and Pons, 2008; Simonneaux et al., 2008). Therefore, it is possible that the limited crop type reference data may be

effectively augmented and extended by identifying the crop types in similar regions based on their visual interpretation and spectral characteristics at specific growing stage/time (i.e., phenology).

The identification of different agriculture crops based on their spectral characteristics is usually performed by classifying multi-date HRI (Castillejo-González et al., 2009; Yang et al., 2011; Conrad et al., 2014). Recently, the classification of HRI using conventional pixel-based classification methodology has been replaced with Object-Based Image Analysis (OBIA) approach to develop more accurate crop type maps (Castillejo-González et al., 2009). OBIA includes the classification of objects into different crop types based on their spectral, spatial, and texture features using different phenology-based classifier approaches such as Rule-Based Classifier (RBC), Decision Tree (DT) (Peña-Barragán et al., 2011), Random Forest (RF) (Tatsumi et al., 2015), and support vector machine (Peña et al., 2014). The RBC is the simplest classifier which uses a condition to determine whether an image object belongs to a class (e.g., crop) or not. The random forest algorithm has the potential to incorporate multiple spectral and texture variables to discriminate different crop types and improve the classification performance (Lawrence et al., 2006; Oliveira et al., 2012). The non-parametric decision tree classifier is capable of handling the regional intra-class variation of a single agriculture crop type that exists at multiple places. Therefore, the phenology-based classifiers (e.g., RBC, RF, and, DT) could be used as effective algorithms to create crop/no-crop and crop type maps from multi-dates of satellite imagery and identify the agriculture crops of similar regions at multiple places.

A well-distributed and consistent crop type reference data set must be collected either from ground-based or non-ground-based sources to create and assess crop type maps. The basic pre-requisites for collecting crop type reference data that must be carefully considered include: (1) the

classification scheme and (2) the sampling strategy (Congalton, 1991). A mutually exclusive and totally exhaustive classification scheme is necessary to define and translate or cross-walk the reference crop type labels to classify the HRI and generate the augmented and extended crop type reference data. The choice of an appropriate sampling strategy is the other basic requirement needed to collect appropriate reference data for the classification and assessment of the crop type maps (Congalton, 1991; Congalton and Green, 2009). A stratified random sample combined with sufficient number of samples for each class has been effectively used by Yadav and Congalton (2018) to perform an assessment of crop extent maps with varying map class proportions. This stratified sampling approach with sufficient samples in each map class is appropriate to generate a valid crop type reference data set in order to conduct an effective accuracy assessment of crop type maps of dominant and rare agriculture crops.

The augmentation and extension of crop type reference data methods proposed in this study could only be developed in the United States (US) where high-quality crop type reference data (e.g., Cropland Data Layer) already exist to compare and evaluate the results. After testing these methods and comparing their results with the CDL reference data in the US, they can be effectively employed in the future to generate consistent and large area crop type reference data for rest of the world. Therefore, the objectives of this study are: (1) to augment the crop type reference data using the photographs collected from Google Street View (GSV), (2) to spatially extend the crop type reference data from Training (TR) to TEst (TE) regions based on the investigation of the use of one, two, and three dates of high spatial resolution imagery (HRI) and (3) to evaluate the results of these augmentation and extension approaches using the CDL reference data of the US.

Study Area

The study areas used in this research includes three pairs (i.e., total six) of approximately 6 km by 6 km regions selected randomly within three different AEZs (Figure 36A) and agriculture field sizes (Figure 36B) in the United States (US). The AEZs were defined based on the length of growing period days of the agriculture crops using the GAEZ (Global Agro-Ecological Zones) layer (Fischer et al., 2012). Likewise, the agriculture field sizes were derived from the IIASA (International Institute for Applied System Analysis) field size layer by grouping the field sizes from 10-40 into three classes: (1) large (35-40 ha), (2) medium (22-35 ha), and (3) small (10-22 ha) (Fritz et al., 2015). Each pair of study area includes a region used for TRaining (TR) and the other to TEst (TE).

Figures 1A and 1B show the location of the three pairs of TR and TE regions (total six regions); one pair in each separate AEZ (e.g., AEZ 6, 10, and 11) and for one of the three field sizes (e.g., small, medium, and large). Table 35 describes the length of the AEZ growing periods in days, the agriculture field sizes, and the states of the US in which each pair of study areas are located.

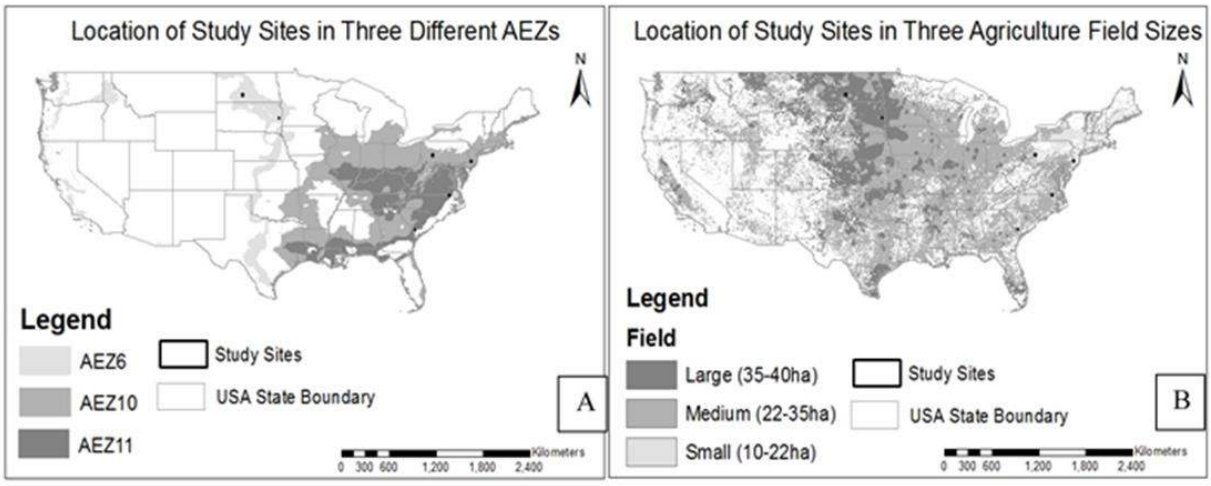

Figure 36A and 36B. The location of three pairs of Training (TR) and TEst (TE) regions selected each in three AEZs and three agriculture field sizes.

Table 35. The description of the six regions selected in three AEZs for different field sizes.

Regions	AEZ (LGP)	Field Size	States of the US
1 TR, 1 TE	AEZ 6 (120-149 days)	Large (35-40ha)	North-Dakota, South-Dakota
1 TR, 1 TE	AEZ 11 (270-299 days)	Medium (22-35ha)	North-Carolina, South-Carolina
1 TR, 1 TE	AEZ 10 (240-269 days)	Small (10-22ha)	New Jersey, Pennsylvania

LGP: Length of Growing Period; TR: TRaining; TE: TEst

The cropping schedule of different crop types was clearly defined to help with the selection of multi-dates of satellite imagery and identification of crop types for each of the six regions (Table 36). The planting and harvesting events for the agriculture crops were described as: (1) begin, (2) active, and (3) end growing stages. The spring (sp), summer (su), fall (f), and winter (w) growing seasons of agriculture crops were divided into early (e), mid (m), and late (l) to represent the months of a year.

Table 36. The cropping calendar of different crop types from three agriculture field sizes.

Crops	Jan (m-w)	Feb (l-w)	Mar (e-sp)	Apr (m-sp)	May (l-sp)	Jun (e-su)	Jul (m-su)	Aug (l-su)	Sep (e-f)	Oct (m-f)	Nov (l-f)	Dec (e-w)
Corn (L)				Planting						Harvesting		
Corn (M)			Planting				Harvesting					
Corn (S)				Planting					Harvesting			
Cotton (M)				Planting					Harvesting			
Soybean (L)					Planting				Harvesting			
Soybean (M)					Planting					Harvesting		
Soybean (S)					Planting					Harvesting		
Alfalfa (L)					Harvesting		Harvesting		Harvesting			
Other Hay (L)						Harvesting						
Other Hay (S)					Harvesting					Harvesting		
Spring Wheat (L)				Planting			Harvesting					
Double Crop (M)					Harvesting Planting				Planting	Harvesting Planting		

L: Large Field Size; M: Medium Field Size; S: Small Field Size; e: early; m: mid; l: late; sp: spring; su: summer; f: fall; w: winter

Datasets

Three different datasets were used to perform the augmentation, extension, and evaluation of the results. The first dataset was the Google Street View (GSV) technology featured in Google Maps and Google Earth that provides panoramic views from positions along many streets in the world since 2007. The agriculture field photos for 2017 were accessed on the Google Maps website (https://www.google.com/maps) to augment the crop type reference data for the three TR regions used in this research.

The second dataset was World View-2 (WV-2) satellite imagery of the year 2015 and derived vegetation indices (Figure 37 and Table 37). The World View-2 satellite imagery has eight multi-

spectral bands (i.e., coastal-blue, blue, green, yellow, red, red-edge, Near Infra-Red (NIR) 1, and NIR 2) at a spatial resolution of 0.6m. These multi-spectral bands were used to derive the vegetation indices for the classification of agriculture crops of the six regions. These indices are listed in Table 3 describing their name, spectral bands used to derive the indices, and the references.

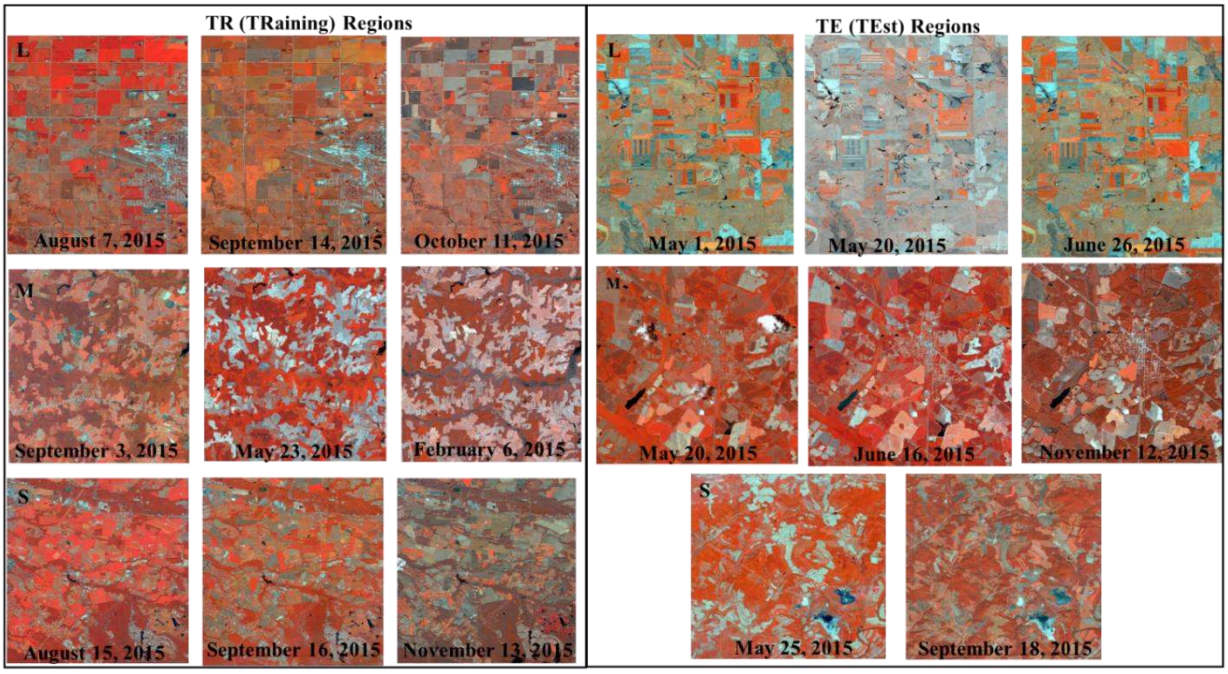

Figure 37. The World View-2 images used to investigate the use of multi-dates of imagery for extending the crop type reference data from the Training (TR) (left panel) to Test (TE) regions (right panel) in large (L), medium (M), and small (S) field sizes.

Table 37. List of vegetation indices that were explored and used in the classification of crop types.

Vegetation Index (VI)	VI Equations derived from WV-2 Spectral Bands	Reference
Difference Vegetation Index (DVI)	NIR – Red	(Erdas Imagine, 2015)
Green Normalized Difference Vegetation Index (GNDVI)	$(NIR - Green)/(NIR + Green)$	(Gitelson and Merzlyak, 1996)
Improved Modified Chlorophyll Absorption Ratio Index (MCARI)	$\frac{(1.5 * (2.5 * (NIR - Red) - 1.3 * (NIR - Green)))}{SQRT((2 * NIR + 1)^{2-(6*NIR-5*SQRT(Red)}}$	(Daughtry, 2000)
Modified Soil Adjusted Vegetation Index (MSAVI)	$2 * NIR + 1 - SQRT(2 * NIR + 1)^{2-(8*NIR-Red}))/2$	(Erdas Imagine, 2015)
Modified Red Edge Simple Ratio Index (MSR)	$((Red\ Edge - Coastal\ Blue))/((Red\ Edge + Coastal\ Blue))$	(Chen, 1996)
Normalized Difference Vegetation Index (NDVI)	$((NIR - Red))/((NIR + Red))$	(Rouse et al., 1973)
Soil and Atmospherically Resistant Vegetation Index (SARVI)	$((NIR - RB) * (1 + L))/(NIR + RB + L)$ RB: Red-Gamma*(Blue-Red); L (Vegetation Cover Correction Factor): 0.5; Gamma (Aerosol Content Stabilization Factor):1	(Kaufman and Tanre, 1992)
Soil Adjusted Vegetation Index (SAVI)	$((NIR - Red) * (1 + L))/((NIR + Red + L))$	(Panda et al., 2010)
Enhanced Vegetation Index (EVI)	$2.5*(((NIR - Red)/(NIR + 6(Red) - 7.5(Blue) + 1)))$	(Huete et al., 1997)

The third dataset was the Cropland Data Layer (CDL) (USDA, NASS) which was used as the reference data to evaluate the results achieved by the augmentation and extension approaches developed in this study for collecting crop type information from additional non-ground-based sources (Figure 38). CDL has been generated annually for all the states at 30m spatial resolution

beginning in 2009 (USDA-NASS and USDA, 2010) and is a reference crop type map developed for agriculture crops using Landsat imagery and ground-based information. The CDLs are 85–95% accurate for major crops in large agricultural states (Boryan et al., 2011). Therefore, CDL could be used to evaluate the augmented crop type reference data (2017) for the three TR regions and extended crop type maps (2015) for the six TR and TE regions. The CDL reference labels were cross-walked (translated) into the same classification scheme used for the six regions in this study (Table 35). The 2015 CDL data were used to evaluate the crop type maps of the TR and TE regions while 2017 CDL was used to evaluate the augmented crop type reference data of the TR regions. Figure 38 shows the six CDL maps of the year 2015 for the three TR (first row) and three TE (second row) regions studied in this research.

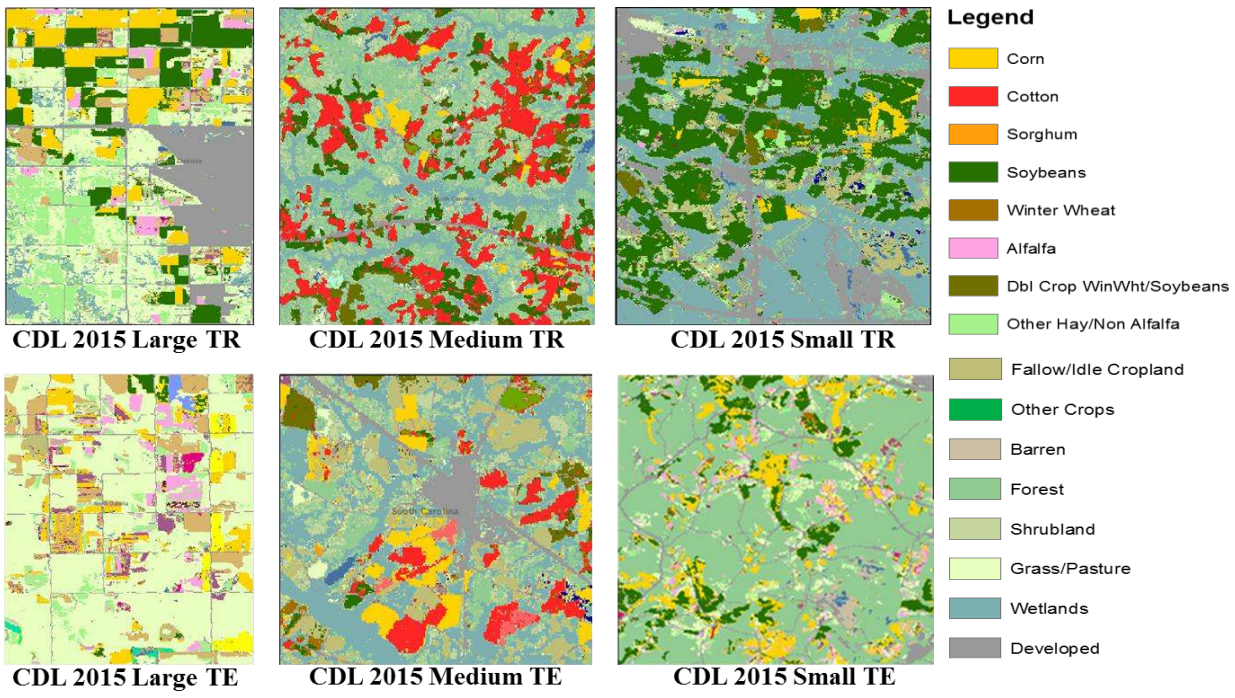

Figure 38. Cropland Database Layer (CDL) of TR (first row) and TE (second row) regions used as reference data to evaluate the results of augmentation and extension approaches.

One of the key elements of collecting additional crop type reference data and developing crop type maps from the classification of the satellite imagery is to use an appropriate classification scheme. A well-defined classification scheme helps to reduce the risk of misclassification of the cropland, fallow land, and different crop types from the satellite imagery. Therefore, a common hierarchical classification scheme was used to cross-walk or translate the reference labels into map labels for the classification of the satellite imagery and collecting reference data for creating and assessing the crop type maps. Figure 39 shows a hierarchical classification scheme which consists of three hierarchical levels to classify the crop, fallow, and non-crop at first level. The first level classes were re-grouped at second level into cropland including fallow and non-crop. At third level, only the cropland classes were classified into different crop types (e.g., Crop 1, 2, 3, and 4) for the six regions.

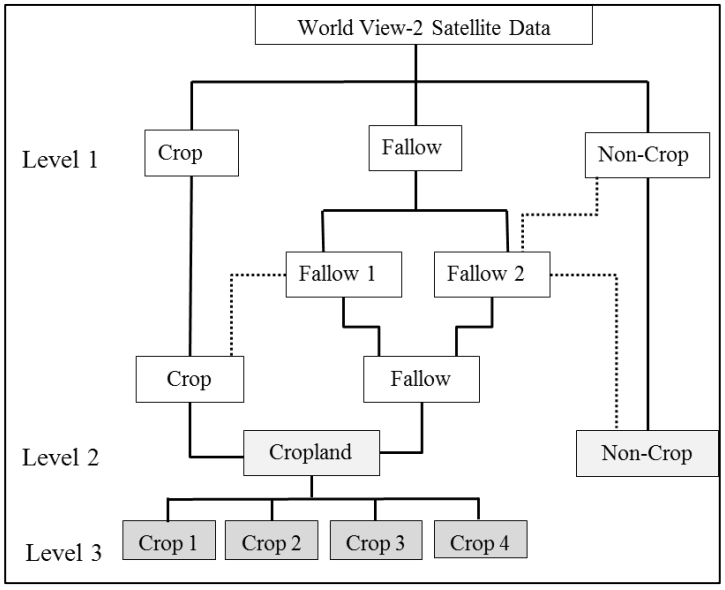

Figure 39. The hierarchical classification scheme followed to classify the agriculture crops of the six regions.

Methods

The objectives of augmenting and extending the limited crop type reference data were accomplished using three main methods. First, the augmentation of the limited crop type reference data was performed using the interpretation of photographs from GSV. Second, the extension of the crop type reference data was performed from the TR to TE region using an object-based image analysis (OBIA) of multi-dates of HRI to classify first as crop, no-crop, and then into agriculture crop types for the six regions. Third, accuracy assessment was performed to evaluate the augmentation and extension approaches by assessing the crop type reference data for the TR regions and crop/no-crop, crop type maps for the six regions, respectively. The following flow chart shows the overall methodology that was followed to augment the crop type reference data and spatially extend the CDL 2015 crop type reference data of the TR regions to TE regions within same AEZ and field by investigating the use of one, two, and three dates of satellite imagery (Figure 40).

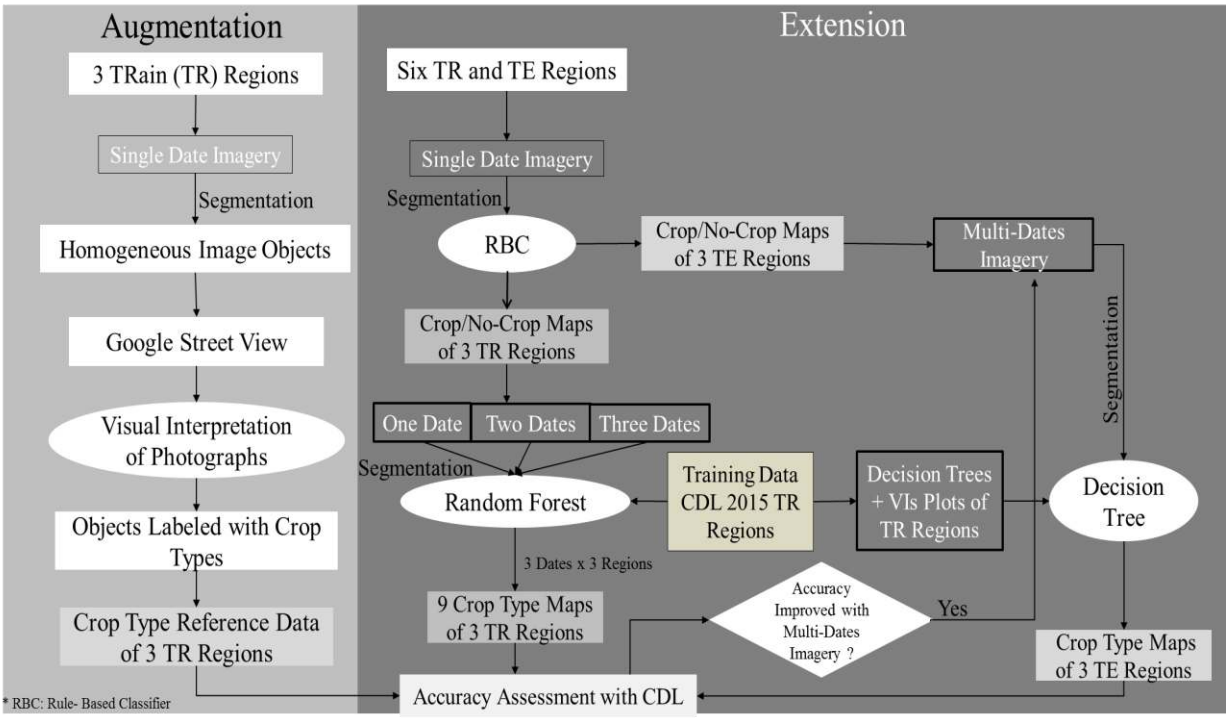

Figure 40. The overall methodology flow chart showing the augmentation and extension of the limited crop type reference data for the six regions.

Augmentation of crop type reference data for the three TR regions

The limited crop type reference data was augmented by interpretation of the agricultural field photographs collected along the major roads from Google Street View (GSV) in the US. The interpretation of photographs was performed by one interpreter based on prior knowledge of the visual characteristics of the different crop types of the three TR regions. The three TR regions of large, medium, and small field sizes were located on the Google Maps of 2017 and the field photographs were interpreted and labeled by the analyst for the different crop types based on the latest cropping calendar and physical characteristics. These interpretations were then compared and evaluated by comparison with the reference data from CDL of the year 2017.

Extension of crop type reference data from the TR regions to the TE regions

To extend the crop type reference data using the classification of satellite imagery from the TR to TE regions, the benefits of one, two, or three dates of satellite imagery were first investigated for the three TR regions. The multi-dates of satellite imagery for each of the six regions (3 TR and 3 TE regions) were created by mosaicking nine 2km by 2km World View-2 scenes. Consequently, a single region was comprised of nine World View-2 scenes, two dates had 18 scenes, and three dates had 27 scenes. The first image date tested was selected using the cropping calendar for the major crop types to show where high spectral variation might exist between the crop, fallow, and no-crop fields to produce crop/no-crop maps for each of the six regions (Figure 37). This first date imagery was subsequently combined with second and third dates of imagery selected using the cropping calendar to further separate different crop types (described in Table 35) to produce crop type maps for the three TR regions for each of the three field sizes. The crop type maps of the three TE regions were then developed based on the results of this TR analysis using best multi-dates of satellite imagery.

The extension of crop type reference data from the TR regions to TE regions was executed in the following five steps:

First, the crop/no-crop maps of the six regions were produced using the hierarchical classification scheme (described in the section 2.2) and an Object-Based Image Analysis (OBIA) of the first date satellite imagery. The imagery of each region were segmented into homogeneous groups of pixels (i.e., objects) based on the spectral, spatial, and texture characteristics using the Multi-Resolution Segmentation (MRS) method in the Trimble eCognition 9.3 version software (Definiens, 2017). The segmentation was performed by defining the scale, color, and shape

parameters using a bottom-up merging approach. A scale of 100, 70, and 60 were used for large, medium, and small agriculture field sizes, respectively which provided an appropriate segmentation of the field boundaries. The color and shape parameters were defined as 0.5 and 0.3, respectively for the three different field sizes, providing more weight to the spectral features of the objects while merging them into homogeneous groups. The homogeneous objects were then classified into crop (cropland and fallow) and no-crop using the Rule-Based Classifier (RBC) based on their mean spectral response and texture values for each of the six regions.

Second, the crop types of the three TR regions were classified within the crop class of the crop/no-crop maps at Level 3 of the hierarchical classification scheme (Figure 39). The crop type classification was performed using the Random Forest (RF) classification algorithm for one, two, and three dates of satellite imagery combined with their Vegetation Indices (VIs) described in Table 36. A total of 50 samples per map class was collected from the 2015 CDL of the TR regions for training the RF algorithm and assessing the crop type maps. These samples were divided into independent training and assessment samples based on a 40-60% split rule. A stratified random sample with 20 training samples for each crop type class was used in the RF classifier to create the crop type maps leaving 30 samples for each crop type to perform the accuracy assessment.

Third, the results of the multi-date image analysis of the TR regions, as described above, was used to select the best imagery for each of the three TE regions. The same training samples used in the RF classification algorithm for the TR regions were used for training the DT algorithm and creating the crop type maps of the TE regions. However, since the training samples of the TR regions are spatially located on the TR imagery, the actual training sample locations could not be directly used for the TE regions. Instead, the statistics derived from the 20 training samples for

each class of the three TR regions were used to derive unique spectral and texture thresholds for the different crop types and applied to a DT algorithm to classify the TE regions. The RF algorithm could not be used to classify the TE regions as this, and many other algorithms, require spatially locating training areas on the imagery. However, a DT algorithm could be used with the training statistics acquired for the TE regions.

Fourth, the thresholds of spectral and texture characteristics (i.e., training statistics for the TE regions) were derived for the different crop types using the following two steps: (1) Decision Tree (DT) modeling on the TR regions and (2) plotting the relationship of VIs for different crop types of the TR regions. The DT modeling created models from the pool of all the spectral and texture features acquired from each TR region using the recursive partitioning platform in the statistical software JMP 8 (SAS Institute Inc., Cary, NC, USA). This binary recursive algorithm splits the training data for each of the three TR regions and builds Decision Trees (DTs) by choosing the features and corresponding values that best fit the partial response in every split. The algorithm examined a very large number of possible splits and determined the most significant ones using the largest likelihood-ratio chi-square ($\chi 2$) statistic. A cross-validation method was applied to define and evaluate each of the models in which samples were randomly separated into 40% for model training and 60% for model validation. This procedure was repeated ten times to generate results using random combinations of training and validation sets (Friedl and Brodley, 1997). The best DTs were chosen for each of the three TR regions by selecting the optimal model which provided the smallest error rate when run on the independent dataset (Mingers, 1989). In addition, the relationship between the Vegetation Indices (VIs) (e.g., NDVI, MSR, DVI, GNDVI, MCARI, SARVI, and EVI) were also plotted to determine the most useful and important indices.

Consequently, the best DTs and plots of VIs were used to determine the threshold values of spectral and texture characteristics for the different crop types.

Finally, the threshold values of spectral and texture characteristics derived from the training samples of the TR regions were used for training the DT classification algorithm to produce the crop type maps for the three TE regions. The crop type maps of the TE regions were assessed using 30 assessment samples for each crop type collected from 2015 CDL of the TE regions.

Accuracy assessment of augmentation and extension

The results of augmentation and extension of the crop type reference data for the six regions were evaluated separately by comparing with the CDL reference data in the form of error matrices. The reference data for each assessment were always collected independently of the training data. The entire augmented reference data collected from the GSV were compared with the 2017 CDL reference data to create the error matrices for each of the three TR regions. The reference dataset consists of 30 samples collected from the 2015 CDL reference data for each crop type to assess the crop type maps of the three TR and three TE regions. In addition to the crop type maps, the crop/no-crop maps of the three TR and three TE regions were also assessed using the reference dataset collected from the 2015 CDL data. The crop/no-crop reference dataset consists of the crop samples which were subsequently derived by combining the crop type samples used in the assessment of crop type maps while the no-crop samples were collected proportional to their area for each of the TR and TE regions.

Finally, the assessment reference data was used to assess the augmented crop type reference data of the three TR regions, the crop/no-crop maps, and the crop type maps of the three TR and

three TE regions in the form of object-based error matrices presenting the accuracy measures (i.e., overall, user's, and producer's accuracy).

Results

The results of this study are presented in the following three sub-sections: (1) augmented crop type reference data from the GSV for the TR regions, (2) the extension of crop type reference data from the TR regions to the TE regions, and (3) the assessment reference data used to generate the error matrices for all the crop/no-crop and crop type maps of the six regions.

Augmented crop type reference data of the three TR regions

The augmented crop type reference data for the three TR regions was generated by the interpretation of photographs collected from GSV. Figure 41 presents the augmented crop type reference data for the large, medium, and small agriculture field size TR regions.

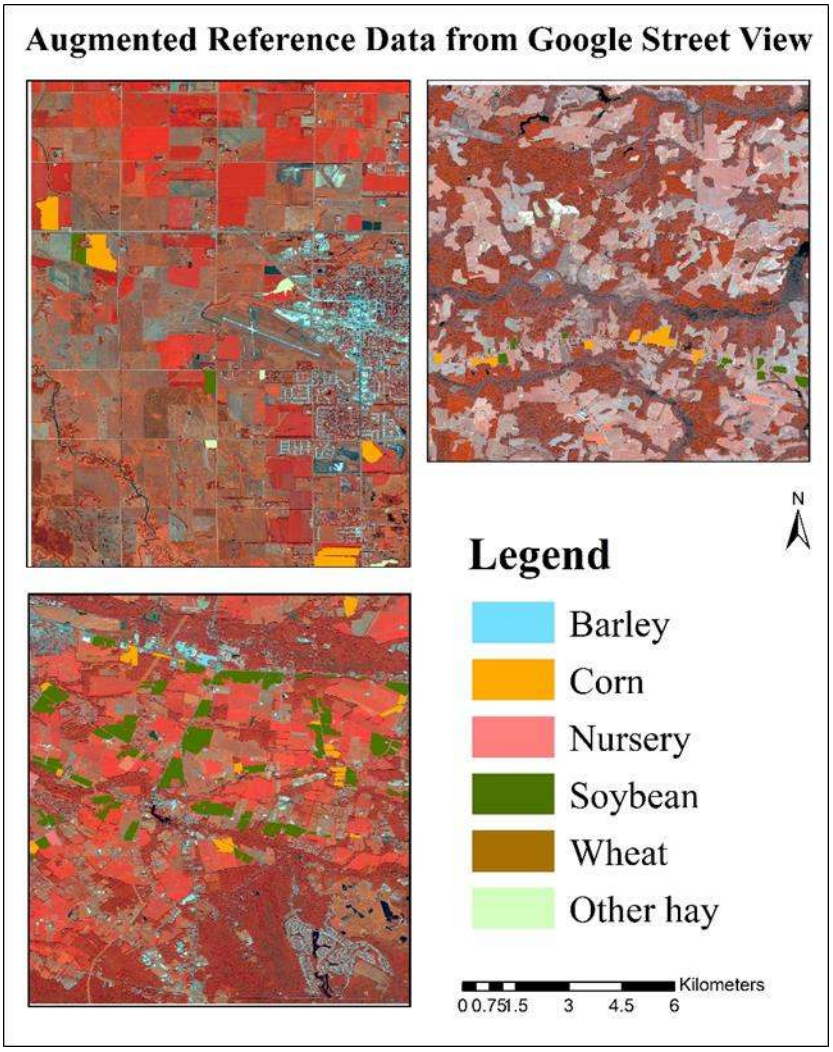

Figure 41. Augmented crop type reference data of three TR regions collected from GSV for large, medium, and small field sizes.

Extension of crop type reference data from the TR regions to TE regions based on the investigation of one, two, and three dates of imagery for the TR regions

The crop/no-crop maps of the six regions (3 TR and 3 TE regions) were first generated from the classification of most appropriate World View-2 satellite imagery using a rule-based classifier and an object-based image analysis. Figure 42 presents the crop/no-crop maps of 3 TR and 3 TE regions in large, medium, and small field sizes.

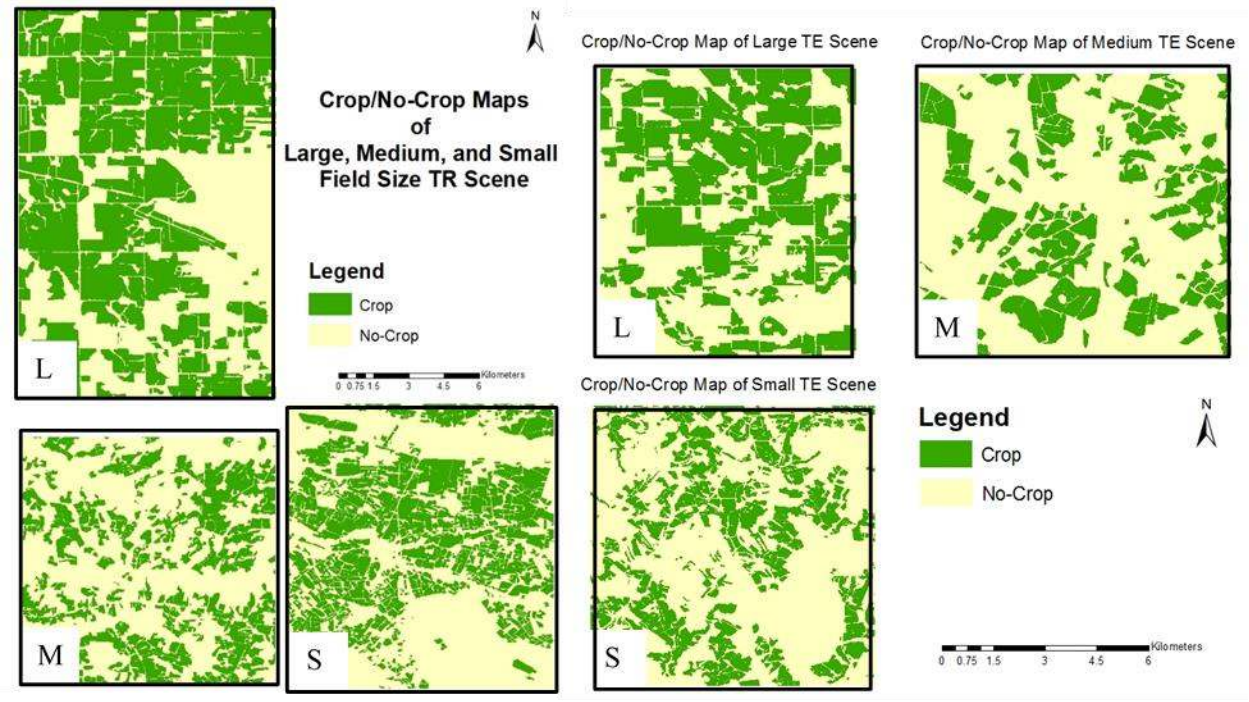

Figure 42. The crop/no-crop maps of the three TR and three TE regions in large (L), medium (M), and small (S) field sizes.

The crop/no-crop maps of the six regions were subsequently classified into the crop types using the phenology-based classification algorithm and training data collected from the 2015 CDL of the TR regions. The crop type maps for the TR regions were produced from the investigation of one, two, and three dates of satellite imagery and reference data collected from the CDL of these regions. While the crop type maps of the TE regions were developed from the multi-dates of satellite imagery and training data derived from the Decision Trees (DT) and the relationship of Vegetation Indices (VIs) of the different crop types of the TR regions.

Figure 43 presents the Decision Trees (DTs) that were used to derive the threshold of the spectral and textural features of different crop types of the TR regions using the hierarchical recursive partitioning algorithm in JMP software. Figure 44, 45, and 46 present the relationship plots of the Vegetation Indices (VI's) for the different agriculture crops of the three TR regions, respectively.

A total of 20 samples for each map class were collected for training the classification algorithms to create the crop type maps of the TR and, by extension, the training statistics used in the TE regions. Table 38 presents the entire training data collected from the 2015 CDL and their derived statistics of the TR regions to classify the crop types of the six regions for each of the field sizes and AEZs.

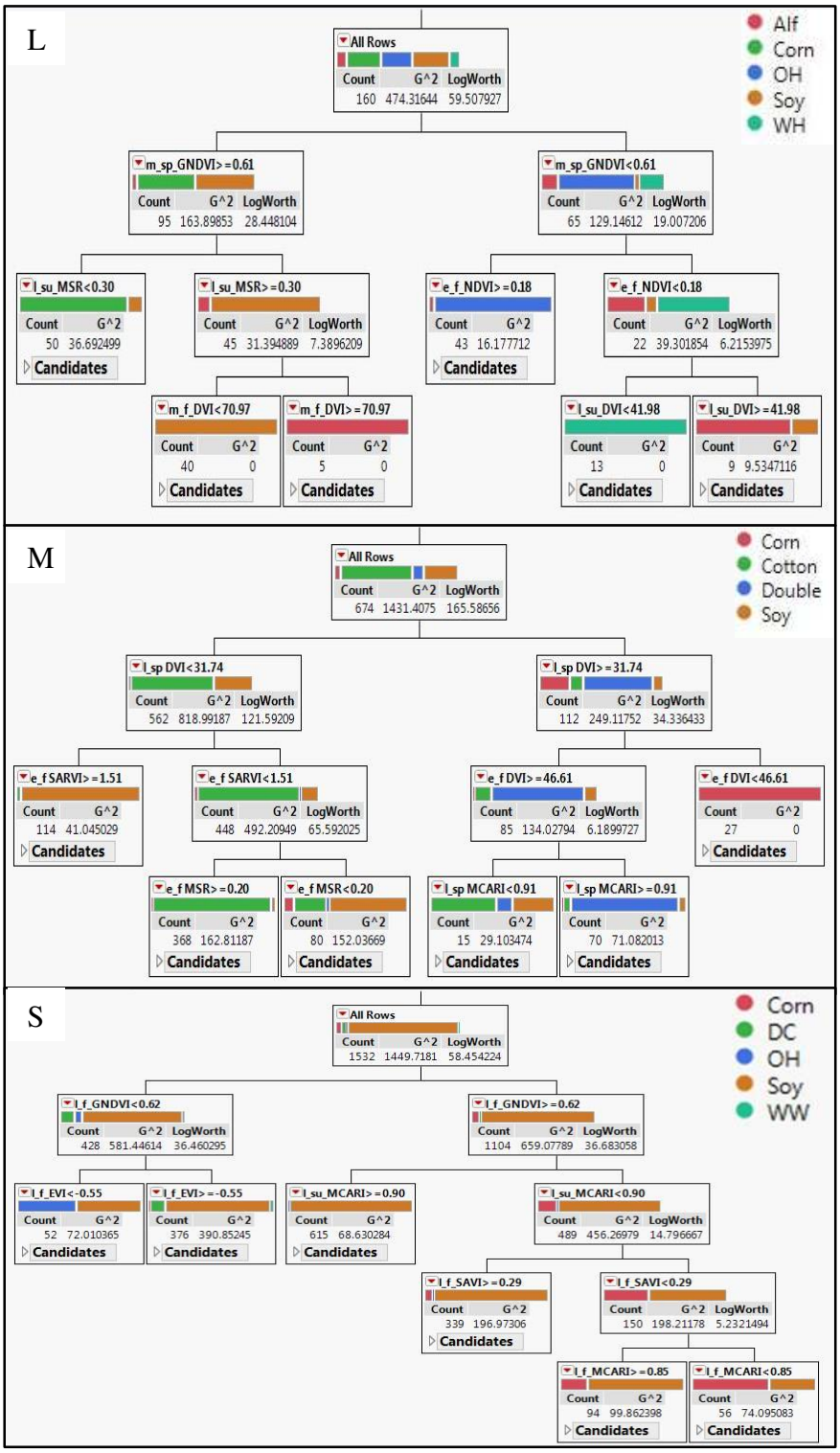
L
All Rows
Count G^2 LogWorth
160 474.31644 59.507927
Alf
Corn
OH
Soy
WH
m_sp_GNDVI>=0.61
Count G^2 LogWorth
95 163.89853 28.448104
m_sp_GNDVI<0.61
Count G^2 LogWorth
65 129.14612 19.007206
l_su_MSR<0.30
Count G^2
50 36.692499
Candidates
l_su_MSR>=0.30
Count G^2 LogWorth
45 31.394889 7.3896209
e_f_NDVI>=0.18
Count G^2
43 16.177712
Candidates
e_f_NDVI<0.18
Count G^2 LogWorth
22 39.301854 6.2153975
m_f_DVI<70.97
Count G^2
40 0
Candidates
m_f_DVI>=70.97
Count G^2
5 0
Candidates
l_su_DVI<41.98
Count G^2
13 0
Candidates
l_su_DVI>=41.98
Count G^2
9 9.5347116
Candidates
M
All Rows
Count G^2 LogWorth
674 1431.4075 165.58656
Corn
Cotton
Double
Soy
l_sp_DVI<31.74
Count G^2 LogWorth
562 818.99187 121.59209
l_sp_DVI>=31.74
Count G^2 LogWorth
112 249.11752 34.336433
e_f_SARVI>=1.51
Count G^2
114 41.045029
Candidates
e_f_SARVI<1.51
Count G^2 LogWorth
448 492.20949 65.592025
e_f_DVI>=46.61
Count G^2 LogWorth
85 134.02794 6.1899727
e_f_DVI<46.61
Count G^2
27 0
Candidates
e_f_MSR>=0.20
Count G^2
368 162.81187
Candidates
e_f_MSR<0.20
Count G^2
80 152.03669
Candidates
l_sp_MCARI<0.91
Count G^2
15 29.103474
Candidates
l_sp_MCARI>=0.91
Count G^2
70 71.082013
Candidates
S
All Rows
Count G^2 LogWorth
1532 1449.7181 58.454224
Corn
DC
OH
Soy
WW
l_f_GNDVI<0.62
Count G^2 LogWorth
428 581.44614 36.460295
l_f_GNDVI>=0.62
Count G^2 LogWorth
1104 659.07789 36.683058
l_f_EVI<-0.55
Count G^2
52 72.010365
Candidates
l_f_EVI>=-0.55
Count G^2
376 390.85245
Candidates
l_su_MCARI>=0.90
Count G^2
615 68.630284
Candidates
l_su_MCARI<0.90
Count G^2 LogWorth
489 456.26979 14.796667
l_f_SAVI>=0.29
Count G^2
339 196.97306
Candidates
l_f_SAVI<0.29
Count G^2 LogWorth
150 198.21178 5.2321494
l_f_MCARI>=0.85
Count G^2
94 99.862398
Candidates
l_f_MCARI<0.85
Count G^2
56 74.095083
Candidates

Figure 43. The Decision Trees (DTs) built from the 2015 CDL reference data of the three TR regions for large (L), medium (M), and small (S) field sizes.

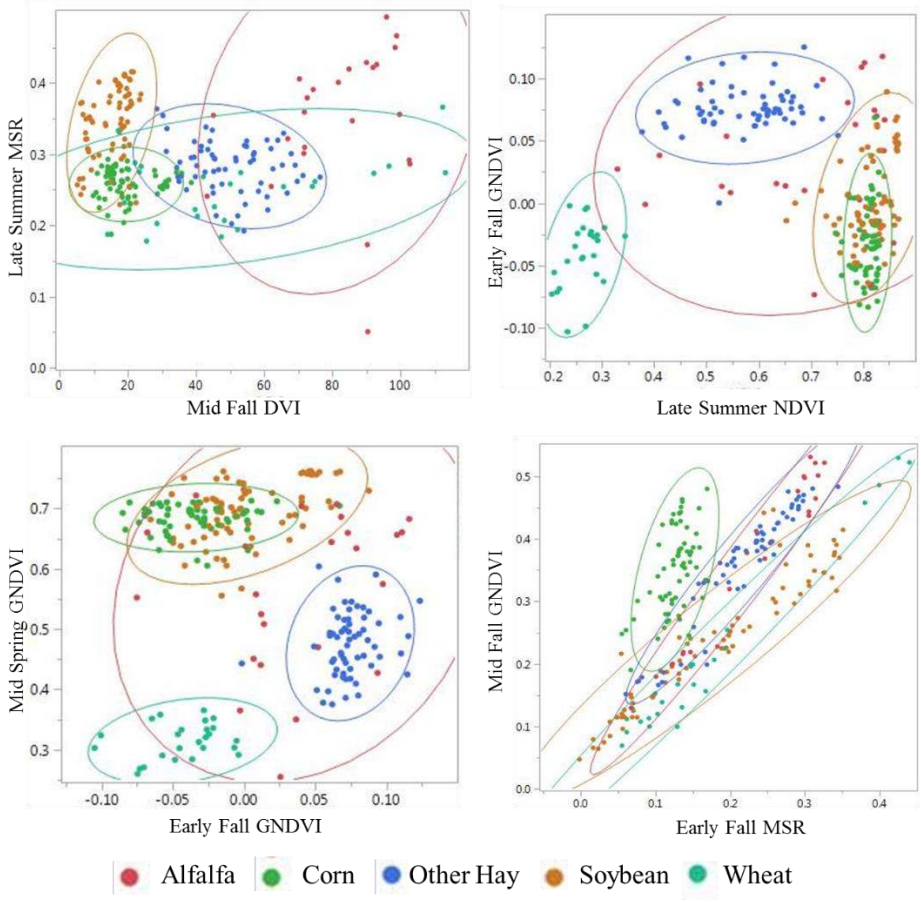

Figure 44. The relationship between Vegetation Indices (MSR, DVI, NDVI, and GNDVI) in different growing seasons in the large agriculture field size TR region.

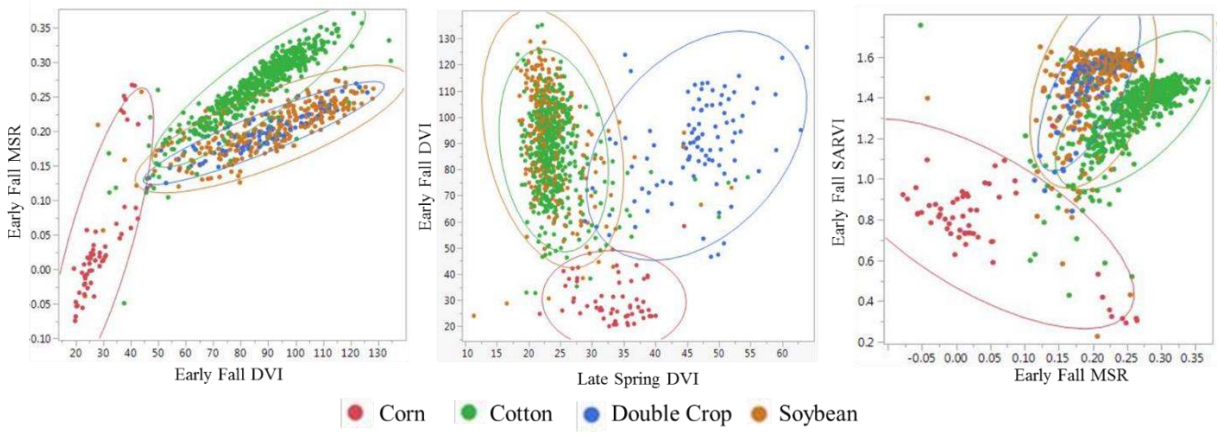

Figure 45. The relationship between Vegetation Indices (MSR, DVI, and SARVI) in different growing seasons in the medium agriculture field size TR region.

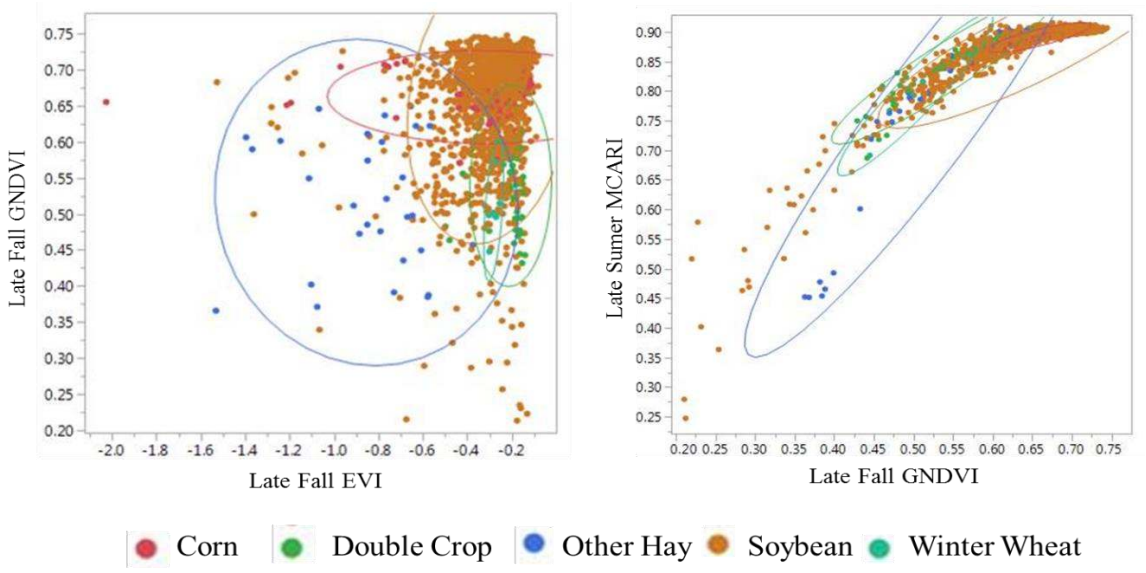

Figure 46. The relationship between Vegetation Indices (GNDVI, EVI, and MCARI) in different growing seasons in the small agriculture field size TR region.

Table 38. The training data collected from the 2015 CDL of the TR regions to classify the crop type maps of the TR and TE regions.

Crop Types	Field Size	AEZ	Training Data (TR)	Training Data (TE)
Corn	Large	AEZ 6	20 x 5=100	85 (5 Crop Types)
Soybean				
Spring Wheat				
Alfalfa				
Other Hay				
Cotton	Medium	AEZ 11	20 x 4=80	63 (4 Crop Types)
Corn				
Soybean				
Double Crop				
Corn	Small	AEZ 10	20 x 5=100	120 (5 Crop Types)
Soybean				
Other Hay				
Double Crop				
Fallow				

The crop type maps of the six regions were produced using the training data described in Table 38. Figure 47 presents the three crop type maps for the three TR regions in the large, medium, and small field sizes. Figure 48 presents the crop type maps for the three TE regions developed from the classification of multi-dates of satellite imagery using the DT algorithm and training samples derived from the DT and VIs of the TR regions.

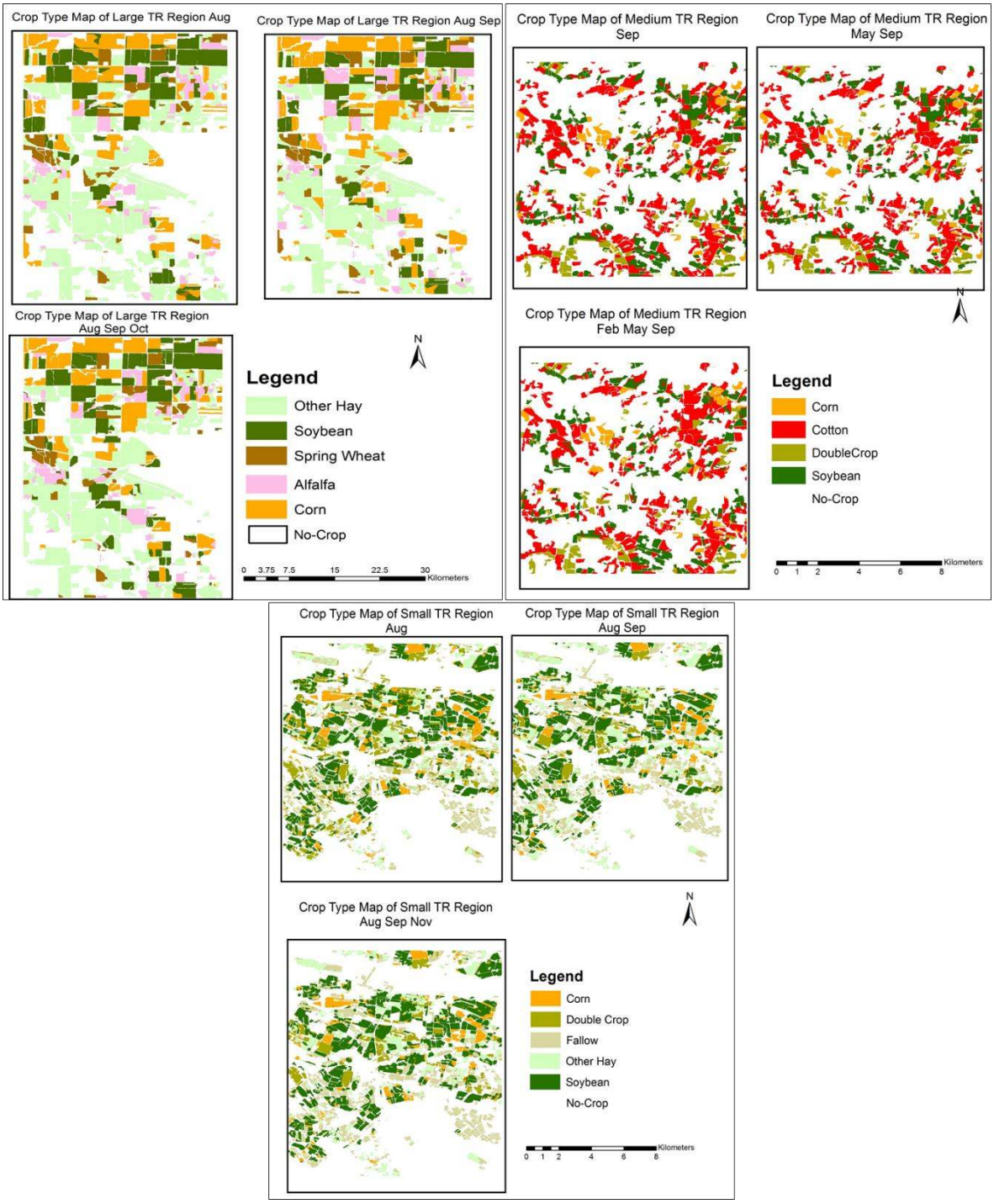

Figure 47. Crop type maps of three TR regions produced from one, two, and three dates of satellite imagery in the large, medium, and small field sizes.

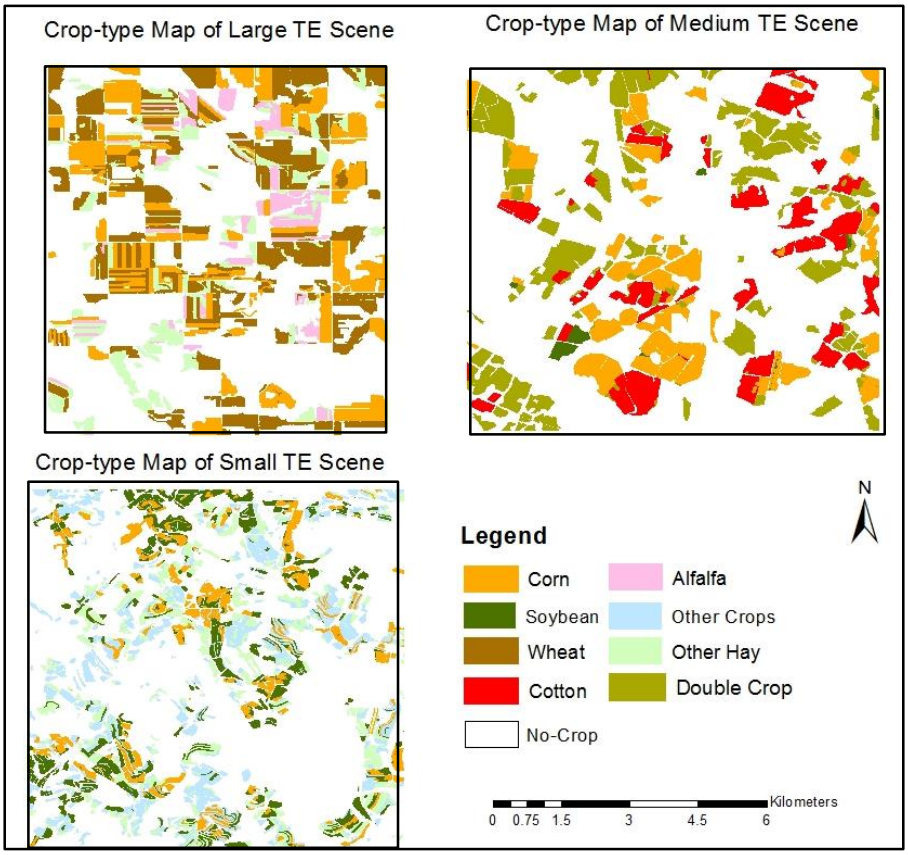

Figure 48. The crop type maps of the three TE regions produced from the classification of multi-dates of satellite imagery in large, medium, and small field sizes.

Accuracy Assessment

The results of the accuracy assessment include the reference data collected to assess the crop/no-crop and crop type maps of the six regions and the accuracy measures generated for the augmented crop type reference data and the crop/no-crop and crop type maps of the six regions. Table 39 presents the assessment reference data collected from the CDL of the US to assess the augmented reference data, crop/no-crop, and crop type maps of the six regions.

Table 39. The reference data used to assess the crop/no-crop and crop type maps of the three TR and three TE regions.

Crop types	Field Size	AEZ	Reference Data (TR Region)	Reference Data (TE Region)	Reference Data (Augmented TR Region)
Corn Soybean Spring Wheat Alfalfa Other Hay	Large	AEZ 6	C: 110* (46%) NC: 130 (54%) Total: 240	C: 120* (38%) NC: 195 (62%) Total: 315	25 (3 Crop Types)
Cotton Corn Soybean Double Crop	Medium	AEZ 11	C: (30x4) =120 (39%) NC: 187 (61%) Total: 307	C: 95* (36%) NC: 170 (64%) Total: 265	19 (2 Crop Types)
Corn Soybean Other Hay Double Crop Fallow	Small	AEZ 10	C: (30x5) =150 (45%) NC: 180 (55%) Total: 330	C: (30x4) =120 (27%) NC: 325 (73%) Total: 445	227 (2 Crop Types)

*minimum 30 sample size not achieved for rare crop types; the cropland and no-cropland area proportions are presented in percentages for each region; C: Crop; NC: No-Crop; TR: TRaining; TE: TEst

The accuracy assessment was performed to assess the augmented crop type reference data of the three TR regions collected from the GSV for large, medium, and small field sizes. The error matrices were generated using the all the reference data available from the GSV and might have insufficient samples for some crop types (Table 39). Table 40 presents the user's, producer's, and overall accuracy of the crop type reference data collected from the GSV for the three TR regions

in the large, medium, and small field sizes. The overall accuracy indicates the percent of correctly labeled agriculture fields from the GSV.

Table 40. The evaluation of the augmented crop type reference data collected from GSV.

Field Sizes	Crop types	Samples collected from GSV	User's Accuracy	Producer's Accuracy	Overall Accuracy
Large	Corn	15	33.3%	83.3%	44.0%
	Other Hay	5	20.0%	100.0%	
	Soybean	5	100.0%	33.3%	
Medium	Cotton	8	50.0%	44.4%	47.4%
	Soybean	11	45.4%	71.4%	
Small	Corn	39	23.1%	23.7%	74.0%
	Soybean	188	84.5%	86.0%	

Second, the accuracy assessment was performed to assess the crop/no-crop and crop type maps of the six regions resulting in the overall, user's, and producer's accuracy in the form of error matrices for large, medium, and small field sizes. Table 41 presents the error matrices of the crop/no-crop maps of the TR and TE regions for large, medium, and small field sizes. The overall accuracy of the crop/no-crop maps of the three TR regions in the large, medium, and small field sizes are 89.58%, 91.86%, and 94.2%, respectively. While the overall accuracy of the crop/no-crop map of the three TE regions in the large, medium, and small field sizes are 97.78%, 96.23%, and 97.98%, respectively. Table 42 presents the overall accuracy of 73.75%, 90.23%, and 83.33%, respectively for the crop type maps of the three TR regions developed from one, two, and three dates of satellite imagery.

Table 41. The error matrices of crop and no-crop maps of TR and TE regions for the large, medium, and small field sizes.

Large TR		Reference Data			
		Crop	No-Crop	Total	User's Accuracy
Map Data	Crop	109	24	133	81.95%
	No-Crop	1	106	107	99.07%
Total		110	130	240	
Producer's Accuracy		99.09%	81.54%		**89.58%**

Large TE		Reference Data			
		Crop	No-Crop	Total	User's Accuracy
Map Data	Crop	119	6	125	95.20%
	No-Crop	1	189	190	99.47%
Total		120	195	315	
Producer's Accuracy		99.17%	96.92%		**97.78%**

Medium TR		Reference Data			
		Crop	No-Crop	Total	User's Accuracy
Map Data	Crop	108	13	121	89.26%
	No-Crop	12	174	186	93.55%
Total		120	187	307	
Producer Accuracy		90.00%	93.05%		**91.86%**

Medium TE		Reference Data			
		Crop	No-Crop	Total	User's Accuracy
Map Data	Crop	95	10	105	90.48%
	No-Crop	0	160	160	100.00%
Total		95	170	265	
Producer's Accuracy		100.0%	94.12%		**96.23%**

Small TR		Reference Data			
		Crop	No-Crop	Total	User's Accuracy
Map Data	Crop	142	11	153	92.81%
	No-Crop	8	169	177	95.48%
Total		150	180	330	
Producer's Accuracy		94.67%	93.89%		**94.24%**

Small TE		Reference Data			
		Crop	No-Crop	Total	User's Accuracy
Map Data	Crop	113	0	113	100.00%
	No-Crop	9	323	332	97.29%
Total		122	323	445	
Producer's Accuracy		92.62%	100.00%		**97.98%**

Table 42. The overall accuracy of the crop type maps of the three TR regions developed from one, two, and three dates of satellite imagery.

Regions	Accuracy (One date)	Accuracy (Two dates)	Accuracy (Three dates)
Large TR	67.1%	69.2%	**73.8%**
Medium TR	88.6%	89.6%	**90.2%**
Small TR	75.8%	80.0%	**83.3%**

Table 43, 44, and 45 present the evaluation of the crop type maps of the three TE regions developed from the extended 2015 CDL reference data of the TR regions and multi-dates of satellite imagery in large, medium, and small field sizes, respectively. The overall accuracy of the extended crop type maps for large, medium, and small fields sizes are 93.65%, 93.21%, and 84.49%, respectively.

Table 43. The error matrix of crop type map generated from multi-dates of World View-2 imagery for the TE region in the large agriculture field size.

Large TE		Reference Data						
		Corn	Alfalfa	Other Hay	Wheat	No-Crop	Total	User's Accuracy
Map Data	Corn	28	0	0	0	0	28	100.00%
	Alfalfa	0	24	4	0	0	28	85.71%
	Other Hay	0	5	24	0	5	34	70.59%
	Wheat	2	1	1	30	1	35	85.71%
	No-Crop	0	0	1	0	189	190	99.47%
Total		30	30	30	30	195	315	
Producer's Accuracy		93.33%	80.00%	80.00%	100.00%	96.92%		**93.65%**

Table 44. The error matrix of crop type map generated from multi-dates of World View-2 imagery for the TE region in the medium agriculture field size.

Medium TE		Reference Data						
		Corn	Soybean	Double Crop	Cotton	No-Crop	Total	User's Accuracy
Map Data	Corn	28	0	0	1	2	31	90.32%
	Soybean	0	4	0	0	0	4	100.00%
	Double Crop	1	1	27	1	6	36	75.00%
	Cotton	1	0	3	28	2	34	82.35%
	No-Crop	0	0	0	0	160	160	100.00%
Total		30	5	30	30	170	265	
Producer's Accuracy		93.33%	80.00%	90.00%	93.33%	94.12%		**93.21%**

Table 45. The error matrix of crop type map generated from multi-dates of World-View 2 imagery for the TE region in the small agriculture field size.

Small TE		Reference Data						
		Corn	Soybean	Other Crops	Other Hay	No-Crop	Total	User's Accuracy
Map Data	Corn	24	11	0	0	0	35	68.57%
	Soybean	5	15	1	0	0	21	71.43%
	Other Crops	1	4	14	2	0	21	66.67%
	Other Hay	0	0	13	23	0	36	63.89%
	No-Crop	2	0	2	5	323	332	97.29%
Total		32	30	30	30	323	445	
Producer's Accuracy		75.00%	50.00%	46.67%	76.67%	100.00%		**84.49%**

Discussion

The crop type mapping at large scales and with high resolution imagery is non-existent in the literature (Inglada et al., 2015). The mapping and accuracy assessment of large area crop type maps heavily depends on quality-assured reference data collected from different sources for generating accurate crop type information (Bayas et al., 2017). There have been numerous small area crop type mapping efforts for limited number of crop type classes where crop type reference data were easily collected from ground-based surveys (Badhwar, 1984; Murthy et al., 2003; Verbeiren et al., 2008; Jain et al., 2016). However, such ground-based reference data might be insufficient to classify the crop types for large areas (e.g., any continent or the entire world) due to inability to access the limited regions of different continents. The limited availability of sufficient crop type reference data is required to be enriched using augmentation and extension approaches for large area crop type mapping and assessment from non-ground-based sources (e.g., Google Street View and High-Resolution Imagery). Therefore, the goals of this research were to evaluate our ability

to augment and extend reference data used for assessing thematic map accuracy. The crop type reference data was extended using multi-date satellite imagery. To generate accurate crop type maps and sufficient reference data, the potential of augmentation, multi-date satellite imagery, and extension approaches must be evaluated and discussed for different field sizes.

Identification of crops to augment the crop type reference data for different field size TR regions

The augmentation of limited crop type reference data involves the identification of crop types based on their physical characteristics through the interpretation of photographs available from the GSV for the TR regions of large, medium, and small field sizes. The quality of such additional crop type reference data collected from the GSV depends on the interpreter's skills and ability to discriminate different crop types. Figure 41 shows the distribution of interpreted crop type reference fields (data) along the major roads for each of the large, medium, and small field size TR regions. The major challenge for collecting augmented crop type reference data is the limited availability of Google Street View along the major roads in specific regions of the world. As a result, the augmentation results demonstrate unbalanced and insufficient sample size for each crop type and therefore, would not be appropriate to perform the classification and assessment of the crop type maps.

Identification of crops to investigate the benefits of multi-dates of imagery for the extension of crop type reference data

The crop/no-crop maps of the six regions were developed from the most appropriate, single date imagery using a spectral and textural rule-based classification algorithm (Figure 42). The most appropriate date of satellite imagery was selected from the available images for each region to develop crop/no-crop maps. Using these crop/no-crop maps, the crop type maps were subsequently developed by selecting one, two, and three dates of imagery using the random forest classifier because of its robustness to the spectral variations of similar crop types (Figure 47). Figure 47 presents nine crop type maps generated from the single, two, and three date satellite imagery for each of the three TR regions with different field sizes. The subsequent addition of two and three dates of satellite imagery provides more temporal variation in spectral responses for discriminating and mapping different crop types with improved accuracy. Consequently, the potential benefits of using multi-dates of satellite imagery for crop type mapping are investigated based on the improved accuracy of crop type maps achieved with classification using more than a single date of imagery. Figure 49 shows multi dates of satellite imagery and the crop type map developed from a combination of three dates of imagery for a medium field size TR region. The first single date of imagery acquired in the month of September provides unique spectral characteristics for discriminating different types of crops including both harvested and standing crops (e.g., corn and soybean) (Figure 49). However, the additional dates of satellite imagery acquired in the month of May and February provide more spectral and textural variations among the crop types (e.g., cotton and double crop). Consequently, the crop type map developed from the three dates of satellite imagery presents the benefits of using multi dates of imagery for effective crop type mapping in different field size regions.

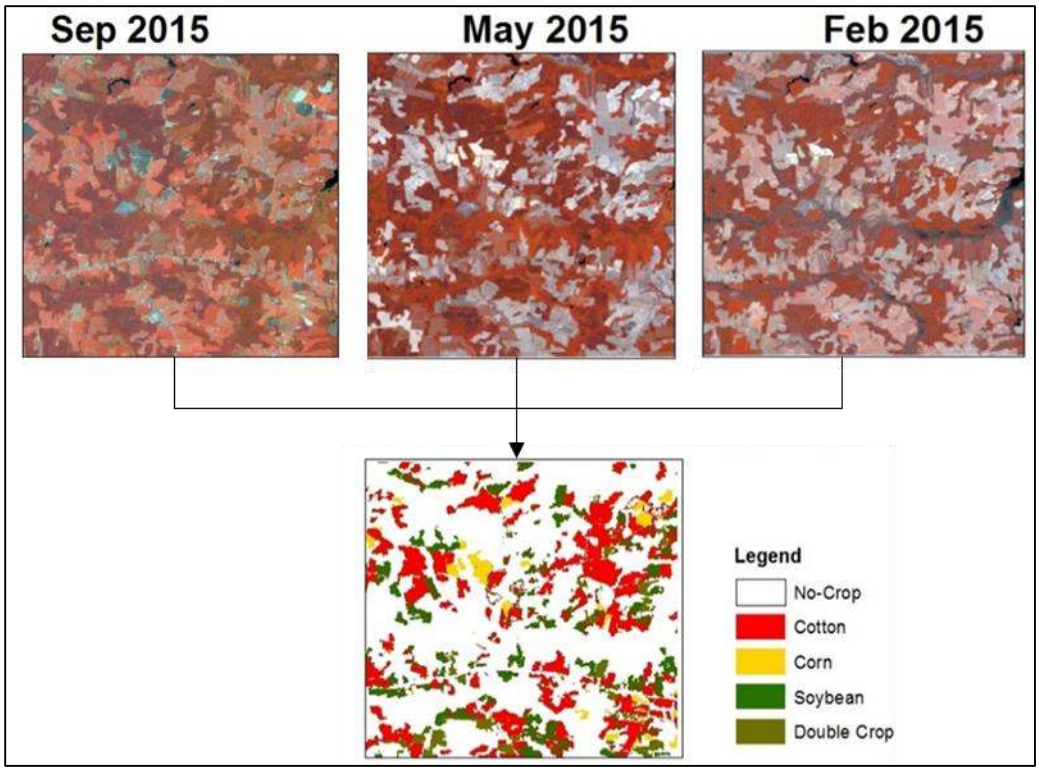

Figure 49. The crop type map developed from the multi dates of World View-2 imagery showing the unique spectral characteristics for the different crop types of the medium field size TR region.

In addition to providing additional spectral characteristics for mapping different crop types of a region, the multi-dates of satellite imagery help to identify the discrepancies and errors (e.g., omission or commission) that existed in crop type reference data. For example, the satellite imagery acquired in the month of November for the small fields size TR region shows unique spectral characteristics as dark red patches in the right lower corner (Figure 50). The agriculture fields with unique spectral characteristics were expected to be some seasonal crop (e.g. cranberry growing in the month of November) and labeled as fallow land on the CDL reference data of the

year 2015 (Figure 50). Comparing the CDL reference data of the year 2014 and 2017 showed that these fields were labeled as cranberry crop. Therefore, the crop type mapping using multi-date satellite imagery acquired in August, September, and November are effective for identifying the omission errors in the reference data existed due to limited field surveys conducted in different parts of the US.

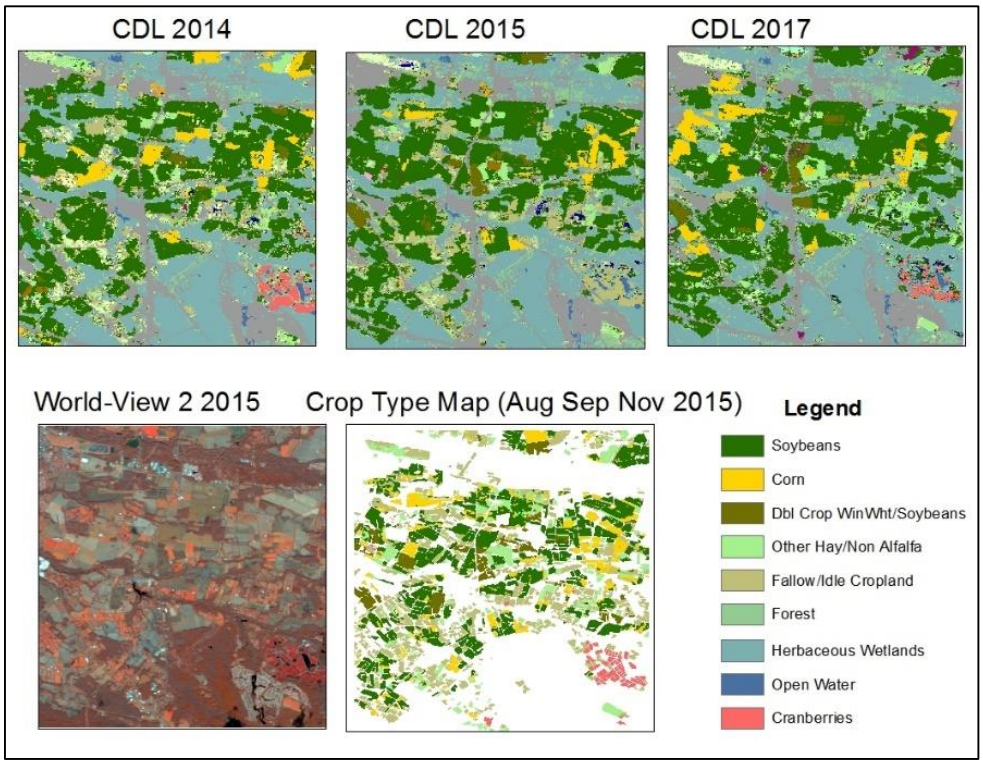

Figure 50. The comparison of CDL reference data of the small field size TR region with the satellite imagery.

The use of three dates of satellite imagery demonstrated advantages over the single and two dates to perform effective crop type mapping for each of the field sizes for the TR regions due to:

(1) spectral and textural variations and (2) capability to identify the errors that existed in the reference data (Ehrlich et al., 1994; Panigrahy and Sharma, 1997; Simonneaux et al., 2008). Based on this multi-date analysis in the TR regions, the best three dates of satellite imagery were selected to perform the classification of crop types for two (large and medium field size) of the TE regions except the small field size TE region for which only two dates of imagery were available.

The extension of limited crop type reference data involves the identification of crop types for collecting additional reference data from the classification of the best multi-dates of HRI for the TE regions. The identification of crop types becomes complex due to their diverse spectral characteristics in different regions. The decision trees (Figure 43) and the relationship of vegetation indices (VI's) (Figure 44, 45, and 46) derived from each of the TR regions were used to identify the crop types for each of the large, medium, and small field sizes in the TE regions.

The crop types of the large field size TR region (Alfalfa, Corn, Other Hay, Soybean, and Wheat) were discriminated by means of a sequence of four VIs (NDVI, DVI, MSR, and GNDVI) (Figure 44). Soybean was characterized by high green vegetation vigor in late summer and low in mid fall. Other Hay was characterized by high vegetation vigor in the late summer and early fall. Wheat was characterized by low vegetation vigor in early fall. Corn was characterized by high vegetation in mid spring. The positive slope in MSR and GNDVI distribution in Alfalfa can be interpreted as increase in the vegetation vigor in early and mid-fall. No texture feature offered a consistent solution for the discrimination between the crops, but several VIs based on NIR bands were useful in the identification of crops. The mid-spring and early fall were selected for this initial step to classify the wheat, other hay, and corn crops in the TE scenes of the large agriculture field sizes (Figure 44).

The crop types of the medium field size TR region (Corn, Cotton, Soybean, and Double Crop) were discriminated by means of a sequence of three VIs (DVI, MSR, and SARVI) (Figure 45). In early fall, the positive slope in DVI and MSR distribution in corn can be interpreted as an increase in the vegetation vigor. A negative slope in MSR and SARVI distribution can be interpreted as decrease in vegetation. Corn was characterized by low vegetation vigor in late spring and early fall. However, in all the acquired scenes, the corn was characterized by low vegetation vigor. Double crop including soybean and winter wheat was characterized by a positive slope in DVI distribution showing an increase in the vegetation vigor in late spring and early fall. Soybean was characterized by high vegetation vigor in early fall and a negative slope in DVI distribution was identified as a decrease from early fall to late spring. Cotton was characterized by high vegetation vigor in DVI, MSR, and SARVI distribution in early fall.

The crop types of the small field size TR region (Corn, Other Hay, Soybean, Winter Wheat, and Double Crop) were discriminated by means of a sequence of three VIs (DVI, MSR, and EVI) (Figure 46). Corn was characterized by high green vegetation vigor in the distribution of GNDVI and EVI in late fall. Other Hay was identified in the zone enclosed by GNDVI values greater than 0.3 in the late fall. Soybean was characterized by high vegetation vigor in GNDVI, EVI, and MCARI distribution in late summer and late fall. The positive slope in GNDVI distribution in soybean can be interpreted as an increase in the vegetation vigor in late fall. No texture feature offered a consistent solution for the discrimination between the crop types, but several VIs based on NIR bands were useful for the indentation of crops.

Potential benefits of augmentation, classification with multi-dates of satellite imagery, and extension of crop type reference data from the TR to TE regions

The evaluation and assessment of the augmentation and extension approaches of collecting additional crop type reference data tested in the US are very crucial to effectively apply them for the rest of the world in the future. Accuracy assessment was performed separately to evaluate the results of augmentation, benefits of using multi-dates of satellite imagery, and extension. The augmented reference data were evaluated by comparing with the CDL reference data to determine the percent of correctly labeled reference data from the GSV. The results presented in Table 40 demonstrate that the augmented crop type reference data collected from the GSV are insufficient to perform the classification and assessment of the crop type maps. Very few agriculture fields were interpreted in the large and medium field sizes along the major roads using the GSVs photographs as compared to the small field sizes, where three or four crop types were identified. Second, dominant and more common crops (e.g., Soybean) of small fields size regions were interpreted and augmented in large clusters due to which the spatial auto-correlation issues could possibly exist between the reference polygons (Figure 41). As a result, the augmentation approach could only be used to collect dominant and common crop types in specific regions due to limited availability of photographs along the major roads.

The benefits of using multi-dates of satellite imagery were established by assessing the crop type maps of the TR region developed from one, two, and three dates of satellite imagery in the form of error matrices presenting the overall, producer's, and user's accuracy. Table 42 shows high overall accuracy of the crop type maps developed from multi-date satellite imagery for the large (73.8%), medium (90.2%), and small (83.3%) field size regions than one and two dates

imagery classification. The benefit of using multi-dates of satellite imagery was established for more accurate crop type mapping in different field size TR regions by improving the map accuracy. The accuracy of the crop types maps was improved when developed from the multi-dates of imagery as compared to one and two dates imagery by providing more spectral and texture features for the discrimination of the different crop types. The accuracy assessment of the crop type maps shows that the maps generated from three dates of imagery in medium field size regions are more accurate than large and small field sizes. The reason of high accuracy is the presence of variations in the non-cropland class of different field size regions. In the medium field size region, forest and agriculture are dominant land cover classes whose objects were easily discriminated based on the texture features. However, the large field size region has more variability in the non-cropland classes with the availability of developed and fallow lands. Therefore, the spectral and texture features of developed class was confused with the fallow land feature.

The extension approach of collecting additional crop type reference data was evaluated by the assessment of crop type maps of three TE regions developed from multi-dates of satellite imagery using the crop type reference data extended from three TR regions representing each field size (Figure 48). These maps were assessed using the reference data collected from the CDL map of the year 2015 (Table 39). The error matrices generated for the crop type maps of the TE region in Table 43, 44, and 45 show that: (1) the crop type reference data of more common agriculture crops was extended with high quality and reliability for three field sizes, (2) rare crop types were spatially extended with high accuracy (80-90%) in the large and medium field sizes, and (3) the extended crop type reference data has lower accuracy (60-70%) and reliability in the small field sizes as compared to the large and medium field sizes for the same crops. Finally, it can be concluded that

the limited crop type reference data can be effectively extended using a phenology-based classification approach and is more efficient than the interpretation of photographs collected from GSV (Yadav and Congalton, 2019b).

Conclusions

In this research, we have presented an innovative and novel approaches of augmenting and extending the limited crop type reference data within similar regions representing different agriculture field sizes in the US where high-quality crop type reference data (e.g., CDL) already exist. The results demonstrate that the interpretation of panoramic views collected from GSV promise to augment more common/dominant agriculture crops while the phenology-based classification approach can efficiently extend the limited crop type reference data to every region within the same AEZ for different field sizes. The most attractive feature of augmentation and extension approaches are that they reduce the need to collect additional field reference data at multiple locations, greatly lowering the cost and time involved in the mapping of crop types for large areas. This is especially important for the regions where reference data are often too scarce to routinely apply the supervised classification methods to effectively map different agriculture crops. Variables related to phenology and spectral features at specific phenological stages were utilized as measurements that reflect the nature of crop types and remain stable over time and space within similar ecological conditions and cropping patterns. Therefore, a phenology-based classification algorithm was developed to identify the crop types based on the prior knowledge on their cropping calendar and spectral properties. Resultant crop type maps demonstrated the

potential and capability of augmenting and extending limited crop type reference data using interpretation and phenology-based algorithms of discriminating agriculture crops at multiple places in similar regions.

The success of this initial application in the United States using the non-ground-based sources of crop type information is encouraging, given the potential of extending the algorithm to other crop types and other remotely sensed data. To identify more crop types in other areas, expert knowledge on local agricultural practices, crop growth modeling, and crop spectral monitoring and simulation (Jacquemoud et al., 2009) are the main factors to consider when defining classification rules. For regions with variable crop types growing throughout the year, the extended automated approach may improve the classification of all the available crop types from a single year by incorporating images from multiple dates. Because the automated algorithm is not image-specific, it is scalable to utilize these datasets with minimal revisions. We are confident that the phenology-based classification approach has great potential in the applications as the technique of generating additional crop type reference data for creating and assessing the crop type maps.

CHAPTER VII

OVERALL CONCLUSIONS

The overall goal of this research was to evaluate and assess the large area cropland extent maps and generate sufficient reference data for creating other cropland products (e.g., crop type maps). Additionally, many of the issues and constraints related with the cropland distribution, pattern, proportion, and reference data availability were examined. Previous existing global cropland extent maps have not been assessed by individual continents to consider the prevalent cropland distribution, area, spatial extent, and pattern of each region. Consequently, meaningful accuracy measures for each individual continent have not been reported in the literature. The results of this research show that large area accuracy assessments of cropland extent maps must be performed using an appropriate sampling strategy with a large cropland reference dataset to achieve meaningful accuracy results not only for the entire world, but also by continent.

The accuracy assessment of the three different cropland extent maps developed at three spatial resolutions shows that the cropland maps becomes more accurate at higher spatial resolutions. However, despite the differences in the overall accuracy of the three different cropland extent maps, each cropland extent map needs to be compared to provide recommendations as which spatial resolution should be applied given different agriculture field sizes. The comparison of the characteristics of the cropland landscape mapped at the three different spatial resolutions is a very effective way to establish the similarity among the cropland extent maps. Therefore, recommendations for using the cropland extent maps developed at different spatial resolution (i.e.,

30m, 250m, and 1km) were made for monitoring cropland in different cropping pattern regions of the world.

As valuable as it is to assess the large area cropland maps, it is just as valuable to report meaningful and appropriate accuracy measures for different cropland proportion regions. Since different regions have different cropland distributions and proportions, it is very important to achieve sufficient sample sizes and meaningful accuracy measures for regions with varying cropland proportions. This research evaluated SRS and SMPS designs for different regions to achieve sufficient sample sizes and appropriate accuracy measures for the rare cropland map class. This evaluation demonstrates that the distribution of samples is more important than increasing or decreasing the number of samples (once a sufficient number of samples is determined) to effectively assess the rare cropland map class of various cropland regions. The regions of <15% CAP that are clustered and limited to small areas cropping pattern can be effectively assessed using the SMPS design as compared to the scattered and uniform cropping pattern. However, the regions of >15% CAP (those maps that do not contain a rare cropland map class) can be effectively assessed using either of the sampling designs at a sample size of 250.

One of the objectives of this research was to generate sufficient crop type reference data for creating large area crop type maps by collecting additional reference data from non-ground-based sources. This research presents an innovative approach to extend and augment crop type reference data for major crop types for three different agriculture field sizes of the US where high-quality crop type reference data (i.e., CDL) are available. After successful implementation of these methods in data rich regions, they can potentially be implemented to generate additional reference data for data limited regions. The most attractive feature of the automated approach is that it

reduces the need to collect additional reference data in multiple regions, greatly lowering the cost of large area crop type mapping. This is especially important for the regions where reference data are often too scarce to routinely apply the supervised classification method. The success of the initial application in the United States using the automated approach is encouraging, given the potential of extending the algorithm to other crop types and other remotely sensed data. For regions with variable crop types growing throughout the year, the extended automated approach may improve the classification of all the available crop types from a single year by incorporating images from multiple dates. We are confident that the phenology-based classifier extension method has more potential applications as the technique of generating additional reference data for the classification and accuracy assessment.

The research conducted for this dissertation contributes to both the cropland monitoring and remote sensing communities in four distinct ways. First, an appropriate large area assessment strategy is suggested for assessing global cropland extent maps. Second, the suitability of different resolution cropland extent maps was recommended for their effective use in monitoring cropland regions of different field sizes. Third, an alternate sampling strategy is suggested to perform an effective assessment of the cropland maps of different cropland regions. Finally, the extension of limited crop type reference data is suggested to generate consistent reference data for creating large area crop type maps using a phenology-based classification of multi-date high spatial resolution imagery.

LITERATURE CITED

Adams, C.R., and Eswaran, H., 2000. Global land resources in the context of food and environmental security. In: S. P. Gawande, Ed., Advances in Land Resources Management for the 20th Century, Soil Conservation Society of India, New Delhi, 655 pp.

AgRISTAR: Agriculture and Resources Inventory Surveys through Aerospace Remote Sensing, 1981. NASA, Lyndon B Johnson Space Center, Houston, Texas, 59:110–123.

Alexandratos, N. and Bruinsma, J., 2012. World agriculture towards 2030/2050: the 2012 revision. ESA Working paper No. 12-03, FAO, Rome, Italy.

Arvor, D., Jonathan, M., Meirelles, M.S.P., Dubreuil, V., and Durieux, L., 2011. Classification of MODIS EVI time series for crop mapping in the state of Mato Grosso, Brazil. *International Journal of Remote Sensing*, 32:7847-7871.

Asner, G.P., Keller, M., Pereira, R., and Zweede, J.C., 2002. Remote sensing of selective logging in Amazonia: Assessing limitations based on detailed field observations, Landsat ETM+, and textural analysis. *Remote Sensing of Environment*, 80: 483–496. doi.org/10.1016/S0034-4257(01)00326-1.

Atzberger, C., Vuolo, F., Klisch, A., Rembold, F., Meroni, M., Mello, M.P., and Formaggio, A., 2015. *Land Resources Monitoring, Modeling, and Mapping with Remote Sensing, First Edition*, Thenkabail, P.S., (Ed.). CRC Press-Taylor and Francis Group: Boca Raton, FL, USA, 849 pp. ISBN 1482217988.

Badhwar, G., 1984. Classification of Corn and Soybeans Using Multitemporal Thematic Mapper Data. *Remote Sensing of Environment*, 16:175–181.

Bai, Y., Feng, M., Jiang, H., Wang, J., and Liu, Y., 2015. Validation of land cover maps in China using a sampling-based labeling approach. *Remote Sensing,* 7:10589–10606. doi:10.3390/rs70810589.

Barrett, E.C. and Curtis, L.F., 1992. *Introduction to Environmental Remote Sensing, Third Edition*. Chapman and Hall, London, 426 pp. ISBN: 0412371707.

Barrett, E.C., 2013. *Introduction to Environmental Remote Sensing, Fifth Edition*. Taylor and Francis, Hoboken, NJ, 480 pp. ISBN: 1134982453.

Bartholome, E., and Belward, A. S., 2005. GLC2000: A New Approach to Global Land Cover Mapping from Earth Observation Data. *International Journal of Remote Sensing*, 26 (9): 1959−1977. doi:10.1080/01431160412331291297.

Baatz, M., and Schäpe, A., 2000. Multiresolution segmentation: An optimization approach for high quality multi-scale image segmentation. *Journal of Photogrammetry and Remote Sensing, 58:*12–23.

Bayas, L., Carlos, J., Lesiv, M., Waldner, F., Schucknecht, A., Duerauer, M., See, L., Fritz, S., Fraisl, D., Moorthy, I., McCallum, I., Perger, C., Danylo, O., Defourny, P., Gallego, J., Gilliams, S., Akhtar, I., Baishya, S. J., Baruah, M., Bungnamei, K., Campos, A., Changkakati, T., Cipriani, A., Das, K., Das, K., Das, I., Davis, K. F., Hazarika, P., Johnson, B. A., Malek, Z., Molinari, M. E., Panging, K., Pawe, C. K., Pérez-Hoyos, A., Sahariah, P. K., Sahariah, D., Saikia, A., Saikia, M., Schlesinger, P., Seidacaru, E., Singha, K., and Wilson, J. W., 2017. A global reference database of crowdsourced cropland data collected using the Geo-Wiki platform. *Nature: Scientific data*, Volume 4, Id: 170136. doi:10.1038/sdata.2017.136.

Beach, R.H., DeAngelo, B.J., Rose, S., Li, C., Salas, W., and DelGrosso, S.J., 2008. Mitigation potential and costs for global agricultural greenhouse gas emissions. *Agriculture Economics*, 38:109–115. doi.org/10.1111/j.1574-0862.2007.00286.

Benz, U.C., Hofmann, P., Willhauck, G., Lingenfelder, I., and Heynen, M., 2004. Multi-resolution, object-oriented fuzzy analysis of remote sensing data for GIS-ready information. *ISPRS Journal of Photogrammetry*, 58(3-4):239–258. doi.org/10.1016/j.isprsjprs.2003.10.002

Bicheron, P., Defourny, P., Brockmann, C., Schouten, L., and Vancutsem, C., 2008. GLOBCOVER—Products Description and Validation Report, 33:1–47, MEDIAS-France: Toulouse, France. doi:10013/epic. 39884.d016.

Biradar, C.M., Thenkabail, P.S., Noojipady, P., Li Y., Dheeravath, V., Turral, H., Velpuri, M., Gumma, M.K., Gangalakunta, O.R.P., Cai, X.L., Xiao, X., Schull, M.A., Alankara, R.D., Gunasinghe, S., and Mohideen, S., 2009. A global map of rainfed cropland areas (GMRCA) at the end of last millennium using remote sensing. *International Journal of Applied Earth Observation and Geoinformation*, 11(2):114. doi.org/10.1016/j.jag.2008.11.002.

Blaschke, T., and Strobl, J., 2001. What's wrong with pixels? Some recent developments interfacing remote sensing and GIS. Zeitschrift fur Geoinformationssysteme, 14(6):12-17.

Blaschke, T., Lang, S., Hay, G.J., 2008. Object-Based Image Analysis: Spatial Concepts for Knowledge-Driven Remote Sensing Applications, First Edition. Springer-Verlag, Berlin, Heidelberg, 817pp. ISBN 978-3-540-77058-9.

Blaschke, T., 2010. Object based image analysis for remote sensing. *ISPRS Journal of Photogrammetry and Remote Sensing*, 65(1):2-16. doi.org/10.1016/j.isprsjprs.2009.06.004.

Blaschke, T., Hay, G.J., Kelly, M., Lang, S., Hofmann, P., Addink, E., Feitosa, R.Q., 2014. Geographic Object-Based Image Analysis Towards a new paradigm. *ISPRS Journal of Photogrammetry and Remote Sensing,* 87(100):180–191. doi: 10.1016/j.isprsjprs.2013.09.014.

Boryan, C., Yang, Z., Mueller, R., and Craig, M., 2011. Monitoring US agriculture: The US Department of Agriculture, National Agricultural Statistics Service, Cropland Data Layer Program. *Geocarto International,* 26:341–358. doi:10.1080/10106049.2011.562309.

Botkin, D.B., Estes, J.E., MacDonald, R.M., and Wilson, M. V., 1984. Studying the Earth's Vegetation from Space. *Bioscience*, 34:508–514. doi.org/10.2307/1309693

Breiman, L., 2001. Random Forests. *Machine Learning, 45*:5–32. doi.org/10.1023/A:1010933404324.

Büttner, G., and Csillag, F., 1989. Comparative study of crop and soil mapping using multitemporal and multispectral SPOT and Landsat thematic mapper data. *Remote Sensing of Environment*, 29: 241–249. doi.org/10.1016/0034-4257(89)90003-5

Card, D., 1982. Using know map category marginal frequencies to improve estimates of thematic map accuracy. *Photogrammetry Engineering and Remote Sensing,* 48(3): 431–439.

Castillejo-González, I.L., López-Granados, F., García-Ferrer, A., Peña-Barragán, J.M., Jurado-Expósito, M., de la Orden, M.S., and González-Audicana, M., 2009. Object- and pixel-based analysis for mapping crops and their agro-environmental associated measures using QuickBird imagery. *Computer Electronics Agriculture,* 68:207–215. doi.org/10.1016/j.compag.2009.06.004.

Champagne, C., McNairn, H., Daneshfar, B., and Shang, J., 2014. A bootstrap method for assessing classification accuracy and confidence for agricultural land use mapping in Canada. *International Journal of Applied Earth Observation and Geoinformatics,* 29:44–52. doi: 10.1016/j.jag.2013.12.016.

Chang, J., Hansen, M.C., Pittman, K., Carroll, M., and Di Miceli, C., 2007. Corn and soybean mapping in the united states using MODIS time-series data sets. *Agronomy Journal*, 99(6):1654-1664. doi: 10.2134/agronj2007.0170.

Chen, J., Cao, X., Peng, S., and Ren, H., 2017. Analysis and Applications of GlobeLand30: A Review. *ISPRS International Journal of Geo-Informatics,* 6:230. doi:10.3390/ijgi6080230.

Chen, J. M., 1996. Evaluation of Vegetation Indices and a Modified Simple Ratio for Boreal Applications. *Canadian Journal of Remote Sensing,* 22:229–242. doi.org/10.1080/07038992.1996.10855178.

Clark, M.L., and Aide, T.M., 2011. Virtual interpretation of earth web-interface tool (VIEW-IT) for collecting land-use/land-cover reference data. *Remote Sens*ing, 3:601–620. doi:10.3390/rs3030601.

Comber, A., Fisher, P.F., Brunsdon, C. and Khmag, A., 2012. Spatial analysis of remote sensing image classification accuracy. *Remote Sensing of Environment*, 127:237–246. doi: 10.1016/j.rse.2012.09.005.

Congalton, R.G., 1988. A comparison of sampling schemes used in generating error matrices for assessing the accuracy of maps generated from remotely sensed data. *Photogrammetry Engineering and Remote Sensing,* 54(5):593–600.

Congalton, R.G., 1991. A review of assessing the accuracy of classifications of remotely sensed data. *Remote Sensing of Environment,* 37:35–46. doi.org/10.1016/0034-4257(91)90048-B.

Congalton, R.G., Balogh, M., Bell, C., Green, K., Milliken, J.A., and Ottman, R., 1998. Mapping and monitoring agricultural crops and other land cover in the Lower Colorado River Basin. *Photogrammetry Engineering and Remote Sensing,* 64:1107–1113.

Congalton, R.G., and Green, K., 1999. *Assessing the Accuracy of Remotely Sensed Data: Principles and Practices, First Edition*. CRC Press: Boca Raton, FL, USA, 137 pp. ISBN 1420055127.

Congalton, R.G., and Green, K., 2009. *Assessing the Accuracy of Remotely Sensed Data-Principles and Practices, Second Edition*. CRC Press: Boca Raton, FL, USA, 200 pp. ISBN 9781420055122.

Congalton, R.G., Gu, J., Yadav, K., Thenkabail, P., and Ozdogan, M., 2014. Global land cover mapping: A review and uncertainty analysis. *Remote Sensing*, 6:12070–12093. doi:10.3390/rs61212070.

Congalton, R. G., 2016. Assessing Positional and Thematic Accuracies of Maps Generated from Remotely Sensed Data. In: Remote Sensing Handbook; Vol. I: Data Characterization, Classification, and Accuracies P. Thenkabail (Editor). CRC/Taylor & Francis, Boca Raton, FL, 583-601 pp.

Congalton, R.G., Yadav, K., McDonnell, K., Poehnelt, J., Stevens, B., Gumma, M.K., Teluguntla, P., and Thenkabail, P.S., 2017. NASA Making Earth System Data Records for Use in Research Environments (MEaSUREs) Global Food Security-Support Analysis Data (GFSAD) @ 30-m: Cropland Extent Validation (GFSAD30VAL), NASA EOSDIS Land Processes DAAC, USGS Earth Resources Observation and Science (EROS) Center: Sioux Falls, SD, USA. doi:10.5067/MEaSUREs/GFSAD/GFSAD30VAL.001.

Conrad, C., Dech, S., Dubovyk, O., Fritsch, S., Klein, D., Löw, F., Schorcht, G., and Zeidler, J., 2014. Derivation of temporal windows for accurate crop discrimination in heterogeneous croplands of Uzbekistan using multitemporal RapidEye images. *Computer Electronics and Agriculture,* 103:63–74. doi.org/10.1016/j.compag.2014.02.003.

CropScape – Cropland Data Layer, United States Department of Agriculture, National Agricultural Statistics Service. Available Online: https://nassgeodata.gmu.edu/CropScape (last date accessed 7 March 2017)

Daughtry, C., 2000. Estimating Corn Leaf Chlorophyll Concentration from Leaf and Canopy Reflectance. *Remote Sensing of Environment,* 74:229–239. doi.org/10.1016/S0034-4257(00)00113-9.

De Wit, A. J.W., and Clevers, and J.G.P.W., 2004. Efficiency and accuracy of per-field classification for operational crop mapping. *International Journal of Remote Sensing*, 25:4091–4112. doi.org/10.1080/01431160310001619580.

Definiens, 2007. Definiens Developer 7. Definiens AG, Munich, Germany, 195 pp.

Defourny, P., Bontemps, S., Schouten, L., Bartalev, S., Cacetta, P., De Wit, A.,Di Bella, C., Gérard, B., Giri, C., Gond, V., Hazeu, G., Heinimann, A., Herold, M., Jaffrain, G., Latifovic, R., Lin, H., Mayaux, P., Mücher, S., Nonguierma, A., Stibig, H., Y. Shimabakuro, Van Bogaert, E., Vancutsem, C., Bicheron, P., Leroy, M., and Arino, O., 2011b. GLOBCOVER 2005 and GLOBCOVER 2009 validation : learnt lessons. In Proceedings of GOFC-GOLD Global Land Cover & Change Validation Workshop, Laxenburg, Austria.

DeGloria, S.D., Laba, M., Gregory, S.K., Braden, J., Ogurcak, D., Hill, E., Fegraus, E., Fiore, J., Stalter, A., and Beecher, J., 2000. Conventional and fuzzy accuracy assessment of land cover maps at regional scale. In Proceedings of the 4th International Symposium on Spatial Accuracy Assessment in Natural Resources and Environmental Sciences, Amsterdam, the Netherlands.

Desclee, B., Bogaert, P., and Defourny, P., 2006. Forest change detection by statistical object-based method. *Remote Sensing of Environment*, 102(1-2):1-11. doi: 10.1016/j.rse.2006.01.013.

Dey, V., Zhang, Y., Zhong, M., 2010. A review on image segmentation techniques with remote sensing perspective. *International Architecture Photogrammetry and Remote Sensing of Spatial Information Science*, 38:31–42.

Di Vittorio, A.V., Kyle, P., and Collins, W.D., 2016. What are the effects of Agro-Ecological Zones and land use region boundaries on land resource projection using the Global Change Assessment Model? *Environment Modeling Software,* 85:246–265. doi: 10.1016/j.envsoft.2016.08.016.

Dong,J. Xiao, X., Kou, W., Qin, Y., Zhang, G., Li, L., Jin, C., Zhou, Y., Wang, J., Biradar, C., Liu, J., and Moore III, B., 2015. Tracking the dynamics of paddy rice planting area in 1986–2010 through time series Landsat images and phenology-based algorithms, *Remote Sensing of Environment,* 160:99-113, ISSN 0034-4257. doi.org/10.1016/j.rse.2015.01.004.

Dronova, I., Gong, P., Clinton, N.E., Wang, L., Fu, W., Qi, S., Liu, Y., 2012. Landscape analysis of wetland plant functional types: The effects of image segmentation scale, vegetation classes and classification methods. *Remote Sensing of Environment*, 127:357–369. doi.org/10.1016/j.rse.2012.09.018.

Duro, D.C., Franklin, S.E., Dubé, M.G., 2012. A comparison of pixel-based and object-based image analysis with selected machine learning algorithms for the classification of agricultural landscapes using SPOT-5 HRG imagery. *Remote Sensing of Environment,118:*259–272. doi.org/10.1016/j.rse.2011.11.020.

Dutta, S., Sharma, S.A., Khera, A.P., Ajai, Yadav, M., Hooda, R.S., Mothikumar, K.E., and Manchanda, M.L., 1994. Accuracy assessment in cotton acreage estimation using Indian remote sensing satellite data. *ISPRS Journal of Photogrammetry and Remote Sensing,* 49:21–26. doi.org/10.1016/0924-2716(94)90011-6.

Ehrlich, D., Estes, J.E., Scepan, J., and McGwire, K.C., 1994. Crop area monitoring within an advanced agricultural information system. *Geocarto International,* 9:31–42. doi.org/10.1080/10106049409354468.

Fischer, G., Nachtergaele, F.O., Prieler, S., Teixeira, E., Toth, G., van Velthuizen, H., Verelst, L., and Wiberg, D., 2012. Global Agro-ecological Zones (GAEZ): Model Documentation, Food and Agriculture Organization (FAO): Rome, Italy, International Institute for Applied Systems Analysis (IIASA): Laxenburg, Austria, 1–179 pp.

Fisette, T., Rollin, P., Aly, Z., Campbell, L., Daneshfar, B., Filyer, P., Smith, A., Davidson, A., Shang, J., and Jarvis, I., 2013. AAFC annual crop inventory: Status and challenges. In Proceedings of the 2013 Second International Conference on Agro-Geoinformatics (Agro-Geoinformatics), Fairfax, VA, USA, 270–274 pp. doi:10.1109/Argo-Geoinformatics.2013.6621920.

Fitzpatrick-Linz, K., 1981. Comparison on sampling procedures and data analysis for a land-use and land-cover map. *Photogrammetric Engineering and Remote Sensing*, 47(3):343-351.

Fletcher, R.S., 2016. Using vegetation indices as input into random forest for soybean and weed classification. *American Journal of Plant Science,* 7:2186–2198. doi: 10.4236/ajps.2016.715193.

Foerster, S., Kaden, K., Foerster, M., and Itzerott, S., 2012. Crop type mapping using spectral-temporal profiles and phenological information. *Computer Electronics and Agriculture*, 89:30–40. doi.org/10.1016/j.compag.2012.07.015

Foley, J. A., Ramankutty, N., Brauman, K. A., Cassidy, E. S., Gerber, J. S., Johnston, M., Mueller, N. D., O'Connell, C., Ray, D. K., West, P. C., Balzer, C., Bennett, E. M., Carpenter, S. R., Hill, J., Monfreda, C., Polasky, S., Rockström, J., Sheehan, J., Siebert, S., Tilman, D., Zaks, D. P., 2011. Solutions for a cultivated planet. *Nature*, 478(7369): 337–42 pp. doi: 10.1038/nature10452.

Food and Agriculture Organization of the United Nations (FAO) Global Forest Resources Assessment, 2010. FAO Forestry Paper 163, Food and Agriculture Organization (FAO): Rome, Italy, 350 pp. ISBN 978-92-5-106654-6.

Foody, G.M., 2002. Status of land cover classification accuracy assessment. *Remote Sensing of Environment*, 80:185–201. doi:10.1016/S0034-425700295-4.

Foody, G.M., 2005. Local characterization of thematic classification accuracy through spatially constrained confusion matrices. *International Journal of Remote Sensing*, 37–41. doi:10.1080/01431160512331326521.

Foody, G.M., 2010. Assessing the accuracy of land cover change with imperfect ground reference data. *Remote Sensing of Environment,* 114:2271–2285. doi: 10.1016/j.rse.2010.05.003.

Foody, G.M., 2015. Valuing map validation: The need for rigorous land cover map accuracy assessment in economic valuations of ecosystem services. *Ecological Economics*, 111:23–28. doi: 10.1016/j.ecolecon.2015.01.003.

Foody, G.M., and Boyd, D.S., 2013. Using Volunteered Data in Land Cover Map Validation: Mapping West African Forests. IEEE J. Sel. Top. *Applied Earth Observation and Remote Sensing*, 6:1305–1312. doi:10.1109/JSTARS.2013.2250257.

Forster, D., Kellenberger, T.W., Buehler, Y., Lennartz, B., 2010. Mapping diversified peri-urban agriculture—Potential of object-based versus per-field land cover/land use classification. *Geocarto International*, 25(3):171–186. doi.org/10.1080/10106040903243416.

Frey, K.E., and Smith, L.C., 2007. How well do we know northern land cover? Comparison of four global vegetation and wetland products with a new ground-truth database for West Siberia. *Global Biogeochemical Cycles*, 21:GB1016. doi:10.1029/2006GB002706.

Friedl, M.A., and Brodley, C.E., 1997. Decision tree classification of land cover from remotely sensed data. *Remote Sensing of Environment*, 61:399–409. doi.org/10.1016/S0034-4257(97)00049-7.

Fritz, S., and See, L., 2008. Identifying and quantifying uncertainty and spatial disagreement in the comparison of Global Land Cover for different applications. *Global Change Biology*, 14:1057–1075, doi:10.1111/j.1365-2486.2007.01519.

Fritz, S., Havlik, P., Schneider, U., Schmid, E., and Obersteiner, M., 2009a. Uncertainties in Global Land Cover Data and its Implications for Climate Change Mitigation Policies Assessment. In Proceedings of the 33rd International Symposium on *Remote Sensing of Environment* (ISRSE-33) "Sustaining the Millennium Development Goals", Stresa, Italy, 1–4 pp.

Fritz, S., McCallum, I., Schill, C., Perger, C., Grillmayer, R., Achard F., Kraxner F., 2009b. Geo-wiki.org: the use of crowdsourcing to improve global land cover. *Remote Sensing*, 1(3):345–354. doi.org/10.3390/rs1030345.

Fritz, S., See L., and Felix R., 2010. Comparison of Global and Regional Land Cover Maps with Statistical Information for the Agricultural Domain in Africa. *International Journal of Remote Sensing*. 31 (9): 2237–2256. doi:10.1080/01431160902946598.

Fritz, S., McCallum, I., Schill, C., Perger, C., See, L., Schepaschenko, D., van der Velde, M., Kraxner, F., Obersteiner, M., 2011a. Geo-Wiki: an online platform for improving global land cover. *Environmental Modelling and Software, 31:110-123*. doi.org/10.1016/j.envsoft.2011.11.015

Fritz, S., See L., McCallum I., Schill, C., Obersteiner, V., Boettcher, H., Havlík, P., and Achard. F., 2011b. Highlighting Continued Uncertainty in Global Land Cover Maps for the User Community. *Environmental Research Letters,* 6(4): No. 044005. doi:10.1088/1748-9326/6/4/044005.

Fritz, S., See, L., You, L., Justice, C., Becker-Reshef, I., Bydekerke, L., Cumani, R., Defourny, P., Erb, K., and Foley, J., 2013. The need for improved maps of global cropland. Eos Trans. American Geophysical Union, 94:31–32, doi:10.1002/2013EO030006.

Fritz, S., See, L., Mccallum, I., You, L., Bun, A., Moltchanova, E., Duerauer, M., Albrecht, F., Schill, C., and Perger, C., 2015. Mapping global cropland and field size. *Global Change Biology*, 21:1980–1992, doi:10.1111/gcb.12838.

Frohn, R., 1997. Remote Sensing for Landscape Ecology: New Metric Indicators for Monitoring, Modeling, and Assessment of Ecosystems, CRC Press-Taylor and Francis, Boca Raton, FL, USA, 99 pp.

Gallego, F.J., 2004. Remote sensing and land cover area estimation. *International Journal of Remote Sensing*, 25:3019–3047. doi:10.1080/01431160310001619607.

Gallego, F.J., Kussul, N., Skakun, S., Kravchenko, O., Shelestov, A., and Kussul, O., 2014. Efficiency assessment of using satellite data for crop area estimation in Ukraine. *International Journal of Applied Earth Observation and Geoinformatics*, 29:22–30. doi: 10.1016/j.jag.2013.12.013.

Ginevan, M.E., 1979. Testing land-use map accuracy: Another look. *Photogrammetry Engineering and Remote Sensing,* 45(10):1371–1377.

Giri, C., Zhu, Z., and Reed, B., 2005. A comparative analysis of the Global Land Cover 2000 and MODIS land cover data sets. *Remote Sensing of Environment*, 94:123–132. doi: 10.1016/j.rse.2004.09.005.

Giri, C., Pengra, B., Long, J., and Loveland, T.R., 2013. Next generation of global land cover characterization, mapping, and monitoring. *International Journal of Applied Earth Observation and Geoinformatics,* 25:30–37. doi: 10.1016/j.jag.2013.03.005.

Gitelson, A., and Merzlyak, M.N., 1996. Signature analysis of leaf reflectance spectra: Algorithm development for remote sensing of chlorophyll. *Journal of Plant Physiology,* 148:494–500. doi.org/10.1016/S0176-1617(96)80284-7.

Global croplands. Available online: https://www.croplands.org/app/map?lat=0&lng=0&zoom=2. (last date accessed 5 March 2017).

Göhmann, H., Herold, M., Jung, M., Schulz, M., and Schmullius, C., 2009. Prototyping a probability-based Best Map Approach for global land cover datasets at 1km resolution using MODIS, GLC2000, UMD and IGBP. In: proceedings of 33rd International Symposium on Remote Sensing of Environment, ISRSE-33, Stresa, Italy, 404-407 pp.

Gong, P., Clinton, N., Yu, L., and Liang, L., 2013a. The 30 m global land cover products from China: Progress and perspectives. In Proceedings of the International Symposium on Land Cover Mapping for the African Continent, Nairobi, Kenya.

Gong, P., Wang, J., Yu, L., Zhao, Y., Zhao, Y., Liang, L., Niu, Z., Huang, X., Fu, H., Liu, S., Li, C., Li, X., Fu, W., Liu, C., Xu, Y., Wang, X., Cheng, Q., Hu, L., Yao, W., Zhang, H., Zhu, P., Zhao, Z., Zhang, H., Zheng, Y., Ji, L., Zhang, Y., Chen, H., Yan, A., Guo, J., Yu, L., Wang, L., Liu, X., Shi, T., Zhu, M., Chen, Y., Yang, G., Tang, P., Xu, B., Giri, C., Clinton, N., Zhu, Z., and Chen, J., 2013b. Finer resolution observation and monitoring of global land cover: first mapping results with Landsat TM and ETM+ data. *International Journal of Remote Sensing*, 34:2607–2654. doi.org/10.1080/01431161.2012.748992.

Google Maps, 2018. www.google.com/maps (last date accessed 18 February 2018)

Grekousis, G., Mountrakis, G., and Kavouras, M., 2015. An overview of 21 global and 43 regional land-cover mapping products. *International Journal of Remote Sensing*, 36:5309–5335. doi:10.1080/01431161.2015.1093195.

Gumma, M.K., Thenkabail, P.S., Maunahan, A., Islam, S., and Nelson, A., 2014. Mapping seasonal rice cropland extent and area in the high cropping intensity environment of Bangladesh using MODIS 500 m data for the year 2010, *ISPRS Journal of Photogrammetry and Remote Sensing*, 91:98-113. doi.org/10.1016/j.isprsjprs.2014.02.007.

Gumma, M.K., Thenkabail, P.S., Teluguntla, P., Oliphant, A.J., Xiong, J., Congalton, R.G., Yadav, K., Phalke, A., and Smith, C., 2017. NASA Making Earth System Data Records for Use in Research Environments (MEaSUREs) Global Food Security-Support Analysis Data (GFSAD) @ 30-m for South Asia, Afghanistan and Iran: Cropland Extent Product (GFSAD30SAAFGIRCE), NASA EOSDIS Land Processes DAAC, USGS Earth Resources Observation and Science (EROS) Center: Sioux Falls, SD, USA. doi: 10.5067/MEaSUREs/GFSAD/GFSAD30SAAFGIRCE.001.

Gumma, M.K., Thenkabail, P.S., Teluguntla, P., Rao, M.N., Mohammed, I.A., and Whitbread, A.M., 2016. Mapping rice-fallow cropland areas for short-season grain legumes intensification in South Asia using MODIS 250 m time-series data. *International Journal of Digital Earth,* 9(10):981-1003. doi.org/10.1080/17538947.2016.1168489.

Hay, A.M., 1979. Sampling designs to test land use map accuracy. *Photogrammetry Engineering and Remote Sensing,* 45(4):529–533.

Hay, G.J., Castilla, G., 2008. Geographic Object-Based Image Analysis (GEOBIA): A new name for a new discipline. In Object-Based Image Analysis, Blaschke, T., Lang, S., Hay, G.J., Eds., Lecture Notes in Geoinformation and Cartography, Springer: Berlin/Heidelberg, Germany, 75–89 pp.

Herold, M., Mayaux, P., Woodcock, C.E., Baccini, A., and Schmullius, C., 2008. Some challenges in global land cover mapping: an assessment of agreement and accuracy in existing 1km datasets. *Remote Sensing of Environment,* 112 (2):2538–2556. doi: 10.1016/j.rse.2007.11.013.

Hord, R.M., and Brooner, W., 1976. Land-use map accuracy criteria. *Photogrammetry Engineering and Remote Sensing,* 42(5):671–677.

Huang, J., Wang, H., Dai, Q., Han, D., 2014. Analysis of NDVI Data for Crop Identification and Yield Estimation. *IEEE Journal of Selected Topics in Applied Earth Observations and Remote Sensin*g, 7 (11): 4374–4384. doi: 10.1109/JSTARS.2014.2334332.

Huete, A.R., Liu, H.Q., Batchily, K., J., and van W., L., 1997. A comparison of vegetation indices over a Global set of TM images for EO -MODIS. *Remote Sensing of Environment*, 59:440–451. doi.org/10.1016/S0034-4257(96)00112-5.

Husak, G.J., Marshall, M.T., Michaelsen, J., Pedreros, D., Funk, C., and Galu, G., 2008. Crop area estimation using high and medium resolution satellite imagery in areas with complex topography. *Journal of Geophysical Resources and Atmosphere*, 113. doi:10.1029/2007JD009175.

Inglada, J., Arias, M., Tardy, B., Hagolle, O., Valero, S., Morin, D., Dedieu, G., Sepulcre, G., Bontemps, S., Defourny, P., and Koetz, B., 2015. Assessment of an Operational System for Crop Type Map Production Using High Temporal and Spatial Resolution Satellite Optical Imagery. *Remote Sensing*, 7:12356-12379. doi:10.3390/rs70912356.

Jacquemoud, S., Verhoef, W., Baret, F., Bacour, C., Zarco-Tejada, P.J., Asner, G.P., François, C., and Ustin, S.L., 2009. PROSPECT + SAIL models: A review of use for vegetation characterization. *Remote Sensing of Environment,* 113: S56–S66. doi.org/10.1016/j.rse.2008.01.026

Jain, M., Srivastava, A.K., Singh, B., Joon, R.K., McDonald, A., Royal, K., Lisaius, M.G., and Lobell, D.B., 2016. *Remote Sensing*, 8(10):860. doi:10.3390/rs8100860.

Jakubauskas, M.E., Legates, D.R., and Kastens, J.H., 2003. Crop identification using harmonic analysis of time-series AVHRR NDVI data. *Computer Electronics and Agriculture*, 37:127–139. doi.org/10.1016/S0168-1699(02)00116-3.

Kaptué Tchuenté, A.T., Roujean, J.-L., and De Jong, S.M., 2011. Comparison and relative quality assessment of the GLC2000, GLOBCOVER, MODIS and ECOCLIMAP land cover data sets at the African continental scale. *International Journal of Applied Earth Observation and Geoinformatics*, 13:207–219. doi: 10.1016/j.jag.2010.11.005.

Kaufman, Y., and Tanre, D., 1992. Atmospherically Resistant Vegetation Index (Arvi) For Eos-Modis. *Geoscience Remote Sensing,* 30(2):261–270. doi: 10.1109/36.134076.

Kenduiywo, B. K., Bargiel, D. and Soergel, U., 2018. Crop type mapping from a sequence of Sentinel-1 images, *International Journal of Remote Sensing*, 39(19):6383-6404. doi: 10.1080/01431161.2018.1460503.

Kooistra, L., Groenestijn, A., Kalogirou, V., Arino, O., Herold, M., 2010. User requirements from the climate modelling community for next generation global products from land cover CCI project. In: Proceedings of ESA-iLEAPS-EGU joint Conference 2010, Frascati, Italy 3–5 November 2010.

Kuenzer, C., van Beijma, S., Gessner, U., and Dech, S., 2014. Land surface dynamics and environmental challenges of the Niger Delta, Africa: Remote sensing-based analyses spanning three decades (1986–2013). *Applied Geography,* 53:354–368. doi: 10.1016/j.apgeog.2014.07.002.

Latifovic, R., Zhu, Z., Cihlar, J., Giri, C., and Olthof, I., 2004. Land cover mapping of North and Central America – Global Land Cover 2000. *Remote Sensing of Environment*, 89 (1):116–127. doi: 10.1016/j.rse.2003.11.002.

Lawrence, R.L., Wood, S.D., and Sheley, R.L., 2006. Mapping invasive plants using hyperspectral imagery and Breiman Cutler classifications (random Forest). *Remote Sensing of Environment,* 100:356–362. doi.org/10.1016/j.rse.2005.10.014.

Lebourgeois, V., Dupuy, S., Vintrou, É., Ameline, M., Butler, S., Bégué, A., 2017. A combined random forest and OBIA classification scheme for mapping smallholder agriculture at different nomenclature levels using multisource data (simulated Sentinel-2 time series, VHRS and DEM). *Remote Sensing,* 9(3):259. doi.org/10.3390/rs9030259.

Leff, B., Ramankutty, N., and Foley, J.A., 2004. Geographic distribution of major crops across the world. *Global Biogeochemical Cycles*, 18. doi:10.1029/2003GB002108.

Li, Q., X. Cao, K. Jia, M. Zhang, and Q. Dong. 2014. Crop type identification by integration of high-spatial resolution multispectral data with features extracted from coarse-resolution time-series vegetation index data. *International Journal of Remote Sensing*, 35 (16):6076– 6088. doi.org/10.1080/01431161.2014.943325.

Liu, D., and Xia, F., 2010. Assessing object-based classification: Advantages and limitations. *Remote Sensing Letters*, 1:187–194. doi.org/10.1080/01431161003743173.

Lobell, D.B., Cassman, K.G., and Field, C.B., 2009. Crop Yield Gaps: Their Importance, Magnitudes, and Causes. Annual Review of Environment and Resources, 34:179-204. doi.org/10.1146/annurev.environ.041008.093740.

Long, J.A., Lawrence, R.L., Greenwood, M.C., Marshall, L., Miller, P.R., 2013. Object-oriented crop classification using multitemporal ETM+ SLC-off imagery and random forest. *GIScience Remote Sensing,* 50:418–436. doi.org/10.1080/15481603.2013.817150.

Löw, F., Duveiller, G., 2014. Defining the spatial resolution requirements for crop identification using optical remote sensing. *Remote Sensing*, 6(9):9034–9063. doi.org/10.3390/rs6099034.

MacDonald, R.B., Bauer, M.E., Allen, R.D., Clifton, J.W., Erickson, J.D., and Landgrebe, D.A., 1971. Results of 1971 the corn blight watch experiment. *LARS Technical Reports.* Paper 107. http://docs.lib.purdue.edu/larstech/107.

MacDonald, R.B., Hall, F.G., and Erb, R.B., 1975. The use of Landsat data in a large area crop inventory experiment (LACIE). In: Laboratory for Applications of Remote Sensing (LARS) Symposia, Paper 46, Purdue University, 1–25 pp. http://docs.lib.purdue.edu/lars_symp/46.

Massey, R., Sankey, T., Congalton, R. G., Yadav, K., Thenkabail, P. S., Ozdogan, M., and Sánchez Meador, A. J., 2017a. MODIS Phenology-Derived, Multi-Year Distribution of Conterminous U.S. Crop Types. *Remote Sensing of Environment*, 198:490–503. doi: 10.1016/j.rse.2017.06.033.

Massey, R., Sankey, T.T., Yadav, K., Congalton, R.G., Tilton, J.C., and Thenkabail, P.S., 2017b. NASA Making Earth System Data Records for Use in Research Environments (MEaSUREs) Global Food Security-Support Analysis Data (GFSAD) @ 30 m for North America: Cropland Extent Product (GFSAD30NACE), NASA EOSDIS Land Processes DAAC, USGS Earth Resources Observation and Science (EROS) Center: Sioux Falls, SD, USA. doi.org/10.5067/MEaSUREs/GFSAD/GFSAD30NACE.001.

Massey, R., Sankey, T. T., Yadav, K., Congalton, R. G., and Tilton, J. C., 2018. Integrating cloud-based workflows in continental-scale cropland extent classification. *Remote Sensing of Environment*, 219:162–179. doi: 10.1016/J.RSE.2018.10.013.

Mathur, A., Foody, G.M., 2008. Crop classification by support vector machine with intelligently selected training data for an operational application. *International Journal of Remote Sensing,* 29(8):2227–2240. doi.org/10.1080/01431160701395203.

Mayaux, P., Eva, H., Gallego, J., Strahler, A. H., Herold, M., and Agrawal, S., 2006. Validation of the global land cover 2000 map. *IEEE Transactions on Geoscience and Remote Sensing*, 44(7):1728–1739. doi: 10.1109/TGRS.2006.864370.

McCallum, I. Obersteiner, M., Nilsson, S., and Shvidenko, A., 2006. A spatial comparison of four satellite derived 1 km global land cover datasets. *International Journal of Applied Earth Observation and Geoinformation*, 8(4):246–255. doi.org/10.1016/j.jag.2005.12.002.

Mingers, J., 1989. An empirical comparison of selection measures for decision tree induction. *Machine Learning*, 3:319–342. doi.org/10.1007/BF00116837

Monfreda, C., Ramankutty, N., and Foley, J. A., 2008. Farming the planet: 2. Geographic distribution of crop areas, yields, physiological types, and net primary production in the year 2000. *Global Biogeochemical Cycles*, 22(1). doi.wiley.com/10.1029/2007GB002947.

Muñoz, X., Freixenet, J., Cufí, X., Martí, J., 2003. Strategies for image segmentation combining region and boundary information. *Pattern Recognition Letters,* 24(1-3):375–392. doi.org/10.1016/S0167-8655(02)00262-3.

Murakami, T., Ogawa, S., Ishitsuka, N., Kumagai, K., and Saito, G., 2001. Crop discrimination with multitemporal SPOT/HRV data in the Saga Plains, Japan. *International Journal of Remote Sensing,* 22:1335–1348. doi.org/10.1080/01431160151144378

Murthy, C.S., Raju, P.V., Badrinath, K.V.S., 2003. Classification of Wheat Crop with Multi-Temporal Images: Performance of Maximum Likelihood and Artificial Neural Networks. *International Journal of Remote Sensing*, 24(23):4871–4890. doi.org/10.1080/0143116031000070490.

Myint, S.W., Gober, P., Brazel, A., Grossman-Clarke, S., Weng, Q., 2011. Per-pixel vs. object-based classification of urban land cover extraction using high spatial resolution imagery. *Remote Sensing of Environment,* 115(5):1145–1161. doi.org/10.1016/j.rse.2010.12.017.

Neumann, K.; Herold, M.; Hartley, A.; and Schmullius, C., 2007. Comparative assessment of CORINE2000 and GLC2000: Spatial analysis of land cover data for Europe. *International Journal of Applied Earth Observation and Geoinformation*, 9(4), 425–437. doi.org/10.1016/j.jag.2007.02.004

Oetter, D.R., Cohen, W.B., Berterretche, M., Maiersperger, T.K., and Kennedy, R.E., 2000. Land cover mapping in an agricultural setting using multiseasonal Thematic Mapper data. *Remote Sensing of Environment* 76:139–155. doi.org/10.1016/S0034-4257(00)00202-9.

Ok, A.O., Akar, O., and Gungor, O., 2012. Evaluation of random forest method for agricultural crop classification. *European Journal of Remote Sensing,* 45(1):421–432. doi.org/10.5721/EuJRS20124535.

Oliphant, A.J., Thenkabail, P.S., Teluguntla, P., Xiong, J., Congalton, R.G., Yadav, K., Massey, R., Gumma, M.K., and Smith, C., 2017. NASA Making Earth System Data Records for Use in Research Environments (MEaSUREs) Global Food Security-Support Analysis Data (GFSAD) @ 30-m for Southeast & Northeast Asia: Cropland Extent Product (GFSAD30SEACE), NASA EOSDIS Land Processes DAAC, USGS Earth Resources Observation and Science (EROS) Center: Sioux Falls, SD, USA. doi.org/10.5067/MEaSUREs/GFSAD/GFSAD30SEACE.001.

Oliveira, J.C., Formaggio, A.R., Epiphanio, J.C.N., and Luiz, A.J.B., 2012. Index for the Evaluation of Segmentation (IAVAS): An Application to Agriculture Mapping Science. *Remote Sensing,* 40:155–169. doi.org/10.2747/0749-3878.40.3.155.

Olofsson, P., Stehman, S.V., Woodcock, C.E., Sulla-Menashe, D., Sibley, A.M., Newell, J.D., Friedl, M.A., and Herold, M., 2012. A global land-cover validation data set, part I: Fundamental design principles. *International Journal of Remote Sensing,* 33:5768–5788. doi:10.1080/01431161.2012.674230.

Olofsson, P., Foody, G.M., Stehman, S.V., and Woodcock, C.E., 2013. Making better use of accuracy data in land change studies: Estimating accuracy and area and quantifying uncertainty using stratified estimation. *Remote Sensing of Environment*, 129:122–131. doi: 10.1016/j.rse.2012.10.031.

Olofsson, P., Foody, G. M., Herold, M., Stehman, S. V., Woodcock, C. E., and Wulder. M. A., 2014. Good Practices for Estimating Area and Assessing Accuracy of Land Change. *Remote Sensing of Environment,* 148:42–57. doi: 10.1016/j.rse.2014.02.015.

Ozdogan, M., and Woodcock, C.E., 2006. Resolution dependent errors in remote sensing of cultivated areas. *Remote Sensing of Environment*, 103:203–217. doi.org/10.1016/j.rse. 2006.04.004.

Palchowdhuri, Y., Valcarce-Diñeiro, R., King, P., and Sanabria-Soto, M., 2018. Classification of multi-temporal spectral indices for crop type mapping: A case study in Coalville, UK. *Journal of Agriculture Science,* 156:24–36. doi.org/10.1017/S0021859617000879.

Pan, Z., Huang, J., Zhou, Q., Wang, L., Cheng, Y., Zhang, H., Blackburn, G.A., Yan, J., and Liu, J. 2015. Mapping crop phenology using NDVI time-series derived from HJ-1 A/B data, *International Journal of Applied Earth Observation and Geoinformation*, 34:188-197, ISSN 0303-2434. doi.org/10.1016/j.jag.2014.08.011.

Panda, S.S., Ames, D.P., and Panigrahi, S., 2010. Application of vegetation indices for agricultural crop yield prediction using neural network techniques. *Remote Sensing* 2:673–696. doi.org/10.3390/rs2030673.

Panigrahy, S., and Sharma, S.A., 1997. Mapping of crop rotation using multidate Indian Remote Sensing Satellite digital data. *ISPRS Journal of Photogrammetry and Remote Sensing,* 52:85–91. doi.org/10.1016/S0924-2716(97)83003-1.

Peña, M.A. and Brenning, A., 2015. Assessing fruit-tree crop classification from Landsat-8 time series for the Maipo Valley, Chile. *Remote Sensing of Environment, 171*:234–244. doi.org/10.1016/j.rse.2015.10.029.

Peña-Barragán, J.M., López-Granados, F., García-Torres, L., Jurado-Expósito, M., Sánchez de la Orden, M., García-Ferrer, A., 2008. Discriminating cropping systems and agro-environmental measures by remote sensing, *Agronomy for Sustainable Development,* 28(2):355-362. doi.org/10.1051/agro:2007049.

Peña-Barragán, J.M., Ngugi, M.K., Plant, R.E., and Six, J., 2011. Object-based crop identification using multiple vegetation indices, textural features and crop phenology. *Remote Sensing of Environment,* 115:1301–1316. doi.org/10.1016/j.rse.2011.01.009.

Peña-Barragán, J.M., Gutiérrez, P.A., Hervás-Martínez, C., Six, J., Plant, R.E., López-Granados, F., 2014. Object-based image classification of summer crops with machine learning methods. *Remote Sensing*, 6:5019–5041. doi.org/10.3390/rs6065019.

Pérez-Hoyos, A., García-Haro, F. J., and San-Miguel-Ayanz, J., 2012. "A Methodology to Generate a Synergetic Land-Cover Map by Fusion of Different: Land-Cover Products." *International Journal of Applied Earth Observation and Geoinformation,* 19(1):72–87. doi: 10.1016/j.jag.2012.04.011.

Pérez-Hoyos, A., Rembold, F., Kerdiles, H., and Gallego, J., 2017. Comparison of global land cover datasets for cropland monitoring. *Remote Sensing*, 9(11):1118. doi.org/10.3390/rs9111118.

Petitjean, F., Kurtz, C., Passat, N., Arski, P.G., 2012. Spatio-temporal reasoning for the classification of satellite image time series. *Pattern Recognition Letter*, 33(13):1805–1815. doi.org/10.1016/j.patrec.2012.06.009.

Pflugmacher, D., Krankina, O.N., Cohen, W.B., Friedl, M.A., Sulla-Menashe, D., Kennedy, R.E., Nelson, P., Loboda, T.V., Kuemmerle, T., and Dyukarev, E., 2011. Comparison and assessment of coarse resolution land cover maps for Northern Eurasia. *Remote Sensing of Environment,* 115:3539–3553. doi: 10.1016/j.rse.2011.08.016.

Phalke, A., Ozdogan, M., Thenkabail, P.S., Congalton, R.G., Yadav, K., Massey, R., Teluguntla, P., Poehnelt, J., and Smith, C., 2017. NASA Making Earth System Data Records for Use in Research Environments (MEaSUREs) Global Food Security-Support Analysis Data (GFSAD) @ 30-m for Europe, Middle-East, Russia and Central Asia: Cropland Extent Product (GFSAD30EUCEARUMECE), NASA EOSDIS Land Processes DAAC, USGS Earth Resources Observation and Science (EROS) Center: Sioux Falls, SD, USA. doi.org/10.5067/MEaSUREs/GFSAD/GFSAD30EUCEARUMECE.001.

Pittman, K., Hansen, M. C., Becker-Reshef, I., Potapov, P. V., and Justice, C. O., 2010. Estimating Global C Extent with Multi-Year MODIS Data. *Remote Sensing,* 2 (7):1844–1863. doi:10.3390/rs2071844.

Portmann, F.T., Siebert, S., and Döll, P., 2010. MIRCA2000—Global monthly irrigated and rainfed crop areas around the year 2000: A new high-resolution data set for agricultural and hydrological modeling. *Global Biogeochemical Cycles,* 24:1–24. doi:10.1029/2008GB003435.

Potapov, P., Hansen, M., Gerrand, A., Lindquist, E., Pittman, K., Turubanova, S., Wilkie, M.L., 2011. The global Landsat imagery database for the FAO FRA remote sensing survey. *International Journal of Digital Earth,* 4(1):2–21. doi.org/10.1080/17538947.2010.492244.

Ramankutty, N., Evan, A.T., Monfreda, C., and Foley, J.A., 2008. Farming the planet: 1. Geographic distribution of global agricultural lands in the year 2000. *Global Biogeochemical Cycles,* 22:1–19. doi.org/10.1029/2007GB002952.

Ran, Y., Li, X., and Lu, L., 2010. Evaluation of four remote sensing-based land cover products over China. *International Journal of Remote Sensing,* 31(2):391–401. doi.org/10.1080/01431160902893451.

Rhode, W.G., 1978. Digital Image Analysis Techniques for Natural Resource Inventories. National Computer Conference Proceedings, 43-106 pp.

Rodriguez-Galiano, V.F., Chica-Olmo, M., Abarca-Hernandez, F., Atkinson, P.M., and Jeganathan, C., 2012. Random Forest classification of Mediterranean land cover using multi-seasonal imagery and multi-seasonal texture. *Remote Sensing of Environment,* 121:93–107. doi.org/10.1016/j.rse.2011.12.003.

Rosenfield, G.H., Fitzpatrick-Lins, K., and Ling, H.S., 1982. No Sampling for thematic map accuracy testing. *Photogrammetry Engineering and Remote Sensing*, 48:131–137.

Rouse, J.W., Hass, R.H., Schell, J.A., and Deering, D.W., 1973. Monitoring vegetation systems in the great plains with ERTS. Third Earth Resources Technology Satellite Symposium. 1:309–317. doi.org/citeulike-article-id:12009708.

Ryerson, R.A., Dobbins, R.N., and Thibault, C., 1985. Timely crop area estimates from Landsat. *Photogrammetry Engineering and Remote Sensing,* 51:1735–1743.

Salmon, J.M., Friedl, M.A., Frolking, S., Wisser, D., and Douglas, E.M., 2015. Global rain-fed, irrigated, and paddy croplands: A new high-resolution map derived from remote sensing, crop inventories and climate data. *International Journal of Applied Earth Observation and Geoinformatics*, 38:321–334, doi: 10.1016/j.jag.2015.01.014.

Scepan, J., 1999. Thematic validation of high-resolution Global Land- Cover Data Sets. *Photogrammetry Engineering and Remote Sensing,* 65 (9):1051–1060.

Schwab, K., Sala-i-Martín, X., Brende, B., Blanke, J., Bilbao-Osorio, B., Browne, C., Corrigan, G., Crotti, R., Hanouz, M.D., Geiger, T., Gutknecht, T., Ko, C., and Serin, C., 2014. The Global Competitiveness Report, World Economic Forum Reports 2014. doi.org/ISBN-13: 978-92-95044-73-9.

Sedano, F., Gong, P., and Ferrão, M., 2005. Land cover assessment with MODIS imagery in southern African Miombo ecosystems. *Remote Sensing of Environment*, 98:429–441. doi: 10.1016/j.rse.2005.08.009.

See, L.M., and Fritz, S., 2005, A user-defined fuzzy logic approach to comparing global land cover products. In 14th European Colloquium on Theoretical and Quantitative Geography, 9–12 September 2005, Lisbon, Portugal.

See, L. M., and Fritz, S., 2006. A method to compare and improve land cover datasets: Application to the GLC-2000 and MODIS land cover products. *IEEE Transactions on Geoscience and Remote Sensing*, 44(7):1740–1746. doi: 10.1109/TGRS.2006.874750.

Seo, S.N., 2014. Evaluation of the Agro-Ecological Zone methods for the study of climate change with micro farming decisions in sub-Saharan Africa. *European Journal of Agronomy*, 52:157–165. doi: 10.1016/j.eja.2013.09.014.

Serra, P., and Pons, X., 2008. Monitoring farmers' decisions on Mediterranean irrigated crops using satellite image time series. *International Journal of Remote Sensing,* 29:2293–2316. doi.org/10.1080/01431160701408444.

Shao, Y., and Lunetta, R.S., 2012. Comparison of support vector machine, neural network, and CART algorithms for the land-cover classification using limited training data points. *ISPRS Journal of Photogrammetry and Remote Sensing*, 70:78–87. doi: 10.1016/j.isprsjprs.2012.04.001.

Simonneaux, V., Duchemin, B., Helson, D., Er-Raki, S., Olioso, A., and Chehbouni, A.G., 2008. The use of high-resolution image time series for crop classification and evapotranspiration estimate over an irrigated area in central Morocco. *International Journal of Remote Sensing,* 29:95–116. doi.org/10.1080/01431160701250390.

Sonobe, R., Tani, H., Wang, X., Kobayashi, N., Shimamura, H., 2012. Parameter tuning in the support vector machine and random forest and their performances in cross- and same-year crop classification using TerraSAR-X. *International Journal of Remote Sensing,* 35(23):260–267. doi.org/10.1080/01431161.2014.978038.

South, S., Qi, J., and Lusch, D.P., 2004. Optimal classification methods for mapping agricultural tillage practices. *Remote Sensing of Environment* 91:90–97. doi.org/10.1016/j.rse.2004.03.001.

Stehman, S.V., 1992. Comparison of systematic and random sampling for estimating the accuracy of maps generated from remotely sensed data. *Photogrammetry Engineering and Remote Sensing*, 58:1343–1350.

Stehman, S.V., 1997. Selecting and interpreting measures of thematic classification accuracy. *Remote Sensing of Environment*, 62:77–89. doi:10.1016/S0034-425700083-7.

Stehman, S V. 1999. Comparing Thematic Maps Based on Map Value. *International Journal of Remote Sensing,* 20 (12):2347–2366. doi:10.1080/014311699212065.

Stehman, S.V., 2009. Sampling designs for accuracy assessment of land cover. *International Journal of Remote Sensing*, 30:5243–5272, doi:10.1080/01431160903131000.

Stehman, S.V., 2012. Impact of sample size allocation when using stratified random sampling to estimate accuracy and area of land-cover change. *Remote Sensing Letters*, 3:111–120. doi:10.1080/01431161.2010.541950.

Stehman, S V, and Czaplewski, R. L., 1998. "Design and Analysis for Thematic Map Accuracy Assessment - an Application of Satellite Imagery." *Remote Sensing of Environment*, 64:331–344. doi:10.1016/S0034-4257(98)00010-8.

Story, M., and Congalton, R.G., 1986. Accuracy assessment: A user's perspective. *Photogrammetry Engineering and Remote Sensing*, 52:397–399. doi:10.1111/j.1530-9290.2010.00257.

Strahler, A.H., Boschetti, L., Foody, G.M., Friedl, M.A., Hansen, M.C., Herold, M., Mayaux, P., Morisette, J.T., Stehman, S.V., Woodcock, C.E., 2006. Global Land Cover Validation: Recommendations for Evaluation and Accuracy Assessment of Global Land Cover Maps, GOFC-GOLD Report No. 25, *European Commission Joint Research Centre,* Ispra, Italy, 48–51 pp.

Stumpf, A., Kerle, N., 2011. Object-oriented mapping of landslides using Random Forests. *Remote Sensing of Environment*, 115(10):2564–2577. doi: 10.1016/j.rse.2011.05.013.

Sun, P., and Congalton, R.G., 2018. Using a Similarity Matrix Approach to Evaluate the Accuracy of Rescaled Maps. *Remote Sensing*, 10:487. doi:10.3390/rs10030487.

Taşdemir, K., Milenov, P., Tapsall, B., 2012. A hybrid method combining SOM-based clustering and object-based analysis for identifying land in good agricultural condition. *Computer Electronics in Agriculture*, 83:92–101. doi: 10.1016/j.compag.2012.01.017.

Tatsumi, K., Yamashiki, Y., Canales Torres, M.A., and Taipe, C.L.R., 2015. Crop classification of upland fields using Random forest of time-series Landsat 7 ETM+ data. *Computer Electronics and Agriculture*, 115:171–179. doi.org/10.1016/j.compag.2015.05.001.

Teluguntla, P.G., Thenkabail, P.S., Xiong, J., Gumma, M.K., Giri, C., Milesi, C., Ozdogan, M., Congalton, R.G., Tilton, J.C., and Sankey, T.T., 2016. Global Food Security Support Analysis

Data at Nominal 1 km (GFSAD1km) Derived from Remote Sensing in Support of Food Security in the Twenty-First Century: Current Achievements and Future Possibilities. In Land Resources Monitoring, Modeling, and Mapping with Remote Sensing, CRC Press: Boca Raton, FL, USA, 131–160 pp. doi:10.1201/b19322-9.

Teluguntla, P., Thenkabail, P. S., Xiong, J., Gumma, M. K., Congalton, R. G., Oliphant, A., Poehnelt, J., Yadav, K., Rao, M., and Massey, R., 2017a. Spectral Matching Techniques (SMTs) and Automated C Classification Algorithms (ACCAs) for Mapping Croplands of Australia Using MODIS 250-m Time-Series (2000–2015) Data. *International Journal of Digital Earth,* 10 (9):944–977. doi:10.1080/17538947.2016.1267269.

Teluguntla, P., Thenkabail, P.S., Xiong, J., Gumma, M.K., Congalton, R.G., Oliphant, A.J., Sankey, T., Poehnelt, J., Yadav, K., and Massey, R., 2017b. NASA Making Earth System Data Records for Use in Research Environments (MEaSUREs) Global Food Security-Support Analysis Data (GFSAD) @ 30-m for Australia, New Zealand, China, and Mongolia: Cropland Extent Product (GFSAD30AUNZCNMOCE), NASA EOSDIS Land Processes DAAC, USGS Earth Resources Observation and Science (EROS) Center: Sioux Falls, SD, USA. doi.org/10.5067/MEaSUREs/GFSAD/GFSAD30AUNZCNMOCE.001.

Teluguntla, P., Thenkabail, P.S., Oliphant, A., Xiong, J., Gumma, M.K., Congalton, R.G., Yadav, K., and Huete, H., 2018. A 30-m landsat-derived cropland extent product of Australia and China using random forest machine learning algorithm on Google Earth Engine cloud computing platform*, ISPRS Journal of Photogrammetry and Remote Sensing*, 144:325-340, ISSN 0924-2716. doi.org/10.1016/j.isprsjprs.2018.07.017.

The World Bank, 2010. Global strategy to improve agricultural and rural statistics (Economic and Sector Work No.56719-GLB). Washington, DC. © World Bank. https://openknowledge.worldbank.org/handle/10986/12402 License: CC BY 3.0 IGO.

Thenkabail, P.S., 2005. Assessing positional and thematic accuracies of map generated from remotely sensed data. In: Remotely Sensed Data Characterization, Classification, and Accuracies, CRC Press-Taylor and Francis Group: Boca Raton, FL, USA, 583–605 pp.

Thenkabail, P.S., Lyon, G.J., Turral, H., and Biradar, C., 2009. *Remote Sensing of Global Croplands for Food Security*, CRC Press-Taylor and Francis Group: Boca Raton, FL, USA, London, UK, 556 pp.

Thenkabail, P. S., Biradar, C. M., Noojipady, P., Dheeravath, V., Li, Y., Velpuri, M., and Gumma, M. K., 2009. "Global Irrigated Area Map (GIAM), Derived from Remote Sensing, for the End of the Last Millennium." *International Journal of Remote Sensing,* 30 (14):3679–3733. doi:10.1080/01431160802698919.

Thenkabail, P.S., 2010. Global croplands and their importance for water and food security in the twenty-first century: Towards an evergreen revolution that combines a second green revolution with a blue revolution. *Remote Sensing*, 2:2305–2312, doi:10.3390/rs2092305.

Thenkabail, P.S., and Wu, Z., 2012. An automated cropland classification algorithm (ACCA) for Tajikistan by combining Landsat, MODIS, and secondary data. *Remote Sensing,* 4(10):2890–2918. doi.org/10.3390/rs4102890.

Tollefson J., 2011. Scientists push for agricultural monitoring. *Nature.* doi:10.1038/news.2011.566.

Tsendbazar, N. E., Bruin, S. D., and Herold, M., 2015. Assessing Global Land Cover Reference Datasets for Different User Communities. *ISPRS Journal of Photogrammetry and Remote Sensing,* 103. International Society for Photogrammetry and Remote Sensing, Inc. (ISPRS): 93–114. doi: 10.1016/j.isprsjprs.2014.02.008.

Tsendbazar, N.E., Bruin, S. De, Fritz, S., and Herold, M., 2015. Spatial Accuracy Assessment and Integration of Global Land Cover Datasets. *Remote Sensing*, 7:15804–15821, doi:10.3390/rs71215804.

Ulabay, F.T., Li, R.Y., and Shanmugan, K.., 1982. Crop Classification Using Airborne Radar and Landsat Data. *IEEE Transactions of Geoscience Remote Sensing*, 20:42–51. doi.org/10.1109/TGRS.1982.4307519.

Ung, C.H., Lambert, M.C., Guidon, L., and Fournier, R.A., 2000. Integrating Landsat-TM data with environmental data for classifying forest cover types and estimating their biomass. In: Proceedings of the 4th International Symposium on Spatial Accuracy Assessment in Natural Resources and Environmental Sciences, 659–662 pp.

USDA-NASS, USDA, 2010. Field Crops Usual Planting and Harvesting Dates, National Agriculture Statistics Services, 1–51 pp.

Ustuner, M., Sanli, F.B., Abdikan, S., Esetlili, M.T., and Kurucu, Y., 2014. Crop type classification using vegetation indices of rapid eye imagery. *International Architect of Photogrammetry Remote Sensing Spatial Information Science* - ISPRS Arch. 40:195–198. doi.org/10.5194/isprsarchives-XL-7-195-2014.

Van Genderen, J., and Lock, B., 1977. Testing land use map accuracy. *Photogrammetry Engineering and Remote Sensing*, 43:1135–1137.

Van Wart, J., van Bussel, L.G.J., Wolf, J., Licker, R., Grassini, P., Nelson, A., Boogaard, H., Gerber, J., Mueller, N.D., and Claessens, L., 2013. Use of agro-climatic zones to upscale simulated crop yield potential. *Field Crops Resources*, 143:44–55. doi: 10.1016/j.fcr.2012.11.023.

Vancutsem, C., Marinho, E., Kayitakire, F., See, L., and Fritz, S., 2013. Harmonizing and combining existing land cover/land use datasets for cropland area monitoring at the African continental scale. *Remote Sensing*, 5:19–41. doi:10.3390/rs5010019.

Verbeiren, S., Eerens, H., Piccard, I., Bauwens, I., Orshoven, J. V., 2008. Sub-Pixel Classification of Spot-Vegetation Time Series for the Assessment of Regional Crop Areas in Belgium. *International Journal of Applied Earth Observation and Geoinformatics*, 10:486–497. doi: 10.1016/j.jag.2006.12.003.

Vieira, M.A., Formaggio, A.R., Rennó, C.D., Atzberger, C., Aguiar, D.A., Mello, M.P., 2012. Object Based Image Analysis and Data Mining applied to a remotely sensed Landsat time-series to map sugarcane over large areas. *Remote Sensing of Environment*, 123:553–562. doi.org/10.1016/j.rse.2012.04.011.

Vinciková, H., Hais, M., Brom, J., Procházka, J., and Pecharová, E., 2010. Landscape Studies Use of remote sensing methods in studying agricultural landscapes – a review. *Journal of Landscape Studies,* 3:53–63.

Vintrou, E., Desbrosse, A., Bégué, A., Traoré, S., Baron, C., Lo Seen, D., 2012. Crop area mapping in West Africa using landscape stratification of MODIS time series and comparison with existing global land products. *International Journal of Applied Earth Observation and Geoinformation*, 14(1):83–93. doi:10.1016/j.jag.2011.06.010.

Waldner, F., Canto, G.S., and Defourny, P., 2015. Automated annual cropland mapping using knowledge-based temporal features. *ISPRS Journal of Photogrammetry and Remote Sensing,* 110:1–13. doi: 10.1016/j.isprsjprs.2015.09.013.

Waldner, F., Fritz, S., Di Gregorio, A., and Defourny, P., 2015. Mapping Priorities to Focus Cropland Mapping Activities: Fitness Assessment of Existing Global, Regional and National Cropland Maps. *Remote Sensing*, 7 (6):7959–7986. doi:10.3390/rs70607959.

Walker, J.S., and Blaschke, T., 2008. Object-based land cover classification for the Phoenix metropolitan area: optimization vs. transportability. *International Journal of Remote Sensing*, 29(7):2021–2040. doi.org/10.1080/01431160701408337.

Wardlow, B.D., and Egbert, S.L., 2008. Large-area crop mapping using time-series MODIS 250 m NDVI data: An assessment for the U.S. Central Great Plains. *Remote Sensing of Environment*, 112:1096–1116. doi: 10.1016/j.rse.2007.07.019.

Wardlow, B.D., Egbert, S.L., and Kastens, J.H., 2007. Analysis of time-series MODIS 250??m vegetation index data for crop classification in the U.S. Central Great Plains. *Remote Sensing of Environment,* 108:290–310. doi.org/10.1016/j.rse.2006.11.021

Warner, T.A., Lee, J.Y., and McGraw, J.B., 1998. Delineation and identification of individual trees in the Eastern Deciduous Forest. Presented at: The International Forum on Automated Interpretation of High Spatial Resolution Imagery for Forestry. February 10-12, Victoria, BC.

Williams, V.L., Philipson, W.R., and Philpot, W.D., 1987. Identifying vegetable crops with Landsat Thematic Mapper data. *Photogrammetry Engineering and Remote Sensing*, 53:187–191.

Wu, W., Shibasaki, R., Yang, P., Zhou, Q., and Tang, H., 2008. Remotely sensed estimation of cropland in China: A comparison of the maps derived from four global land cover datasets. *Canadian Journal of Remote Sensing*, 34:467–479. doi:10.5589/m08-059.

Wu, Z., Thenkabail, P.S., Mueller, R., Zakzeski, A., Melton, F., Johnson, L., Rosevelt, C., Dwyer, J., Jones, J., and Verdin, J.P., 2014. Seasonal cultivated and fallow cropland mapping using MODIS-based automated cropland classification algorithm. *Journal of Applied Remote Sensing*, 8:83618–83685. doi: 10.1117/1.JRS.8.083685.

Wulder, M.A., Masek, J.G., Cohen, W. B., Loveland, T.R., and Woodcock, C.E., 2012. Opening the archive: how free data has enabled the science and monitoring promise of Landsat. *Remote Sensing of Environment*, 122:2–10. doi.org/10.1016/j.rse.2012.01.010.

Xiong, J., Thenkabail, P.S., Gumma, M.K., Teluguntla, P., Poehnelt, J., Congalton, R.G., Yadav, K., and Thau, D., 2017a. Automated cropland mapping of continental Africa using Google Earth Engine cloud computing. *ISPRS Journal of Photogrammetry and Remote Sensing,* 126:225–244. doi: 10.1016/j.isprsjprs.2017.01.019.

Xiong, J., Thenkabail, P. S., Tilton, J. C., Gumma, M. K., Teluguntla, P., Oliphant, A., Congalton, R. G., Yadav, K., and Gorelick, N., 2017b. Nominal 30-m C Extent Map of Continental Africa by Integrating Pixel-Based and Object-Based Algorithms Using Sentinel-2 and Landsat-8 Data on Google Earth Engine. *Remote Sensing,* 9 (10):1065. doi:10.3390/rs9101065.

Xiong, J., Thenkabail, P.S., Tilton, J.C., Gumma, M.K., Teluguntla, P., Congalton, R.G., Yadav, K., Dungan, J., Oliphant, A.J., and Poehnelt, J., 2017c. NASA Making Earth System Data Records for Use in Research Environments (MEaSUREs) Global Food Security-Support Analysis Data (GFSAD) @ 30-m Africa: Cropland Extent Product (GFSAD30AFCE), NASA EOSDIS Land Processes DAAC, USGS Earth Resources Observation and Science (EROS) Center: Sioux Falls, SD, USA. doi.org/10.5067/MEaSUREs/GFSAD/GFSAD30AFCE.001.

Yadav, K., and. Congalton R. G., 2018a. Issues with Large Area Thematic Accuracy Assessment for Mapping C Extent: A Tale of Three Continents. *Remote Sensing,* 10 (1): 53. doi.org/10.3390/rs10010053.

Yadav, K., and Congalton, R. G., 2018b. Accuracy Assessment of Global Food Security-Support Analysis Data (GFSAD) Cropland Extent Maps Produced at Three Different Spatial Resolutions. *Remote Sensing,* 10 (11):1800. doi.org/10.3390/rs10111800.

Yadav, K., and Congalton, R. G., 2019a. Evaluating Sampling Designs for Assessing the Accuracy of Cropland Extent Maps in Different Cropland Proportion. In Prep.

Yadav, K., and Congalton, R. G., 2019b. Augmenting and Extending Limited Crop Type Reference Data using an Interpretation and Phenology-Based Approach. In Prep.

Yan, L., Roy, D.P., 2014. Automated crop field extraction from multi-temporal Web Enabled Landsat Data. *Remote Sensing of Environment*, 144:42–64. doi.org/10.1016/j.rse.2014.01.006.

Yan, L., Roy, D.P., 2015. Improved time series land cover classification by missing-observation-adaptive nonlinear dimensionality reduction, *Remote Sensing of Environment*, 158:478-491. doi.org/10.1016/j.rse.2014.11.024.

Yang, C., Everitt, J.H., and Murden, D., 2011. Evaluating high resolution SPOT 5 satellite imagery for crop identification. *Computers and Electronics in Agriculture*, 75(2):347–354. doi.org/10.1016/j.compag.2010.12.012.

Yu, L., Wang, J., Clinton, N., Xin, Q., Zhong, L., Chen, Y., and Gong, P., 2013. FROM-GC: 30 m global cropland extent derived through multisource data integration. *International Journal of Digital Earth*, 6:521–533. doi:10.1080/17538947.2013.822574.

Zhong, L., Gong, P., and Biging, G.S., 2014. Efficient corn and soybean mapping with temporal extendability: A multi-year experiment using Landsat imagery. *Remote Sensing of Environment,* 140:1–13. doi.org/10.1016/j.rse.2013.08.023

Zhong, Y., Giri, C., Thenkabail, P.S., Teluguntla, P., Congalton, R.G., Yadav, K., Oliphant, A.J., Xiong, J., Poehnelt, J., and Smith, C., 2017. NASA Making Earth System Data Records for Use in Research Environments (MEaSUREs) Global Food Security-Support Analysis Data (GFSAD) @ 30-m for South America: Cropland Extent Product (GFSAD30SACE), NASA EOSDIS Land Processes DAAC, USGS Earth Resources Observation and Science (EROS) Center: Sioux Falls, SD, USA. doi.org/10.5067/MEaSUREs/GFSAD/GFSAD30SACE.00.

Zhou, M., Shu, J., Song, C., and Gao, W., 2014. Sensitivity studies for atmospheric carbon dioxide retrieval from atmospheric infrared sounder observations. *Journal of Applied Remote Sensing,* 8(1):083697. doi.org/10.1117/1.JRS.8.083697.